EXTRACTIVE AMMONIA (EA): A NOVEL AMMONIA-BASED PRETREATMENT TECHNOLOGY FOR LIGNOCELLULOSIC BIOMASS

By

Leonardo da Costa Sousa

A DISSERTATION

Submitted to
Michigan State University
in partial fulfillment of the requirements
for the degree of

Chemical Engineering – Doctor of Philosophy

2014

ABSTRACT

EXTRACTIVE AMMONIA (EA): A NOVEL AMMONIA-BASED PRETREATMENT TECHNOLOGY FOR LIGNOCELLULOSIC BIOMASS

By

Leonardo da Costa Sousa

Large scale production of economically viable biofuels can only be achieved from widely available resources, notably lignocellulosic biomass. This feedstock is largely composed by complex carbohydrates, which can be enzymatically hydrolyzed and converted to fuels and chemicals by fermentative organisms. Lignocellulosic biomass is recalcitrant to enzymatic degradation and therefore, a pretreatment step is required for achieving acceptable sugar yields. Recent research has improved our fundamental understanding about the physico-chemical events occurring during ammonia pretreatment of biomass that correlate with enzymatic hydrolysis yields. From this understanding, a novel Extractive Ammonia (EA) pretreatment was developed and is presented herein for the first time. This technology allows the conversion of naturally occurring cellulose I (CI) to cellulose III (CIII) and the selective extraction of lignin from the plant cell wall with liquid ammonia. These extractives are collected in a separate stream as a valuable byproduct. While CIII is known to improve enzymatic hydrolysis rates up to two fold compared to native CI, lignin is acknowledged as a major inhibitor for both enzymes and microbes. Other key events include ester-bonds cleavage via ammonolysis and hydrolysis reactions during EA. Ester bonds play an important role in cross-linking lignin and carbohydrates and therefore, their cleavage disrupts the complex cell wall architecture, allowing carbohydrates to be more easily accessible by enzymes.

The effect of pretreatment variables on CIII conversion was studied using isolated cellulose from commercial sources (Avicel). These studies revealed that samples of higher CIII crystallinity can significantly increase enzymatic activity, which contradicts the current paradigm based on CI results, which show that higher CI crystallinity reduces enzymatic activity of cellulases. In the present work, EA performance was evaluated using corn stover (CS) as primary biomass feedstock. An empirical model was created using statistical design of experiments to predict EA pretreatment effectiveness on lignin extraction, ester-bond cleavage and sugar yields as a function of pretreatment conditions. The results show that EA allows extraction of up to ~ 50 % of the lignin present in corn stover, while cleaving about 70 % of the ester bonds. These effects, in synergy with cellulose III formation, allow maximum monomeric glucose and xylose conversions of 93 % and 79 %, respectively, using 15 mg/g glucan of enzyme for 24 h, at 1% glucan loading enzymatic hydrolysis. At 15 % to 20% solid loadings, EA allows up to 2.7 fold reduction of enzyme loading during enzymatic hydrolysis compared to AFEX^{TM}-CS. The benefits of EA on fermentation were also explored using the novel RaBIT process, which is capable of doubling biofuel productivity while decreasing enzyme loading by 30 % compared with traditional SHF. By coupling EA and RaBIT technologies was possible to efficiently generate 191 g ethanol/Kg biomass in 48 h. using 7.5 mg/g glucan of enzyme loading.

The viability of the EA process depends on enzyme savings and on the utilization of lignin streams. From this perspective, EA lignin extracts were fractionated by sequential precipitation generating a fraction composed by ~92 % lignin, which represented about 32 % of the lignin initially present in CS. Techno-economic evaluation of the EA biorefinery was also performed and will be presented along with recommendations for further improvement of this technology.

Dedicated to my dear daughter Maria Madalena and to my parents

ACKNOWLEDGEMENTS

I would like to express my gratitude to my research advisor, Prof. Bruce Dale, and to Prof. Venkatesh Balan for accepting me in their team and for supporting me during my PhD.

A special acknowledgement goes to my Committee members Prof. Dan Jones, Prof. Carl Lira and Prof. Dennis Miller for their support and suggestions to improve my work.

When I joined Prof. Dale's lab in 2007, I found a vibrant group of people working in synergy to overcome the challenges of lignocellulosic biomass conversion to fuels and chemicals. The work presented herein would never be possible without the help of many of my colleagues, their support and contribution. I would like to highlight the contribution of Shishir Chundawat, Mingjie Jin, James Humpula, Nirmal Uppugundla, Vijay Bokade, Margie Magyer, Christa Gunawan, Bryan Bals, Andrea Orjuela, Xiaoyu Tang and Prof. Albert Cheh to this work. I would also like to highlight the contribution of various collaborators, notably Prof. Marcus Foston, Prof. John Ralph, Ali Azarpira and Fachuang Lu, who brought their expertise in lignin characterization to this work.

A special thanks goes to my colleagues Ming Woei Lau, Dahai Gao, Rebecca Ong and Cory Sarks for the vibrant discussions, support, friendship and for providing me a pleasant work environment.

I would also like to exend my gratitude to Pete Donald, Brandon Guthrie, Aaron Vigil and Lucas Holcomb for their hard work and commitment. They were a vital part of this project, as they

helped me building reactors, performing pretreatment experiments and composition analysis on many of my samples.

I would like to thank the Great Lakes Bioenergy Research Center (GLBRC) and Fundacao para a Ciencia e Tecnologia (FCT) for funding my PhD work.

A very important acknowledgment goes to those who supported me in the good and bad times during my stay in US. Thanks to my friends Anchita, Durga, Alvaro, Ven, Mingjie, Shishir and my ex-wife Xana for their support and encouragement.

Finally, I would like to express my gratitude to my family, especially to my parents Celeste Sousa and Mateus Sousa, and to my daughter Madalena, for their love, support, motivation and encouragement.

TABLE OF CONTENTS

LIST OF TABLES

LIST OF FIGURES

CHAPTER 1 - INTRODUCTION

1.1. Project objectives

The increasing interest in exploring renewable sources of energy derives from several factors which include increasing oil consumption, depleting oil reserves, environmental concerns due to green-house gas (GHG) emissions, national security and energy independence issues. Among the different renewable sources of energy, lignocellulosic biomass is considered to be the only sustainable resource, capable of delivering liquid fuels and chemicals on a large scale [1]. Biochemical processing of lignocellulosic biomass to liquid fuels takes advantage of the fact that the plant cell wall is composed of carbohydrate polymers (cellulose and hemicellulose), which can be hydrolyzed by cellulolytic enzymes and fermented by microorganisms to produce fuel molecules (e.g. ethanol, butanol). Since biomass is extremely recalcitrant to enzyme degradation, efficient enzymatic hydrolysis cannot be obtained before a pretreatment step, which improves accessibility of enzymes to the substrate. Ammonia Fiber Expansion (AFEX^{TM}) is one the leading pretreatment technologies available today, capable of improving enzymatic hydrolysis yields from 3-10 folds, depending on the nature of the substrate [1]. This technology shows a vast potential to solve major bottlenecks in the biorefinery. However, current biorefinery scenarios, including AFEX^{TM}-based scenarios, still have important issues that must be addressed before turning the bioeconomy into a reality. For example, cellulolytic enzymes are expensive and their price contributes in large extent to the operation cost of the biorefinery, which can only be solved by decreasing enzyme utilization. One major problem observed during enzymatic hydrolysis is related to the fact that industrially relevant conditions require cellulose loadings

higher than 6% (w/w), allowing the production of high concentration of fermentable sugars which can translate to high concentrations of ethanol (>40g/L) after fermentation. Under these conditions, sugar yields are severely reduced comparing to low cellulose loadings (e.g. 1% (w/w)), possibly due to decreased water activity and lower hydration of the cellulose surface [2, 3]. As a consequence of this issue, a higher enzyme loading is required to effectively hydrolyze lignocellulosic biomass at industrially relevant conditions. Solving this problem requires either engineering the substrate during the pretreatment step, or engineering the enzymes to work effectively under those conditions. In our perspective, little technological advances have been observed in the pretreatment area, where relevant contributions to solve these important bottlenecks remain scarce. In realistic terms, the properties of lignocellulosic biomass can be manipulated and engineered by the pretreatment to improve downstream processing, allowing existing microorganisms and enzymes to perform efficiently at industrially relevant conditions. From this point of view, this work attempts to understand and be able to control key events occurring during ammonia pretreatment of corn stover. Moreover, it proposes to modify the current AFEX^{TM} pretreatment methodology in order to maximize the potential of ammonia as a pretreatment chemical and therefore be able to:

1) Reduce enzyme loading from ~20mg/g glucan to < 10mg/g glucan without highly affecting enzymatic hydrolysis yields;

2) Improve enzymatic hydrolysis yields at higher solid loadings by minimizing the negative impact of solids on enzymatic hydrolysis yields;

4) Create conditions to valorize lignin streams derived from pretreated biomass.

For these objectives, the creation of a novel pretreatment technology is proposed herein, where naturally occurring cellulose I is modified to a more hydrophilic cellulose III, thereby improving enzymatic hydrolysis rates at low and high solid loading. Also, due to the inhibitory role of lignin toward enzymes and microbes, we propose to use this novel pretreatment technology to extract lignin from the plant cell wall, thereby reducing enzyme and microbial inhibition during downstream processing. This novel technology, denominated by Extractive Ammonia (EA) pretreatment is proposed herein for the first time and consists of contacting lignocellulosic biomass with liquid ammonia, at high liquid-to-solid ratio and relatively mild temperatures (~120 $^{\circ}$C) for short residence times. The effect of this treatment on the plant cell wall chemistry will be determined by measuring 1) the impact of treatment conditions in cellulose III conversion, 2) the degree of ester bond cleavage on the plant cell wall through ammonolysis and hydrolysis reactions and also by 3) determining the extent of lignin extractability during EA pretreatment.

The effect of plant cell wall modifications proposed herein on downstream processing will be also evaluated by studying high solid loading enzymatic hydrolysis. Empirical modeling will be performed using statistical design of experiments to correlate sugar yields with enzymatic hydrolysis conditions, notably solids loading, enzyme loading and incubation time. The extracted lignin and its potential for valorization to fuels and chemicals will be also evaluated by a detailed physico-chemical characterization.

State-of-the-art fermentation technology will be used to test the novel EA pretreated substrate performance. The novel Rapid Bioconversion with Integrated Enzyme Recycling Technology (RaBIT) process has demonstrated to be capable of saving an extra 30 % of enzyme due to its enzyme recycling capability on AFEX^{TM} pretreated corn stover (AFEX^{TM}-CS) [4]. Therefore, by integrating a more digestible substrate to the RaBIT technology, we expect that enzyme loading could be further reduced to lower levels.

The objectives proposed here and their relevance will be supported by techno-economic evaluation. Major economics information will include calculation of the minimum ethanol selling price (MESP), using current downstream technology coupled with EA processes, based on experimental data and empirical predictive models. The feedstock of interest in this study will be corn stover in all cases.

Finally, the information obtained from these studies will be used to formulate appropriate recommendations to improve EA pretreatment technology and allow it to play a major role in future biorefineries.

CHAPTER 2 – LITERATURE REVIEW

2.1. Lignocellulosic Biomass

The main components of the plant cell wall are cellulose, hemicellulose, lignin, protein and ash. The ratio between these components varies among families of plants, like grasses, softwoods and hardwoods (**Table 2-1**).

Table 2-1 Composition of lignocellulosic materials in cellulose, hemicellulose, lignin and ash [5-7].

Lignocellulosic Materials	Cellulose (%)	Hemicellulose (%)	Lignin (%)	Ash (%)
Hardwoods	40-55	24-40	18-25	<1
Softwoods	45-50	25-35	25-35	<1
Grasses	25-40	35-50	10-30	1-12

These plant cell wall components form a complex interlinked structure that can provide both support and a defense mechanism against invading microbes [6], [5], [8]. This is one of the reasons why plant cell walls are highly recalcitrant towards fungal and bacterial enzymes and why a pretreatment is required to disrupt this complex cell wall architecture prior to enzymatic hydrolysis [9], [1]. The chemical structure of these components defines their role in the plant cell wall architecture, which will be discussed herein.

2.1.1. Cellulose

Cellulose is the main polysaccharide in the plant cell wall. Its structure is identical for all plants; however woody biomasses have a higher cellulose content compared to grasses. The primary structure of cellulose is a linear (i.e., non-branched) chain consisting of β-(1,4)-linked D-glucose

residues. Several of these chains are assembled in parallel through hydrogen bonding to form a secondary structure, called cellulose *microfibril* [10]. In plants, these microfibrils are composed by a more abundant fraction of ordered (crystalline) cellulose and a smaller fraction of less ordered (amorphous) cellulose [11]. Crystalline cellulose occurs naturally in two different polymorphs denominated by cellulose I_α and I_β [12]. These crystalline structures are organized in parallel chains connected by hydrogen bonds that allow the formation of cellulose sheets. In cellulose I_α and I_β there is no strong hydrogen bonding between the cellulose sheets. The only difference between these two polymorphs of cellulose I is the relative displacement of the sheets in the chain direction, resulting in triclinic and monoclinic unit cells for cellulose I_α and I_β , respectively. The only cellulose allomorph present in plants is cellulose I_β, while cellulose I_α can be found in cell walls of bacteria and algae. In some organisms, notably in *Valonia*, is interesting to see that cellulose is consistently composed of an eight-chain unit cell, accommodating both native cellulose polymorphs, i.e. cellulose I_α and I_β [13].

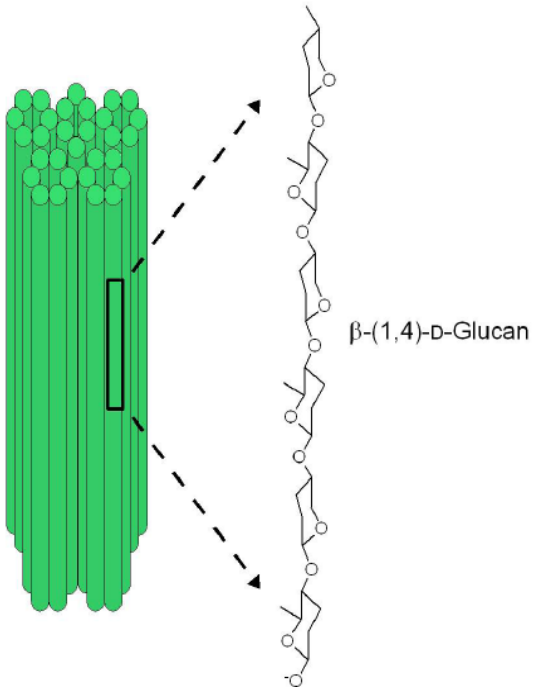

Figure 2-1 Graphical representation of the structure of cellulose microbibrils. Cellulose microfibrils (green) are composed of chains of β-(1,4)-linked D-glucose subunits.

2.1.2. Hemicelluloses

Hemicelluloses are the second major polysaccharides found in plant cell walls and are mainly composed of aldopentoses (i.e., arabinose and xylose) and play an important role in cross-linking cellulose microfibrils. In grasses, the most abundant hemicelluloses are xyloglucans and arabinoxylans.

Xyloglucan has a backbone similar to cellulose, decorated with xylose side-residues linked to every 3 of 4 glucose monomers (**Figure 2-2**). This polymer is thought to either bind spontaneously to adjacent cellulose microfibrils, maintaining their link, or bind covalently to pectin polysaccharides [10]. Arabinoxylans have a β-(1,4)-D-xylan backbone, branched with arabinose residues. Glucuronic and ferulic acid branches are also present in the arabinoxylan

structure. Ferulic acid residues are responsible for cross-linking arabinoxylans to lignin. There are between nine and ten ferulic acid ester-ether bridges every 100 C6-C3 lignin monomers [14], [15].

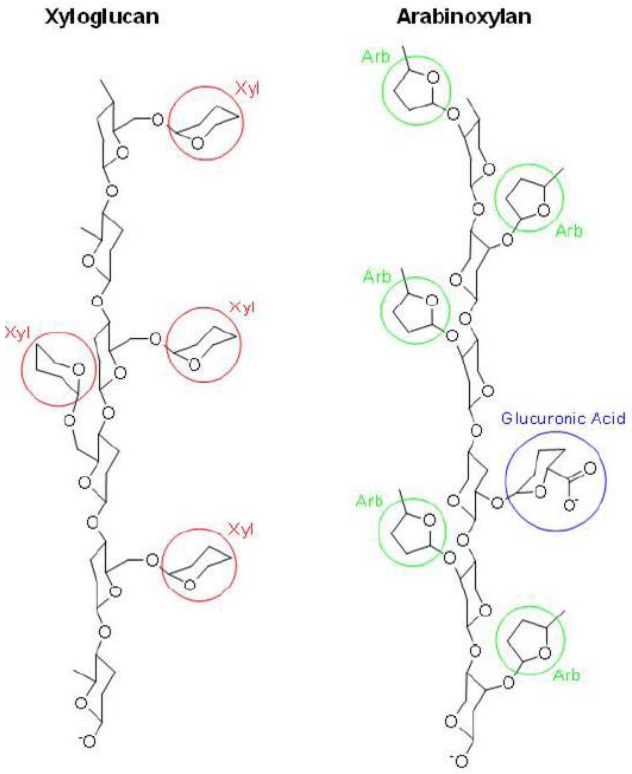

Figure 2-2 Graphical representations of the major hemicellulose structures in grasses, i.e., Xyloglucan (left) and Arabinoxylan (right). Xyloglucan is composed by a glucan backbone decorated by xylose residues (circled in red, Xyl). Arabinoxylan is composed by a xylan backbone decorated with arabinose residues (circled in green, Arb) and glucuronic acid residues (circled in blue).

In softwoods the major hemicelluloses are galactoglucomannan, glucomannan and arabinoxylan. From these types galactoglucomannan is the most important in softwoods and it is composed of a β-(1,4)-linked D-mannopyranose and D-glucopyranose backbone decorated with D-galactopyranose residues, which are linked as single-unit side chains by α-(1,6) bonds [14]. The

hydroxyl groups in the C2 and C3 positions of the backbone residues are partially substituted by O-acetyl groups. On an average, is possible find one O-acetyl group per 3-4 hexose units.

In hardwoods the main hemicellulose component is *O*-acetyl-4-*O*-methyilglucurono-β-D-xylan. As in softwoods and grasses, the backbone consists of β-(1,4)-D-xylan units, however in hardwoods most of the hydroxyl groups at the carbons C2 and/or C3 are substituted by acetyl groups. In addition, xylose units are substituted with α-(1-2)-linked 4-*O*-methylglucuronic acid residues, normally at every tenth xylose unit [16]. Unlike in softwoods and grasses, hardwood xylans do not contain arabinose in their side chains.

2.1.3. Pectins

Pectins are a complex and heterogeneous group of polysaccharides with different domains that are believed to be covalently linked together. The more important pectin domains include rhamnogalacturan I and II, galactans and arabinans (**Figure 2-3**). Rhamnogalacturan I is a polymer constituted by alternating residues of galacturonic acid and rhamnose, while rhamnogalacturan II is constituted by a complex structure of eleven different sugar residues, linked to a backbone chain of galacturonic acid molecules that is called homogalacturonan when no side chains are attached. On the other hand, when side branches of xylose are covalently bound to this chain, it is called xylogalacturonan.

Arabinans are branched polymers constituted by arabinose, that can be linked to a backbone of β-(1,4)-D-galactan creating a new structure called arabinogalactan. The neutral arabinans and arabinogalactans can be linked to the acidic pectins, promoting flexibility to the cell wall [10, 16].

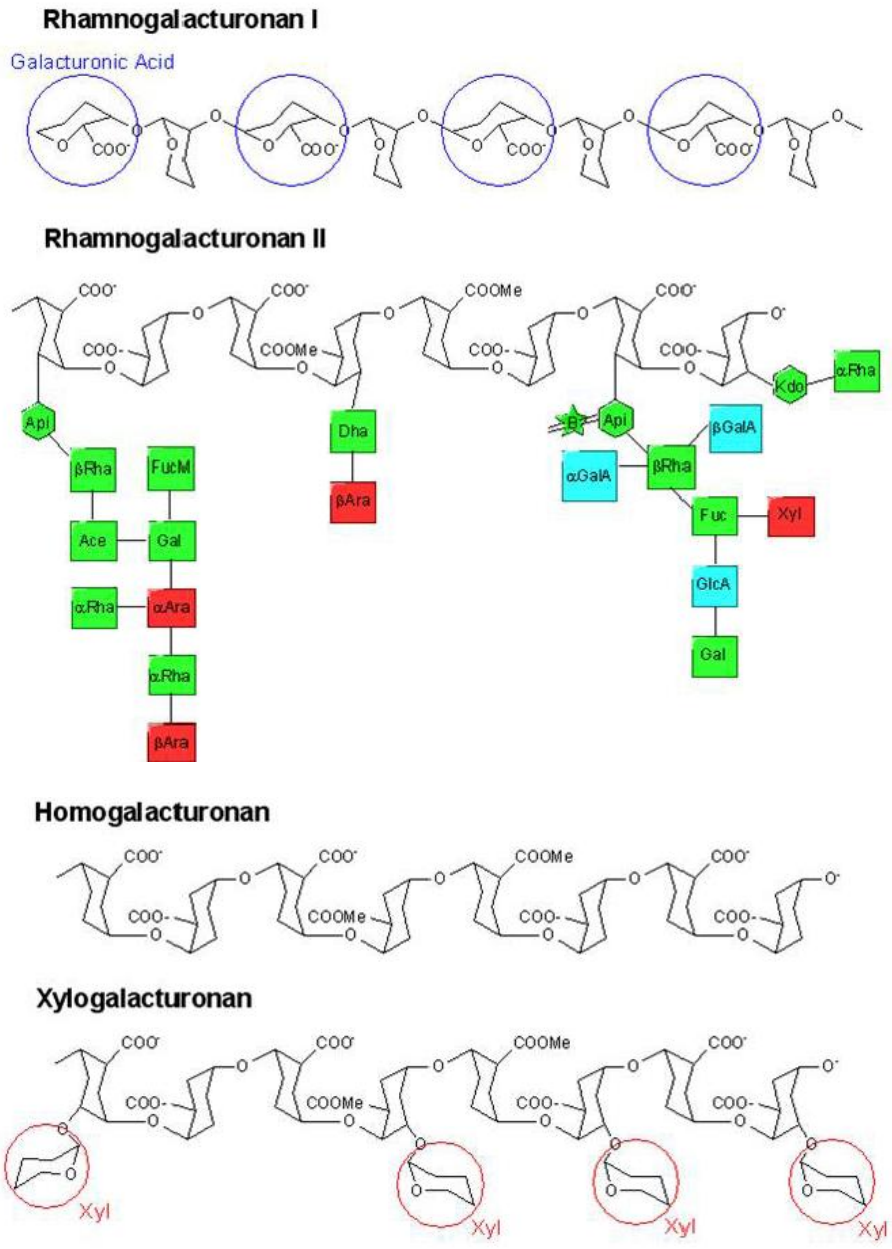

Figure 2-3 Representation of the major pectin domains present in plants.

2.1.4. Lignins

In angiosperms, the lignin polymer is produced by dehydrogenative polymerization of three different cinnamyl alcohols (p-coumaryl, coniferyl, and sinapyl alcohol) that differ in the degree of methoxylation at the C3 and C5 positions of the aromatic ring (**Figure 2-4**).

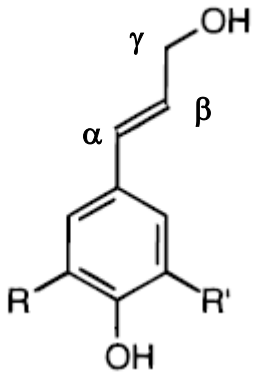

Figure 2-4 Representation of the general precursor of lignin biosynthesis in angiosperms. (p-coumaryl alcohol: R = R'=H ; coniferyl alcohol: R = H, R'= OCH3 ; and sinapyl alcohol: R = R' = OCH3).

When these alcohols are transformed in lignin polymers, are called p-hydroxyphenyl (H), guaiacyl (G) and syringyl (S) units of the polymer, respectively. In addition to these three main components, lignin polymers incorporate compounds that derive from incomplete biosynthesis of components H, G and S, as well as other phenylpropanoid units such as acetates, hydroxycinnamyl aldehydes and others [17].

A variety of chemical linkages, including ether and carbon-carbon bonds, connects the units of a complex network of different compounds. This polymer complexity and heterogeneity depends on the relative proportions of the three main monolignol units (H, G and S). Lignin from grasses incorporates G and S units at comparable levels and more H units than dicots. In the case of softwoods, lignin is essentially made of G units while in hardwoods is made of G and S units.

Lignin rich in G units has relatively more carbon-carbon bonds than lignin rich in S units. For this reason, grasses and softwoods are less susceptible to Kraft delignification than hardwoods. Kraft delignification is a process used by the paper industry during the pulping process, breaking down the non-condensed ether β-O-4-linkages in lignin using alkali agents (e.g. NaOH). The carbon-carbon bonds are more resistant to chemical degradation, so they are not affected during this process. In plants, lignification of the cell wall is an important defense mechanism to various pathogens, notably fungi and bacteria, and helps provide the required strength to plant tissues. Cell walls of the various plant organs and tissues contain different lignin contents as well as different ratios of the three monolignols referred above [18].

2.2. Lignocellulosic Biorefinery

As a result of the organization and interaction between these polymeric structures, the plant cell wall is naturally recalcitrant to biological degradation [19]. In the context of biological conversion of lignocellulosic biomass to ethanol (**Figure 2-5**), a pretreatment step before enzymatic hydrolysis is required to facilitate the access of the enzymes to its substrates, enhancing the rate of hydrolysis by 3–10-fold, depending on the type of pretreatment and nature of the substrate. Several economic models acknowledge that pretreatment is a major unit operation in a lignocellulosic biorefinery, accounting for 16–19% of its total capital investment [20] and being the second largest expense after the power plant generator [21]. For this reason it is important to mature existing technologies and develop new methodologies to decrease the economic impact of pretreatment on the overall biorefinery system. Enzymatic hydrolysis is another important unit operation, where the polymeric carbohydrates are simplified into fermentable sugars by a group of enzymes containing a gamut of activities that synergistically

hydrolyze cellulose and hemicelluloses [22]. In this process, achieving high sugar yields (>80%) at high solid loadings (> 20%) using enzyme additions below 10mg/g glucan is one of the major goals towards a commercially viable biorefinery. To achieve such goal, enzyme companies such as Novozymes (Bagsvaerd, Denmark) and DuPont (Wilmington, DE, USA) have been working on the development of cellulase and hemicellulase cocktails, with improved enzyme properties, notably improved specific activity and thermal stability. In parallel, the development of pretreatment technologies that perform critical structural modifications of the plant cell wall, including reduction of crystallinity of cellulose, modification of cellulose crystalline structure, cleavage of hemicellulose side chains and lignin-carbohydrate-complex (LCC) bonds, will also contribute to higher enzyme activity and further reduction of enzyme loading [23].

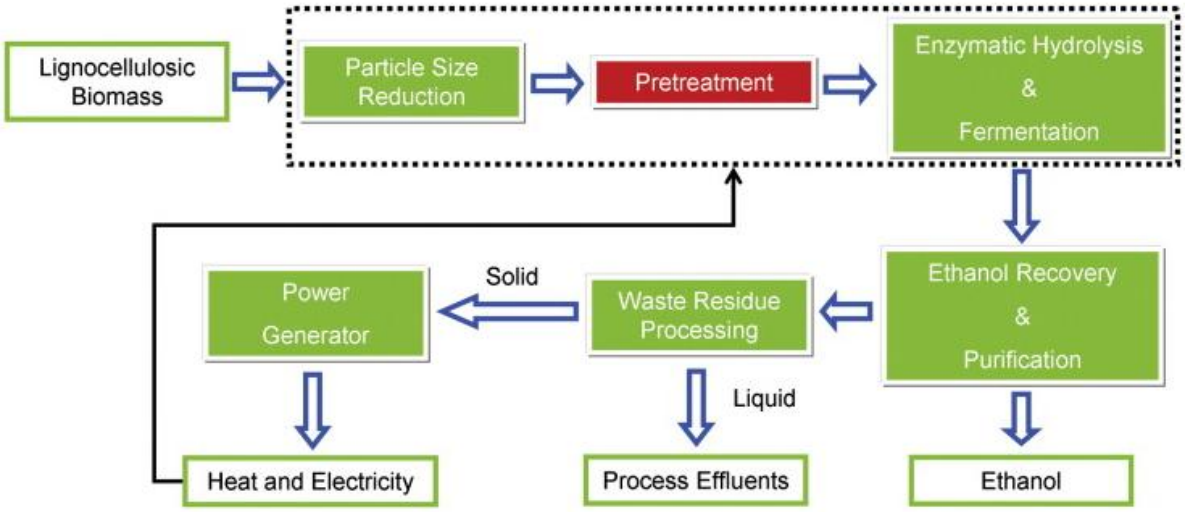

Figure 2-5 Process flow diagram representing the unit operations for biological conversion of lignocellulosic biomass into ethanol [1].

Enzymatic hydrolysis and fermentation can be performed in the biorefinery in two separate unit operations, typically denominated by *Separate Hydrolysis and Fermentation* (SHF). Alternatively, these two unit operations can be combined in one process denominated by

Simultaneous Saccharification and Fermentation (SSF). Finally, another processing possibility involves microorganisms than can produce and secrete cellulolytic enzymes, which are able to hydrolyze the pretreated biomass to fermentable sugars. These sugars are further converted to fuel molecules by the same organisms in a process denominated by *Consolidated Bioprocessing* (CBP).

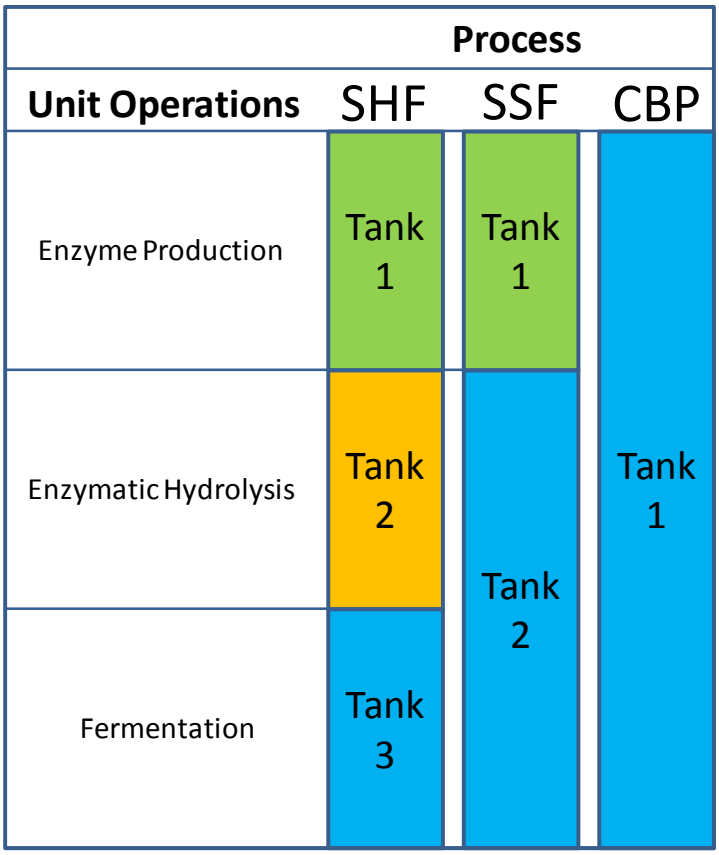

Figure 2-6 Description of the various biorefinery process configurations and the number of tanks required for each configuration.

These three different processes present advantages and disadvantages. In one hand, SHF allows the operation of enzymatic hydrolysis and fermentation at optimal conditions for enzymes and microbes. While enzymatic hydrolysis occurs typically at 50°C, efficient microbial fermentation occurs between 30°C and 40°C, depending on the organism. The optimal pH of both processes is

often slightly different, as fungal enzymes usually operate at pH between 4.5 and 5, while yeast fermentation is usually efficient at pH 5.5. One major drawback of SHF is that the accumulation of soluble sugars above certain concentrations inhibits cellulases and hemicellulases, thereby decreasing the hydrolysis rate and final product yields. The SSF process does not allow the concentration of sugars to accumulate during enzymatic hydrolysis since microorganisms simultaneously consume these sugars as they are produced. Also, the SSF process is performed in one single vessel, which has some economic impact due to capital investment reduction. However, SSF processes operate under non-optimal conditions for both enzymatic hydrolysis and fermentation, which usually need to be fine-tuned for maximizing ethanol yields. Also, the ethanol produced by microorganisms is inhibitory to enzymes and therefore, some of the advantages gained by eliminating the sugar inhibition may be lost by ethanol inhibition [24]. While SHF and SSF require external enzyme production and supplementation to the process, CBP processes eliminate the need for dedicated vessels to produce enzymes. However, CBP microorganisms are often susceptible to plant- and pretreatment-derived inhibitors that impact the rate and yields of fuel production [25]. Developing robust CBP organisms and eliminating possible plant-derived inhibitors from the fermentation media are two possible strategies that are being explored to enable this type of process in a future biorefinery [25].

In most biorefinery models, the biomass components that do not participate in fuel production via fermentation are subjected to waste treatment, of which results a solid stream that is used to feed the power plant generator where electricity and heat are produced for the biorefinery. However, one approach to possibly improve the economics of lignocellulosic biofuels is to provide value addition to this waste stream. An obvious component of this solid waste stream that has good potential for value addition is lignin. Lignin is the major renewable source of

phenolic compounds in nature and has multiple applications in the areas of biofuels, chemical precursors, polymers and resins [26-28]. Electricity and heat production is a rather low-end application for lignin and may not be the most economical solution for the biorefinery. The lignin can be isolated from the plant cell wall in the front of the biorefinery during the pretreatment process or downstream after fermentation and waste residue treatment (**Figure 2-5**). Lignin removal before enzymatic hydrolysis provides several process advantages, as the presence of lignin inhibits cellulolytic enzymes and microbes [29, 30]. Moreover, as lignin is not a substrate for enzymes and microbes, its presence occupies non-productive volume in the reactors, which represents an increase in capital investment.

One other form to reduce enzyme cost in the biorefinery is proposed by several authors and consists on the implementation of enzyme recycling techniques to partially recover the added enzymes for the following process cycle [31, 32]. This technique, associated with novel bioprocessing methods such as Fast-SSF or Fast-SHF (also known as RaBIT processes), can reduce enzyme loading up to 30% and presents improvements in biofuel productivity [4].

2.3. Importance of Pretreatment in the Lignocellulosic Biorefinery Context

In plants, the cell wall acts naturally as a physical protection against pathogens [33]. Some of these pathogens carry hydrolytic enzymes that target different plant cell wall components promoting the disruption of the fibers [33]. From the evolutionary perspective, the plant cell wall structure developed naturally to avoid pathogen penetration. Substrate-related factors affecting enzymatic digestibility are normally associated on a macroscale with cell wall porosity [34] and biomass particle size [35]. On a microscale, these factors are associated with cellulose crystallinity and degree of polymerization [36], hemicellulose side-chain branching [37], lignin

composition [18], and coumarate and ferulate crosslinking [18, 38] . For an efficient biological conversion of cellulose into fermentable sugars, it is important to modify the physical and chemical properties of the plant cell wall, which can be done through a pretreatment step. Different pretreatments have varying chemistries and ways of interacting with the plant cell wall components. Also, there is an extensive variety of lignocellulosic materials, ranging from grasses, softwoods, and hardwoods, which also have different physical and chemical properties. For this reason there is interdependence between pretreatment, the type of substrate, and the way it is eventually processed.

Moreover, it is evident that the choice of pretreatment will also impact the physicochemical properties of the pretreated biomass. These properties will also profoundly affect downstream processes such as enzyme and microbial selection, preconditioning, by-product utilization, waste residue handling, and ethanol recovery (**Figure 2-7**). Consequently, the choice of pretreatment will have an economic impact on each one of the biorefinery stages. These aspects make pretreatment the central unit operation in a biologically based sugar-platform for processing lignocellulosic biomass into fuels and chemicals.

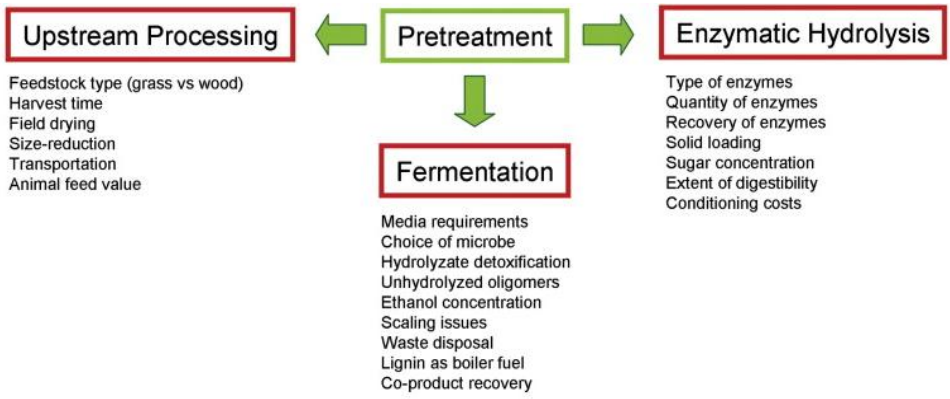

Figure 2-7 Pretreatment choice affects all biorefinery related operations. This fact gives pretreatment a central role affecting the design and economic viability of a lignocellulosic biorefinery [1].

2.4. Important Pretreatment Technologies Available Today

Several pretreatment technologies are available today, which can be classified, based on the nature of the cell wall disruption, into four categories: 1) physical; second; 2) fractionation; 3) chemical; and 4) biological pretreatment.

2.4.1. Physical Pretreatment

Physical pretreatments operate based on the principle of particle size reduction by mechanical stress. This can be obtained by dry, wet vibratory, and compression based ball milling procedures [39-41], increasing the enzyme performance by improving the surface area to volume ratio and in some cases by reducing degree of polymerization and crystallinity of cellulose [36]. Although physical pretreatments are not sufficient to dramatically increase sugar conversions, most other pretreatments require a minimal particle size reduction in order to be effective, especially to overcome mass and heat transport problems. It is also important to notice that beyond a certain particle size this type of pretreatment becomes economically unfeasible due to the extensive energy requirements associated with the milling process.

2.4.2. Solvent Fractionation

This category of pretreatment technologies applies the principle of differential solubilization and partitioning of various components of the plant cell wall, including cellulose, by the disruption of the hydrogen bonding between microfibrils [42]. Several fractionation methodologies are available today; however, the most attractive ones are the organosolv process, phosphoric acid fractionation, and ionic liquids based fractionation.

Organosolv process uses organic solvents, usually alcohols in the presence of an acidic catalyst to extract lignin from lignocellulosic biomass [43]. In this pretreatment, operating temperatures

range between 90 and 120°C for grasses and 155 and 220°C for woods, with a residence time ranging from 25 to 100 min. Depending on the substrate, catalyst concentration can vary from 0.83 to 1.67% and alcohol concentration from 25 up to 74% (v/v). Lignol Innovation Corporation, Vancouver, Canada, is investing in the organosolv process using ethanol as a preferred solvent. In their process, the insoluble cellulose fraction is used to produce fermentable sugars via enzymatic hydrolysis, while the liquid phase containing lignin, furfural, xylose, acetic acid, and lipophilic extracts is processed to recover these compounds [44]. Also, oligosaccharides are subjected to a mild acid hydrolysis to convert them into fermentable sugars to produce more ethanol. The solvent is recovered by distillation and reused while the lignin is used as an additive binder for other applications.

In phosphoric acid fractionation, a series of different solvent extractions using phosphoric acid, acetone, and water at temperatures around 50°C are used to fractionate the plant cell wall into amorphous cellulose, hemicellulose, lignin, and acetic acid. The fractionation is possible owing to the preferential solubility of various plant cell wall components in different solvents. Using this methodology, it is possible to decrystallize cellulose fibers, removing at the same time most of the hemicelluloses and lignin [45]. This pretreatment has several advantages, since it can operate at a low temperature and pressure (atmospheric pressure) giving at the same time high yields of glucose and xylose [46]. However, the challenges facing this method have to do with finding economical ways of recovering and purifying phosphoric acid (and other solvents) for recycle at the end of each pretreatment batch.

Only recently ionic liquids were first applied as a pretreatment technology to convert lignocellulosic biomass into fermentable sugars [47]. Ionic liquids have the capability to form hydrogen bonds with cellulose at high temperatures, because of the presence of anions like

chloride, formate, acetate, or alkyl phosphonate. This pretreatment uses ionic liquids in a ratio of 1:10 (biomass:ionic liquid, w/w) and temperatures ranging from 100 to 150°C. The soluble biomass is regenerated using antisolvents such as water, methanol and ethanol, and then subjected to enzymatic hydrolysis to produce fermentable sugars. One important factor is the fact that residual ionic liquids remaining in the biomass after regeneration could interfere with hydrolytic enzyme activities (and downstream fermentation steps), affecting the final sugar and biofuel yields [48]. After regeneration, ionic liquids may be recovered from antisolvents by flash distillation and reused in the process [49]. Ionic liquids have tremendous potential for pretreating lignocellulosic biomass, producing a substrate that can achieve more than 90% cellulose digestibility [50]; however, the cost of these chemicals must be significantly reduced or their recovery made highly efficient, in order to make this technology a serious candidate for an industrially based biorefinery process.

2.4.3. Chemical Pretreatment

Most of the leading pretreatment technologies are represented in this category, which comprises acidic, alkaline and oxidative based pretreatments. Optimal operational conditions for some leading chemical pretreatments to maximize enzymatic digestibility of corn stover are summarized in **Table 2-2**. In this category, most pretreatments differ in the types of chemistries and mechanisms that are responsible for cell wall ultrastructural and chemical modifications (**Table 2-3**) that result in improved enzyme accessibility and higher sugar yields.

2.4.3.1. Acidic pretreatments

Several acidic pretreatment technologies are available, such as concentrated and dilute acid, steam explosion, and liquid hot water pretreatment. Although the chemistry governing these

pretreatments is quite similar, they operate using different methodologies. While dilute acid uses an externally added acid catalyst, steam explosion, and liquid hot water pretreatments operate in acidic conditions due to the fact that water behaves like an acid at high temperatures and also due to liberation of acetic acid from hemicellulose under these conditions [51]. The acid is responsible for chemical hydrolysis, targeting mainly hemicelluloses and lignin, solubilizing a great part of these components from the plant cell wall structure and improving the enzyme accessibility to cellulose. However, during this process several degradation products are formed, mainly furfural, 5-hydroxymethylfurfural, phenolic acids and aldehydes, levulinic acid, and other aliphatic acids which can inhibit both enzymatic hydrolysis and fermentation [52, 53].

Dilute-acid pretreatments typically use sulfuric acid as a catalyst for hemicellulose and lignin solubilization at low acid concentrations (0.05–5%), and temperatures ranging from 160 to 220°C [54, 55], in order to minimize the formation of degradation products. Naturally, minimizing the sugar degradation contributes to higher sugar yields at the end of the process. However, this methodology requires extensive washing of the cellulose-rich slurry fraction after pretreatment and/or detoxification of the hydrolyzates before fermentation [53, 56]. One advantage of this pretreatment is that hemicellulose hydrolytic enzymes (e.g. xylanases) need not be added during enzymatic hydrolysis, which can be considered a definite cost saving feature. However, most microbes have been unable to ferment xylose from the pretreatment liquor without substantial detoxification [56].

Steam explosion has been one of the most widely implemented pretreatment technologies, being successfully applied to several types of lignocellulosic biomass (e.g. softwoods, hardwoods, and agricultural residues). This pretreatment has been demonstrated in several variants, with and without the presence of several chemical catalysts (e.g. sulfuric acid, sulfur dioxide, sodium

hydroxide, and ammonia) before steam explosion [57-61]. It operates at high temperature (160–290°C) and pressure for a certain duration of time (ranging from a few seconds to several minutes) before the pressure is explosively released [57-60].

Liquid hot water pretreatment uses water at high temperatures (160–230°C) and pressures (>5 MPa), in order to maintain water in the liquid state [51]. Several methodologies have been developed to promote an effective contact between the biomass and the liquid water, varying from co-current, counter-current, and flow-through [62]. Recent variants of this pretreatment allow better pH control between 4 and 7, minimizing the nonspecific degradation of polysaccharides [63].

In addition, several other mineral and organic acids (nitric, carbonic, succinic, fumaric, maleic, and citric acid) have been used successfully as pretreatment catalysts [64-66].

2.4.3.2.Alkaline pretreatments

This kind of pretreatment uses alkaline catalysts, such as calcium oxide (lime), ammonia, and sodium hydroxide. Most of these chemicals specifically target hemicellulose acetyl groups and lignin–carbohydrate ester linkages [75, 76]. These reactions help solubilize and extract lignin from the biomass, reducing nonspecific binding during enzymatic hydrolysis [71]. However, cell wall chemical and ultrastructural modifications still need to be understood for most alkaline pretreatments in order to develop proper enzyme mixtures that can effectively hydrolyze both cellulose and hemicellulose.

Table 2-2 Optimum operating conditions of some of the leading pretreatment technologies that maximize enzymatic digestibility of pretreated corn stover [67-70].

Pretreatment type	Temp. (°C)	Reaction time (min)	Chemical used	Chemical loading (g/g dry biomass)	Water loading (g/g dry biomass)	Specific notes
Dilute acid	160	20	Sulfuric acid	0.015	3	Batch process
Sulfur dioxide Steam Explosion	190	5	Sulfur dioxide	0.03	4	Soaked overnight in 3% acid solution before pretreatment
Controlled pH liquid hot water	190	15			5.25	Flow-through mode
AFEX	90	5	Ammonia	1	0.6	Liquid ammonia added to moist biomass before heating reactor
ARP	170	10	Ammonia	0.5	2.8	Flow-through mode using 5 ml/min of ammoniacal solution, 15% (w/w)
Lime	55	4 weeks	Calcium hydroxide	0.5	10	Purged with air

Table 2-3 Effect of leading thermochemical pretreatments on the physicochemical properties of corn stover and respective glucan and xylan conversion after enzymatic hydrolysis.

Pretreatment type	Cellulose CrI	% cellulose removed	% hemicellulose removed	% lignin removed	Cellulose DP	% acetyl groups removed	% glucan conversion	% xylan conversion
Dilute acid	53	5-10	70-75	18	2700	55	92	93
Sulfur dioxide steam explosion	ND	3-5	40	40-45	3000	55	87[a]	78[a]
Controlled pH liquid hot water	45	5-10	40	ND	5600	55	91	81
AFEX	36	0	0	0	6600	30-35	96	91
ARP	26	1-5	50-60	75-85	4600	85-90	90	88
Lime	56	1-3	30-35	55-60	3200	90-95	94	76

Enzymatic hydrolysis was conducted using 15 FPU/g glucan cellulase loading (Spezyme CP, Genencor). Glucan and xylan conversions were calculated relative to the initial composition of corn stover, including both monomeric and oligomeric sugars. The cellulose crystallinity index for untreated corn stover is 50 units and the degree of polymerization is 7000 [54, 63, 67, 69, 71-74]. ND: not determined; CrI: Crystallinity Index; DP: Degree of Polymerization.

[a]Enzymatic hydrolysis was performed using Celluclast 1.5 L at 65 FPU/g mixture and 17 beta-glucosidase IU/g mixture.

Ammonia fiber expansion (AFEX^{TM}) is a lower temperature process (60–140°C) where concentrated ammonia is used as a catalyst (0.3–2 kg ammonia per kg of dry weight biomass). Ammonia is added to prewetted biomass (0.6–2 kg moisture per kg of dry weight biomass) in a high-pressure reactor and is cooked for 5–45 min before the pressure is rapidly released. The volatility of ammonia allows it to be recovered and reused, leaving the dried biomass ready for enzymatic hydrolysis [77]. Because ammonolysis reactions do not produce major inhibitors (e.g. organic acids) for enzymes and microbes, it is possible to ferment and hydrolyze this substrate without any sort of detoxification [78, 79]. However, AFEX^{TM} treated biomass requires the utilization of hemicellulose hydrolytic enzymes in addition to cellulases to produce fermentable sugars. X-ray diffraction studies have also revealed that ammonia decrystallizes cellulose [80], facilitating enzyme activity on this substrate.

Other ammonia based methodologies (e.g. *Ammonia Recycle Percolation* (ARP), *Soaking in Aqueous Ammonia* (SAA), *Supercritical Ammonia* and *Ammonia-Hydrogen Peroxide* pretreatments[81, 82] are available, differing mostly in the thermodynamic state of ammonia–water mixtures, and ammonia concentrations. For example, ARP is carried out in a flow-through, recycle mode by percolating ammoniacal solutions (5–15% concentration) through a packed bed reactor with the biomass under pressure and high temperatures. During this process, hemicellulose and lignin are removed from the biomass in the liquid phase.

2.4.3.3.Oxidative pretreatments

Oxidizing agents can also be used to remove lignin and hemicellulose from biomass, in order to increase enzymatic digestibility of cellulose [83]. These agents can react selectively with lignin aromatics and alkyl/aryl ether linkages or also target hemicellulose and cellulose, which will

contribute negatively to the final sugar hydrolysis yields. Several kinds of degradation products may be formed (primarily aliphatic aldehydes and aliphatic organic acids) that have been found to inhibit enzymatic hydrolysis of cellulose.

Alkaline wet oxidation is a form of oxidative pretreatment which operates under alkaline conditions and high temperatures (170–220°C) using pressurized air/oxygen or hydrogen peroxide as oxidant [84, 85]. The alkali in this pretreatment is sodium carbonate, which helps solubilize hemicelluloses [84] and also minimizes the formation of furan based degradation products that could inhibit enzymes.

2.4.4. Biological pretreatment

Biological pretreatments, as opposed to chemical based pretreatments, are non-energy intensive processes [86], normally performed using fungi (e.g. white rot basidiomycetes) and certain actinomycetes. During pretreatment, these organisms secrete extracellular enzymes like lignin peroxidases and laccases that help remove a considerable amount of lignin from the biomass [87]. However, biological processes require longer residence time (several hours to few days) [88], which constitutes a serious limitation for its application in large-scale biorefinery related operations. Also, most microbes typically consume some part of the carbohydrates available in the biomass during growth, which will negatively impact the sugar yield at the end of the process. Important advantages of this pretreatment may be more evident when less recalcitrant genetically modified plant materials are available with higher carbohydrate content, requiring milder pretreatments.

2.5. Considerations for an ideal pretreatment technology

The evaluation of a pretreatment should comprise not only technological factors, but also economical and environmental criteria. Feedstock cost represents the highest variable cost in a biorefinery [20]. For this reason, sugar yield contributes in a large extent to the overall economical feasibility of the biorefinery. Also, sugar concentration is an important factor contributing to both economical and environmental aspects of the biorefinery (e.g. volume of reactors, size of product recovery operations, energy inputs, etc.). At the same time environmental impacts owing to land use management factors [89] and waste residue production would also affect the biorefinery economics. In the pretreatment point of view, energy requirements are associated with chemical and water utilization, temperature, pressure, mixing and chemical recovery during its operation. These parameters have economical and environmental impacts; however, it is important not to place boundaries around the pretreatment step only, because the pretreatment method will impact all other unit operations in a biorefinery [90] (**Figure 2-5**). For example, one some pretreatments require preconditioning of hydrolyzates because of inhibitory compounds produced during pretreatment [53], contributing to additional costs and solid-waste management concerns. The type of chemicals utilized is also a criterion to take into consideration. Besides the reactor volume, the construction material is also going to affect the total capital investment for pretreatment. A less corrosive chemical with low toxicity would contribute for reducing this cost as well as increasing safety and environmental benefits.

Lignin recovery is also an important criterion; because this component of the plant cell wall can be used as a precursor to manufacture valuable chemicals [44]. This area of research is rapidly evolving and could be considered a valuable option in the future, contributing to the economical feasibility of a biorefinery. Moreover, some pretreatments have the potential to produce dry

pretreated substrates, which could benefit distributed processing facilities because of lower transportation costs. Currently, biomass transportation and storage is considered a technical, economical, and environmental concern [91] and should be addressed before choosing a certain pretreatment technology for large-scale implementation. Some of these pretreatment technologies (e.g. AFEX^{TM}) also have the potential to process biomass for animal feed [92], increasing its digestibility and reducing the feedstock requirements for animal production [91]. This application can create conditions for sustainable land use management, both for bioenergy and feed production, promoting at the same time the desired environmental benefits of lignocellulosic biofuels.

2.6. Ammonia and Alkaline Pretreatment Chemistry

2.6.1. Reactions involving hydroxyl ions and lignocellulosic biomass.

2.6.1.1. Reactions with polysaccharides.

Initial reactions consist of the solvation of hydroxyl groups by hydroxyl ions, causing the biomass to swell. At higher temperatures, there are many chemical reactions that can occur. The most important ones are considered [93]: (i) Dissolution of un-degraded polysaccharides; (ii) Peeling of end-groups and the formation of alkali stable end-groups; (iii) Alkaline hydrolysis of glucosidic bonds and acetyl groups and (iv) Degradation and decomposition of dissolved polysaccharides and peeled monosaccharides.

Loss of polysaccharides and decrease in the degree of polymerization during alkali treatments are in large extent due to peeling and hydrolytic reactions. These are the most important reactions to monitor in order to preserve the integrity of the polysaccharides. At temperatures

around 100ºC, the degradation of polysaccharide chains starts from the existing reducing end groups, which is commonly called the primary peeling reaction. At temperatures around 150ºC, polysacharide chains start to be degraded by alkaline hydrolysis and the new reducing ends formed in this process will be also subject to endwise peeling reactions (also known as secondary peeling) [94].

Peeling reactions of polysaccharides involve the elimination of the reducing end groups, forming a number of different carboxylic acid compounds. Sjöström [94] proposed a mechanism for endwise peeling where monomeric sugars resulting from peeling reactions can be tautomerized to a dicarbonyl compound that can be rearranged to yield isosaccharinic acids. Other degradation products that can result from these reactions include lactic acid, 2-hydroxybutanoic acid and 2,5-dihydroxypentanoic acid. Some of these compounds can be found in AFEX^{TM} pretreated corn stover, however they exist in small amounts due to low reaction temperatures and residence times during AFEX^{TM} operation [95].

Hemicelluloses are in general much more vulnerable to these types of chemical reactions in alkali media than cellulose. Moreover, is also possible to see differences among the various kinds of hemicellulose components. For example, xylans are more stable and less vulnerable than glucomanans and arabinans. Interestingly, early cleavage of arabinose side-groups in softwood xylans has a stabilizing effect against alkaline peeling, since an alkali-stable metasaccharinic acid end group is formed after the loss of the arabinose side group [93].

The reactions that occur during endwise peeling terminate when competing reactions start to take place. These reactions are called stopping reactions and are very important in preventing the disruption of the polysaccharide fibers and their degradation [93]. They are initiated by a β-

hydroxy elimination at the C2 position, producing a tautomeric intermediate that is converted to an alkali stable metasaccharinic acid group or C2-methylglyceric acid [94].

Other small molecular weight acids are also formed in alkali conditions, including acetic acid and formic acid. Formic acid is a product of peeling reactions of polysaccharides while acetic acid is formed by cleavage of the acetyl side chain groups present in grasses and hardwoods xylans. Glucuronic acid side groups of xylan are also hydrolyzed during intensive alkaline pretreatment [93, 94]. All these compounds are found in AFEX^{TM} pretreated corn stover [23].Therefore, minimization of peeling reactions would be important to minimize sugar decomposition as well as formation of highly inhibitory organic acids to enzymes and microorganisms.

2.6.1.2. Reactions with Lignin

In any discussion about lignin degradation, the most important aspect is the varied behavior and stability of the possible bonds that exist in the lignin polymer. The most labile bonds in alkaline conditions are ester bonds and aryl-ether bonds, which are mostly cleaved during kraft pulping treatment. Also, aryl-alkyl or alkyl-alkyl bonds are typically destroyed in alkaline medium, but to a lesser extent than the aryl-ether bonds. Diaryl ether and C-C bonds are normally stable in these conditions, meaning they usually remain unaltered during alkali treatment.

In hardwoods and softwoods, the most common linkages are of the types α- and β-aryl ether, which means these are the most important linkages to cleave to promote lignin degradation. As α- and β-aryl ether linkages are relatively easy to cleave, their cleavage is independent of the hydroxyl ion concentration and is normally the main reaction that occurs in the initial phase of the alkaline pulping processes [93]. During alkaline treatment of biomass, a great variety of

compounds can be formed from lignin. Most are aromatic acids, aromatic aldehydes and phenolic compounds, which can have an inhibitory effect on enzymes and microorganisms.

Ester linkages are abundantly present in grasses (e.g. corn stover), participating in ferulate and di-ferulate cross-linking with hemicellulose and lignin [96]. These linkages are easily hydrolyzed by hydroxyl ions resulting in the formation of ferulic acid and di-ferulates. These components can be found in AFEX^{TM} pretreated corn stover [23, 95], as well as their amide counterparts, which result from competing reactions involving ammonia, i.e. ammonolysis reactions.

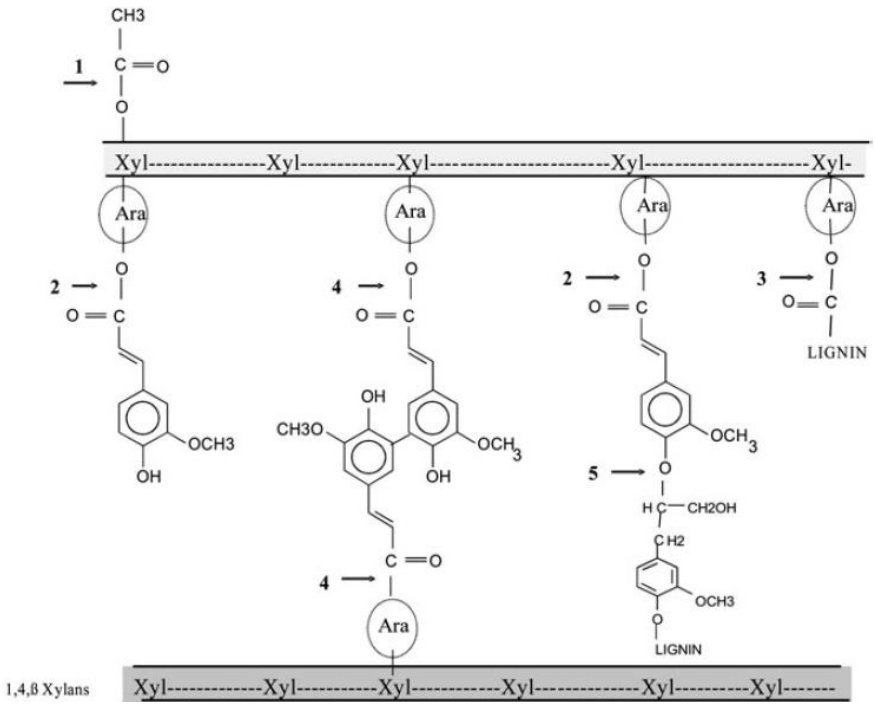

Figure 2-8 Simplified diagram of proposed ferulate and diferulate cross linkages with lignin and arabino-xylans. 1- Acetyl decoration in xylan backbone; 2- Ester linked ferulate to arabino-xylan; 3- Ester linked arabinose to lignin; 4- 5-5 ester linked ferulate dimer cross-linking arabino-xyalan chains; 5 –Ether-linked ferulate to lignin.

2.6.2. Reactions involving ammonia and lignocellulosic biomass

2.6.2.1. Ammonolysis Reactions

In the special case of AFEX™ pretreatment of lignocellulosic biomass, ammonia not only participates in the production of hydroxyl ions, which can drive a variety of reactions as mentioned above, but also acts as a reactant itself. Amidation of organic compounds via ammonolysis occurs during AFEX™ pretreatment, as was evident when considerable amounts of acetamide and phenolic amides were found in water extracts of AFEX™ treated corn stover [16, 95].

Ammonolysis reactions can occur in aqueous solutions or in the vapor-phase and target mainly ester linkages present in the plant cell wall. As mentioned above, this type of bonds are abundant in grasses and can be found in arabinoxylan acetyl groups, ferulate and di-ferulate cross-linking of lignin and hemicellulose as well as *p*-coumarate residues which occupy terminal sites in lignin polymers. Ammonolysis products of these interactions yield amides that can be found in AFEX™ pretreated corn stover [23, 95, 97]. The correlation between enzymatic hydrolysis yields and extent of cleavage of these ester bonds is evident from **Figure 2-9**, proving that these chemical interactions are important to maximize in order to have efficient enzymatic activity on AFEX™ substrates. Therefore, understanding ammonolysis and hydrolysis reactions of structural ester bonds in the plant cell wall is extremely relevant for improving ammonia-based pretreatments of lignocellulosic biomass.

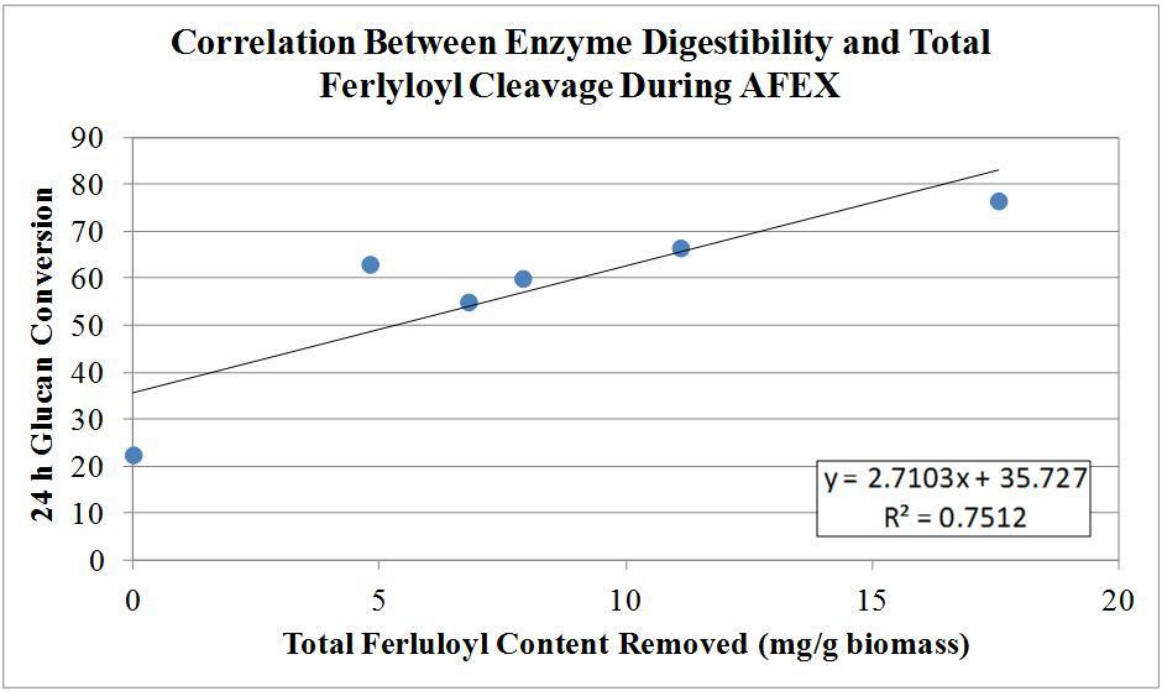

Figure 2-9 Correlation between enzymatic digestibility of AFEX^{TM} pretreated corn stover and total feruloyl cleavage (amide + acid) during AFEX^{TM} pretreatment [23].

H. E. French et al. [98] has studied the effect of aqueous ammonia solutions in a variety of esters containing different leaving groups with different molecular weights. It was found that the ratio of ammonolysis to hydrolysis decreases with increasing molecular weight of the alcohols associated with the different esters. Moreover, the reactivity decreases by increasing the molecular weight of the ester, especially in the case where the leaving group had side chains close to the ester bond (e.g. isopropyl acetate). The justification for this fact may relate to stereochemical factors during the chemical reaction and the accessibility of ammonium ions compared with hydroxyl ions to access the carbonyl group. Gordon Maxwell et al. [99] described the catalytic effect of some solvents during ammonolysis reactions, ranging from glycerol (higher catalytic activity) to butanol, methanol and dioxane (lower catalytic activity). According to the authors, these differences may relate to the polarization of the nitrogen-hydrogen bond,

increasing the reactivity of ammonia as a nucleophilic agent. Also, P.M Williamson et al.[100] and L.L. Fellinger et al.[101] described catalytic effects during ammonolysis reactions caused by electrolytes, such as sodium and ammonium salts. AFEX^{TM} pretreatment utilizes aqueous ammonia as a reactant medium, and therefore is possible to accelerate ammonolysis reactions by introduction of more advantageous solvent systems, coupled with the presence of inorganic salts. Understanding the effect of solvents and salts during pretreatment will help to better design ammonia-based pretreatment methodologies. Ammonolytic reactions target not only ester bonds, but also react with phenolic compounds, alkyl halogens and alcohols.

2.6.3. Maillard Reactions

Ammonia (or amino compounds) can react with polysaccharides generating the so-called Maillard reaction products. Maillard chemistry is typically composed by an extremely complex network of reactions. More than fifty reaction products have been identified after reacting ammonia with D-glucose, which belong to a variety of families of compounds such as pyrazines, imidazoles, ketones, aldehydes and amides [102]. Some of the Maillard products identified in AFEX^{TM} treated corn stover were listed by Chundawat et al. (2009) [23].

2.6.4. Rearrangement of cellulose crystalline state (Cellulose I_β to III_I)

Cellulose I_β is the predominant allomorph of cellulose present in plants. Thermochemical pretreatments are known to affect cellulose crystallinity at different levels by i) transforming cellulose I_β into amorphous cellulose, ii) increasing cellulose crystallinity I_β due to degradation of the amorphous regions of cellulose or by iii) converting it to different allomorphs. It has been

reported in the literature that a mild decrystallization of cellulose occured in conventional AFEX^{TM} [38], however there is no evidence of formation of other cellulose allomorphs.

Anhydrous ammonia is known to modify cellulose I_{β} crystal structure to cellulose III_I (**Figure 2-10**). This modification is defined as the rearrangement of intracrystalline hydrogen bonds and stacking interactions between glucose units. X-Ray and neutron diffraction have elucidated the formation of an intermediate complex (i.e. ammonia-cellulose I complex) before cellulose III_I conversion, where ammonia molecules trapped inside the cellulose crystal form hydrogen bonds with neighboring hydroxyl groups from cellulose [103, 104]. Cellulose III_I is formed once ammonia is removed from the intermediate complex, allowing a rewiring of hydrogen bond network and adjustments on the packing of cellulose glucan chains. Our recent work has demonstrated that this crystalline allomorph of cellulose enhances depolymerization rate by 2 to 2.5 folds, improving synergistic effects between endocellulases and exocellulases, especially when endocellulases of GH family 5 and 7 are involved [105] (**Figure 2-10**).

From the different pretreatment technologies available today, ionic liquid pretreatment and phosphoric acid pretreatment produce cellulose II [106] and amorphous cellulose [107] respectively. Both pretreatments show the highest improvements in enzymatic digestibility among the pretreatment technologies available in the literature. However, high cost of the chemicals used in these methods and catalyst recovery bottlenecks are still major problems to solve before they can be economically viable.

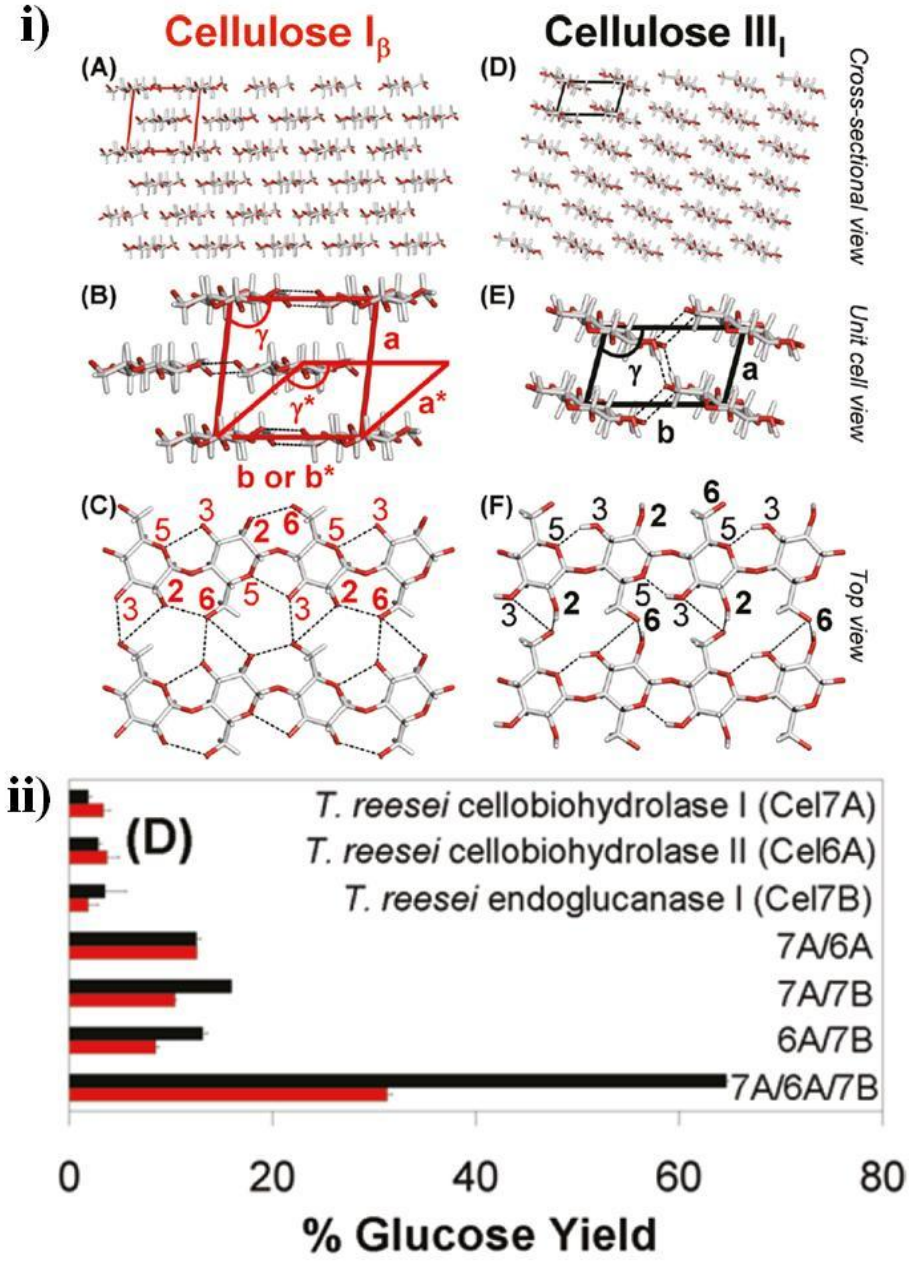

Figure 2-10 i) Representation of cellulose Iβ and III_I crystal structure, including hydrogen bonding network and glucan chain organization. ii) Synergistic effect of endocellulases and exocellulases in cellulose I_β (red) and IIII (black) hydrolysis [105].

From our recent work, we concluded that by forming cellulose III_I, using liquid anhydrous ammonia, enzymatic hydrolysis yields improve above cellulose II result for commercial enzyme

mixtures (Spezyme CP and Novozyme 188 by Genencor and Novozymes, respectively). However, amorphous cellulose is still the most digestible form of cellulose available (**Figure 2-11**).

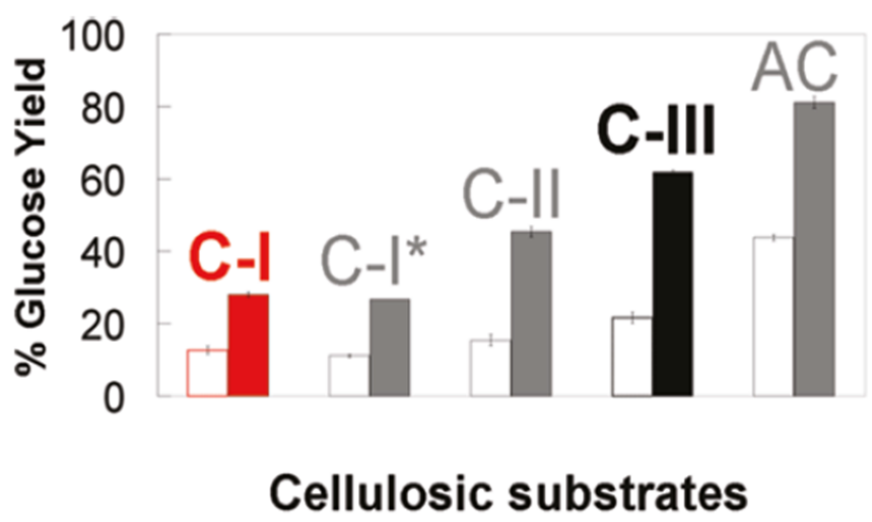

Figure 2-11 Glucose yields after enzymatic hydrolysis of the different cellulose substrates. Enzymatic hydrolysis was performed using 1.5 FPU Spezyme CP cellulase/g glucan and 6.4 p-NPGU Novo188 β-glucosidase /g glucan. Left and right bars represent 6 h and 24h enzymatic hydrolysis data [105].

From this set of results, it is clear that cellulose crystallinity is the ultimate barrier for efficient biomass degradation to fermentable sugars. Therefore, is important to define strategies to modify AFEX^{TM} pretreatment to produce cellulose III_I in an efficient, economic viable fashion.

2.7. Major downstream processing bottlenecks in the biorefinery

2.7.1.“Solids effect” and enzyme loading

“Solids effect” is defined as the decrease in sugar yields caused by increasing the initial solids loading of enzymatic hydrolysis. This phenomenon is one of the most important bottlenecks to solve in the biorefinery, since one important goal is to produce high concentrations of

fermentable sugars so they can be fermented to high concentrations of product (e.g. ethanol). This will decrease the level of water handling in the biorefinery and decrease the size and energy spent in downstream unit operations (e.g. fermentors and distillation column size).

Most, if not all, leading pretreatment technologies are not able to solve the "solids effect" problem [3]. Several authors have been studying possible reasons for this phenomenon, of which the reduction of water activity by the presence of solids gained particular attention [2]. In **Figure 2-12 ii)** is possible to observe that higher T_2 relaxation times (a measure of water activity) are associated with improvement of glucose yields after 24h of enzymatic hydrolysis. Water activity decreases with increasing solid loading (**Figure 2-12 iii)**) and, as a consequence, diffusivity coefficients for proteins and for sugars released during enzymatic hydrolysis are negatively affected, thereby decreasing sugar yields at higher solid loading [2].

Kristensen, J.B. et al [3] suggested decrease in cellulase binding at high solid loadings as one of the factors that contribute for the "solids effect". In fact, is possible to observe a linear correlation between enzyme binding and enzymatic conversion with respect to initial solids loading (**Figure 2-13 i)**). From our previous work, we found that enzyme binding is not so important to convert cellulose III into monomeric glucose (**Figure 2-13 ii)**), since is possible to improve enzymatic digestibility by 2-2.5 folds with lower enzyme bound to cellulose. This finding, coupled with the fact that the surface of cellulose III is more hydrophilic than cellulose I, brings us to the hypothesis that is possible to minimize the effect of solids by converting cellulose I_β to cellulose III_I.

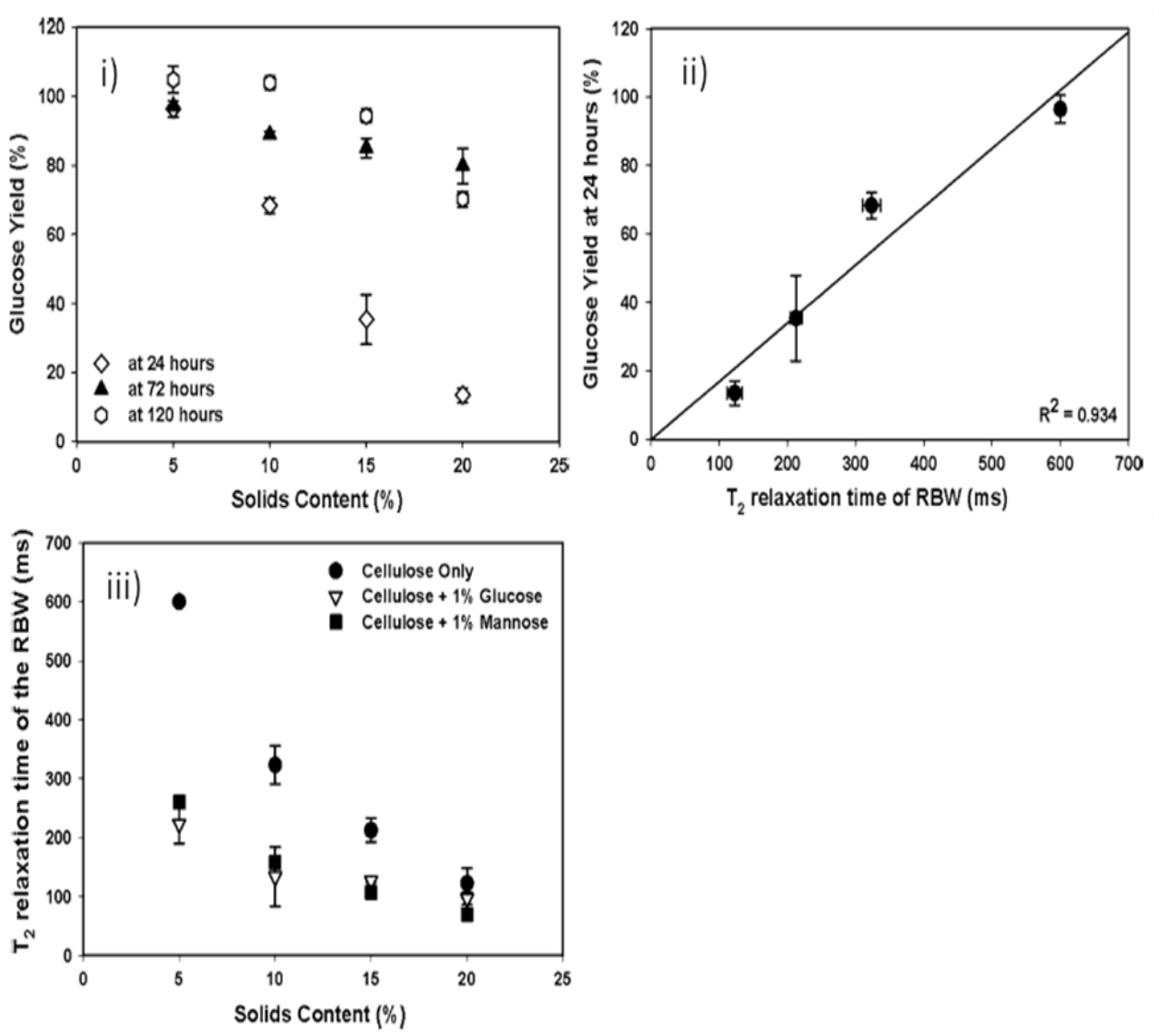

Figure 2-12 i) Solids effect observed for different time points of enzymatic hydrolysis. ii) Effect of T2 relaxation time of restricted bulk water (RBW) on enzymatic digestibility after 24h. iii) Effect of solids content on T2 relaxation time of RBW [2].

For conventional AFEX^{TM} pretreatment, typical enzyme loadings to convert 80% of the cellulose into monomeric glucose from corn stover range 20-30 mg enzyme/g glucan, at high solids loading. Optimal enzyme loading has been decreasing as novel commercial enzyme cocktails have been evolving to efficiently convert cellulose into monomeric glucose. However,

to be competitive in the biofuels area is important to look at the level of enzyme loading required to degrade starch into glucose in the corn grain ethanol industry. Currently, is possible to efficiently hydrolyze starch using ~2 mg enzyme/g glucan in an industrial setup. Our previous results show that by converting cellulose I to III, enzymatic hydrolysis rates can increase 2 to 2.5 fold [105]. If this holds true for higher solids loading and if cellulose III reduces the effect of solids during enzymatic hydrolysis, it may be possible to decrease enzyme loading to the single digit region while hypothetically maintaining enzymatic hydrolysis yields around 80%.

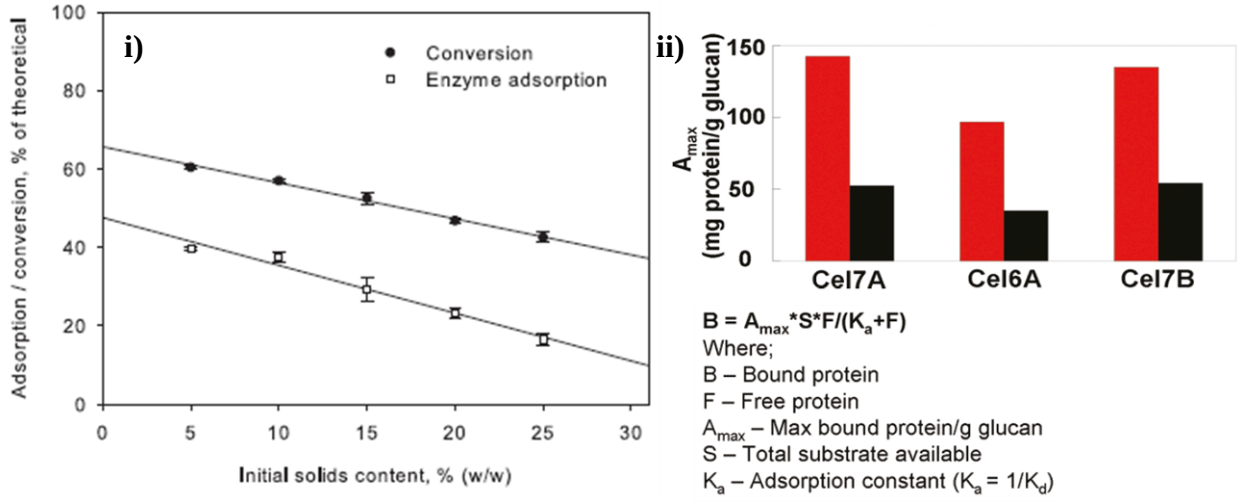

Figure 2-13 i) Relationship between enzyme adsorption and initial solids content [3]. ii) Maximum cellulase adsorption on cellulose I (red) and cellulose III (black) for three different kinds of cellulases [105].

2.7.2.Enzyme and microbial inhibition

Even though AFEX^{TM} pretreatment is known to produce highly digestible substrates and fermentable hydrolyzates without detoxification procedures, it does produce decomposition products that inhibit enzymes and microbes to certain extent [108].

Jin, M. et al. [109] has identified the sources of inhibition from AFEX^{TM} corn stover hydrolyzate and quantified the contribution of each one of them to the final decrease in fermentation performance of *S.cerevisiae* 424A (LNH-ST) (**Figure 2-14**). From this work, is possible to observe that AFEX^{TM} decomposition products reduce cell growth by 22% and specific xylose consumption rate by 13%. Therefore, is important to identify major components that contribute to this inhibition and study mechanisms to control the production of major components during pretreatment.

Inhibition factors tend to be even more critical for the case of CBP, where a single organism is able to produce enzymes, digest lignocellulosic biomass and produce ethanol simultaneously. Recent work has demonstrated that AFEX^{TM} corn stover inhibits the enzymatic hydrolysis performance during CBP when compared with pure cellulose (Avicel) [110].

For the reasons mentioned above, it is clear that the presence of lignin and other AFEX^{TM} decomposition products are negatively affecting major downstream processing operations, especially in the case of CBP fermentation. CBP methodology is considered to be a long term solution for the lignocellulosic biofuels industry; however, pretreatment methodologies as well as microorganisms must be perfected before this technology becomes economically viable.

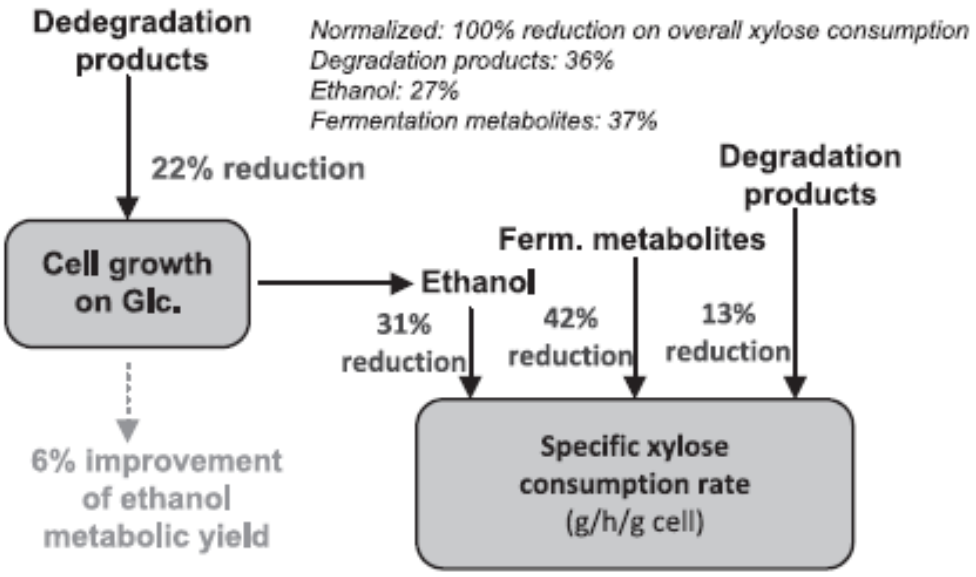

Figure 2-14 Contribution of AFEX^{TM} decomposition products, ethanol and fermentation metabolites on xylose consumption rate and cell growth of S.cerevisiae 424A(LNH-ST) [109].

Lignin has also been known to act as a natural inhibitor to both microbes and enzymes. The recalcitrant nature of the lignin molecule has been largely explained by effects such as its role on increasing non-productive binding of cellulases, restriction of enzyme accessibility to the carbohydrates and inhibitory effects caused by the water soluble lignin-derived compounds [111-113]. Also, authors have demonstrated that the inhibitory role of lignin is largely dependent on the nature of the molecules that compose the lignin polymer. For example, phenolic hydrolyxyl groups were found to be critical to the inhibitory effect of lignin to cellulolytic enzymes by Pan et al. (2008) [30]. Therefore, reducing the effect of lignin inhibition, ideally through an extraction process during pretreatment, would possibly improve downstream operations during biofuel production and would also create a new source of revenue to the biorefinery due to the high market potential of lignin.

CHAPTER 3 - FACTORS THAT CONTRIBUTE TO CELLULOSE III CONVERSION AND ASSOCIATED IMPACT ON ENZYMATIC DIGESTIBILITY OF CELLULOSE.

3.1. Abstract

The crystalline nature of cellulose is considered a natural barrier to enzymatic action, preventing efficient decomposition of cellulose to simple sugars during microbial attack. The crystalline allomorph of plant-derived cellulose, i.e., cellulose I_β (CI), can be altered by ammonia treatment to form a more amenable substrate to enzymatic degradation, designated by cellulose III (CIII). In this work, we studied several aspects of CIII conversion, including the effect of ammonia-to-cellulose ratio, ammonia concentration in organic solvent, incubation time and incubation temperature on the formation of CIII. To evaluate the crystal allomorph composition of ammonia-treated samples, XRD spectra were processed based on a new strategy that combines amorphous subtraction and peak deconvolution methods. Kinetic data show that the amorphous content of cellulose increases substantially for the first few seconds of ammonia incubation. After this early event, a slow reduction of the amorphous content is observed, being replaced by the formation of CIII for extended incubation times. These observations suggest that incomplete disruption of hydrogen bonding during formation of the ammonia-cellulose complex, promote a disordered assembly of the cellulose chains upon evaporation of ammonia. Elevated temperatures accelerate ammonia penetration into the cellulose fibers and formation of the ammonia-cellulose intermediate, generating cellulose samples of higher CIII crystallinity after 30 min of incubation time. As CIII crystallinity increases, we also observed improvement of enzymatic hydrolysis rates up to 2 folds compared to native CI. This observation contradicts the

current paradigm that supports the idea that lower cellulose crystallinity benefits enzymatic degradation of cellulose. Furthermore, the utilization of co-solvents, such as ethanol, along with ammonia seems to be compatible with CIII conversion, as no reversion to CI was observed when the ammonia-cellulose intermediate is formed. From our results, cellulose treated with 60 wt% at 25 °C for 30 min incubation time, allow approximately two folds increase in enzymatic hydrolysis rates as compared to CI. This solvent compatibility enables the reduction of operating pressure at higher pretreatment temperatures, which can be economically advantageous in the context of a lignocellulosic biorefinery.

3.2. Introduction

One of the major bottlenecks associated with biological conversion of lignocellulosic biomass to fuels and chemicals, derives from the structural organization of cellulose in tightly packed microfibrils, sustained by a complex network of hydrogen bonds [114-116]. This naturally occurring crystalline arrangement of cellulose, denominated by cellulose I_β (CI), is highly recalcitrant to cellulases, representing the final barrier for sugar conversion [114]. Amorphous cellulose (AC) and other non-native forms of crystalline cellulose are known to be more vulnerable to cellulase activity, generating substantial improvements to the rate of enzymatic hydrolysis [105]. For example, Chundawat et al. (2011) converted CI derived from Avicel PH-101 into cellulose III (CIII) using anhydrous ammonia, thereby improving enzymatic hydrolysis rates by two folds compared to the original CI [105]. Previously, Igarashi et al. (2007) [117] had already observed that cellulose III promoted about five fold higher enzymatic hydrolysis rate using Cel7A enzyme on algal-derived cellulose. The reasons for such improvement are far from being totally understood, however several pieces of work have unveiled interesting phenomena

that contradicted some of the paradigms established for enzymatic hydrolysis of CI. For example, Gao et al. (2013) [118] observed recently that cellulases tend to bind less effectively to CIII than to CI, even though their specific activity is higher on CIII. Computational simulations suggested that this enhancement is derived from favorable free energies during decrystallization of individual cellulose chains, as well as intrinsic kinetic factors related to processivity of bound enzymes to the CIII substrate.

Several authors have studied the factors that impact cellulose III conversion [119]. Liquid anhydrous ammonia and primary amines have been successfully used as swelling agents of cellulose, as they intercalate onto the crystalline structure of cellulose by hydrogen bonding [80, 120-122]. CIII is formed from these cellulose complexes of larger crystallite size upon removal of the mentioned swelling agents [80, 120]. Ammonia has been the most commonly used swelling agent for CIII conversion in the literature. Ammonia treatment has been performed at various conditions that include its usage in supercritical state or liquid state at ambient pressures [80, 117]. Other authors cycle temperature from -33 °C to 25 °C or higher prior to ammonia evaporation [123]. However, all processing conditions referred by those authors are energy intensive and do not benefit the implementation of CIII conversion in a lignocellulosic biorefinery context. Ideally, the most favorable conditions would be performed at constant and close to ambient temperatures, thereby reducing energy cost and capital cost due to milder operating pressures.

The effect of temperature during ammonia evaporation has been considered a major factor impacting conversion of CI to CIII [80]. Higher temperatures can improve significantly crystallinity indices (CrI) of the treated cellulose samples, while ammonia treatment time has been reported to reduce CrI [80] as well as the CI content of cellulose. To our knowledge, a

systematic understanding of how temperature, time and ammonia loading impact CIII conversion is not yet been reported in the literature. Also, the impact of crystalline CIII composition on enzymatic hydrolysis yields is a question that remains to be answered in a systematic manner. Therefore, the work presented herein attempts to create analytic methodologies to measure relative ratios of CI, CIII and AC in samples treated under various processing regimes, thereby allowing understanding of the effect of cellulose allomorph composition on enzymatic hydrolysis efficiency. Moreover, the effect of ammonia treatment variables (i.e., temperature, time, ammonia loading and concentration in the presence of co-solvents) on cellulose allomorph composition will be evaluated in detail in this work.

3.3. Experimental

3.3.1. Reaction apparatus

A reaction apparatus was designed and assembled to convert cellulose I_β (CI) to cellulose III_I (CIII) under controlled conditions. As shown in **Figure 3-1**, the apparatus consisted of two major sections that include ammonia delivery (1-6) and reaction equipment (7-12). As it was important to accurately deliver the appropriate amounts of ammonia at set-point temperature, an ammonia preheating vessel (1 – Parr Instrument Company, Moline, IL, USA) equipped with temperature controller (2) was installed on the top of a balance (5 – A&D, Inc., San Jose, CA, USA). This balance was used to measure the displaced weight of ammonia from the preheating vessel to the reactor by a jacketed syringe pump (4 – Teledyne Isco Model 500D, Lincoln, NK, USA). To avoid heat losses during ammonia delivery, the syringe pump jacket was temperature controlled by a circulating water bath (3 – VWR, Radnor, PA, USA). Ammonia was delivered to the

reaction vessel (7 – HEL, Inc., Hertfordshire, UK) at constant pressure with the help of a backpressure regulator (6 – Parker, Cleveland, OH, USA). An online temperature PID controller (8 – Julabo, Seelbach, Germany) was installed to maintain the desired temperature during reaction time. Reaction pressure was controlled by HEL, Inc. software (12) actuating two solenoid valves (9 and 10) for nitrogen inlet and outlet, respectively. Reaction temperature and mixing controls were also activated via computer software designed by HEL, Inc. (12). Cellulose suspensions were sampled through a valve connected to a deep tube (11) that was installed in top of the reaction vessel.

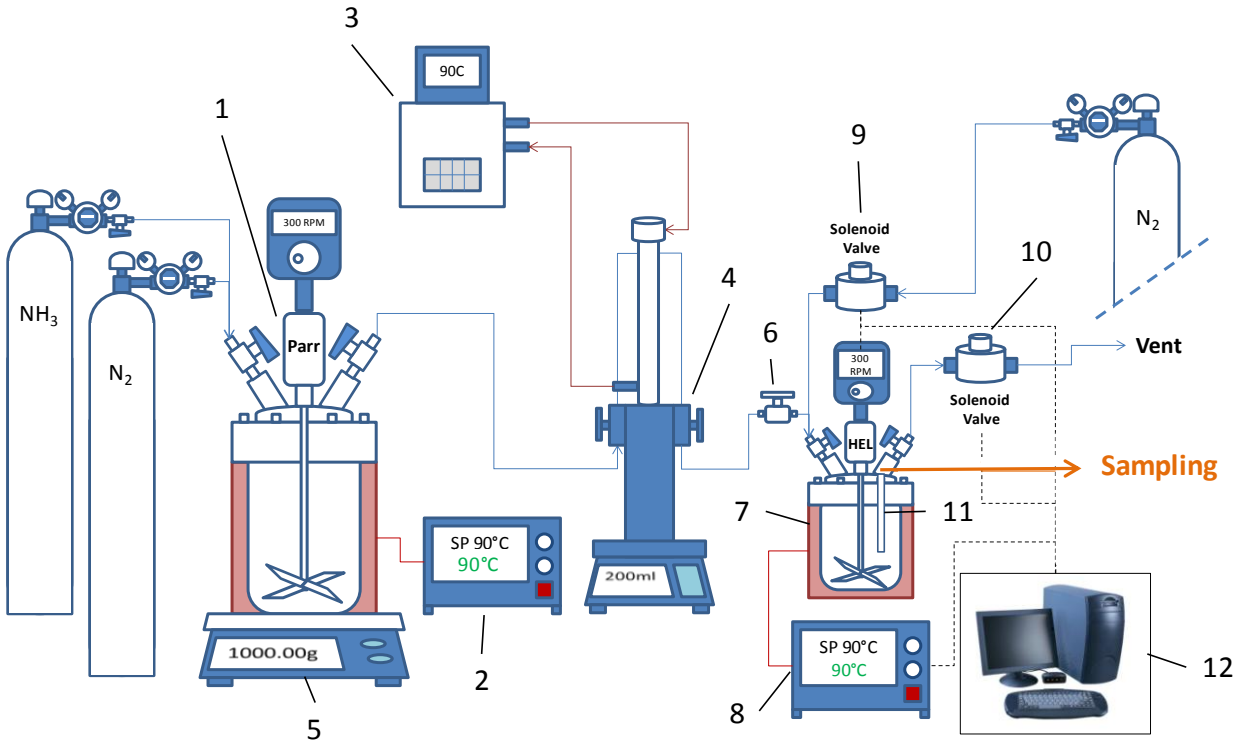

Figure 3-1 Instrumental apparatus for conversion of CI to CIII: 1) High-pressure mixing vessel and mantle used to preheat ammonia to set-point temperature; 2) Temperature controller for ammonia preheating vessel; 3) Water circulator used to heat the syringe pump to reaction set-point temperature; 4) Syringe pump to pump the desired volume of ammonia; 5) Balance to confirm the delivery of the desired ammonia loading; 6) Backpressure regulator; 7) High-pressure mixed reaction vessel and mantle for cellulose III conversion; 8) Temperature controller

Figure 3-1 (cont'd)

for reaction vessel; 9) Solenoid valve for pressure control (nitrogen inlet); 10) Solenoid valve for pressure control (nitrogen outlet), also used for venting the system; 11) Deep tube sampling port; 12) computer controls and data logging.

3.3.2. Cellulose III conversion studies

3.3.2.1. Impact of sampling solvent on the conversion of ammonia-cellulose complex to CIII

The ammonia-cellulose complex was formed in a high pressure reaction vessel (**Figure 3-1**, 7) by contacting anhydrous ammonia with Avicel PH-101 (Sigma-Aldrich, St.Louis, MO, USA) using 6:1 ammonia-to-celullose ratio, at 90 °C for 20 min residence time. The reaction occurred under 1000 psi of nitrogen overpressure to assure all the loaded ammonia was in the liquid phase. Suspensions of ammonia-cellulose complex in liquid ammonia were sampled into vessels containing excess of various solvents at 25 °C. These vessels were kept in a temperature controlled water bath to reduce temperature drop during ammonia evaporation. The solvents used in this study were acetone, methanol, ethanol and water, in a proportion of approximately 30:1 (v/v) solvent-to-sample. Ammonia pressure was released from the top of the sampling vessel and the resulting cellulose fibers were filtered using a Millipore (Billerica, MA, USA) vacuum-filtration system equipped with a glass microfiber filter (Whatman GF/A, Kent, UK). The treated cellulose samples were further washed with the respective solvents and dried overnight in the hood to evaporate residual solvent. Samples were stored in zip sealed plastic bags at 4°C prior to usage. XRD was performed in these treated samples within the first 48 hours after reaction completion.

3.3.2.2. Effect of ammonia loading on CIII conversion

The ammonia-cellulose complex was formed using various loadings of anhydrous ammonia, notably 1:1, 2:1, 3:1 and 6:1 ammonia-to-cellulose ratio, at 90 °C for 10 min residence time. The microcrystalline cellulose used in this study was Avicel PH-101 (Sigma-Aldrich, St. Louis, MO, USA). The ammonia-cellulose complex activation occurred under 1000 psi of nitrogen overpressure to assure all the loaded ammonia was in the liquid phase. A suspension of that intermediate complex was transferred to 100 % ethanol in a ratio of approximately 30:1 solvent-to-sample, which was maintained at 25 °C in a temperature controlled water bath. Ammonia pressure was released from the top of the sampling vessel and the resulting cellulose fibers were filtered using a Millipore (Billerica, MA, USA) vacuum-filtration system equipped with a glass microfiber filter (Whatman GF/A, Kent, UK). The treated cellulose samples were further washed with absolute ethanol and dried overnight in the hood to evaporate residual solvent. Samples were stored in zip sealed plastic bags at 4 °C prior to usage. XRD was performed in these treated samples within the first 48 hours after reaction completion.

3.3.2.3. Effect of temperature on cellulose III conversion

In these experiments, ammonia was added to a reaction vessel (**Figure 3-1**, 7) containing Avicel PH-101 at set point temperature, using a syringe pump (Teledyne Isco Model 500D, Lincoln, NK, USA). Ammonia-cellulose complexes were formed solely with anhydrous ammonia, using 6:1 ammonia-to-cellulose ratio, at various temperatures (ranging from -30 °C to 90 °C). All incubations were performed for 30 min residence time and 1000 psi of nitrogen overpressure to assure that all added ammonia was in liquid state and in contact with cellulose. In this study, it was important to differentiate between the effects of temperature during ammonia-cellulose

complex formation and temperature of CIII conversion during ammonia evaporation. For this purpose, ammonia-cellulose complexes formed at the various temperatures were sampled to a vessel containing excess of 100 % ethanol at a constant temperature of 25 °C. The cellulose suspensions in ethanol, obtained after ammonia evaporation from the sampling vessel, were further filtered using a Millipore (Billerica, MA, USA) vacuum-filtration system equipped with a glass microfiber filter (Whatman GF/A, Kent, UK). Residual ammonia was further removed by flowing 100 % ethanol through the sample while applying vacuum to the filtration system. Ammonia-treated cellulose samples were further dried in the hood overnight to evaporate residual ethanol. Samples were stored in zip sealed plastic bags at 4 °C prior to usage. XRD was performed in these treated samples within the first 48 hours after reaction completion.

3.3.2.4. Effect of ethanol:ammonia solvent system on CIII conversion

Avicel PH-101 was placed in the high pressure reactor (**Figure 3-1**, 7) in the presence of calculated amounts of 100 % ethanol. Appropriate volumes of ammonia were loaded in the reactor with a syringe pump at 25 °C. Several concentrations of ammonia in ethanol were tested, ranging from 17 wt% to 60 wt% ammonia. Liquid-to-solid ratios were also varied for a fixed ammonia concentration, ranging from 4:1 to 10:1 (w/w). Avicel PH-101 was incubated in these ammonia solutions at 25 °C for 30 min residence time before being transferred through a sampling valve to a vessel containing absolute ethanol at 25 °C. Ammonia was further evaporated from the sampling vessel and the cellulose suspension was transferred to a vacuum filtration system (EMD Millipore, Billerica, MA, USA), equipped with glass microfiber filters (Whatman GF/A, Kent, UK). The treated cellulose was extensively washed with 100 % ethanol to remove residual ammonia. Treated cellulose samples were air dried overnight in the hood to

evaporate residual ethanol prior to storage in zip sealed plastic bags at 4 °C. XRD was performed in these treated samples within the first 48 hours after reaction completion.

3.3.3. Preparation of cellulose standards

High purity (>95 %) microcrystalline CI, purchased from Sigma-Aldrich (Avicel PH-101), served as CI standard in this study. The CIII standard was produced from Avicel PH-101 using liquid anhydrous ammonia, prepared in a high-pressure stirred batch reactor (**Figure 3-1**) at 90 °C for 30 min residence time, using 6:1 ammonia-to-cellulose ratio. The reactor pressure was maintained constant at 1000 psi with nitrogen. After reaction completion, ammonia was slowly evaporated from the reactor through a venting valve (**Figure 3-1**, 10). During this process, the temperature of the reactor slowly decreased due to heat of vaporization of ammonia and was stabilized at 25 °C with a heating controller. After reaching atmospheric pressure, the cellulose sample was removed from the reactor, transferred to a flat container and placed overnight in the hood to evaporate residual ammonia. No visual differences in color were observed after ammonia treatment of cellulose at these conditions. The CIII standard was stored at 4 °C in a zip sealed bag prior to usage. The amorphous cellulose (AC) standard was produced using phosphoric acid treatment as described in the literature [124]. Phosphoric acid swollen cellulose (PASC) was freeze dried and stored at 4 °C in zip sealed bags prior to further usage.

3.3.4. X-ray powder diffraction (XRD)

XRD was performed on an X-ray powder diffractometer with beam parallelized by a Gobel mirror (D8 Advance with Lynxeye detector; Bruker, Bruker AXS Inc., Madison, WI, USA). CuKα radiation (wavelength = 1.5418 Å) was generated at 40 kV and 40 mA. Detector slit was set to 2.000 mm. Sample was analyzed using a coupled 2θ/θ scan type with a continuous PSD

fast scan mode. 2θ started at 8.000° and ended at 30.0277° with increments of 0.02151°, while θ started at 4.0000° and ended at 15.0138° with increments of 0.01075°. Step time was 1.000 sec (i.e., 1025 total steps, effective total time 1157 sec per run). Cellulose samples (approximately 0.5 g) were placed in a specimen holder ring made of PMMA with 25 mm diameter and 8.5 mm height, rotating at 5 degrees per minute during analysis.

3.3.5. XRD data analysis

To determine the relative amounts of the various crystalline allomorphs of cellulose (CI and CIII) as well as the level of AC in a sample, a series of standards were produced as described previously and further analyzed by XRD. As the CI and CIII standards contained a relatively high content of AC, it was required to remove the amorphous portion of the XRD spectra, thereby reproducing spectra correspondent to 100 % crystalline CI and CIII. For this purpose, AC standard (PASC) was used in a technique designated by amorphous subtraction method (ASM) [125, 126]. **Figure 3-2** shows how the ASM method was applied to the CI and CIII standards. The yellow area, representing the AC spectrum, was subtracted from the XRD spectra of CI and CIII, generating new XRD spectra representative of 100 % crystalline CI and CIII.

These XRD spectra representing 100 % CI and CIII were further used in peak deconvolution of several ammonia treated samples produced in this study. As example, **Figure 3-3** shows a sample containing a mixture of AC, CI and CIII, which was deconvoluted using standard spectra of CI, CIII and AC. The deconvolution was performed using the following equation:

$$Model\ XRD\ Spectra = \alpha \cdot AC + \beta \cdot CI + \gamma \cdot CIII \qquad \textbf{(3-1)}$$

Where,

AC = amorphous cellulose spectra; *CI* = 100 % cellulose I standard spectra; *CIII* = 100% cellulose III standard spectra. The coefficients α, β *and* γ control the proportion of each crystal in the mixture.

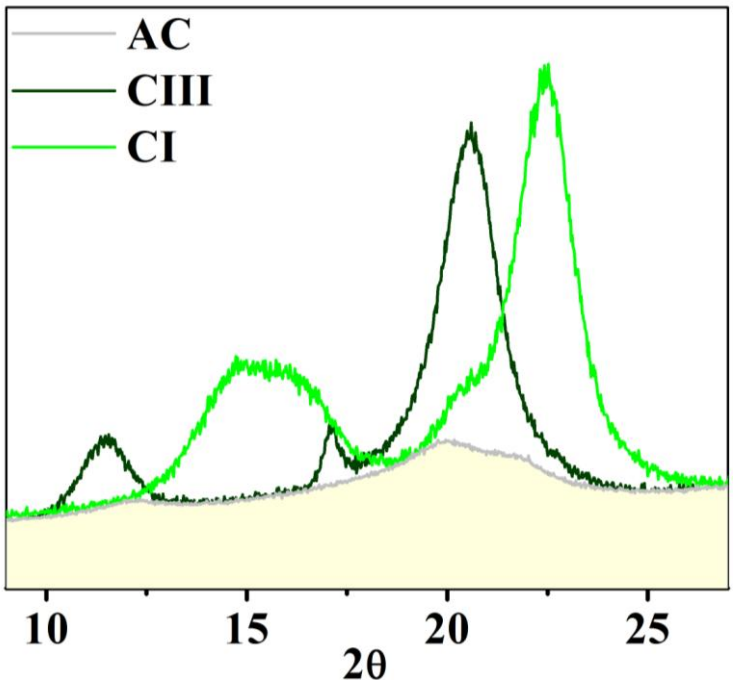

Figure 3-2 Example of the XRD spectra of cellulose I (CI), cellulose III (CIII) and amorphous cellulose (AC). Amorphous subtraction method was applied to CI and cellulose CIII standards for this study. The yellow area was subtracted from the XRD spectra of CI and CIII standards as described in this figure to recreate the 100 % crystalline CI and CIII spectra used for XRD spectra deconvolution.

The coefficients α, β *and* γ from the model XRD spectrum were determined using the least squares method. The resulting model XRD spectra was further evaluated for statistical significance, showing in all cases *P* values of 0.00 and R^2 values above 0.99. In **Figure 3-3** is possible to observe an example of a model curve (in red) fitting the XRD spectra of a sample containing unknown composition of CI, CIII and AC. The composition of a designated sample containing CI, CIII and AC was analyzed based on the relative area occupied by each standard

XRD spectrum after deconvolution. For all the model fits reported in this manuscript, R^2 values were always higher than 0.99, demonstrating the ability of the model to fit XRD spectra obtained for the various conditions.

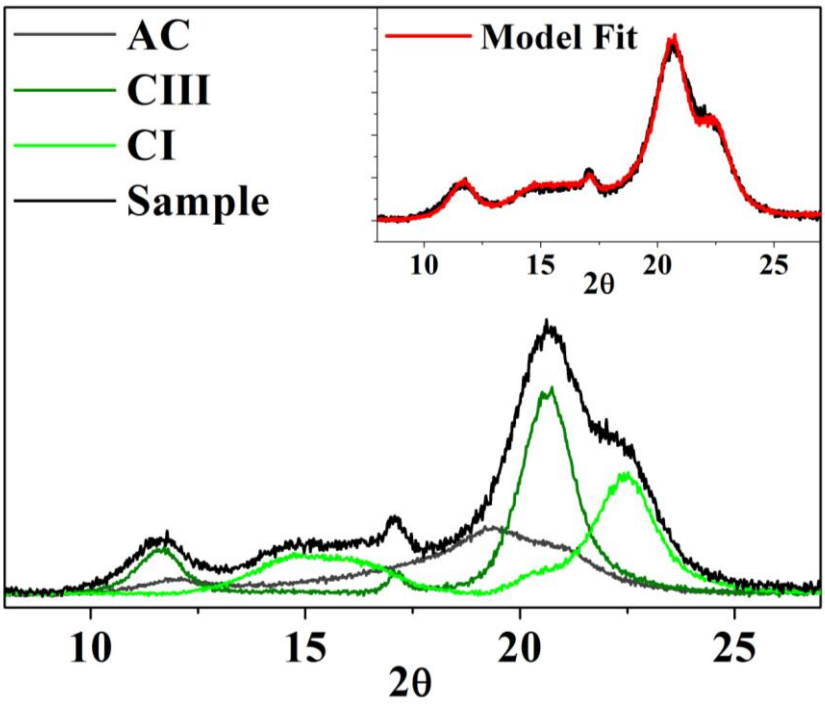

Figure 3-3 Example of an XRD peak deconvolution applied to a sample containing a mixture of amorphous cellulose (AC), cellulose I (CI) and cellulose III (CIII). The model spectra (red line), contrasting with the sample XRD spectra (black line) is presented in the top right corner.

Peak deconvolution methods have been used in the literature to calculate the crystallinity index of cellulose samples [126-129], however they are usually performed summing a combination of Gaussian, Lorentzian or Voigt functions to fit XRD spectra of the sample. However, multiple curves are required to describe a mixture of various cellulose allomorphs, and the high number of degrees of freedom increases the number of possible combinations of intensity for the curves that describe the XRD spectrum of the sample. The method described herein, eliminates this problem

in great extent, as the ratio between each peak is maintained constant within the standard XRD spectrum of CI, CII and AC. Therefore, the method produces consistent results, favoring our analysis, which is will be mainly a relative comparison between samples as opposed to a discussion about absolute values.

3.3.6. Enzymatic hydrolysis

Cellulose samples were subjected to enzymatic hydrolysis at 1% glucan loading. The total protein loadings used during reaction was 4.0 or 7.5 mg/ g glucan of Accellerase 1500 enzymes (DuPont, formerly Genencor, Palo Alto, CA, USA), depending on the experiment. When 4 mg enzyme/g of glucan was used, sugar yields were evaluated for 24h residence time, while for 7.5 mg/g glucan, enzymatic hydrolysis was evaluated for 4 h residence time. In all experiments, the reaction pH was adjusted to 4.8 prior to incubation at 50 °C in an orbital shaking incubator set at 200 RPM (New Brunswick, Innova 44, Enfield, CT, USA). Monomeric glucose was quantified using a Shimadzu HPLC system equipped with an Aminex HPX-87P carbohydrate analysis column (Biorad, Hercules, CA) and Waters 410 refractive index detector (RID). Degassed HPLC grade water with 5 mM H_2SO_4 was used as a mobile phase at 0.6 mL/min. Injection volume was 20 µL with a run time of 20 minutes.

3.4. Results and Discussion

3.4.1. Effect of sampling media on cellulose III conversion

The mechanism for converting CI to CIII proposed by Schuerch (1963) [130], involves the penetration of anhydrous ammonia into the cellulose crystal, followed by the disruption of hydrogen bonding, creating a crystalline complex with a larger unit cell than CI, designated by

ammonia-cellulose complex. After evaporating ammonia, the hydrogen bonding is rewired in a completely different pattern, generating a new crystal designated by CIII. During this operation, the heat of vaporization of ammonia is often large enough to reduce the temperature in the surface of the cellulose fibers below 0 °C. As described by Menachem Lewin et al. (1971) [80], the temperature at which CIII is formed, i.e., during ammonia evaporation, can affect the crystallinity of cellulose and therefore, is necessary a good control of this parameter to avoid misleading experimental results during CIII formation. For this purpose, a "heat sink" composed by a large enough volume of solvent was prepared. The ammonia-cellulose complex, suspended in liquid ammonia, was sampled from the high-pressure reactor into a "heat sink" prior to ammonia evaporation. The cellulose sample was further filtered and washed extensively with solvent to remove residual ammonia before being dried in the hood overnight at room temperature. For this experiment, acetone, ethanol, water and methanol were evaluated as sampling solvents. The ammonia-cellulose complex was generated using Avicel PH-101 and ammonia at 90 °C with 6:1 ammonia-to-cellulose ratio for 20 min. The glass vials containing the sampling solvents were also kept at 25 °C in a temperature-controlled water bath. As ammonia evaporated from the solvent, temperature did not decrease below 20 °C for all cases and therefore, the solvents tested herein could potentially be used to control temperature during assembly of the CIII crystal. However, similarly to temperature, the presence of a solvent can also affect the way CIII crystals are assembled and the final crystallinity of the sample. Therefore, this work attempted to evaluate differences between the various solvents tested herein in order to select the one that can offer the best environment for CIII conversion.

By performing XRD on the treated cellulose samples (**Figure 3-4)**, it was possible to observe differences in CIII conversion as a function of the sampling solvent used. CIII formation was

evaluated based on crystallinity index (CrI) measurements, which were performed according to the amorphous subtraction method, as described earlier. The range of values available on the literature for CrI of Avicel PH-101 can vary significantly from ~39 to ~90 %, depending on the calculation method [126, 131]. Amorphous subtraction methods usually generate crystallinity indexes between ~60 and ~75 % for Avicel PH-101 [126, 131], however the result obtained in this work was 50.1%, which is slightly lower than most reports from the literature. As these values of CrI are not consistent among authors, our discussion will be based on relative differences between the various samples generated in this work, instead of focusing on comparing absolute values with literature results. The XRD data shown in **Figure 3-4** clearly reveal the importance of the environment at which hydrogen bonding is formed during CIII crystal assembly. From the organic solvents used in this study, ethanol was the one that allowed higher conversion to CIII and consequently higher glucose conversion. Also, methanol seemed to provide a better environment for CIII formation as compared to acetone and air, which generated similar results. The reasons behind such differences are still to be determined and more work is required to clarify this observation. As ethanol was the most effective sampling media for CIII conversion, it was defined as the choice of sampling solvent for the subsequent experimental work.

The most distinct result was generated by sampling the ammonia-cellulose complex into water. This sample generated an undefined XRD pattern that could not be effectively deconvoluted by the method described earlier in the materials and methods section, and therefore, it suggests that this sample of low crystallinity cannot be described as a mixture of solely CI, CIII and AC produced by phosphoric acid treatment. These results also suggest that water interferes with rewiring of the hydrogen bonding once ammonia leaves the ammonia-cellulose complex,

creating a less ordered pattern of hydrogen bonds that is reflected by the amorphous-like XRD spectrum (**Figure 3-4 ii.b**). Lewin et al. (1971) [80], performed a similar experiment with cotton cellulose, reporting a complete reversion to CI after drying the sample at 65 °C. Others studies conducted by Barry et al. (1936) [132] and Clark et al. (1937) [133] revealed that aqueous ammonia treatment is able revert CIII back to CI, after drying at 105 °C. The cellulose type and drying method used by these studies are two major differences contrasting with the work presented herein, where Avicel PH-101 was used as the cellulose source and freeze drying was used as the preferred method to remove water from the sample. The rationale behind this choice of drying process was purposely to avoid reversion of CIII back to CI, as our preliminary evaluation revealed that freeze drying does not allow reversion of fully converted CIII to CI and has low impact on the final cellulose crystallinity [data not shown].

Enzymatic digestion of the water-sampled cellulose resulted in lower sugar yields compared with cellulose sampled to organic solvents, even though the former presents lower crystallinity. This observation is not concordant with the current paradigm that supports the idea that less crystalline cellulose allows higher enzymatic hydrolysis yields [114]. The definition of AC as being a sample with no ordered structural pattern can contribute to the misleading idea that all AC is made alike. However, this data suggests that this paradigm can no longer be applied for cellulose III in all instances. Another relevant observation supporting this idea is that higher CIII crystallinity improved cellulose vulnerability to enzymatic digestion, which usually is not observed for CI [114, 134, 135]. This topic will be further explored in this manuscript, where new evidence supporting this idea will be presented and discussed.

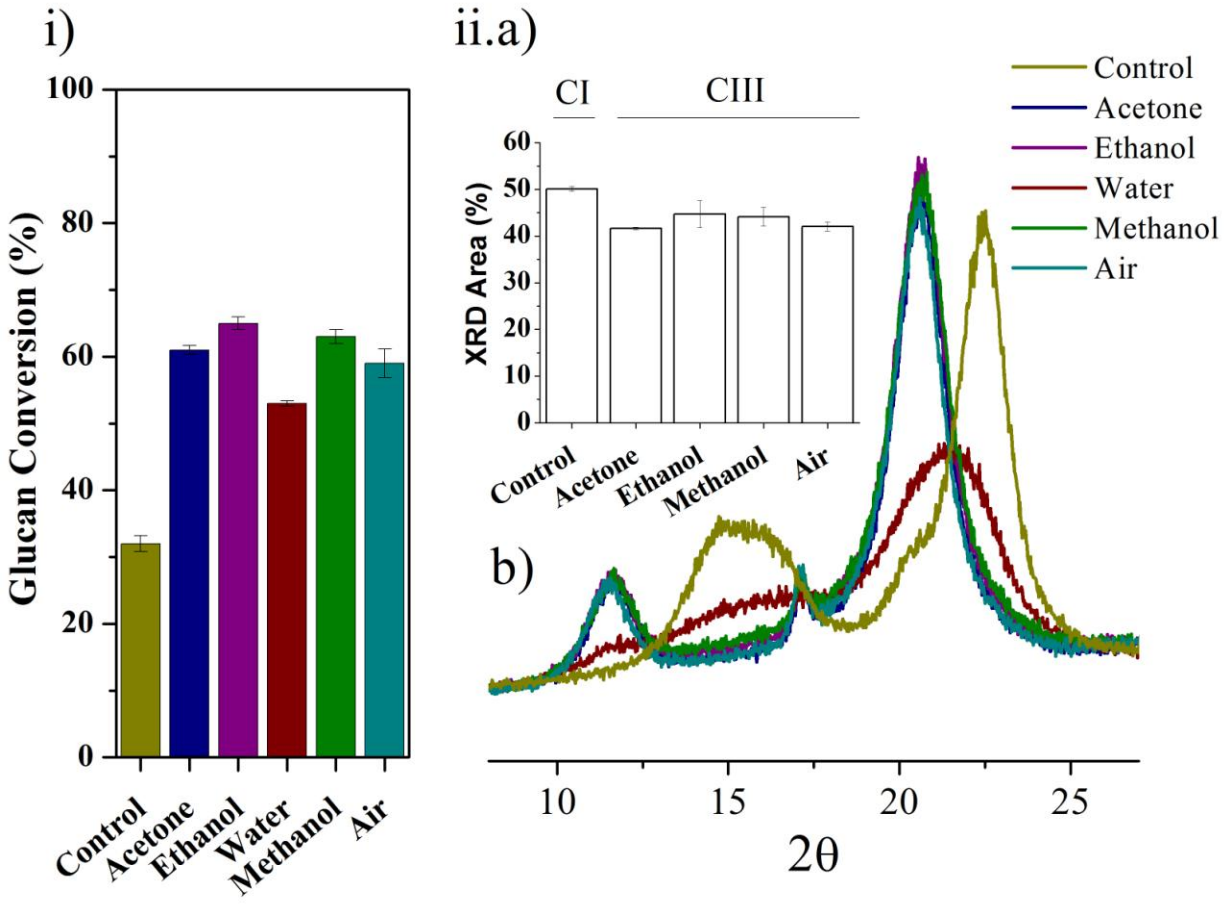

Figure 3-4 i) Glucose conversion of cellulose treated at 90 °C with 6:1 (w/w) ammonia-to-cellulose ratio for 20 min residence time, sampled to various solvents and to no solvent (air). The control experiment corresponds to cellulose I (Avicel PH-101). Enzymatic hydrolysis was performed using 4 mg/g glucan of Accellerase 1500 enzymes for 24h; ii. a) Crystallinity index (CrI) of the various samples of ammonia treated cellulose sampled to different solvents and to no solvent (air). CrI measurement was performed by amorphous subtraction method of the XRD spectra showed in b).

3.4.2. Effect of ammonia loading on cellulose III conversion

Ammonia loading is one of the key factors contributing to the effectiveness of ammonia-based pretreatments on lignocellulosic biomass [136, 137]. Most of these pretreatments use aqueous ammonia at elevated temperatures to improve the accessibility of enzymes to cellulose. Although

these pretreatments can partially decrystallize cellulose fibers [138], the presence of elevated proportions of water inhibits modifications to the crystalline morphology of cellulose, notably the formation of CIII. Efficient conversion of CI to a more easily digestible CIII crystal requires contact of the cellulose fibers with liquid anhydrous ammonia for a period of time at a range of temperatures (effect of temperature and time will be further discussed in this manuscript). The ammonia-to-cellulose ratio can impact both the rate of liquid ammonia penetration to the cellulose fibers and the number of hydrogen bonding sites that will be activated by ammonia. Incomplete formation of the ammonia-cellulose complex will affect cellulose III conversion and enzymatic hydrolysis performance. As ammonia usage has economic implications to the biorefinery, is important to optimize ammonia loading to efficiently convert CI to CIII using minimum ammonia-to-biomass ratio. To determine the minimum ammonia loading that allows efficient CIII conversion, anhydrous ammonia was put in contact with microcrystalline CI (Avicel PH-101) at various ammonia-to-cellulose ratios ranging from 1:1 to 6:1 (w/w). In **Figure 3-5**, **it** is possible to observe (i) the extent of CIII conversion by XRD and (ii) the respective impact on enzymatic hydrolysis for this range of ammonia loadings. From the XRD spectra presented in **Figure 3-5 ii)** it is evident that ammonia-to-cellulose ratios of 1:1 and 2:1 are not sufficient to completely modify the native crystal state of cellulose in 10 min of ammonia treatment. Efficient conversion of CI to CIII is only observed at ammonia-to-cellulose ratios above or equal to 3:1. From the XRD spectra, it is also clear that the CIII peaks are sharper and taller for 6:1 than for 3:1 ammonia loading, leading to a more effective CIII conversion. This result suggests that higher ammonia loadings (e.g., 6:1) can improve the mass action responsible for efficient penetration of ammonia in the cellulose crystal, being able to activate the ammonia-cellulose complex at faster rate than the lower ammonia loadings (e.g., 3:1). It is possible that for

the lower ammonia loadings, some hydrogen bonding sites are not activated by ammonia within the first 10 min of treatment, leading to a poorer alignment between cellulose chains during ammonia evaporation which resulted in a product of lower CIII crystallinity. For ammonia-to-cellulose ratios above 6:1 it was not possible to observe significant changes in CIII conversion (data not shown), suggesting a saturation of the ammonia loading effect around 6:1. For this reason, 6:1 was the maximum ammonia loading used in this study.

Other authors have successfully converted cellulose I to III using ammonia loadings between 2:1 and 3:1 for longer periods of time (30-90 min), while ramping the temperature from -75 °C to 25 °C or higher [123]. Also, literature reports show that is possible to achieve high CIII conversion with ammonia in the supercritical state [139]. However, these techniques are not practical for an industrial pretreatment method, as supercritical conditions and temperature fluctuations of those amplitudes often require high energy demands. Therefore, we chose to deliver ammonia in subcritical conditions, at set-point temperature and allow it to contact cellulose for the desired residence time. This more practical technique showed to be effective on producing CIII, which can be confirmed by the various XRD results presented in this study.

The enzymatic hydrolysis results from **Figure 3-5 i)** show a progressive increase of glucose yields as a function of CIII conversion. Also, the results are concordant to our previous observation, showing that higher CIII crystallinity favors improved enzymatic hydrolysis rates. Sugar yields increased up to approximately two fold for the most crystalline sample of CIII (i.e., 6:1), as compared to native CI (from ~32 % to ~ 59 %). This level of improvement has been observed by other authors in the literature, notably Chundawat et al. (2011) [105], using similar substrate and enzyme cocktail. However, in the literature it is possible to find a wide range of results. For example, Igarashi et al. (2007) [117] observed even higher improvements when

applying purified enzymes on algae-derived CIII, resulting in approximately five folds higher glucose conversion compared with algae-derived cellulose I. On the other hand, Mittal et al. (2011) [123] recently showed significantly lower improvements, or even no improvements during 24h enzymatic hydrolysis of CIII compared with CI. However, a different cellulase cocktail and enzyme loading were used in that work, which could partially explain some of the variability with respect to this and other reports from the literature.

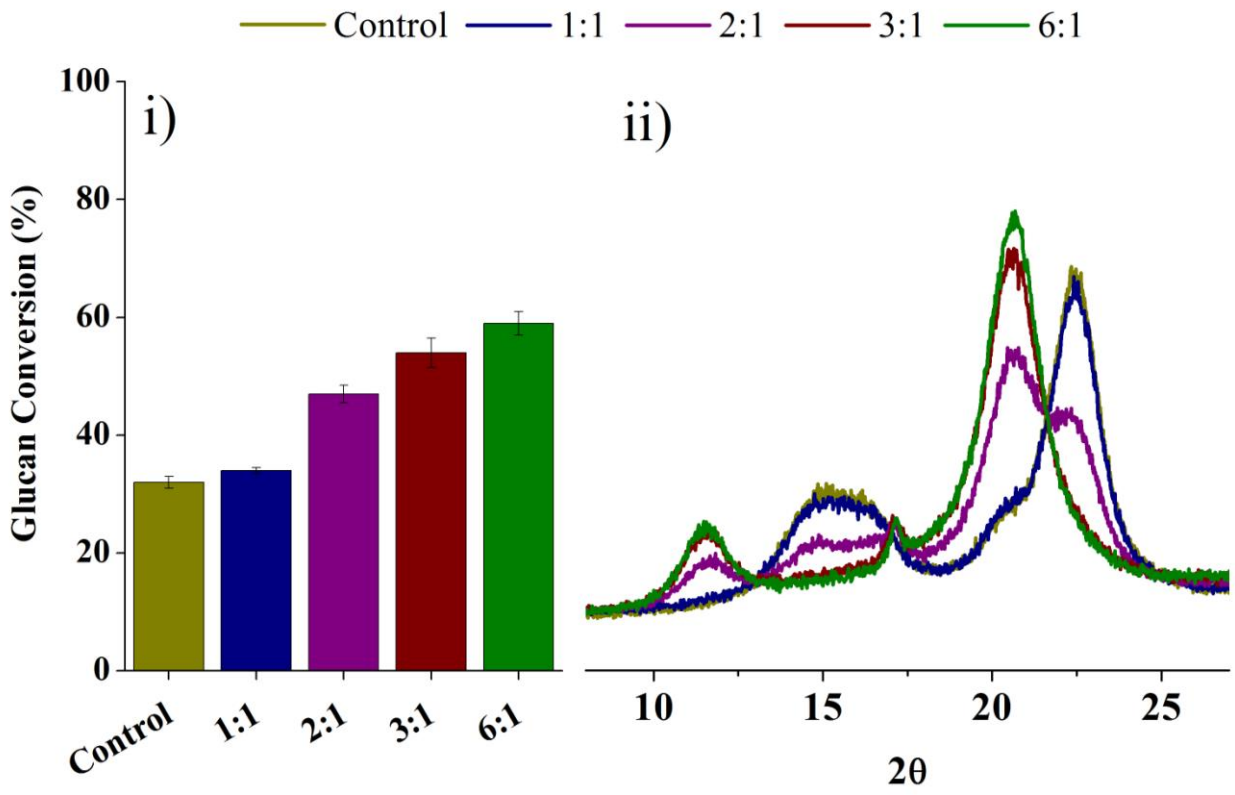

Figure 3-5 i) Glucose conversion of ammonia treated cellulose under various ammonia:cellulose ratios, varying from 1:1 to 6:1 (w/w), compared to the control (Avicel PH-101). Enzyme loading used in the experiment was 4 mg/g glucan for a residence time of 24h; ii) XRD spectra of ammonia treated cellulose using various ammonia:cellulose ratios at 90 °C for 10 min residence time.

3.4.3. Effect of temperature and time on cellulose III conversion

Temperature is another key factor contributing to CIII conversion as reported by a number of authors in the literature [80, 123]. This factor is not only important during evaporation of ammonia, but also plays an important role during formation of the ammonia-cellulose intermediate [140]. In this work, the temperature during ammonia evaporation was set constant at 25 °C. This temperature was controlled using absolute ethanol as the sampling solvent, which was placed in a temperature-controlled water bath as described earlier. Ammonia treatment was conducted at 25 °C and 90 °C to evaluate the effect of temperature in the process of CIII conversion. These two temperatures are reasonably far apart from each other, allowing CIII conversion differences to be noticeable. Also, 90 °C was the maximum temperature limit observed for effective CIII conversion without thermally decomposing the sample. Decomposition products derived from high temperature treatments could inhibit enzymes during cellulose digestion [108] and affect the correlations between sugar yields and CIII conversion performed in this study.

Residence time is also important for CIII conversion, as observed initially by Clark et al. (1937) [133] and Lewin et al. (1971) [80]. The latter observed a decrease in equatorial CrI with increasing time of ammonia treatment from 2 sec to 5 min. In his experiment, ammonia was evaporated from cotton samples that were dried at 105 °C. Lewin et al. (1971) also described the transition of CI to CIII as a function of treatment time, with increasing proportions of CIII for larger residence times. However, these authors did not quantify the proportions of AC, CI and CIII as a function of time and only allowed a maximum treatment time of 5 min. In **Figure 3-6** it is possible to clearly observe the transition between these various forms of cellulose as a function of treatment time. For this experiment, Avicel PH-101 was treated with 100 % anhydrous

ammonia at 25 °C and 90 °C in order to evaluate CIII conversion profiles at low and high temperatures. **Figure 3-6 i)** clearly shows an abrupt increase of CIII content within the first minute of treatment, while CI was rapidly depleted from the sample at 25 °C. This observation shows that CIII can be formed at 25 °C with no further heat requirement. It also confirms the results obtained by Mittal et al. (2011), who observed full CIII conversion at 25 °C for Avicel PH-101 and other sources of cellulose [123], including corn stover cellulose. **Figure 3-6 i.a)** also shows a rapid increase of the amorphous content of cellulose (AC) in the first minute of treatment, which slowly decreases with treatment time. One possible justification for this result is that ammonia could fully activate some accessible areas of cellulose during the first minutes of treatment, generating mainly CIII after ammonia evaporation. As ammonia could not access less exposed regions of the cellulose microfibrils and activate the ammonia-cellulose intermediate, they remained intact as CI. Other areas could be partially activated by ammonia through the disruption of some hydrogen bonds, which during rapid ammonia evaporation could not align properly to generate a crystalline structure, resulting in an amorphous XRD pattern. The results obtained by Lewin et al. (1971) [80] also showed an increase of the amorphous content of cotton in the first 5 min of treatment time. As 5 min was the maximum residence time tested by this author, it may have not been long enough for ammonia to effectively penetrate well packed cotton fibers and therefore, it was not possible to observe the expected reduction of the amorphous content.

At 90 °C, a similar CIII conversion profile could be observed, with a rapid increase of the amorphous content of cellulose, followed by its reduction for increasing treatment times. At the same time, a rapid increase of CIII conversion was observed as CI was depleted from the sample. However, a major difference between treatment at 25 °C and 90 °C is that at higher temperatures

CIII is converted at a much faster rate, generating a sample of higher crystallinity than at lower temperatures. For example, the maximum amorphous content obtained at 90 °C was ~62 %, comparing with ~66 % at 25 °C, both occurring at 30 sec of treatment. This result suggests that temperature plays a role on promoting ammonia penetration in the cellulose fiber and creating faster formation of the ammonia-cellulose complex. It is also experimental evidence supporting previous computational simulation results obtained by Bellesia et al. (2011) [140] that clearly suggests an increase of ammonia penetration rate with temperature.

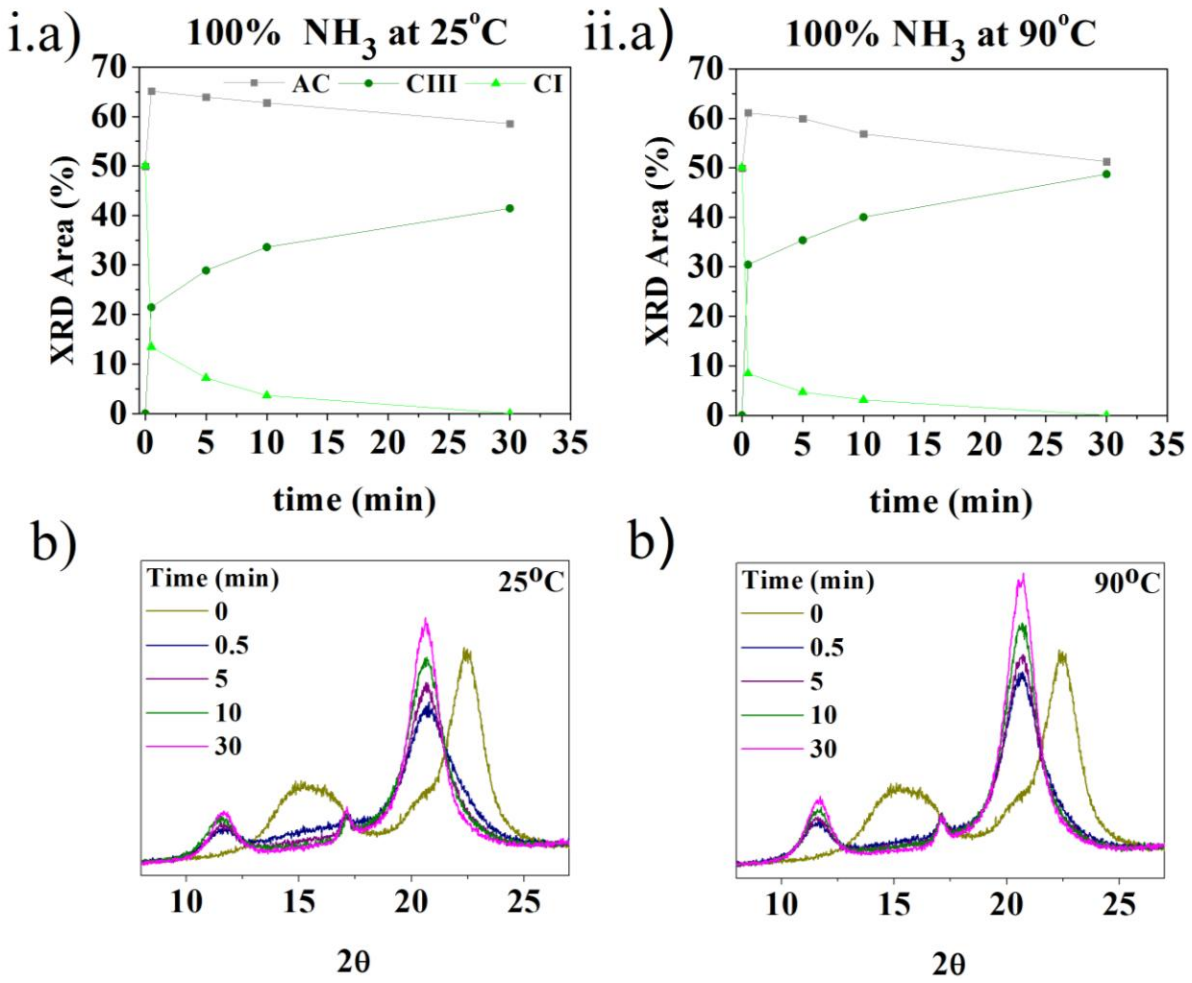

Figure 3-6 i) Relative proportions of cellulose III (CIII), cellulose I (CI) and amorphous cellulose (AC) during anhydrous ammonia treatment of Avicel PH-101 at 25 °C, as a function of

Figure 3-6 (cont'd)

residence time (a) and respective XRD spectra used to calculate CIII, CI and AC contents at 25 °C (b). ii) Relative proportions of cellulose III (CIII), cellulose I (CI) and amorphous cellulose (AC) during anhydrous ammonia treatment of Avicel PH-101 at 90 °C, as a function of residence time (a) and respective XRD spectra used to calculate CIII, CI and AC contents at 90 °C.

At 30 min residence time, the treated cellulose was totally depleted of CI and was composed mainly by AC and CIII at both 25 °C and 90 °C (**Figure 3-6**). The main difference between the two samples at this time point was that at 90 °C, the sample contained approximately 49 % of CIII, while at 25 °C it contained about 41 % of CIII. The effect of temperature during ammonia treatment of Avicel PH-101 was also reported by Mittal et al. (2011) [123], who also observed increase of the CrI for samples treated at higher temperatures. However, a comprehensive kinetic profile has never been presented in the literature showing the evolution of AC, CI and CIII as a function of time and temperature.

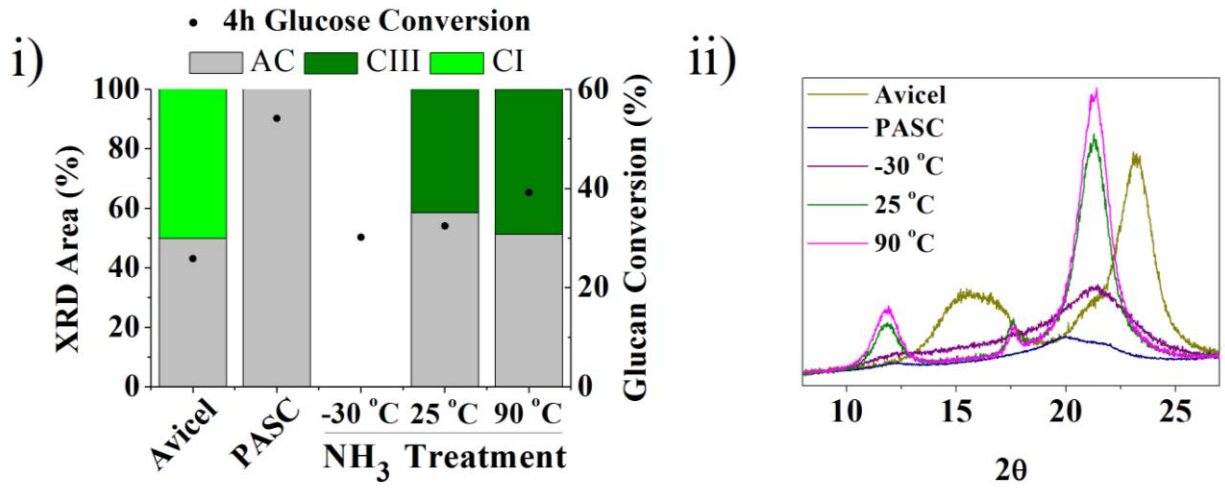

Figure 3-7 i) Comparison between amorphous content of Avicel PH-101 treated at various temperatures and correspondent effect on 4h glucose conversion during enzymatic hydrolysis. Enzymatic hydrolysis was performed with 7.5 mg/g glucan of Accelerase 1500 enzymes at 50 °C. ii) XRD spectra of Avicel PH-101 treated with phosphoric acid (PASC) and with ammonia at -30, 25 and 90 °C. At 25 and 90 °C treatment, ammonia was evaporated at 25 °C in ethanol, while at -30 °C ammonia was vacuum filtered and dried in the hood at ambient temperature.

To evaluate the effect of temperature and crystalline composition of cellulose on enzymatic hydrolysis, Avicel PH-101 was treated at -30, 25 and 90 °C for 30 minutes. Samples treated at 25 and 90 °C were transferred to ethanol at 25 °C prior to ammonia evaporation, while the sample treated at -30 °C was vacuum filtered and dried in the hood overnight at ambient temperature. The results presented in Figure 3-7 demonstrate that was possible to obtain cellulose samples with various levels of amorphous content. While at 25 and 90 °C it was possible to deplete the sample completely from native CI, being converted to CIII and AC, ammonia treatment at -30 °C generated an undefined XRD pattern that could not be completely deconvoluted and quantified as a mixture of AC, CI and CIII. This XRD pattern suggests that ammonia treatment -30 °C promotes the formation of highly disordered cellulose. This fact was also observed by other authors, namely Saafan et al. (1984) [141] and Mittal et al. (2011) [123], however the impact of this structural modification of cellulose on enzymatic digestibility was never reported in the literature. Supporting our previous observations, the results presented in **Figure 3-7** also show that ammonia-treated cellulose samples with higher CIII content are more vulnerable to enzymatic activity. According to the current paradigm, cellulose of higher amorphous content should be more digestible by cellulases [114, 134, 135], contradicting the results shown in **Figure 3-7**. However the observations used to create the current theory were based on results obtained in native cellulose (CI) and amorphous cellulose generated by ball milling or phosphoric acid treatment [107, 142]. From **Figure 3-7** it is possible to confirm that highly disordered cellulose created by ammonia treatment at -30 °C is more digestible than untreated Avicel (CI) composed by approximately 49.9 % of AC. However, the same figure shows that PASC, composed only by AC, presents approximately 1.5-fold improvement with respect to the ammonia treated sample at -30 °C. These observations suggest that different methods for

creating AC generate quite distinct responses to enzymatic activity. Future work is required to understand the basis for these differences at the structural level of cellulose, including evaluation of the level of hydrogen bonding, hydrophilicity and surface area. These studies also must be correlated with enzyme-substrate interaction measurements, such as binding affinity and catalytic activity of cellulases on the various amorphous substrates.

From the perspective of ammonia pretreatment of lignocellulosic biomass, it is important to treat cellulose in order to obtain the highest possible content of CIII, which translates to a more efficient enzymatic digestion by cellulases. This work clearly shows that various levels of CIII, CI and AC content can be achieved by controlling pretreatment variables such as temperature, time and ammonia loading.

3.4.4. Effect of solvent concentration on cellulose III conversion

CIII conversion has been traditionally performed using 100 % liquid anhydrous ammonia, applying heat for relatively short periods of time (< 1h) [80]. As this method uses a liquefied gas, i.e. ammonia, pressure can be considered a potential issue for economic and safety reasons. For example, when operating at 120 °C, pressure can increase up to approximately 1300 psi to maintain ammonia in the liquid state. To avoid such levels of operating pressure and possibly improve the economics and safety of the process, would be important to test the usage of less volatile co-solvents, preferably polar solvents that can allow CIII to be formed. As previously discussed in this manuscript, water does not allow CIII to be formed and therefore, is not a viable option for this process. Our previous work defined ethanol as a very compatible solvent to be used as a heat sink during ammonia evaporation. Ethanol and ammonia are also chemically compatible at temperatures below 150 °C while in the absence of catalysts [143, 144].

Ultimately, ethanol is a cheap chemical, widely available and is considered one of the major biofuel products produced by lignocellulosic biorefineries. Therefore, this chemical could be considered a good candidate to be used as a co-solvent in an ammonia-based pretreatment of lignocellulosic biomass.

Figure 3-8 shows the vapor-liquid equilibrium (VLE) curve of ammonia-ethanol mixture at 120 °C. This curve was obtained using the Non-Random Two Liquid (NRTL) thermodynamic model, estimating the missing parameters with UNIFAC model in ASPEN Plus (v.7.1). This VLE curve can help us determine the thermodynamic state of a two component mixture (ammonia/ethanol) as a function of pressure for a temperature of 120 °C. Analyzing this curve it is evident that is possible to decrease the operating pressure below 750 psi for mixtures consisting of < 60 wt% ammonia. However, is important to evaluate the range of concentrations of ammonia that allow efficient CIII conversion.

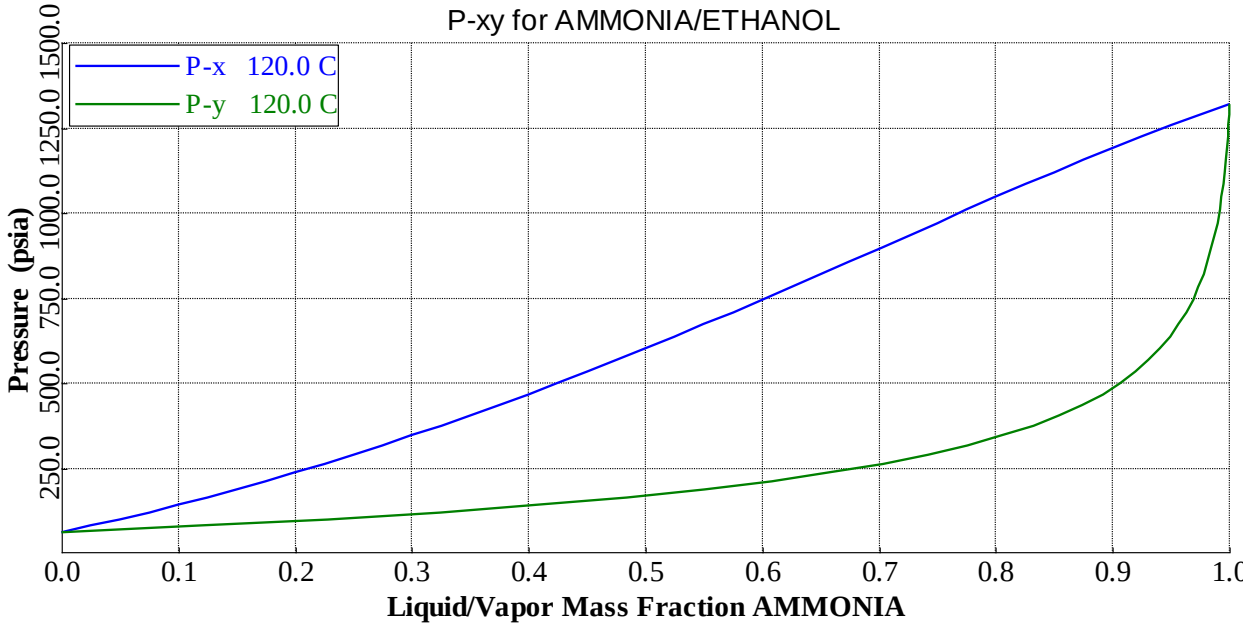

Figure 3-8 Vapor-liquid equilibrium curve (P-xy) for ammonia/ethanol mixture at 120 °C. The curve was predicted using NRTL model, estimating missing parameters using UNIFAC by Aspen Plus (v.7.1) software.

To determine the impact of co-solvent on CIII conversion, Avicel PH-101 was put in contact with various concentrations of ammonia in ethanol, ranging from 17 to 60 %, at different liquid-to-solid ratios, ranging from 4:1 to 10:1 (**Figure 3-9**). These experiments were performed at 25 °C for 30 min residence time. The results show that both 17 and 33 wt% ammonia solutions are not concentrated enough to allow effective penetration of ammonia in the cellulose crystals and disrupt hydrogen bonding. Most of the cellulose (CI) remains intact after pretreatment under such conditions. Using a 50 wt% ammonia solution was possible to observe some CIII conversion (21-27 %), especially at 6:1 and 10:1 ammonia-to-cellulose ratios. At 4:1 there was a slightly lower CIII conversion compared to the later, which may have occurred due to mass action limitations. It is important to note that 4:1 liquid-to-solid ratio, using a 50 wt% ammonia solution, represents 2:1 ammonia-to-cellulose ratio. From the results obtained in this experiment, CIII conversion could only be obtained after increasing the concentration of ammonia from 33 wt% to 50 wt%. It is possible that not only ammonia mass action is responsible for the formation of the ammonia-cellulose complex intermediate. For example, pH may be also responsible for improving solvation of the cellulose crystal by ammonia and perhaps facilitate the penetration of ammonia in the cellulose crystal. To prove such hypothesis, a new set of studies is required where pH should be monitored and controlled during contact of CI with ammonia.

When the concentration of ammonia was increased to 60 wt%, CIII conversion increased substantially for all liquid-to-solid ratios. As demonstrated in **Figure 3-9 iv)**, CIII conversion did not vary significantly within the range of liquid-to-solid ratios used in this study. These results also show that not all the CI was activated by ammonia, since about 5 % of CI was still present in the various treated samples with 60 wt% ammonia. Nevertheless, was possible to obtain approximately 40 % of CIII and 55 % of AC in all these samples.

The enzymatic hydrolysis performance was also measured as a function of ammonia concentration and liquid-to-solid ratio, being also presented in **Figure 3-9**. These results show a trend comparable with previously reported data from this manuscript, where higher glucose yields tend to be achieved with increasing content of CIII in the treated sample. For the best condition tested herein, i.e. treatment with 60 wt% ammonia, our results show 55-57 % glucan conversion in the first 24h of enzymatic hydrolysis with 4 mg/g glucan of enzyme loading, independently of the liquid-to-solid ratio used. This result suggests that is possible to achieve an increase of approximately 2 fold comparing with naturally occurring CI hydrolyzed under the same conditions (compare with control in **Figure 3-4**). At 4:1 liquid-to-solid ratio, the ammonia loading represents about 2.4 g/g of cellulose and an ethanol loading of 1.6 g/g of cellulose. In this study, the effect of temperature was not evaluated for the ammonia-ethanol system, since the major goal of this work was to determine the potential utilization of ethanol as a co-solvent during CIII conversion. In this context, our results indicate that ethanol is a suitable co-solvent for such application, generating a substrate rich in CIII and allowing enzymatic hydrolysis results comparable to the ones obtained by a 10 min treatment using anhydrous ammonia at 25 °C. Also, the utilization of ethanol enables the possibility of operating at lower pressures during ammonia treatment, which could be a determinant factor for the industrial implementation of a pretreatment technology based on CIII conversion of lignocellulosic biomass.

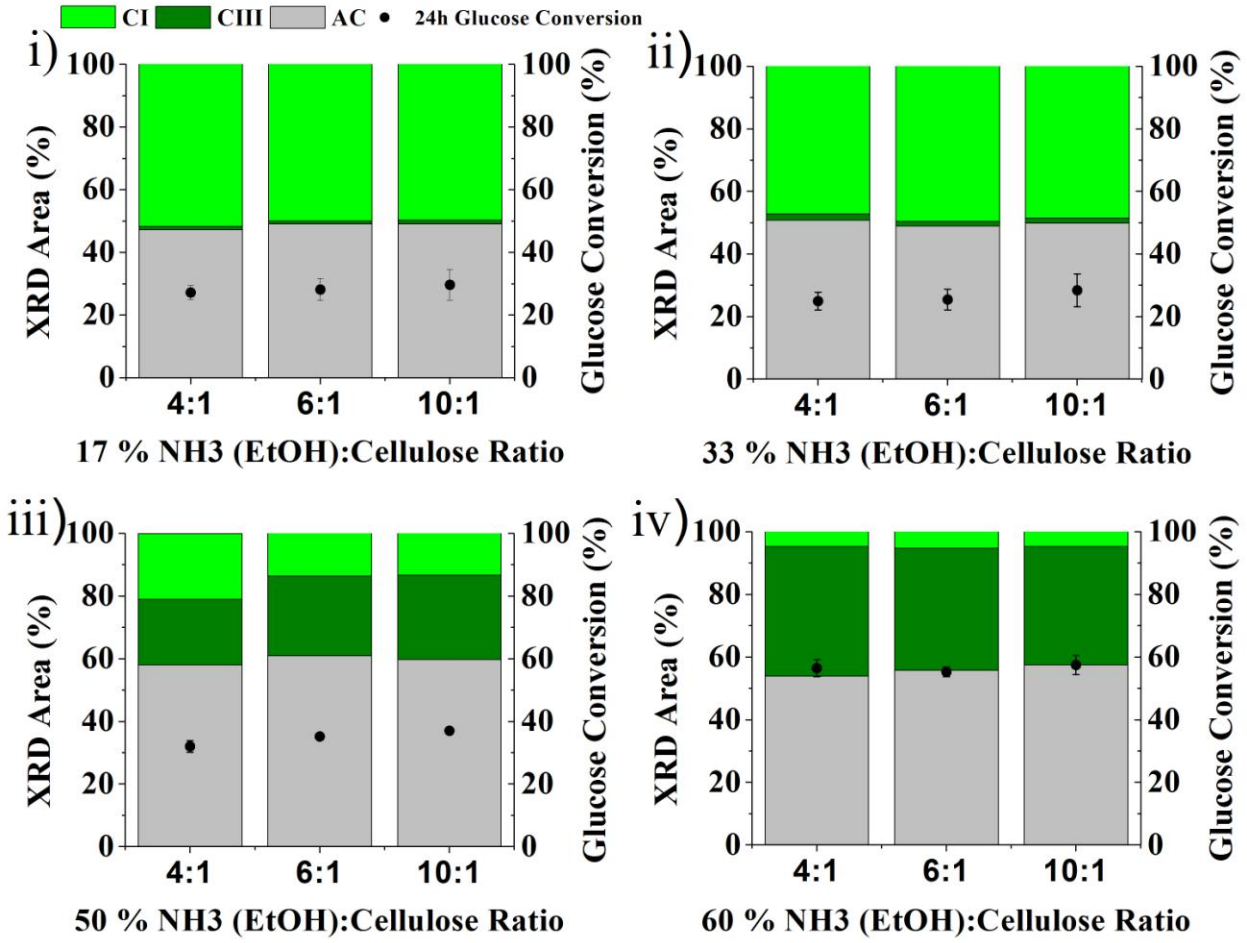

Figure 3-9 Relative proportions of cellulose I (CI), cellulose III (CIII) and amorphous cellulose (AC) as a function of ammonia concentration and liquid-to-solid ratio during ammonia treatment. The ammonia concentrations used in this study were 17 wt% (i), 33 wt% (ii), 50 wt% (iii) and 60 wt% (iv). Ammonia treatment was performed at 25 °C for 30 min residence time using 4:1, 6:1 and 10:1 liquid-to-solid ratios for all ammonia concentrations. The crystalline composition of cellulose was correlated with 24h glucose conversion using 4 mg/g glucan of enzyme for the various samples.

3.5. Conclusion

In this work, the key factors contributing to CIII conversion of Avicel PH-101 and its impact on enzymatic digestibility of cellulose were studied. For this purpose, a hybrid methodology for XRD analysis, consisting of the combination of amorphous subtraction and peak deconvolution

methods was successfully developed and implemented to determine relative amounts of CI, CIII and AC. To better understand the impact of variables such as incubation temperature, ammonia loading and residence time, it was also important to have constant temperature during ammonia release, which was revealed to be challenging due to heat of evaporation of ammonia. For this reason, another innovation was introduced in this work, consisting of the transfer of the ammonia-cellulose complex to ethanol before ammonia was evaporated. This method allowed the ammonia evaporation at relatively stable temperatures avoiding inconsistent and misleading results.

CIII conversion requires the access of liquid ammonia to the crystalline structure of cellulose and therefore, this process needs a minimum ratio of ammonia-to-cellulose to be effective. From our experiments, 3:1 was the minimum ammonia loading that could totally convert CI into CIII and AC. Higher ammonia loadings, such as 6:1 could improve CIII conversion by reducing the amorphous content of the treated sample. From kinetic data using 6:1 ammonia-to-cellulose ratio, we could observe that CI is converted to different proportions of AC and CIII, depending on ammonia incubation time and temperature. In our experiments, the amorphous content of treated cellulose increased in the first few moments of ammonia impregnation, possibly due to incomplete activation of the ammonia-cellulose complex before ammonia evaporation. As time progressed, ammonia could incorporate more effectively into the crystalline structure of cellulose allowing a complete formation of the ammonia-cellulose complex, which was better converted to CIII after ammonia evaporation. This resulted in a decrease of the amorphous content of treated cellulose as a function of time. From enzymatic hydrolysis results, we concluded that higher CIII content benefits sugar conversion from cellulose, contrasting with what has been reported for CI. Also, the AC generated by ammonia treatment cannot be compared with AC from PASC, for

example. This fact suggests that not all amorphous cellulose sources are created equally and possibly have very distinct properties. To maximize CIII conversion and reduce AC contents of treated samples it is important to use higher temperatures of incubation for longer residence times, with ammonia-to-cellulose ratios larger than 3:1. However, in the perspective of an ammonia-based pretreatment of lignocellulosic biomass, higher severity translates into additional processing costs. One of the most important processing issues when operating with ammonia at elevated temperatures is the high pressure. To be able to decrease operating pressure while effectively converting CI to CIII and improving enzymatic hydrolysis yields, ammonia was used in solution with ethanol as co-solvent. From the results in this study, we observed that 60 wt% ammonia in ethanol allowed efficient conversion of CI to CIII, enhancing enzymatic hydrolysis rates by 2 fold compared to untreated Avicel PH-101.

CHAPTER 4 - EXTRACTIVE AMMONIA (EA) PRETREATMENT OF CORN STOVER: REACTIONS IN ANHYDROUS AMMONIA.

4.1. Abstract

The development of a novel pretreatment technology, denominated as Extractive Ammonia (EA) pretreatment, was inspired by recent understanding of ammonia- plant cell wall interactions and mechanism of ammonia pretreatment of lignocellulosic biomass. This pretreatment technology is proposed herein for the first time and is defined by the formation of a less recalcitrant crystal of cellulose, i.e., cellulose III, and a highly selective lignin solubilization, followed by extraction. In this work, a response surface design approach was used to develop a mathematical model that is able to predict sugar conversions (glucan and xylan), lignin extraction yields and extent of ester bond cleavage as a function of pretreatment variables (temperature, ammonia-to-biomass ratio and time) for corn stover. From the experimental results it was possible to observe that sugar conversions during enzymatic hydrolysis is highly correlated with cellulose III formation, lignin extraction yields and ester bond cleavage. Process optimization predicted the condition that maximize sugar conversion as being 121.8 °C, 6.2:1 NH3:Biomass loading and 30.2 min residence time. At this condition is possible to achieve 93 % of glucan conversion to glucose and 79 % xylan conversion to xylose in 24 h enzymatic hydrolysis using 15 mg protein/g glucan, at 1 % glucan loading. At the same processing conditions, the regression model predicts an extraction of 48 % of the lignin initially present in corn stover. Operational details about this pretreatment method and equipment design will be also highlighted here.

4.2. Introduction

From the understanding built in the past few years of how ammonia interacts with plant cell wall components, it is clear that certain events have great impact in enzymatic digestibility of lignocellulosic biomass. Recent work from Chundawat et al. [23, 105, 145] has suggested a mechanism of action for a leading ammonia pretreatment technology, designated as AFEX^{TM}. During this pretreatment, moisture is added to the biomass, which allows an exothermal reaction to occur when in contact with ammonia, generating a sudden increase of temperature that can go up to 140 °C. This interaction reduces the need for external heat during pretreatment, which could be advantageous from the economic stand point. However, addition of water inhibits the formation of cellulose III [80], which can be 2-5 times more digestible than native cellulose I, when performing studies in Avicel [105, 117]. Therefore, AFEX^{TM} pretreatment, similarly to the other ammonia-based pretreatments proposed in the literature [146], is not able to transform the crystalline structure of native cellulose, which is highly recalcitrant to cellulolytic enzymes. Another important feature of ammonia as pretreatment chemical is the ability to cleave ester bonds. These bonds are highly abundant in lignin-carbohydrate complexes (LCC) from grasses and the cleavage of these cross-linkages is thought to help disrupt the complex network of polymers that constitute the plant cell wall. Ammonolysis of ester bonds are known to be facilitated by the presence of polar solvents such as water, which also can provide hydroxyl ions capable of performing hydrolysis of these same bonds [95, 99]. However, little is known about the conditions that favor these reactions in lignocellulosic biomass, especially in the absence of water or other organic solvents.

Also according to Chundawat et al [23, 95, 145], ammonia is able to solubilize cell wall components such as lignin and hemicellulose, which are condensed on the surface of the biomass after ammonia is vaporized by the sudden release of pressure during AFEX^{TM} pretreatment. TEM visualization has demonstrated that this delocalization leaves behind porous structures and delamination zones that are thought to expose cellulose to enzymatic activity, thereby contributing to the increase of digestibility of AFEX^{TM} pretreated biomass [145]. Lignin is known to be a highly inhibitory component of the cell wall to enzymes and also to fermentative microbes [29, 30]. Therefore, removal of lignin from the bioprocessing operations would potentially benefit both enzymatic hydrolysis and fermentation.

To better integrate all these known benefits derived from ammonia interactions with the plant cell wall, we propose to perform ammonia pretreatment in the absence of water, allowing cellulose III to be formed. To allow this transformation, higher ammonia-to-biomass ratios are required which can potentially benefit lignin solubilization and increase lignin removal from the system. This novel pretreatment technology, denominated Extractive Ammonia (EA) pretreatment, will be presented herein for the first time and this work will include the description of the EA reactor and pretreatment methodology. This work will also present a global overview of the important aspects of this new pretreatment technology. Using anhydrous ammonia in the absence of water or other organic solvents, we will present how pretreatment conditions will impact ester bond cleavage from ferulic and coumaric acids, and highlight the importance of this event to enzymatic digestibility of corn stover. Further, lignin solubilization and extraction will also be modeled as a function of pretreatment variables using a statistical design of experiments, which will allow us to define the range of conditions that promote efficient lignin extraction.

Moreover, enzymatic digestibility will be studied as a function of pretreatment variables and correlated with factors such as lignin extraction, cellulose III conversion and ester bond cleavage. Optimization of pretreatment conditions that maximize sugar yields from corn stover will be also presented in this study.

4.3. Experimental

4.3.1. Untreated corn stover

Untreated corn stover (UT-CS), a Pioneer 36H56 hybrid, was harvested in September 2009 in Wisconsin (USA) and oven dried at 60 ºC for approximately 2 weeks. The biomass was further passed through a 5 mm screen installed in a Christy hammer mill (Christison Scientific LTD, England) and stored at 4 ºC in heat sealed bags prior to utilization. The moisture content of the dried and milled corn stover was approximately 6 % on a wet weight basis. The biomass composition analysis was performed using NREL protocols NREL/TP-510-42618 and NREL/TP-510-42620. Based on this protocol, the untreated corn stover contained approximately 38 % glucan, 23 % xylan, 1 % galactan, 3 % arabinan, 14 % Klason lignin, 2 % acid soluble lignin, 5 % ash and 15 % extractives (i.e. ethanol and water soluble compounds), on a dry weight basis.

4.3.2. Extractive Ammonia (EA) pretreatment reactor construction

In Figure 4-1 is possible to visualize a schematic description of the EA equipment parts. This equipment is composed of two parts, with distinct functions, i.e., the EA reactor (**Figure 4-1 A**), where biomass is put in contact with ammonia for a desired temperature and residence time; and

the extractives collector (**Figure 4-1 B**), where the ammonia-soluble biomass components are collected after filtration and also where ammonia is evaporated from the system.

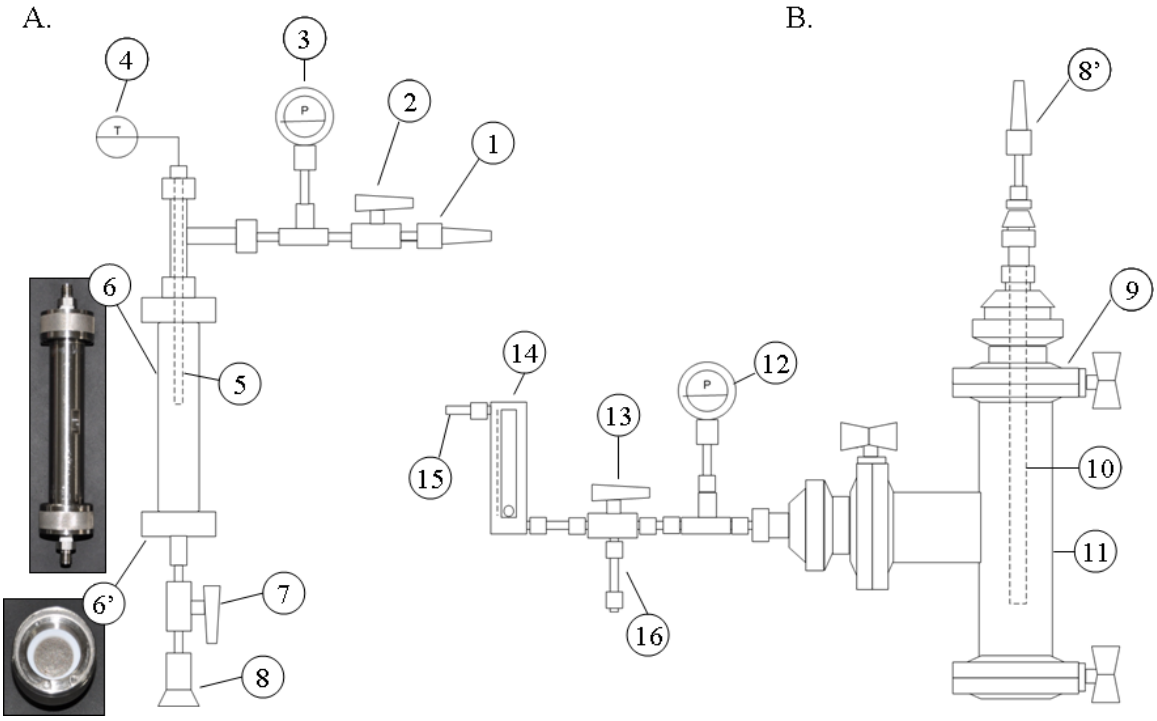

A. EA pretreatment reactor
1 – Connection inlet for NH_3 and N_2
2 – Inlet ball valve
3 – EA reactor pressure gauge
4 – Thermocouple
5 – Thermowell
6 – EA reactor cell
6' – Stainless steel filter installed in cap
7 – Outlet ball valve
8 – Connection outlet for Extractives

B. Extractives collector (flash tank)
8' – Connection inlet for Extractives
9 – Extraction collector lid
10 – Deep tube
11 – Extraction collector (T shape)
12 – Pressure gauge
13 – Gas outlet/inlet valve
14 – Metering valve
15 – Gas outlet
16 – N_2 inlet

Figure 4-1 Schematic drawing of the EA pretreatment reactor (A.) and extractives collector (B.). The pictures of the reaction cell (6) and of the stainless steel filter installed in the cap of the reactor (6') are highlighted. The EA reactor outlet connector (8) is attached to the extractives collector inlet connector (8') during operation.

Extractive ammonia (EA) pretreatment reactors (**Figure 4-1 A**) were constructed using 33 mL stainless steel cells from the Accelerated Solvent Extractor (ASE) system, manufactured by Dionex (Thermo Scientific, Sunnyvale, CA, USA). These cells were modified appropriately to

be used independently from the ASE equipment and to be able to handle liquefied gases, such as ammonia. The cells consist of two caps that screw into a threaded pipe. In the top cap, a thermowell, a pressure gauge and a ball valve were installed. In the bottom cap, a sintered stainless steel filter (80 μm pore size) was installed to separate the solid biomass from the liquid extractives during EA (6'). Also, the bottom cap holds a ball valve that is used to maintain the reaction components in the cell during EA pretreatment.

The extractives collector (**Figure 4-1 B**) is composed of a sanitary tee tube of 1" diameter (11), capped in the top with a sanitary fitting (9) that holds a deep tube (10), which is used to release the extractives in the bottom of the collector after EA reaction is completed. During EA reaction, the deep tube is fixed to the bottom of the EA reactor by joining together the "quick connectors" 8 and 8'. The side fitting of the collector holds a pressure gauge (12) and a 3-way valve (13), followed by a metering valve (14). The 3-way valve was installed to permit a nitrogen inlet (16) for pressurizing the collector and also to release the gases from the collector. The metering valve function is to control the evaporation rate of the ammonia as well as the flow of gases through the system.

This reactor system was designed to handle pressures up to 1500 psi and temperatures up to 140 °C, holding approximately 3 g of biomass (dry weight) per reaction run (depending on the biomass). This reactor system is flexible, as it can be adapted to several lengths of reactor pipe, allowing the user to control the working reaction volume down to 1mL, if required. In our design, five of these units were built in parallel and assembled in a permanent frame. In this frame was also installed a customized heating block, made of aluminum that was machined to perfectly enclose the five reactors (including the caps) simultaneously. The temperature was controlled by a PID controller connected to the heating elements on the block and the respective

temperature sensors. This configuration allowed the possibility of performing small scale, high-throughput reactions for determination of optimum EA pretreatment conditions of various substrates. However, the scope of this work will be centered on the understanding of important factors that affect EA pretreatment effectiveness in both sugar conversions and lignin extraction yields.

4.3.3. EA Pretreatment of corn stover

EA pretreatment was conducted in the tubular reactors described above and shown in **Figure 4-1**. The moisture in the corn stover was raised to 10 % (wet weight basis) by spraying appropriate amounts of distilled water homogeneously throughout the corn stover (3.2 g on a dry weight basis) before transferring it to the reactor cells (**Figure 4-1, 6**). The desired amount of ammonia was loaded with a syringe pump (Harvard Apparatus - model PHD 2000, Holliston, MA, USA) calibrated to deliver ammonia to a 0.01 g accuracy in the reactors, which were pre-heated to reaction temperature. Immediately after loading ammonia, the reactors were heated to the desired temperature. The top fitting was connected to a nitrogen line (**Figure 4-1, 1**) and the bottom fitting was connected to the extractives collector (**Figure 4-1, 8 and 8'**). The extractives collector was pressurized with nitrogen to equalize the pressure developed in the reactor during the course of pretreatment. After reaching the desired residence time, the valve between the reactor and collector (**Figure 4-1, 7**) was opened and the extractives were filtered and drained into the collector. Nitrogen overpressure of 1200 psi was applied to the reactor to maintain ammonia in the liquid state before opening the outlet ball valve and metering valve connected to the extractives collector (**Figure 4-1, 13 and 14**). The valve in the top of the reactor (**Figure 4-1, 2**) was kept opened to allow a pressure of approximately 1200 psi to be maintained in the system

for ~5 min. During this process, nitrogen was allowed to slowly flow through the system while helping ammonia and the respective extractives to be filtered and drained to the collector. After 5 min, the nitrogen inlet valve was closed and the system was depressurized slowly (~3 to 5 min). The pretreated biomass was transferred from the reactor to a tray, which was placed under the hood overnight to remove any residual ammonia from the biomass. Note that the biomass was fairly dry after EA pretreatment and this extra drying procedure was performed to stabilize the biomass with respect to moisture and residual ammonia contents. After collecting the pretreated biomass, the reactor was reconnected to the extractives collector and all the system lines were cleaned with 70 % ethanol and 90 % acetone (both in water) to remove residual extractives from the lines, which were drained to the extractives collector. After drying, the total weight and moisture content of the EA pretreated corn stover (EA-CS) was measured with an analytical balance and moisture analyzer A&D MX-50 (A&D Engineering, Inc., San Jose, CA, USA), respectively. The samples were stored at 4 °C in sealed bags prior to further usage in compositional analysis and enzymatic hydrolysis studies.

4.3.4. Experimental design for pretreatment

A statistical design of experiments (DOE) was used in this study to evaluate the effect of temperature, ammonia-to-biomass ratio (NH_3:BM) and residence time on % lignin extraction and ferulate/coumarate release during EA pretreatment of corn stover. The effect of the same variables on the sugar release of EA-CS during enzymatic hydrolysis was also determined herein. For this purpose, a Box Behnken experimental design was created using Minitab software (Minitab Inc., State College, PA, USA), with two replicates, an alpha value of 1.15 and with high

and low values for each factor as shown in **Table 4-1**. The resulting experimental conditions and respective experiment order are shown in **Table 4-2**.

A full quadratic response surface analysis was performed on the experimental results (notably glucan and xylan conversions, % lignin extraction and ferulate/coumarate release during EA pretreatment of corn stover) as a function of temperature, NH_3:BM and residence time. All interaction effects between factors were considered in this analysis and parameters were included in the model based on their *P* value, as well as their influence on the predictive ability of the model. The regression equations were used to predict the responses of the various effects as a function of the pretreatment conditions within the boundaries set by the experimental design shown in **Table 4-1**.

Table 4-1 High and low limits defined for the experimental points using Box Benhken design.

Factor	Low	High
Temperature (°C)	25	115
NH_3:BM	3	6
Time (min)	5	30

Table 4-2 EA pretreatment conditions defined by a Box Benhken design.

RunOrder	Temperature (°C)	NH_3:BM[a]	Time (min)
1	25	6	30
2	25	6	30
3	70	4.5	17.5
4	25	3	5
5	25	6	5
6	25	3	5
7	70	4.5	17.5
8	25	6	5

Table 4-2 (cont'd)

9	115	3	5
10	115	3	5
11	70	4.5	17.5
12	115	3	30
13	70	4.5	17.5
14	70	4.5	17.5
15	25	3	30
16	70	4.5	17.5
17	115	6	30
18	115	6	30
19	115	6	5
20	70	4.5	17.5
21	115	6	5
22	115	3	30
23	25	3	30
24	70	4.5	17.5
25	70	4.5	31.875
26	70	4.5	3.125
27	70	2.775	17.5
28	70	4.5	17.5
29	18.25	4.5	17.5
30	70	4.5	17.5
31	121.75	4.5	17.5
32	70	4.5	17.5
33	70	6.225	17.5
34	121.75	4.5	17.5
35	70	4.5	17.5
36	18.25	4.5	17.5
37	70	4.5	31.875
38	70	4.5	3.125
39	70	2.775	17.5
40	70	6.225	17.5

[a] NH_3:BM – Ammonia to biomass ratio.

4.3.5. Composition analysis of plant cell wall components

UT-CS and EA-CS were subjected to compositional analysis according to the standard NREL protocols NREL/TP-510-42618 and NREL/TP-510-42620. One exception for the analysis of EA-CS was the absence of water and methanol extraction, to avoid removing water and ethanol soluble lignin from the biomass and thereby overpredict % lignin extraction. Mass balances on glucan, xylan, arabinan and lignin were performed around the EA pretreatment.

For determining ester-linked ferulic and coumaric acid contents remaining in the pretreated cell walls, 40 mg of milled biomass (0.5 mm mesh size) was subjected to ethanol extraction by adding 6 mL of 80% ethanol to a capped test tube. This mixture was incubated at 50 °C for 1 hour with periodic mixing (every 15 min) to facilitate mass transfer. After incubation, the sample was centrifuged for 4 min at 3500 rpm. The supernatant was aspirated from the tube prior to a second addition of 6 mL of 80 % ethanol. The sample was gently vortexed at room temperature and centrifuged for 4 min at 3500 rpm before the liquid was aspirated from the tube. To facilitate drying, the sample was washed twice with 6 mL of 100 % ethanol. The extracted biomass was left in a 50 °C oven overnight to dry before digestion. Quantification of ester-linked hydroxycinnamic acids in the biomass was performed using a 2 M sodium hydroxide (NaOH) digestion as described in the literature [147, 148]. Diethylether extraction of the hydroxycinnamic acids after NaOH digestion was not performed to avoid error propagation. Instead, the alkaline mixture was filtered (0.22 μm syringe filter) into a microcentrifuge tube and diluted prior to quantification using LC-MS. LC-MS analyses were done using a QTRAP 3200 mass spectrometer (AB/Sciex) equipped with binary LC-20AD pumps (Shimadzu, Japan), a SIL-HTc autosampler and Ascentis Express C18 column (5 cm x 2.1 mm; 2.7 μm particle size). The

analytes were eluted with a reversed phase gradient using Solvent A (0.15 % aqueous formic acid) and Solvent B (methanol). Total solvent flow was maintained at 400 μm/min, and a gradient elution was performed using the following solvent compositions: initial, 5% B, held for 1 min; linear gradient to 18 % B at 8 min and then to 50 % B at 9 min; sudden increase to 99 % B at 9.01 min and held until 10 min; and finally returned to initial condition at 10.1 min and held until 12 min. Injection volume and column temperature were 5 μL and 50 °C, respectively. Enhanced Product Ion (EPI) scans were generated for the $[M+H]^+$ ions of coumaric and ferulic acids using electrospray ionization in positive ion mode to identify abundant product ions. Parent ions selected for fragmentation were the protonated molecular species of coumaric and ferulic acids. This analysis was performed to select suitable product ions for Multiple Reaction Monitoring (MRM) analysis. Source and gas parameters were all optimized for the standards to generate signals with highest intensity. After optimization, source parameters were as follows: curtain gas, 20 (arbitrary units); ion spray voltage, 4,500 V; temperature, 500^{o}C; gas 1, 25 (arbitrary units); gas 2, 25 (arbitrary units). Compound dependent parameters after optimization are shown in the table below:

Table 4-3 Compound-dependent parameters after mass spectrometry optimization.

Compound name	MRM transition	DP (V)	EP (V)	CE (V)
Coumaric acid	165 > 91	20	8	35
Ferulic acid	195 > 117	20	10	30

DP: Declustering potential; EP: Entrance potential; CE: Collision Energy

All mass spectrometric data were acquired and processed using Analyst v. 1.4.2 software from AB/Sciex. The quantification of ester-linked hydroxycinnamic acids was performed in quadruplicates for each EA-CS sample as well as the untreated corn stover control, using appropriate standard curves. The results were further processed to calculate the percent of ester-

linked coumaric and ferulic acids that were cleaved during EA pretreatment, with respect to the untreated corn stover.

4.3.6. Enzymatic hydrolysis of EA pretreated corn stover

Enzymatic hydrolysis was performed at 1 % glucan loading, using 15 mg of enzyme per gram of glucan in 15 mL vials, incubated at 50 ºC, with pH 4.8 for 24 h in an orbital shaking incubator (New Brunswick, USA). The enzymes utilized in this work were Cellic® CTec2 (138 mg protein/ml, batch No.VCNI0001) and Cellic® HTec2 (157 mg protein/ml, batch No.VHN00001), generously provided by Novozymes (Franklinton, NC, USA). The protein concentration for the enzymes was determined using the Kjeldahl nitrogen analysis method (AOAC Method 2001.11, Dairy One Cooperative Inc., Ithaca, NY, USA). The enzyme ratios utilized in this work were 50 % Cellic® CTec2 and 50 % Cellic® HTec2 in a dry protein weight basis. These ratios were previously optimized to maximize total sugar conversion on EA pretreated corn stover. After enzymatic hydrolysis, samples of the hydrolyzate were prepared for glucose and xylose analysis using HPLC equipped with a Bio-Rad Aminex HPX-87H column (Bio-Rad, Hercules, CA, USA) as previously described [88].

4.3.7. X-Ray Diffraction (XRD) of EA pretreated corn stover

XRD was performed on an X-ray powder diffractometer with beam parallelized by a Gobel mirror (D8 Advance with Lynxeye detector; Bruker AXS Inc., Madison, WI, USA). Cukα radiation (wavelenghth = 1.5418 Å) was generated at 40 kV and 40 mA. The detector slit was set to 2.000 mm. Sample was analyzed using a coupled 2θ/θ scan type with a continuous PSD fast scan mode. 2θ started at 8.000° and ended at 30.0277° with increments of 0.02151°, while θ started at 4.0000° and ended at 15.0138° with increments of 0.01075°. Step time was 1.000 sec

(i.e., 1025 total steps, effective total time 1157 sec per run). EA-CS samples (approximately 0.5 g) were placed in the specimen holder ring made of PMMA, with 25 mm diameter and 8.5 mm height, rotating at 5°/min during analysis.

4.4. Results and Discussion

4.4.1. Extraction of *p*-coumarate and ferulate from corn stover during EA pretreatment

4.4.1.1. Analysis of ester-linked p-coumarate and ferulate in untreated and EA pretreated corn stover

Similarly to other warm season grasses, maize contains a considerable amount of ester-linked phenolic compounds in the plant cell wall [149, 150], notably hydroxycinnamic acids like *p*-coumaric (*p*CA) and ferulic acid (FA). *p*CA is known to be ester-linked to lignin [151] and there are no evidences in the literature suggesting that this compound has an important role in cross-linking cell wall polymers. In the other hand, FA is described in the literature as being an important bridge, cross-linking arabinoxylan polymers (in the case of diferulates) or even cross-linking arabinoxylans with lignin polymers [152, 153]. By cleaving these ester bonds, is possible to disrupt the ultra-structure of the plant cell wall and therefore, is possible to improve enzyme accessibility to carbohydrate substrates. Most chemical pretreatments have the ability to cleave ester linkages, as both acidic and alkaline conditions result in hydrolysis reactions yielding phenolic acids as the respective products. Ammonia based treatments like EA can also break ester linkages through ammonolysis reactions that yield products like phenolic amides [23, 95, 97]. To evaluate the effect of pretreatment conditions on *p*CA and FA cleavage, a 2 M NaOH treatment at room temperature was performed on UT-CS (control) as well as EA-CS pretreated

under the various conditions (see Box Benhken design on **Table 4-2**). From this analysis, UT-CS showed a *p*CA content of 14.17 mg/g of dried corn stover and an ester-linked FA content of 5.66 mg/g of dried corn stover. *p*CA and ester-linked FA contents in corn stover vary significantly across the various plant tissues. For example, Akin et al. (2006) [148] observed variations of *p*CA from 1.5 mg/g (leaf-blade lamina) to 32.1 mg/g (stem rind) in a Pioneer 3085 corn hybrid. In the same study, ester-linked FA varied from 2.5 mg/g (leaf-blade lamina) to 6.6 mg/g (stem rind). The corn stover used in this study contains a milled mixture of the various fractions of the plant and therefore, the measured amounts of esterified hydroxycinnamic acids are a weighted average from the harvested plant. Literature reports show a large range of *p*CA and FA contents for the whole corn plant, which depends on the hybrid and maturity of the plant [148, 150, 154]. The values measured in this study for *p*CA and FA in untreated corn stover were similar to the numbers reported in the literature.

The esterified *p*CA and FA contents of EA-CS varied significantly with respect to the pretreatment conditions. It is important to note that the measured ester-linked *p*CA and FA from EA-CS, is a result of alkaline hydrolysis of previously extracted samples with ethanol. This extraction method was used to remove residual *p*CA and FA that were cleaved by ammonia, but not totally extracted from the biomass during pretreatment, and therefore provide means to quantify the ester-bound hydroxycinnamic acids in EA-CS. The % cleavage of ester-linked hydroxycinnamic acids after EA pretreatment increased as a function of pretreatment severity, ranging from 5.70 % to 71.96 % for *p*CA and 0.13 % to 76% for FA (% loss referenced to the ester-linked *p*CA and FA in UT-CS). This result suggests that under certain conditions, ammonia is able to effectively cleave ester linkages in the absence of polar solvents, which are often known to catalyze ammonolysis reactions [99]. To further understand how the EA pretreatment

variables affect ester bond cleavage and further extraction of from the plant cell wall during EA pretreatment, a mathematical model based on statistical DOE was implemented. The results for this model will be further discussed below.

4.4.1.2. Response surface analysis: % cleavage of p-coumarate and ferulate as a function of pretreatment conditions.

To obtain a mathematical model describing how ester linkages are cleaved as a function of EA conditions, 40 experimental data points were acquired for *p*CA and FA % cleavage and were subjected to surface response analysis using a full quadratic regression. The terms considered for the regression model were based on their *P* value ($P < 0.05$) and also based on the predictive ability of the resulting model, considering R^2 values, variance and residual analysis. The statistical results obtained in this study are shown in **Figure 4-2** and **Figure 4-3**, which include residual plots, histograms, probability plots, regression coefficients and predicted R^2 values for % cleavage of *p*Ca and FA as a function of the terms considered for each model. The residual plots show that in both cases the residuals are mostly within ± 6 % range. The histograms do not always show a perfect "bell" shaped curve centered in zero, however the greater fraction of the residuals are present between ± 2.5%, as can be observed by the normal probability plots. The goodness of the fits can be evaluated by measuring the R^2 values shown in **Figure 4-2 B** and **Figure 4-3 B**. The predicted R^2 (R-Sq (pred)) value for the regression of % *p*CA cleavage was 98.11 %, while for % FA cleavage was 97.32 %, using the coefficients for the terms shown in **Figure 4-2 B** and **Figure 4-3 B**. These values indicate the ability of the models to predict responses for new observations, and since they are similar to the R^2 and adjusted R^2 values, the

models do not seem to overfit and have adequate predictive ability. The resulting response surface equations for % *p*CA and % FA cleavage are given below:

$$\textbf{\% pCA Cleavage} = (-24.7923) + (0.6028\ X_1) + (3.2131\ X_2) + (1.3931\ X_3) - (0.001\ X_1X_1) - (0.0192\ X_3X_3) + (0.0053\ X_1X_3) - (0.125\ X_2X_3) \quad \textbf{(4-1)}$$

$$\textbf{\% FA Cleavage} = (-14.2344) - (0.204\ X_1) + (2.771\ X_2) + (0.8119\ X_3) + (0.0048\ X_1X_1) - (0.0201\ X_3X_3) + (0.0112\ X_1X_3) - (0.0696\ X_2X_3) \quad \textbf{(4-2)}$$

Where,

X_1 = Temperature (°C) [18.25 to 121.75 °C]; X_2 = NH_3:BM [2.78 to 6.23]; X_3 = Time (min) [3.13 to 31.88 min].

Analyzing the regression coefficients for *p*CA % cleavage it is possible to observe that *temperature*, *NH_3:BM* and *time* are important factors that explain the variability of the experimental data (i.e., $P < 0.05$). Interaction factors *NH_3:BM*NH_3:BM* and *Temperature*NH_3:BM* did not seem to explain the variability of the experimental data, showing *P* values above 0.05 and did not contribute to the improvement of the model. Therefore, these terms were not considered in **Equation (4-1)**.

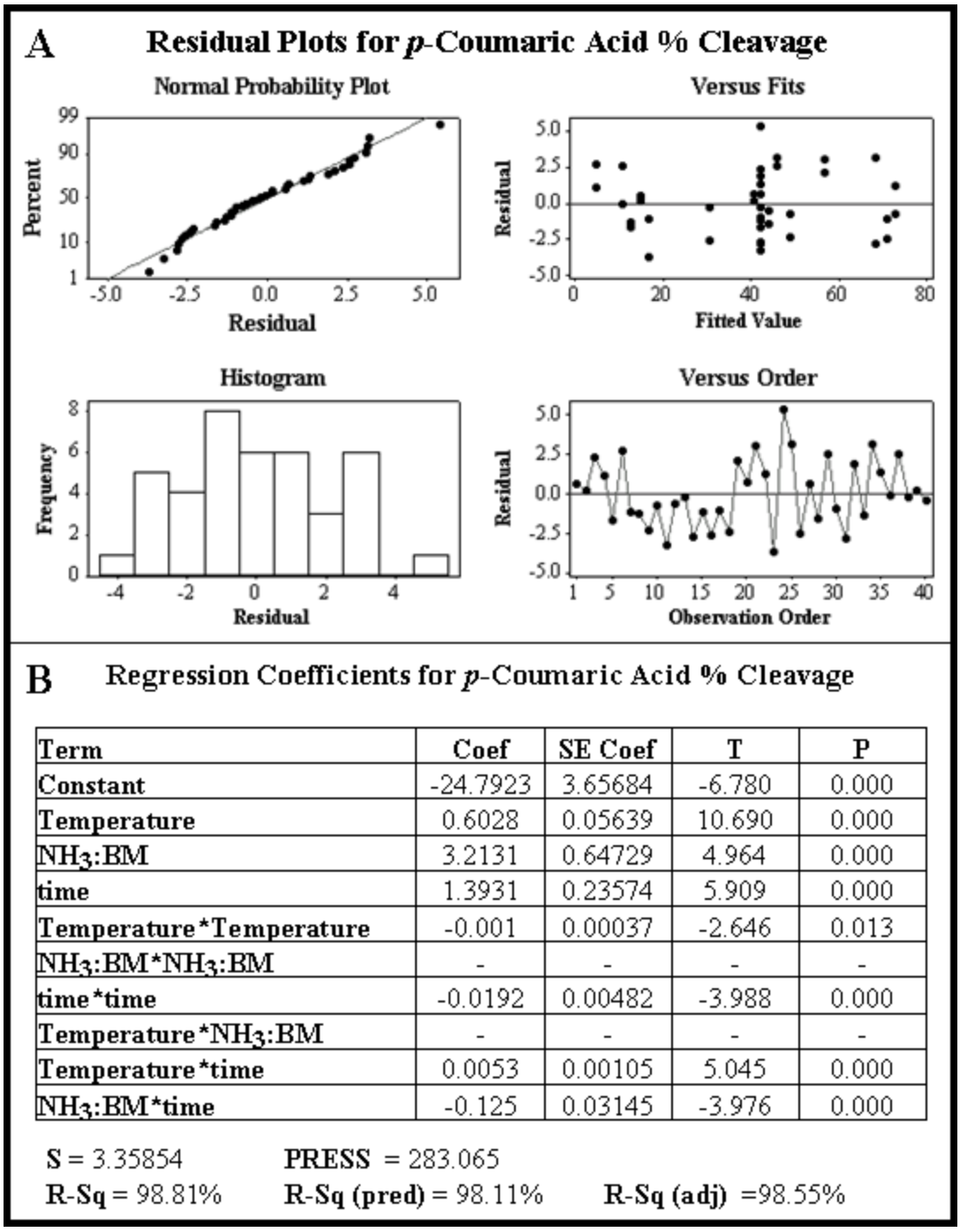

B Regression Coefficients for *p*-Coumaric Acid % Cleavage

Term	Coef	SE Coef	T	P
Constant	-24.7923	3.65684	-6.780	0.000
Temperature	0.6028	0.05639	10.690	0.000
NH_3:BM	3.2131	0.64729	4.964	0.000
time	1.3931	0.23574	5.909	0.000
Temperature*Temperature	-0.001	0.00037	-2.646	0.013
NH_3:BM*NH_3:BM	-	-	-	-
time*time	-0.0192	0.00482	-3.988	0.000
Temperature*NH_3:BM	-	-	-	-
Temperature*time	0.0053	0.00105	5.045	0.000
NH_3:BM*time	-0.125	0.03145	-3.976	0.000

S = 3.35854 **PRESS** = 283.065
R-Sq = 98.81% **R-Sq (pred)** = 98.11% **R-Sq (adj)** =98.55%

Figure 4-2 (A) Residual plots for the regression of ester-linked *p*CA % cleavage as a function of pretreatment variables (temperature, time and NH_3:BM ratio) and respective interaction terms. Residuals and fitted values are expressed in (% cleavage). Regression terms were only considered if their *P* value was smaller than 0.05. (B) Estimation of regression coefficients and *P* values for the terms affecting ester-linked *p*-coumaric acid % cleavage. Parameters that determine the goodness of the fit are also shown.

A

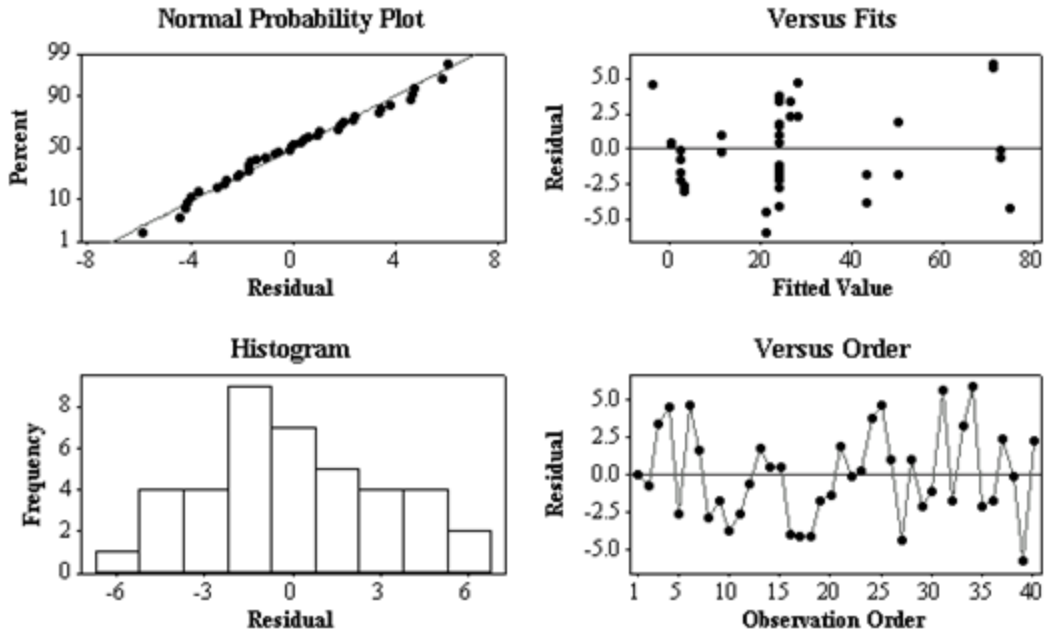

B Regression Coefficients for Ferulic Acid % Cleavage

Term	Coef	SE Coef	T	P
Constant	-14.2344	5.22436	-2.725	0.01
Temperature	-0.204	0.08056	-2.532	0.016
NH_3:BM	2.771	0.92475	2.996	0.005
Time	0.8119	0.3368	2.411	0.022
Temperature*Temperature	0.0048	0.00053	9.016	0
NH_3:BM*NH_3:BM	-	-	-	-
time*time	-0.0201	0.00689	-2.922	0.006
Temperature*NH_3:BM	-	-	-	-
Temperature*time	0.0112	0.0015	7.486	0
NH_3:BM*time	-0.0696	0.04493	-1.55	0.131

S = 3.36954 **PRESS** = 594.655
R-Sq = 98.36% **R-Sq (pred)** = 97.32% **R-Sq (adj)** = 98.00%

Figure 4-3 (A) Residual plots for the regression of ester-linked FA % cleavage as a function of pretreatment variables (temperature, time and NH_3:BM ratio) and respective interaction terms. Residuals and fitted values are expressed in (% cleavage). Regression terms were only considered if their *P* value was smaller than 0.05. (B) Estimation of regression coefficients and *P* values for the terms affecting ester-linked ferulic acid % cleavage. Parameters that determine the goodness of the fit are also shown.

The model used to predict ester-linked FA % cleavage considered the same terms used in the *p*CA % cleavage model. An important aspect that was taken in consideration during the formulation of this model is related to the interaction term *NH_3:BM*time*, that shows a *P* value above 0.05 (**Figure 4-3 B**), suggesting that this term is not related to ester-linked FA % cleavage. However, during optimization of the model, this term impacted the goodness of the fit (R^2), the predictive ability of the model (predicted R^2) and residual values. Therefore, this term was included in **Equation (4-2)**.

To simplify this discussion and visualize the effects of the various pretreatment parameters on the cleavage of ester-linked *p*CA and FA during EA pretreatment, graphical representations of the two models are shown in **Figure 4-4 A** and **Figure 4-4 B**, respectively. The contour plot from **Figure 4-4 A-I** predicts a gradual increase in ester bond cleavage from *p*CA with respect to temperature for a fixed NH_3:BM loading of 6:1. It is also possible to observe a positive effect of pretreatment time on *p*CA % cleavage from the same counter plot. In **Figure 4-4 A-II**, it can be observed an almost linear increase of *p*CA % cleavage with respect to temperature and practically no dependence of NH_3:BM loading for a fixed time of 30 min. At the same time, **Figure 4-4 A-III** shows some dependence between *p*CA % cleavage and NH_3:BM loading for the lower residence times, while at the higher residence times (approaching 30 min) this dependence is significantly decreased (for a fixed temperature of 115 °C). Taking in consideration that this reaction is heterogeneous, is possible that this profile is a result of transport phenomena, where a longer time is required for the ammonia to reach the inner pores of the biomass particles for the lower NH_3:BM loadings. However, detailed kinetic studies should

be performed to confirm this dependence and properly determine transport and reaction parameters, which are not included in this study.

A similar reaction profile was achieved for FA cleavage. However, major differences between rates of FA and *p*CA cleavage seem to be associated with kinetic parameters, notably activation energy (Ea), as the temperature dependence profile is the most distinct between the two reactions. For example, it is clear that the ester bonds linking FA to carbohydrates start to be effectively cleaved at temperatures above 40 °C, while ester-linked *p*CA is effectively cleaved even at 20 °C. Also, is visible that at higher temperatures, similar percentages of ester bonds are cleaved in FA as in *p*CA. This observation supports the idea that the differences between these two reactions could derive mainly from differences in Ea, as is clear that the rate of cleavage of ester bonds from FA is more sensitive to temperature (**Figure 4-4 A-I** and **B-I**).

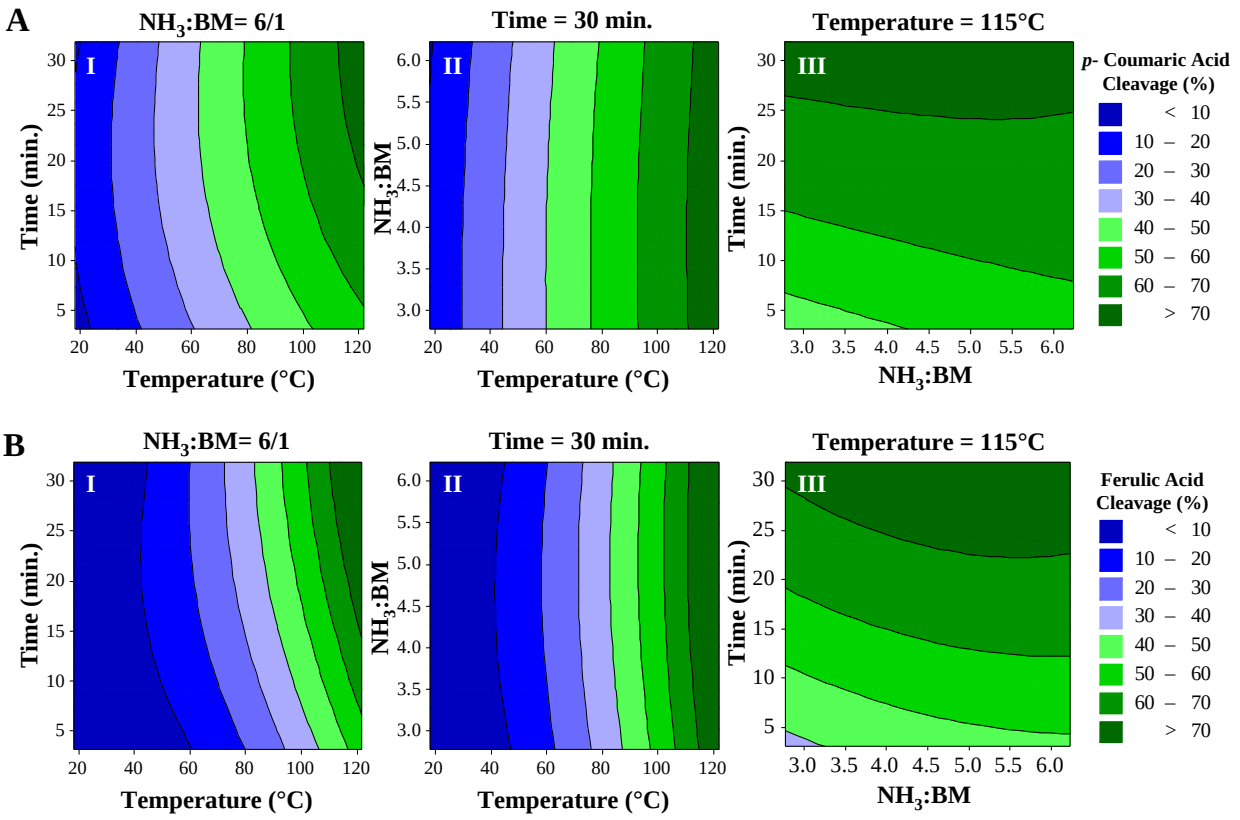

Figure 4-4 Contour plots describing % cleavage of ester-linked *p*-coumaric (A) and ferulic acid (B) as a function of EA pretreatment conditions. Experimental values were calculated based on the content of ester-linked *p*-coumaric and ferulic acids present in corn stover prior to EA pretreatment. The contour plots represent a small area of the universe described by the respective mathematical models, with fixed values of NH3:BM = 6/1 (I), time = 30 min (II) and temperature = 115 °C (III).

4.4.2. Extraction of lignin from corn stover during EA pretreatment

4.4.2.1. Analysis of lignin extraction in untreated and EA pretreated corn stover

The lignin present in EA-CS was quantified using the NREL protocol, excluding both ethanol and water extraction steps, as these solvents can remove lignin components from the pretreated biomass. If we included these steps in the composition analysis method, we would be overpredicting lignin extraction during EA pretreatment. The untreated corn stover was analyzed

according to the original protocol and showed 14 % Klason lignin and 2 % acid soluble lignin contents. The % lignin extraction was calculated based on the lignin content determined before and after pretreatment.

During EA pretreatment of corn stover, several components of the biomass were extracted, of which lignin was the most abundant. Lignin extraction values ranged from 16.1 to 45.5 wt% of the original lignin present in untreated corn stover. Ammonia is known to be a good solvent for lignin extraction and has been used for lignocellulose pulping, usually in aqueous solutions with and without potassium hydroxide [155]. It has also been used in the supercritical state for pulping feedstocks like bamboo or yellow poplar [156]. A recent study from Zhongguo Liu and co-workers (2012) [157], showed that by using aqueous ammonia at concentrations around 30 wt% and temperatures of 120 °C was possible to extract about 61.7 wt% of the lignin from *Miscanthus*. From the same study, a temperature of 180 °C achieved a delignification of 76.9 wt%. However, such conditions also promoted the decomposition and extraction of carbohydrate components, notably cellulose (~88 to ~94 wt% recovery) and hemicellulose (~39 to ~69 wt% recovery). The technology proposed in this manuscript (i.e., EA pretreatment) attempts to maximize lignin extraction while preserving the structural carbohydrates intact in the solid phase, which can then be converted to fermentable sugars during enzymatic hydrolysis. In **Figure 4-5** it is possible to compare the composition of EA-CS referenced with respect to UT-CS. In this chart, EA pretreatment was performed under conditions that maximize lignin extraction within the boundaries of this study and the limitations of the equipment, i.e., temperature = 120 °C, NH_3:BM = 6:1 and time = 30 min. From these results, it is clear that while lignin was the major component removed from corn stover, structural carbohydrate

composition was not significantly reduced during EA pretreatment (< 5 % reduction). Comparing these results to the study by Liu and co-workers (2012) [157], where lignin from *Miscanthus* was extracted using aqueous ammonia, EA pretreatment reveals lower effectiveness for biomass delignification (~44 wt% compared with ~62 wt% at similar processing conditions). However, an important advantage is that anhydrous ammonia appears to be more selective to lignin extraction than aqueous ammonia. For example, Liu and co-workers (2012) [157] showed cellulose and hemicellulose recoveries of 94.4±0.9 % and 69.2±1.0 %, respectively, while the lowest glucan and xylan recoveries obtained during EA pretreatment were 93.6 ± 0.2 % and 95.6 ± 0.4 %, respectively. Other authors that used aqueous ammonia solutions for delignification, often in supercritical state, observe lower recoveries of hemicellulose than cellulose [158]. This trend was not observed when treating corn stover with anhydrous ammonia under sub-critical conditions, as both xylan and glucan recoveries were approximately equal.

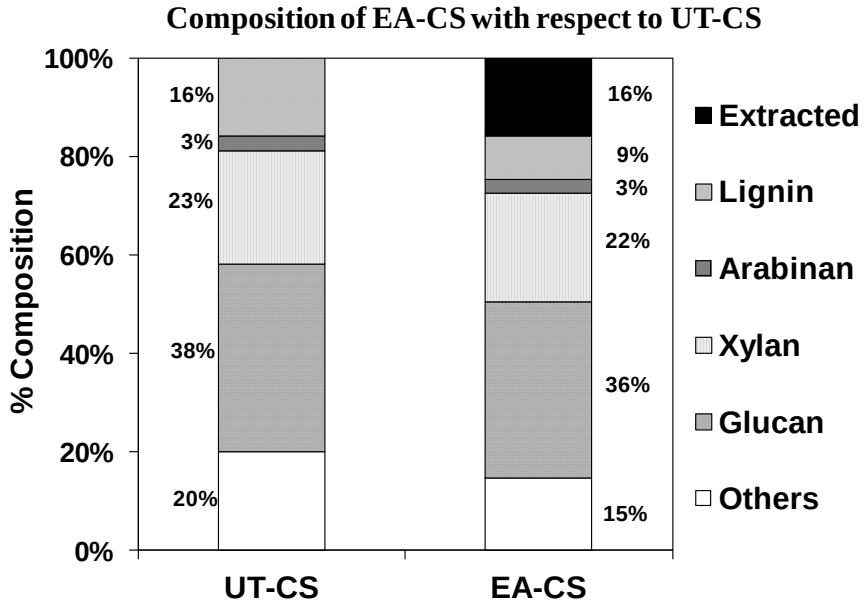

Figure 4-5 Stacked bar chart comparing the mean values for the composition of EA pretreated corn stover (EA-CS) with respect to the untreated corn stover (UT-CS). The pretreatment

Figure 4-5 (cont'd)

condition used for this chart was temperature = 121.8 °C , NH_3:BM loading of 6.2:1 and residence time of 32 min, which represents the highest severity within the boundary conditions defined for EA pretreatment in this work. In this analysis, only structural carbohydrates from the plant cell wall and Klason lignin were considered. Coefficients of variation were below 2.5 % for all measurements.

4.4.2.2. Response surface analysis: % lignin extraction as a function of pretreatment conditions

A mathematical model was formulated based on 40 experimental points expressing the % delignification at various pretreatment conditions (see **Table 4-2** for the experimental design). A surface response analysis using a quadratic regression model was performed using the terms with a *P* value below 0.05 and also other terms that improved the predictive ability of the model, considering predicted R^2 values, variance and residual analysis of the regression. The statistical results obtained in this study are shown in **Figure 4-6**. The residual plots in **Figure 4-6 A** show that the residuals for the regression model were mostly within ± 5 % range. The predicted R^2 value of this regression was 84.83 %, which was relatively similar to the R^2 (90.30 %) and adjusted R^2 (88.54 %) values. These results suggest that the model has good ability to predict unknown observations and is not overfitting experimental data.

The residuals are randomly spread around the regression line, implying the absence of a systematic lack-of-fit. The histogram does not show a perfect "bell shape" curve, however most of the residuals have a value close to zero. The highest number of residuals are located in the negative region of the histogram, however many of these negative residuals correspond to

replicates of the middle point condition, which fit below the regression curve as it can be observed in the residual ("versus fits") plot from **Figure 4-6 A**.

A

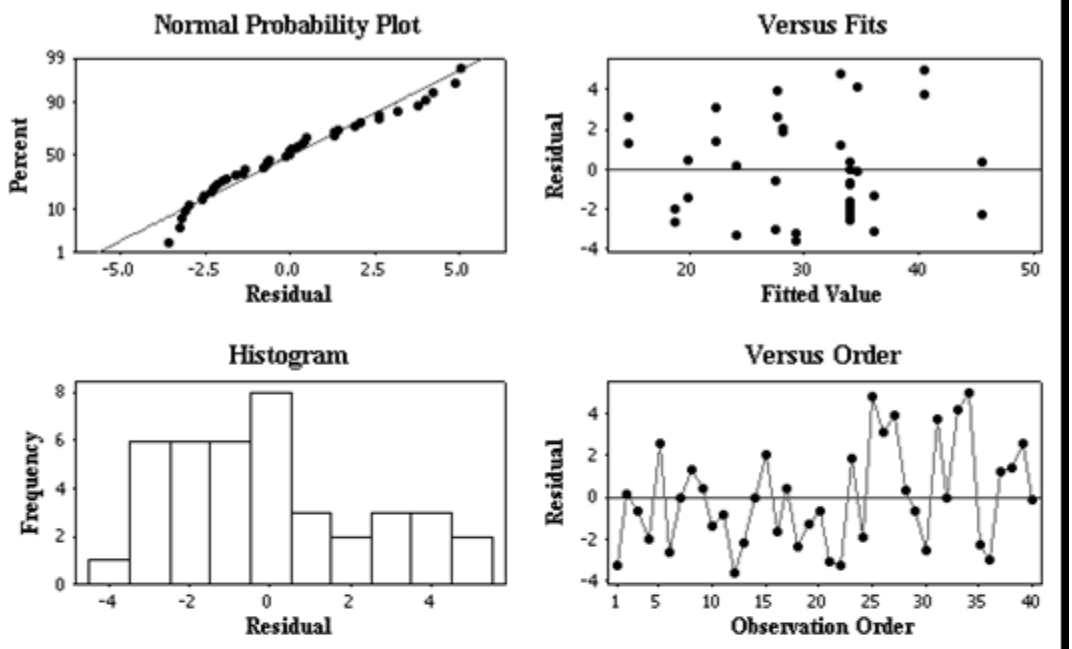

B

Regression Coefficients for Lignin % Extraction

Term	Coef	SE Coef	T	P
Constant	4.27832	7.7474	0.552	0.585
Temperature	-0.21178	0.04595	-4.609	0
NH_3:BM	5.48885	3.4754	1.579	0.124
Time	1.43314	0.19506	7.347	0
Temperature*Temperature	0.0048	0.00053	9.016	0
NH_3:BM*NH_3:BM	-0.96579	0.37614	-2.568	0.015
time*time	-0.03028	0.00542	-5.59	0
Temperature*NH_3:BM	0.07482	0.00981	7.627	0
Temperature*time	-	-	-	-
NH_3:BM*time	-	-	-	-

S = 2.64888 **PRESS** = 362.983
R-Sq = 90.30% **R-Sq (pred)** = 84.83% **R-Sq (adj)** = 88.54%

Figure 4-6 (A) Residual plots for the regression of % lignin extraction as a function of pretreatment variables (temperature, time and NH3:BM ratio) and respective interaction terms.

Figure 4-6 (cont'd)

Residuals and fitted values are expressed in (% extraction). (B) Estimation of regression coefficients and *P* values for the terms affecting % lignin extraction. Parameters that determine the goodness of the fit are also shown.

Figure 4-6 B shows the terms that were considered in the mathematical model describing % lignin extraction as a function of EA pretreatment conditions. The *constant* and *NH_3:BM* terms have a *P* value higher than 0.05, suggesting that are not related to % lignin extraction. However, they were included in the regression model as they impacted substantially the goodness of the fit to the experimental data and the predictability of the model (predicted R^2). The interaction terms *temperature*time* and *NH_3:BM*time* were not considered in the model as their *P* value was higher than 0.05 and they did not improve the fit of the model to the experimental data. As a result, the mathematic equation that best described % lignin extraction as a function of pretreatment conditions is as follows:

$$\textbf{\textit{\% Lignin Extraction}} = (4.27832) - (0.21178\ X_1) + (5.48885\ X_2) + (1.433314\ X_3) + (0.0048\ X_1X_1) - (0.96579\ X_2X_2) - (0.03028\ X_3X_3) + (0.07482\ X_1X_2) \quad \textbf{(4-3)}$$

Where,

X_1 = Temperature (°C) [18.25 to 121.75 °C]; X_2 = NH_3:BM [2.78 to 6.23]; X_3 = Time (min) [3.13 to 31.88 min].

A series of contour plots expressing % lignin extraction as a function of pretreatment conditions are shown in **Figure 4-7**. These contour plots represent a region of the universe described by **Equation (4-3)**, with fixed parameters at 120 °C, NH_3:BM loading of 6:1 and 30 min of residence time. **Figure 4-7 I** shows the increase in delignification as a function of temperature and time, where a minimum delignification of ~11% (at 18.25 °C and 3 min) and a maximum delignification of ~48% (at 120 °C and 25 min) were achieved according to the regression model. Kinetic models based on ammonia pulping experiments often show three phases of delignification, with distinct rates and temperatures at which delignification occurs. Lignin is a heterogeneous polymer, with various levels of hydrophilicity, molecular weights and diverse chemical linkages. Therefore, the decomposition and solubilization of these various fractions of lignin require distinct conditions. In contrast with most pulping methods that use hydroxyl ions as a primary reactant, EA pretreatment uses anhydrous ammonia, which acts as a solvent and a reactant. Ammonia is expected to cleave ester bonds in the biomass but not the abundant ether bonds that support the lignin structure. Pulping methods that use high concentrations of hydroxyl ions are able to cleave ether bonds, reducing the lignin molecular weight and thereby facilitating solubilization as well as extraction [159]. Lower molecular weights and hydrophilic lignins should also be more susceptible to ammonia solubilization and it is possible that these are the native properties of the lignin extracted at lower temperatures and residence times. However, future research should be performed to confirm this hypothesis. *p*-Coumarate ester bond cleavage during EA pretreatment occurs at mild conditions, as can be observed in **Figure 4-4 A**. This fact suggests that even at these conditions ester-linked components of the lignin are being cleaved and solubilized by ammonia. As a general observation, is important to mention that in

the literature, lignin from grasses such as rice straw or wheat straw can be delignified with milder temperatures and shorter residence times compared to wood [155, 156, 160]. This difference is often attributed to a higher porosity observed in grasses that facilitates the penetration of the pulping chemicals and differences in lignin chemistry [155, 160]. These distinct properties of grass lignins compared with lignins from woods are becoming more evident in recent years. For example, recent work developed by Jose C. del Rio and coworkers (2012) [161] about characterization of lignin from wheat straw, showed a substantial level of tricin units incorporated in the lignin, which has not been observed in wood lignin.

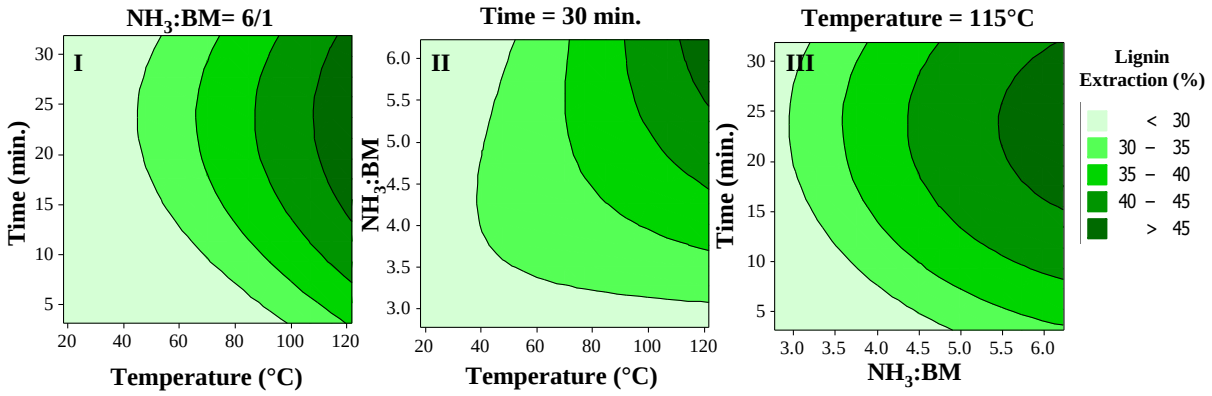

Figure 4-7 Contour plots describing % lignin extraction as a function of EA pretreatment conditions. Experimental values were calculated based on the lignin content in corn stover prior to EA pretreatment. The contour plots represent a small area of the universe described by the respective mathematical models, with fixed values of NH3:BM = 6/1 (I), time = 30 min (II) and temperature = 115 °C (III).

Figure 4-7 II and **III** shows the expected profile, where delignification is improved with increasing temperature and NH_3:BM loading. These contour plots show that efficient delignification (>45 %) occurs at temperatures ranging between 115 and 120 °C with residence times above 15 min and NH_3:BM loadings above 5.5:1. This result suggests that delignification

is favored by high liquid-to-solid ratios and higher temperatures, which consequently generates higher operating pressures (~1200 psi), increasing pretreatment capital cost. However, the effect of delignification on downstream processing, including enzymatic hydrolysis and fermentation must be evaluated before a balanced economic assessment is done. Moreover, lignin valorization is an area of great economic potential [26, 162] and the development of new technologies for lignin upgrading could be instrumental towards the feasibility of this process.

4.4.3. Enzymatic hydrolysis of EA pretreated corn stover

4.4.3.1. Enzymatic digestibility of EA pretreated corn stover

Enzymatic digestibility of the EA-CS was evaluated as a function of pretreatment conditions. In this work, monomeric glucan and xylan conversions after 24h enzymatic hydrolysis were calculated based on the composition of the EA pretreated biomass. However, the carbohydrate loss is not significant in most of the pretreatment conditions, reaching a maximum of 6.4 ± 0.2 % glucan and 4.4 ± 0.4 % xylan for the most severe conditions (i.e. Temperature = 121.8 °C , NH_3:BM loading of 6.2:1 and residence time of 32 min). The variables temperature, NH_3:BM loading and residence time are known to significantly impact the physicochemical properties of ammonia treated cell walls [145]. By varying ammonia pretreatment conditions it is possible to generate a wide variety of properties, which include cellulose III conversion, degree of delignification, level of ester bond cleavage, porosity and level of inhibitory compounds for microbes and enzymes [23, 95, 105, 145]. These properties have significant effects on enzymatic digestibility of the plant cell wall and therefore, pretreatment can be manipulated to create favorable conditions for enzymatic action. Not all these properties will be discussed and

analyzed here, however, it is important to discuss those aspects that are unique in this novel ammonia-based pretreatment, notably cellulose III conversion and degree of delignification. The importance of ester bond cleavage will be also discussed herein, as it shows a good correlation to enzymatic digestibility of corn stover.

From **Figure 4-8 (A1, B1 and C1)** it is possible to observe glucan and xylan conversions (24h enzymatic hydrolysis) achieved by EA-CS pretreated in a wide range of temperatures, NH_3:BM loadings and residence times. These conditions were established by a Box Behnken design, as described previously. The same EA pretreated samples were subjected to XRD analysis to differentiate the crystalline state of cellulose. From these analyses, a series of spectra were generated and are presented in **Figure 4-8 (A2, B2 and C2)**. A substantial amount of work has been done on cellulose III, where improvements of 2-5 fold have been observed for monomeric glucose conversions in isolated cellulose (e.g. Avicel). However, to our knowledge there are no reports of the effect of cellulose III conversion on the enzymatic hydrolysis of lignocellulosic biomass, including corn stover, which will be discussed herein.

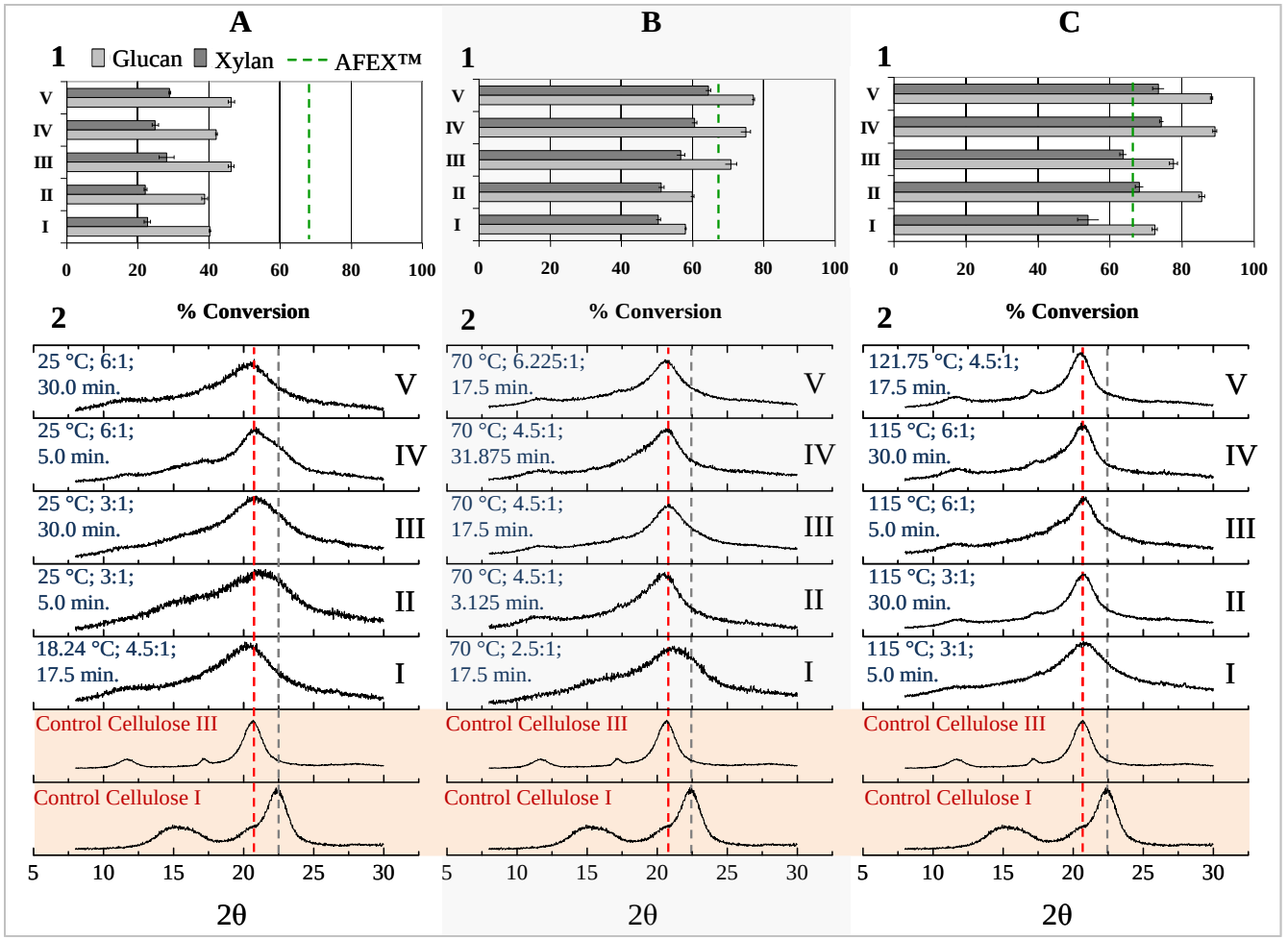

Figure 4-8 Conversions to monomeric glucose and xylose after 24 h enzymatic hydrolysis of various EA-CS samples (A1-C1). Glucan conversion of optimally pretreated AFEX-CS is indicated by a green dashed line. XRD spectra from EA-CS as a function of pretreatment conditions (A2-C2). EA conditions are located in the top left corner of each XRD spectra and include temperature; NH_3:BM loading and time, in this respective order. Cellulose I and III controls are Avicel and ammonia treated Avicel, respectively.

One of the major bottlenecks when analyzing cellulose crystallinity from lignocellulosic biomass is that there is a lack of quantitative methods to measure amorphous cellulose, cellulose I and III when they are simultaneously present in same sample. Besides the peak convolution problem in techniques like XRD, the major difficulty is associated with the presence of lignin and other amorphous components that compose lignocellulosic biomass, which may vary significantly between samples that were treated under different regimes. Biomass bleaching followed by FT-Raman is a potential technique that can help solve this problem in the future [163, 164]. However, as this method is still not developed for cellulose III, it could not be applied in the present research. Despite the analytical limitations, it is possible to perform a qualitative evaluation of the effects that each pretreatment condition had on the crystallinity of the pretreated sample by XRD analysis. From the results shown in **Figure 4-8**, it was possible to conclude that cellulose III is formed for all the conditions within the boundaries of this study. One of the important requirements of cellulose III conversion is that the biomass must be in contact with liquid ammonia, in the absence of moisture [80]. However, our work shows that even at an NH_3:BM ratio of 2.5:1 and 10% moisture in the corn stover, some level of cellulose III conversion occurred (**Figure 4-8 B2-I**), revealed by the presence of a peak at 2θ = ~20.5° (highlighted by a red dashed line). Nevertheless, it is clear that higher liquid-to-solid ratios accelerate the formation of cellulose III in corn stover by analyzing the XRD spectra in **Figure 4-8 A2-II to A2-V** and **C2-I to C2-IV**. As was previously observed in Avicel (**CHAPTER 1**), lower temperatures in the vicinity of 25 °C are sufficient to observe cellulose III conversion, however it was clear that higher temperatures favor the rate at which cellulose III is converted. For example, at 6:1 NH_3:BM loading cellulose I was not fully transformed into cellulose III at

25 °C and 5 min residence time (**Figure 4-8 A2-IV**), while at 115 °C, total conversion to cellulose III is shown by the disappearance of a peak at 2θ = ~22.5° (highlighted by a grey dashed line) (**Figure 4-8 D2-III**). Also at higher temperatures, it is clear that the XRD peaks from cellulose III become sharper. This phenomenon is a result of higher cellulose III conversion (as discussed in **CHAPTER 1**) and of the lower lignin content of samples that were pretreated at higher temperatures (**Figure 4-7**). The combination of these two properties (i.e., cellulose III formation and lignin removal) was expected to improve enzymatic digestibility of lignocellulosic biomass and, indeed, these results suggest that samples with higher levels of cellulose III conversion and lower lignin content are the most susceptible to enzymatic digestion of the carbohydrates, as demonstrated by the sugar conversions from **Figure 4-8 (A1-C1)**. The lowest glucan and xylan conversions obtained in this study were 38.7 % and 22.1%, respectively, which corresponded to an EA pretreatment performed at 25 °C, with 3:1 NH_3:BM loading and 5 min of residence time (**Figure 4-8 A-II**). From the XRD spectra, this sample has low crystallinity and contains a mixture of cellulose I and III from the presence of convoluted peaks in the region of 2θ between ~20.5 and ~22.5°. The highest sugar yields were observed at higher temperatures and liquid–to-solid ratios, from EA conditions **C-IV** and **C-V**. Both conditions had similar enzymatic hydrolysis results, showing 89.0 % and 88.1 % of glucan conversion, respectively. Xylan conversions were 74.3 % and 73.4 %, respectively. The XRD spectra of these samples confirm total cellulose III conversion and lower levels of amorphous components in the biomass compared to other conditions, which shows that a substantial amount of lignin is removed during EA pretreatment at higher temperatures. Even though XRD data does not allow a quantitative correlation between cellulose III conversion and sugar yields, lignin correlations with enzymatic

hydrolysis performance can be measured to support our hypothesis that lignin removal is an important factor that enhances enzymatic hydrolysis yields in EA pretreatment. **Figure 4-9** correlates % glucan conversion with % lignin extraction, where we observe a positive correlation between these two variables. The R^2 shown in **Figure 4-9** measures the variability in the data set that is accounted by the linear regression model in the same figure. Therefore, this linear model can explain 52.9 % of the variability in the experimental points. This result can be explained by the fact that lignin removal is not the only factor contributing to higher cellulose digestibility; however, is certainly a factor that contributes positively to glucan conversion, as the *P* value for this regression term was 0.000. The *P* value is the observed significance level of the test, i.e., the hypothesis that there is a correlation between glucan conversion (%) and lignin extraction (%).

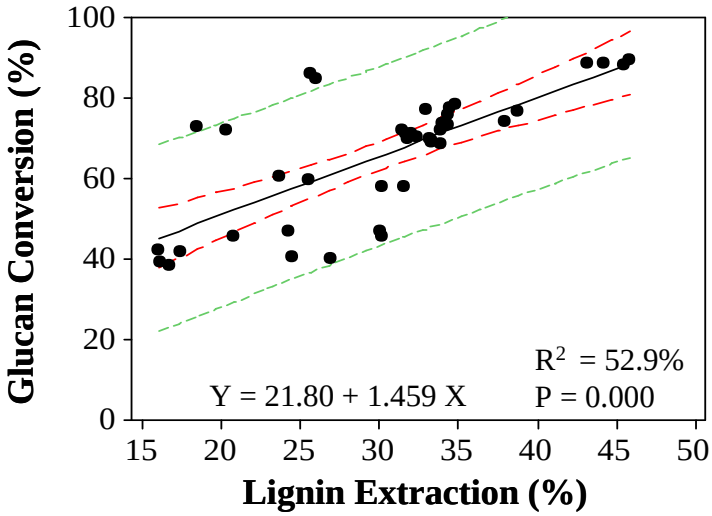

Figure 4-9 Correlation of % glucan conversion as a function of % lignin extraction. The regression had a *P* value = 0.000 for the term % lignin extraction, suggesting that lignin extraction is related to % glucan conversion. The regression (black line), 95 % confidence interval (red line) and 95 % prediction interval (green line) are shown in the graphic.

As the *P* value is lower than the significance level (i.e., 0.05), we can reject the null hypothesis that states that there is no significant correlation between the two variables in the test. The

correlation between glucan conversion and lignin extraction was previously observed by other authors when performing other pretreatments of lignocellulosic biomass [157, 165].

Another factor that is important for sugar conversion is the level of ester bond cleavage in the biomass. The cleavage of ferulic acid and *p*-coumaric acid by ammonia are critical events for disrupting the ultra-structure of the plant cell wall, including cross-links between lignin and carbohydrates. In AFEX^{TM} pretreatment, these reactions help to release cell wall components that are further solubilized and deposited in the surface of the biomass [145]. In EA pretreatment, is likely that these same components are being extracted from the cell wall, creating pores and better access routes for enzymes to target the carbohydrates, similarly to AFEX^{TM} [145]. Previous work has correlated enzymatic digestibility with ferulate and coumarate cleavage for AFEX^{TM} [23], however this correlation was not yet been confirmed under operating conditions such as the ones used during EA pretreatment. Therefore, the results obtained for ferulate and coumarate cleavage during EA pretreatment were correlated with glucan and xylan conversions (**Figure 4-10**).

In all cases presented in **Figure 4-10**, it is possible to observe good linear correlation with R^2 values between 73.5 % and 93.1 %. The *P* values for all linear regressions were 0.000, which means that the terms ferulic acid and *p*-coumaric acid % cleavage are related with glucan and xylan conversions. It is also possible to observe that *p*-coumaric acid cleavage seems to be a better indicator of sugar conversion than ferulic acid, given the higher R^2 values and better fit to the linear regression (**Figure 4-10 B and D**). This result is derived from the fact that the points of low ferulic acid cleavage do not follow the linear trend of the remaining points and therefore,

a quadratic regression would result in a better fit for these correlations (**Figure 4-10 A and C**). However, the main purpose of these correlations is to prove the importance of such events during ammonia pretreatment, providing insight to the scientific community about the aspects that most contribute to biomass recalcitrance, so they can be addressed properly in future research.

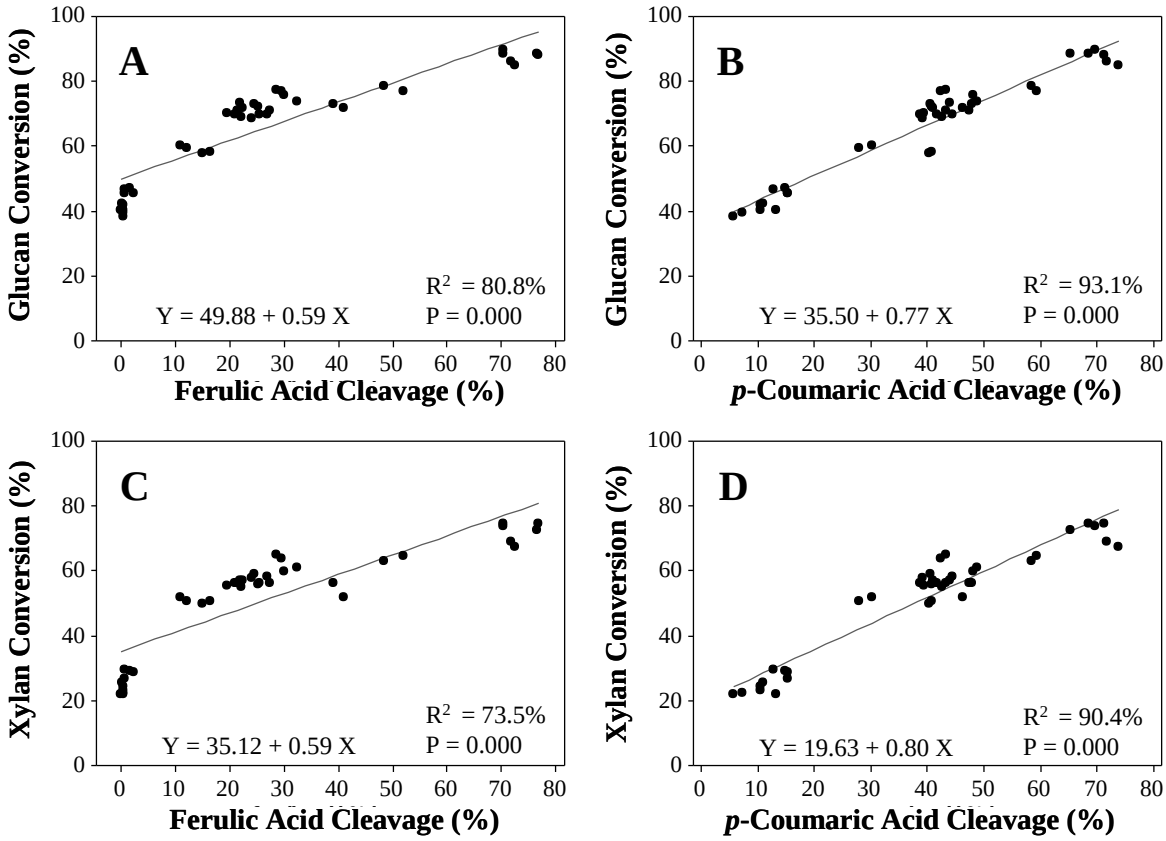

Figure 4-10 Linear regressions correlating glucan (A) and xylan (C) conversions with ferulic acid cleavage, as well as correlating glucan (B) and xylan (D) conversions with p-coumaric acid cleavage. Regression equations P values and R2 values are indicated in the bottom of each graphic.

4.4.3.2.Response surface analysis of enzymatic hydrolysis performance of EA pretreated corn stover

A response surface analysis was also performed on glucan and xylan conversion as a function of pretreatment conditions. The same Box Behnken experimental design used in lignin and ester bond cleavage analysis was applied for sugar conversion. Enzymatic hydrolysis results were obtained after 24 h incubation with an optimized enzyme cocktail as described in the Methods section. **Figure 4-11** shows the residual plots, histograms and the coefficients associated with the terms that better describe glucan conversion with respect to EA pretreatment conditions. From the residual plots, we can observe that the experimental points are relatively dispersed and evenly cover all the range of fitted values. There is no recognizable pattern in the residual plot (versus fits), however there is a region between 45 and 70% conversion where the all residuals are negative. This indicates that in that region the model overpredicts glucan conversion. Nevertheless, the residuals vary between -6 and 7 % and the highest residuals were observed between 5 and 70% glucan conversion. The histogram shows a good "bell shape" curve centered on zero, which means that most of the values fitted the model well. The regression coefficients used in this model are presented in **Figure 4-11 B** and were the coefficients that gave a better fit to the experimental data. Most of the terms used in this model have a *P* value below 0.05 with the exception of the constant (P value = 0.327) term and time (P value = 0.079). This suggests that these two terms do not relate to glucan conversion. However, the absence of these terms in the mathematical model impacts negatively the fit to experimental data. Considering these terms, the predicted R^2 value for this model is 94.73 %, which is similar to the R^2 (96.64 %) and adjusted R^2 (96.03 %) values. This result suggests that the model has a good fit to the

experimental data. The resulting model equation that predicts 24h % glucan conversion as a function of EA pretreatment variables is as follows:

$$\textbf{24h \% Glucan Conversion} = (-8.4167) - (0.7285\ X_1) + (12.3293\ X_2) + (0.2021\ X_3) - (0.0025\ X_1X_1) - (1.1312\ X_2X_2) + (0.0028\ X_1X_3) \quad \textbf{(4-4)}$$

Where,

X_1 = Temperature (°C) [18.25 to 121.75 °C]; X_2 = NH_3:BM [2.78 to 6.23]; X_3 = Time (min) [3.13 to 31.88 min].

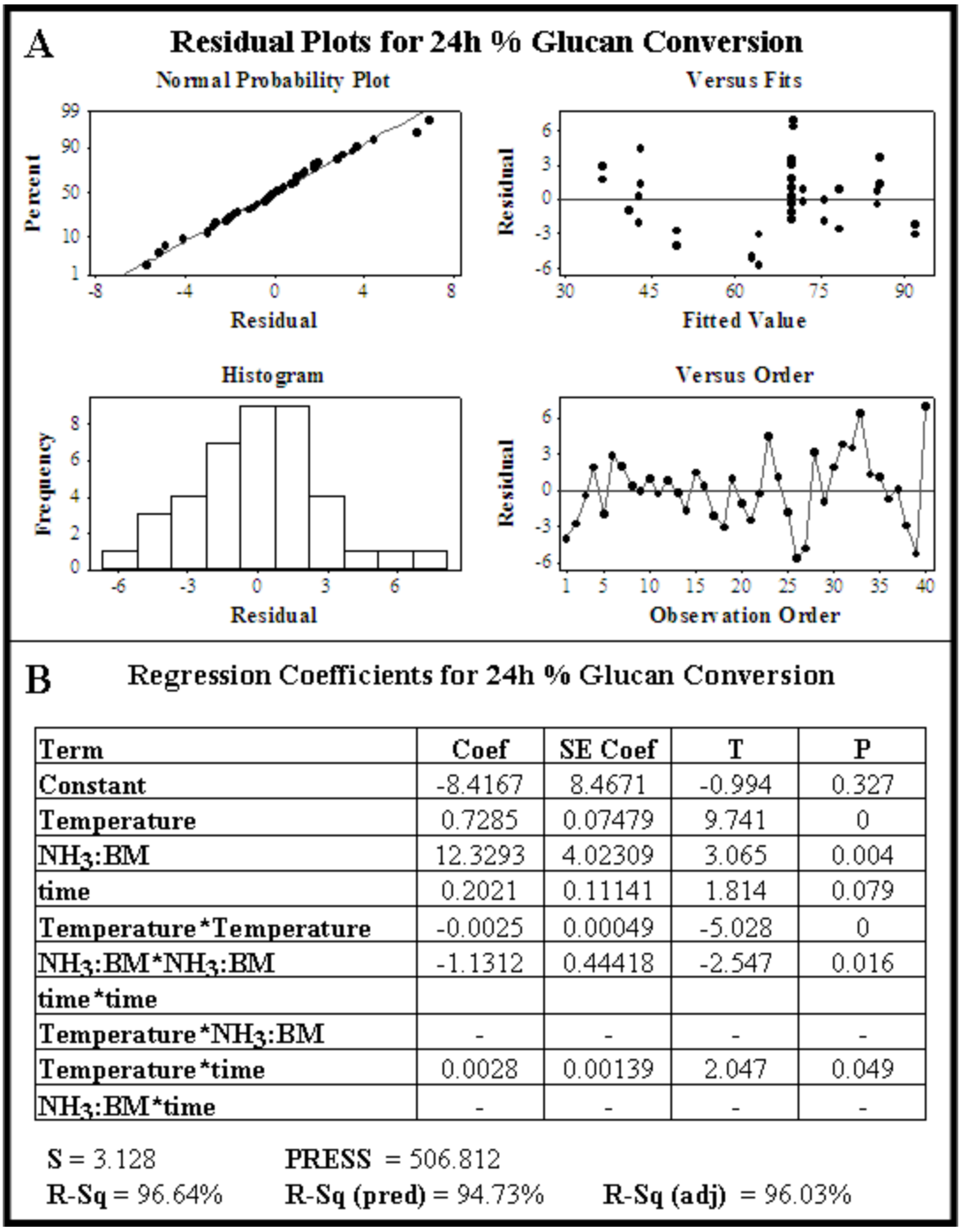

B Regression Coefficients for 24h % Glucan Conversion

Term	Coef	SE Coef	T	P
Constant	-8.4167	8.4671	-0.994	0.327
Temperature	0.7285	0.07479	9.741	0
NH_3:BM	12.3293	4.02309	3.065	0.004
time	0.2021	0.11141	1.814	0.079
Temperature*Temperature	-0.0025	0.00049	-5.028	0
NH_3:BM*NH_3:BM	-1.1312	0.44418	-2.547	0.016
time*time				
Temperature*NH_3:BM	-	-	-	-
Temperature*time	0.0028	0.00139	2.047	0.049
NH_3:BM*time	-	-	-	-

S = 3.128 **PRESS** = 506.812
R-Sq = 96.64% **R-Sq (pred)** = 94.73% **R-Sq (adj)** = 96.03%

Figure 4-11 (A) Residual plots for the regression of 24h % glucan conversion to monomeric glucose as a function of pretreatment variables (temperature, time and NH3:BM ratio) and respective interaction terms. Residuals and fitted values are expressed in (% conversion). (B) Estimation of regression coefficients and *P* values for the terms affecting % glucan conversion. Parameters that determine the goodness of the fit are also shown.

The same methodology was applied to develop a regression model that predicts xylan conversion with respect to pretreatment variables. **Figure 4-12** shows the residual plots and histogram for the regression, as well as the coefficients from the terms used in this model. From the residual we can observe that the residuals show a small range, between -4 and 4%. This is a good indication that all the predicted values are close to the experimental values. The residuals are randomly spread; however there is a slight tendency to observe greater residual values at higher xylan conversions. One other remark about this model is that, in the region between 40 and 50 % xylan conversion, there are no experimental data to fit the curve. Therefore, the model could not be properly tested in that region of the curve, which could lead to a flawed prediction. However, as this is a relatively small area of xylan conversions, the model was still considered acceptable. The histogram shows a profile close to a normal distribution, which indicates the model predictions are more often closer to the experimental results than the opposite. The terms used in the regression model are presented in **Figure 4-12 B**, as well as the respective coefficients. Most of the terms have a *P* value below 0.05, with the exception of NH_3:BM and NH_3:BM*NH_3:BM, which were included in the model due to the fact that their absence decreases the predicted R^2 value and increases the amplitude of the residuals. Nevertheless, these terms seem to be unrelated to 24h % xylan conversion from the *P* value analysis. For this model, the *P* value for the F test was 0.000 and the predicted R^2 value was 96.78 %, which was close to the R^2 (98.15 %) and adjusted R^2 (97.74 %) values. Therefore, these results suggest that the model shows a good fit to experimental data, as well as good ability to predict new observations.

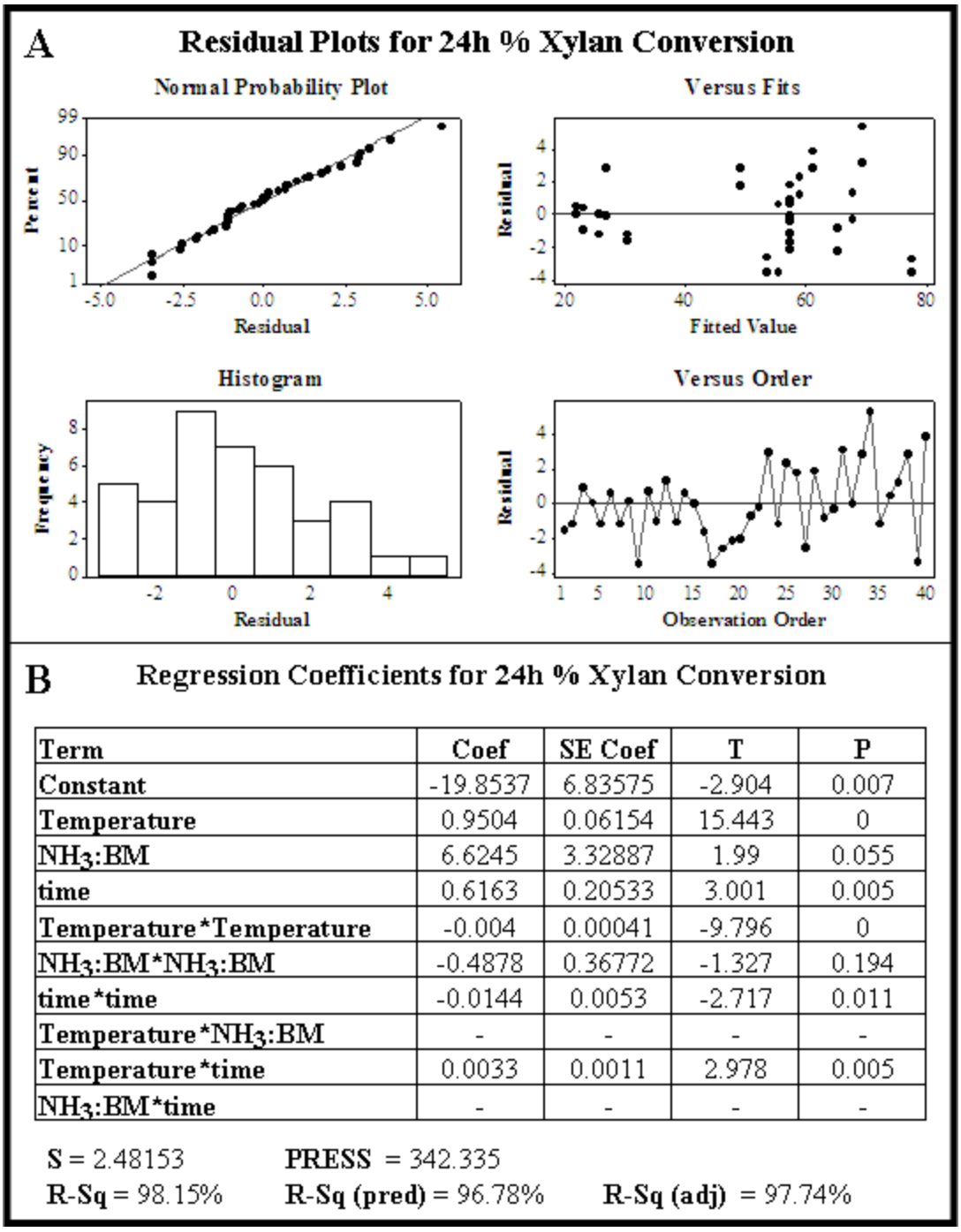

B Regression Coefficients for 24h % Xylan Conversion

Term	Coef	SE Coef	T	P
Constant	-19.8537	6.83575	-2.904	0.007
Temperature	0.9504	0.06154	15.443	0
NH_3:BM	6.6245	3.32887	1.99	0.055
time	0.6163	0.20533	3.001	0.005
Temperature*Temperature	-0.004	0.00041	-9.796	0
NH_3:BM*NH_3:BM	-0.4878	0.36772	-1.327	0.194
time*time	-0.0144	0.0053	-2.717	0.011
Temperature*NH_3:BM	-	-	-	-
Temperature*time	0.0033	0.0011	2.978	0.005
NH_3:BM*time	-	-	-	-

S = 2.48153 **PRESS** = 342.335
R-Sq = 98.15% **R-Sq (pred)** = 96.78% **R-Sq (adj)** = 97.74%

Figure 4-12 (A) Residual plots for the regression of 24h % xylan conversion to monomeric xylose as a function of pretreatment variables (temperature, time and NH3:BM ratio) and respective interaction terms. Residuals and fitted values are expressed in (% xylan conversion). (B) Estimation of regression coefficients and *P* values for the terms affecting % xylan conversion. Parameters that determine the goodness of the fit are also shown.

The resulting model equation that predicts 24h % xylan conversion as a function of EA pretreatment variables is as follows:

$$\textbf{\textit{24h \% Xylan Conversion}} = (-19.8537) - (0.9504\ X_1) + (6.6245\ X_2) + (0.6163\ X_3) - (0.004\ X_1X_1) - (0.4878\ X_2X_2) - (0.0144\ X_3X_3) + (0.0033\ X_1X_3) \quad \textbf{(4-5)}$$

Where,

X_1 = Temperature (°C) [18.25 to 121.75 °C]; X_2 = NH_3:BM [2.78 to 6.23]; X_3 = Time (min) [3.13 to 31.88 min].

To visualize the effects of EA pretreatment variables on both 24h glucan and xylan conversions a series of contour plots were prepared, as shown in **Figure 4-13**. The plots cut a section at fixed values of (I) NH_3:BM = 6:1, (II) time = 30 min and (III) temperature = 115 °C, respectively. **Figure 4-13 A** shows the dependence of 24h % glucan conversion with respect to temperature and time. As EA pretreatment time and temperature increases, glucan conversion also increases progressively, achieving values above 90 % conversion after 25 min, at 120 °C. A similar profile is observed with respect to temperature and NH_3:BM loading. However, NH_3:BM does not seem to impact glucan conversion very significantly for loadings above ~ 4:1, at fixed temperature and 30 min of residence time. At high temperature (115 °C), we can observe an increase of glucan conversion with respect to time and also NH_3:BM, and it is possible to achieve conversions above 90 % using NH_3:BM ratios of 4:1 and 30 min or residence time. Similar conversions can

be achieved at higher NH_3:BM loadings and lower residence times as shown in **Figure 4-13 A-III**.

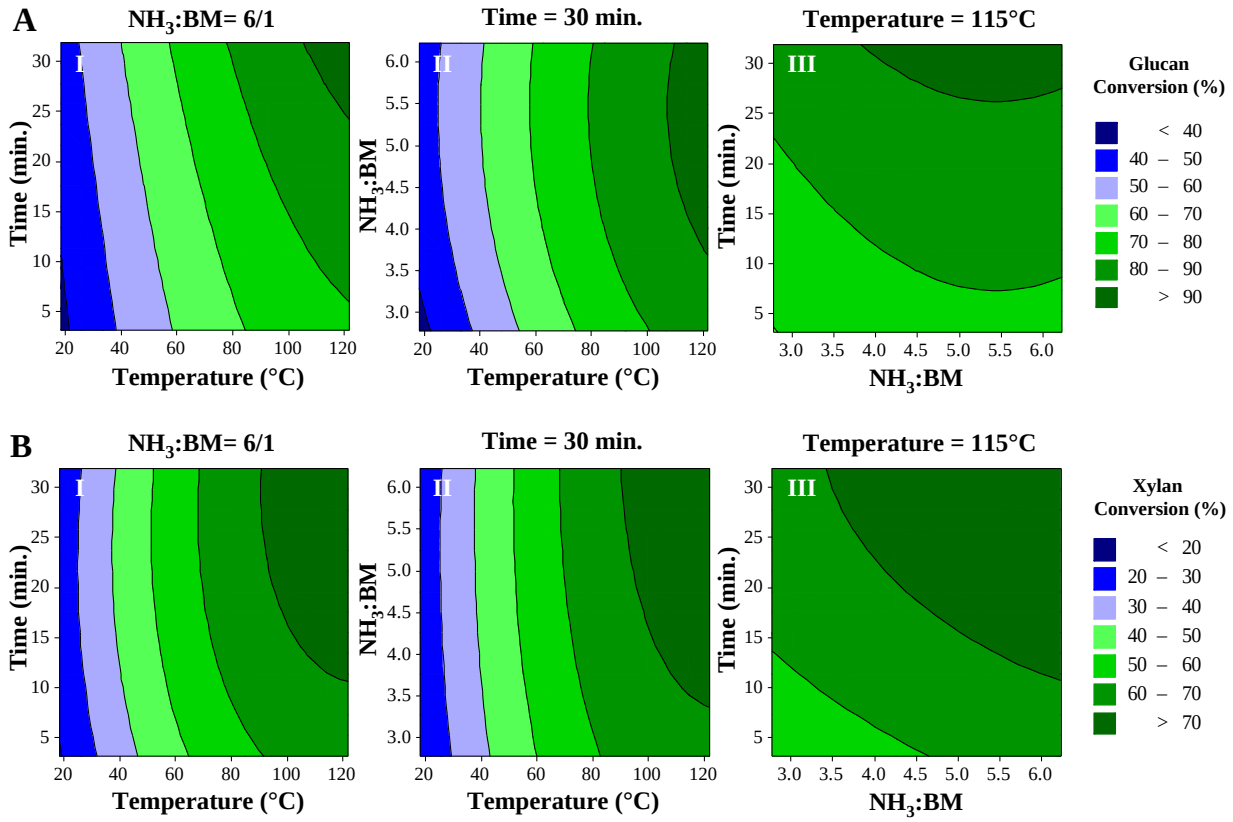

Figure 4-13 Contour plots describing monomeric 24h % glucan (A) and % xylan (B) conversions as a function of EA pretreatment conditions. Experimental values were calculated based on the glucan and xylan contents of the EA pretreated biomass. Maximum glucan and xylan loss during pretreatment was 6.4 % and 4.4 %, respectively, at maximum severity conditions (i.e. temperature = 121.8 °C, NH_3:BM loading of 6.2:1 and residence time of 32 min). The contour plots represent a small area of the universe described by the respective mathematical models, with fixed values of NH3:BM = 6/1 (I), time = 30 min (II) and temperature = 115 °C (III).

From **Figure 4-13 B-I**, it is possible to observe that xylan conversion varies significantly with respect to temperature, but not as significantly with respect to time. Monomeric xylan

conversions can reach values above 70% for temperatures of approximately 90 °C and residence times of 25 min. However, the reaction time can be reduced to approximately 10 min by increasing the temperature, while achieving similar monomeric xylan conversions. It is important to note that the maximum experimental value for xylan conversion was 74.3 ± 0.59 % and the region > 70 % xylan conversion is already near the maximum achieved during enzymatic hydrolysis. In **Figure 4-13 B-II**, xylan conversion is predicted as a function of temperature and NH_3:BM ratio. As observed before, temperature is a major factor contributing to the effectiveness of pretreatment, as demonstrated by the gradual increase in xylan conversion. The NH_3:BM ratio does not play a significant role at lower temperatures, however at higher temperatures, high NH_3:BM ratios are important to maximize xylan conversion. For example, at ~90 °C and 6:1 NH_3:BM ratio is possible to achieve xylan conversions above 70 %, however, by increasing temperature to 120 °C the same conversions can be achieved at 3.5:1 NH_3:BM loading. From **Figure 4-13 B-III**, it can be observed that at 115 °C, both time and NH_3:BM loading contribute to improve xylan conversions from ~50 % to > 70 %. At this temperature, it is possible to achieve > 70 % monomeric xylan conversions at 3.5 NH_3:BM ratio and 30 min residence time. The same conversion can be obtained with progressively lower residence time as we increase ammonia loading during EA pretreatment. From this analysis, we can observe that while maximum glucan conversion is possible in a very narrow range of conditions, maximization of xylan conversion can be obtained in a much broader range, overlapping the conditions that maximize glucan conversion.

4.4.4. Model integration and process optimization

Finally, it is important to integrate the knowledge obtained for the various elements studied herein and elaborate on the predicted conditions that maximize monomeric glucan and xylan conversions, as well as lignin extraction.

The results presented in this work clearly define ester bond cleavage and lignin extraction as major events that relate to improved digestibility of EA-CS. However, from our analysis, ester bond cleavage does not necessarily correlate with higher lignin extraction [results not shown]. This fact results from the presence of variables that are important to extract lignin, such as NH_3:BM ratio, which do not impact ester bond cleavage in such a high extent (within the boundaries of this study). Cellulose crystallinity index (CrI) coupled with cellulose III formation are also important factors that drive monomeric sugar conversion during enzymatic hydrolysis. Though cellulose III conversion does not seem to depend on lignin extraction, CrI of the biomass is highly dependent of the presence of lignin, since lignin is a major amorphous component in the biomass. Lignin negatively impacts enzymatic hydrolysis [30, 165] and therefore, higher crystallinity of the biomass sample often benefit its digestibility if cellulose is not being decrystalized. One big advantage of EA compared to major lignin extraction methods is that it is highly selective to lignin, leaving the carbohydrates behind for further processing to fermentable sugars during enzymatic hydrolysis. This property is extremely advantageous, because lignin extraction by EA pretreatment will not carry other detrimental events such as loss of hemicellulose, which would affect the final sugar yields.

From the model equations determined in this study, it is possible to calculate maximum monomeric sugar conversion and the associated lignin extraction yields. Also, the conditions that

will allow this can be determined within the boundaries of our experimental design. Therefore, theoretical results show that the maximum monomeric glucan conversion (24h of enzymatic hydrolysis) for EA pretreatment is about 93% and xylan conversion is approximately 79%. The pretreatment conditions that allow maximum sugar yields is 121.8 °C, 6.2:1 NH_3:BM loading and 30.2 min of residence time, according to the regression model. At this condition, the model also predicts a lignin extraction of approximately 48%.

Choosing a 3:1 ammonia loading while maintaining the same temperature of 121.8 °C and 30.2 min of residence time, the model predicts a slight decrease in glucan conversion to ~87 %, while xylan conversion drops to ~68 %. Sugar yields may not be impacted greatly according to the model; however, lignin extraction drops significantly to ~29% yield by reducing NH_3:BM loading to 3:1.

The models presented in this work probably cannot be generalized to all maize varieties, since is possible to observe high variability between biomass samples, including within the same species. They also cannot be generalized to all enzymatic hydrolysis time points and glucan loadings. However, the models provide useful insights about how sugar yields and lignin extraction depend on pretreatment variables. The models also show how ester bond cleavage depends on the operating conditions during pretreatment and how they correlate to sugar yields. More importantly, they are a useful tool to help optimize pretreatment conditions and prepare economic analyses for a future EA-based biorefinery.

Further studies are required to fully unveil the mechanism by which EA pretreatment operates. These studies might include imaging techniques, porosity analysis and proper measurement of cellulose III conversion in pretreated biomass. However, the study presented herein provides

clear guidelines about some of the elements that contribute to EA pretreatment effectiveness, which could be potentially used to further improve this pretreatment methodology of lignocellulosic biomass.

Even though this pretreatment method constitutes a novel approach to ammonia pretreatment, with beneficial results for both enzymatic hydrolysis and lignin extraction, some drawbacks are present and should be considered for future work. One important topic to consider is the elevated operating pressure during this pretreatment, reaching 1200 psi for the optimal conditions. High-pressure systems are common in industry; however process economics and ammonia safety would benefit from decreasing operating pressure, which can be achieved to a certain extent by the addition of a polar co-solvent during pretreatment, which does not compromise cellulose III conversion (e.g. ethanol).

4.5. Conclusion

EA pretreatment is a novel ammonia-based pretreatment technology that shows significant potential to decrease the recalcitrance of lignocellulosic biomass toward enzymatic digestion. This benefit is created by the conversion of cellulose III, disruption of important cross-links present in the biomass (e.g. ester-linked ferulates and coumarates), followed by lignin solubilization and extraction. All these factors show good correlation with sugar yields, suggesting that a mechanistic understanding of EA process should involve a deeper analysis of how these events are interdependent and synergize to facilitate biomass deconstruction. The combination of these features is unique from this pretreatment technology and has been proposed here for the first time.

A statistical design of experiments was also implemented to predict monomeric glucan and xylan conversions, lignin extraction yields and ester bond cleavage in corn stover as a function of EA pretreatment variables (i.e., temperature, NH_3:BM ratio and time). The resulting regression models were evaluated based on the goodness of the fit, residual plots and histograms, before being considered reliable. The regression models show that ester bond cleavage in the plant cell wall does not depend on NH_3:BM loading as much as temperature or time (within the boundaries of this study). In the other hand, lignin extraction and sugar yields increase significantly with increasing values of temperature, NH_3:BM loading and time. Sugar yields are maximized at 121.8 °C, 6.2:1 NH_3:BM loading and 30.2 min of residence time, according to our model, yielding ~93 % monomeric glucan conversion and 79 % monomeric xylan conversion after 24h enzymatic hydrolysis at 1 % glucan loading. Under these pretreatment conditions, the model also predicts extraction of approximately 48 % of the lignin present in untreated corn stover, which could be further upgraded to fuels and chemicals. Characterization of this lignin stream is important to define its value and potential for further usage in the biorefinery. The valorization of lignin will be instrumental to offset some of the negative aspects related to this technology, which impact the economics of the process in comparison to other ammonia pretreatments (e.g. AFEX™). A major drawback of this pretreatment is the fact that it operates at high pressure, up to 1200 psi at the most severe conditions tested herein. However, it is possible to develop strategies to further improve the EA method and decrease the operating pressure by the usage of co-solvents, such as ethanol. Higher ammonia loadings are also another important drawback, which will require attention in future research. Detailed economic evaluation and process

engineering studies should be performed in future research to define strategies for minimizing ammonia loading and operating pressure during EA pretreatment, while achieving similar levels of ester bond cleavage, lignin solubilization and cellulose III conversion.

APPENDIX

Table 4-4 Pretreatment conditions used for the Box Benhken design and the respective number for reference of model fit plots below.

Experiment Number	Temperature	NH3:BM	time
1	18.25	4.5	17.5
2	25	3	5
3	25	3	30
4	25	6	5
5	25	6	30
6	70	2.775	17.5
7	70	4.5	3.125
8	70	4.5	17.5
9	70	4.5	31.875
10	70	6.225	17.5
11	115	3	5
12	115	3	30
13	115	6	5
14	115	6	30
15	121.75	4.5	17.5

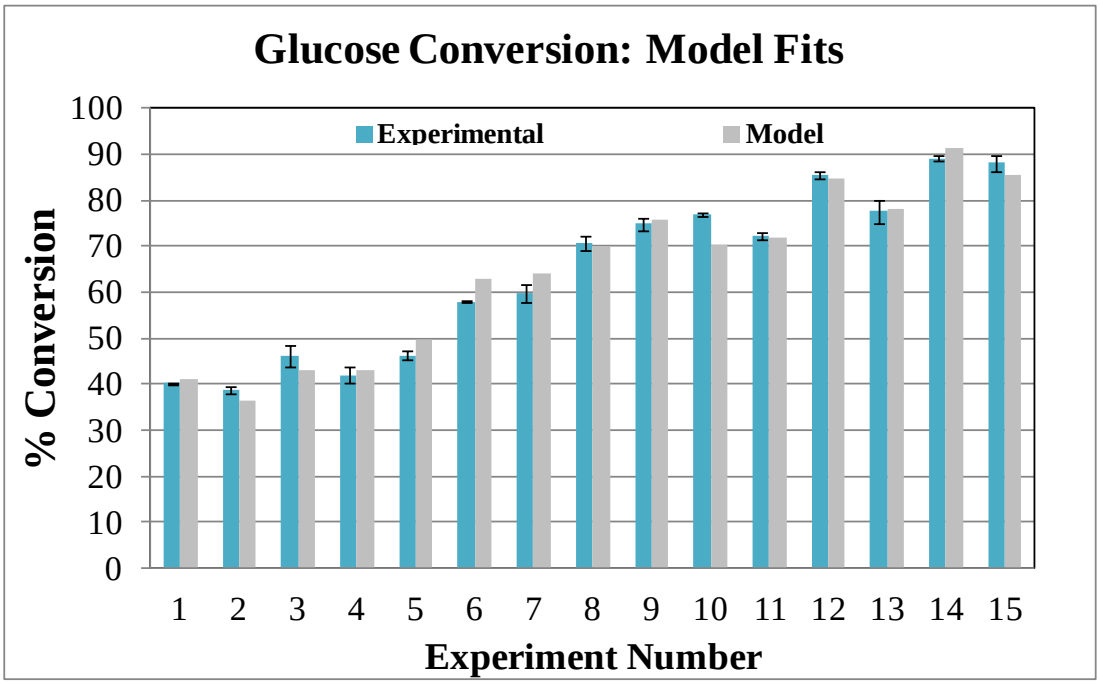

Figure 4-14 Model prediction fits to experimental data for 24h glucose conversion as a function of EA conditions.

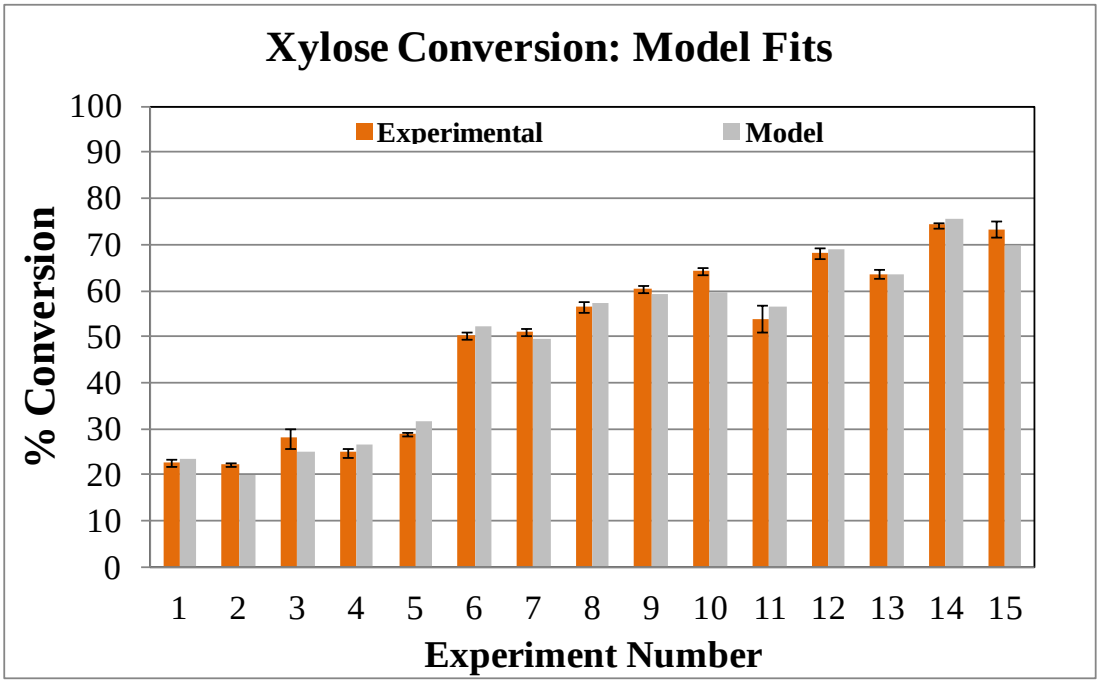

Figure 4-15 Model prediction fits to experimental data for 24h xylose conversion as a function of EA conditions.

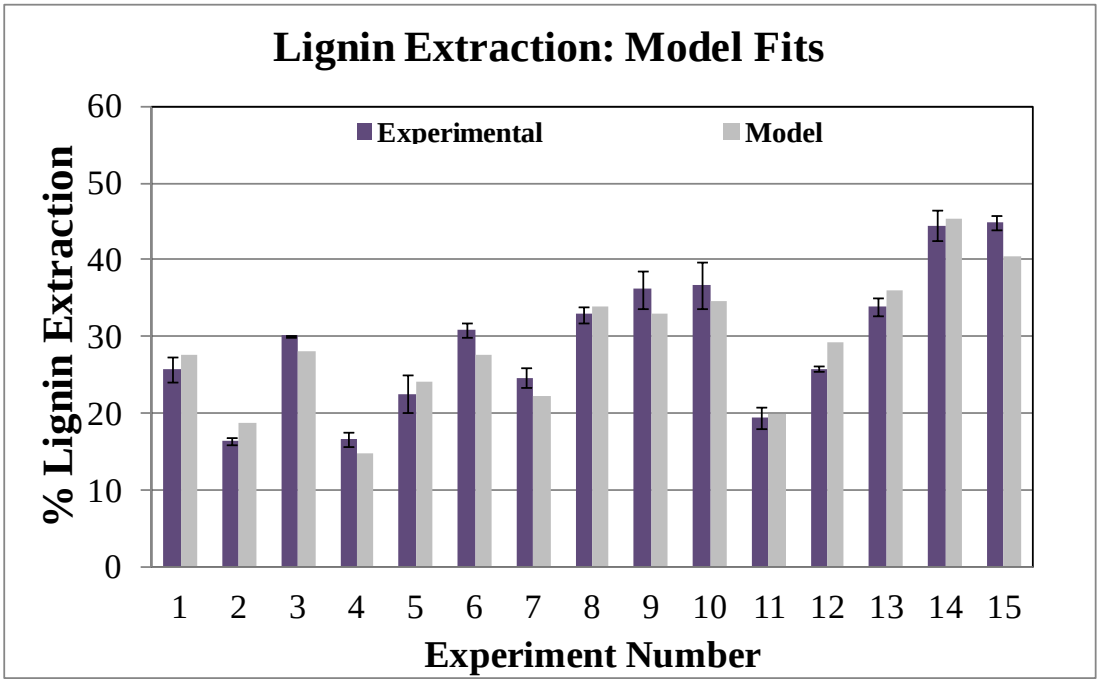

Figure 4-16 Model prediction fits to experimental data for lignin extraction as a function of EA conditions.

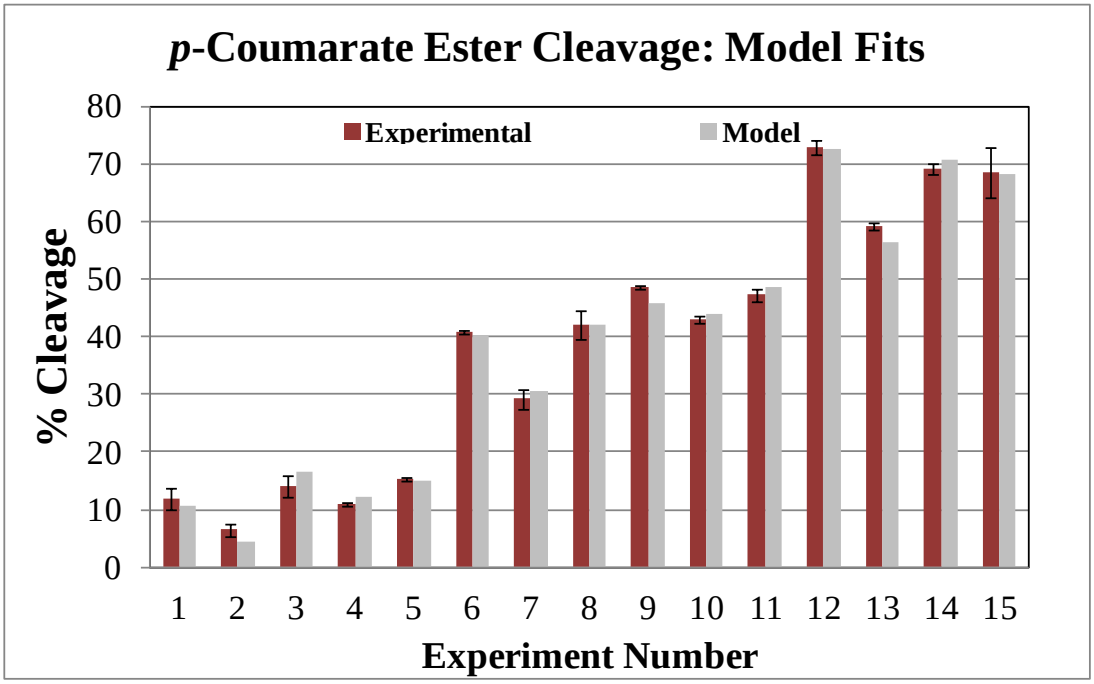

Figure 4-17 Model prediction fits to experimental data for *p*-coumarate ester cleavage as a function of EA conditions.

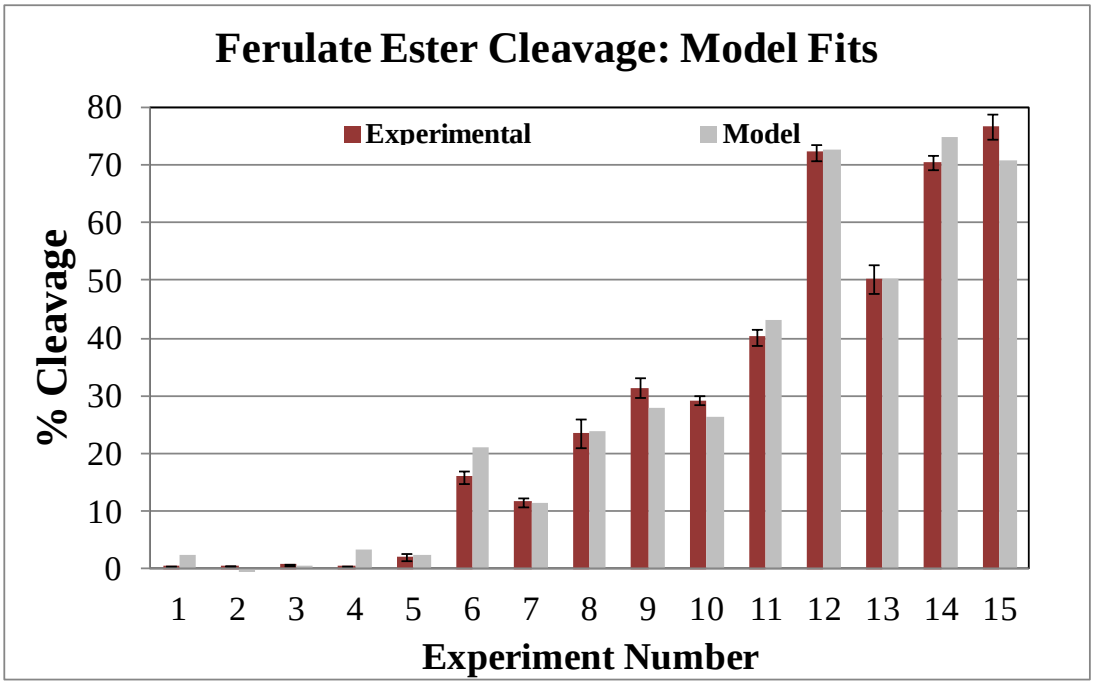

Figure 4-18 Model prediction fits to experimental data for ferulate ester cleavage as a function of EA conditions.

CHAPTER 5 – HIGH SOLID LOADING ENZYMATIC HYDROLYSIS OF EXTRACTIVE AMMONIA (EA) PRETREATED CORN STOVER

5.1. Abstract

In this work, the performance of EA pretreated corn stover (EA-CS) during enzymatic hydrolysis will be compared with AFEX^{TM}-CS at high solid loadings and evaluated as a function of 1) solid loading, 2) enzyme loading and 3) hydrolysis time. A statistical design of experiments (Box Benhken) was applied for these three variables and a full quadratic regression was performed to determine model equations that statistically represent monomeric glucose and xylose conversions as a function of those variables and their respective interaction parameters. To fulfill the feedstock demand for these experiments, a larger scale EA pretreatment reactor was also constructed. This new EA system operation was validated for corn stover and the results were successfully compared with the model predictions defined in **CHAPTER 4** for sugar conversion and lignin extraction. The appropriate EA pretreatment condition was defined based on sugar yields and lignin extraction. Enzymatic hydrolysis analysis was performed using model predictions and the benefits of EA pretreatment were compared with AFEX^{TM}. From this analysis, EA-CS presents better performance than AFEX^{TM} at high solid loadings, where 95 % glucose and 85 % xylose conversions can be achieved for 30 mg/g glucan of enzyme loading at 15 % solids, comparing with 85 % and 70 % obtained for AFEX^{TM}-CS, respectively. The most significant benefit of EA pretreatment was observed at 7.5 mg/g glucan enzyme loadings for 15 % solid loading, where absolute improvements reached approximately 23 % and 15 % for

glucose and xylose conversion, respectively, compared with AFEX^{TM}-CS. Under these conditions, EA-CS can reach approximately 88 % and 76 % glucose and xylose conversion, respectively. This result can only be achieved by AFEX^{TM}-CS when enzyme loadings are above 20 mg/g glucan, which represents a 2.7 fold increase in enzyme loading.

5.2. Introduction

The novel Extractive Ammonia (EA) pretreatment is known to improve enzymatic hydrolysis of lignocellulosic biomass (**CHAPTER 4**) by extracting lignin from the plant cell wall, while simultaneously converting naturally occurring cellulose I (CI) to cellulose III (CIII). Modern pretreatment technologies are required to enhance enzymatic hydrolysis at high solid loadings, as commercial processes require high concentration of sugars in the hydrolysate to potentiate high biofuel concentrations after fermentation. This requirement is important to facilitate biofuel separation and purification. For example, economically viable distillation of ethanol in a biorefinery requires a minimum concentration of 4 wt% ethanol after fermentation [166] and to achieve this concentration, a minimum of 6 % glucan loading (assuming a corresponding 4 % xylan loading) is required during enzymatic hydrolysis [167]. However, high solid loading enzymatic hydrolysis has its own bottlenecks, as sugar yields tend negatively affected by increasing solids loading [168-170], a phenomenon usually described as the “solids effect” [170]. Though authors have correlated the “solids effect” with transport phenomena, water activity, product inhibition, lignin inhibition and pretreatment decomposition products inhibition [2, 169, 170], the reason behind the “solids effect” is still not well understood. In the scope of this work, enzymatic hydrolysis at high solid loadings will be studied for EA pretreated corn stover (EA-

CS). The enzymatic hydrolysis profile will be evaluated as a function of solids loading, enzyme loading and incubation time during enzymatic hydrolysis. For this purpose, a statistical design of experiments will be implemented followed by regression using a full quadratic equation. The performance of EA-CS during enzymatic hydrolysis will be compared with the same feedstock pretreated using a leading ammonia-based pretreatment technology designated by AFEX™. AFEX™ technology is currently on the path for commercialization by Michigan Biotechnology International (MBI) and is known to be highly effective on grasses, such as corn stover, achieving glucose conversions that range 75-80 % during high solid loadings enzymatic hydrolysis [78, 171]. From the empirical regression models developed for EA and AFEX™ pretreated corn stover, it is possible to compare the kinetics of enzymatic hydrolysis for various solid loadings and enzyme loadings. The improvements offered by EA pretreatment technology during high solids loading enzymatic hydrolysis will be analyzed in detail as a function of enzyme loading and solids loading.

5.3. Experimental

5.3.1. Untreated corn stover

Untreated corn stover (UT-CS), a Pioneer 36H56 hybrid, was harvested in September 2009 in Wisconsin (USA) and oven dried at 60 ºC for approximately 2 weeks. The biomass was further passed through a 5 mm screen installed in a Christy hammer mill (Christison Scientific LTD, England) and stored at 4 ºC in heat sealed bags prior to utilization. The moisture content of the dried and milled corn stover was approximately 6 % on a wet weight basis. The biomass

composition analysis was performed using NREL protocols NREL/TP-510-42618 and NREL/TP-510-42620. On a dry weight basis, the untreated corn stover contained approximately 38 % glucan, 23 % xylan, 1 % galactan, 3 % arabinan, 14 % Klason lignin, 2 % acid soluble lignin, 5 % ash and 15 % extractives (i.e. ethanol and water soluble compounds).

5.3.2. Extractive Ammonia (EA) pretreatment reactor

For this work, a new EA reaction system was constructed based on the design presented on **Section 4.3.2**. This version is composed of 3 reactors of ~600 mL each, which are capable of working in parallel and extracting biomass components to a single extraction collector. This new system is capable of producing larger amounts of pretreated biomass, which can be used in high solid loading enzymatic hydrolysis and fermentation studies. Each reactor is made of 316 stainless steel sanitary tubing of 2" x 12" (OD x H) and can pretreat ~40 g of corn stover per batch, per reactor. Sanitary tubes are connected to inlet and outlet fittings through high-pressure bolted clamps, sealed with PTFE gaskets, which can withstand a maximum pressure of 1200 psi. The bottom fitting clamped to the reactor was customized to fit a stainless steel filter of 80 μm pore size, sealed with a custom made PTFE gasket. This connection is linked to a valve that separates the reactors from the extractives collector. All three reactors are equipped with individual heating mantles, connected to a single PID controller (Chemglass Life Sciences, Vineland, NJ, USA) that can be programmed to control temperature of each reactor independently.

The ammonia delivery system is composed of a tubular high-pressure vessel made of 316 stainless steel, containing liquid ammonia at room temperature. This vessel is secured on top of a balance (A&D, Inc., San Jose, CA, USA) and connected to the high-pressure reactors through

flexible tubing made of stainless steel and lined with PTFE. Ammonia delivery is measured by weight displacement from the vessel located on top of the balance to the pretreatment reactors. For accurate delivery measurements all lines from the ammonia vessel to the reactors must be primed with liquid ammonia.

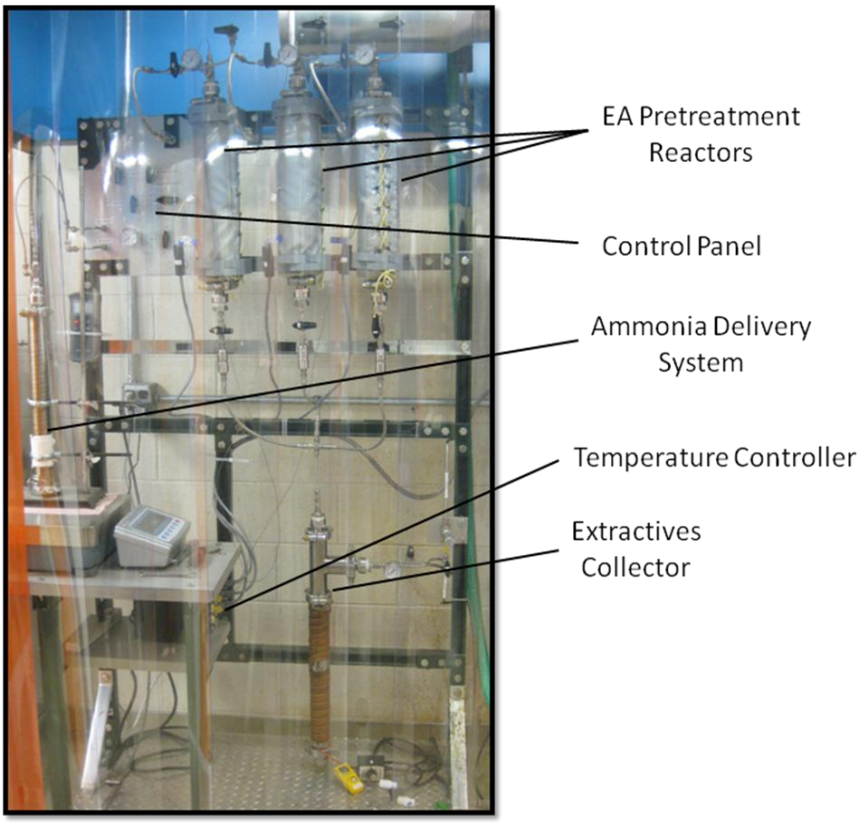

Figure 5-1 Picture of scaled-up EA pretreatment system, composed by 3 high-pressure reactors of 600 mL each, ammonia delivery system and extractives collector.

The extractives collector is also made with stainless steel 316 sanitary tubing of 2" x 12" (OD x H), connected to a sanitary tee tube on the top. A deep tube was installed from the top fitting of the sanitary tee tube to be able to drain the extractives from the reactor to the bottom of the collector. A valve was installed on the side fitting of the tee tube, which can be used to control the ammonia evaporation rate during extractives condensation. Heating tape was installed around

the outer surface of the extractives collector to better control ammonia evaporation, as it absorbs energy from the surroundings, resulting in a significant temperature drop. **Figure 5-1** shows a picture of the reactor system fully assembled.

5.3.3. Pretreatment of corn stover

EA pretreatment was conducted in the tubular reactors described above (**Figure 5-1**). The moisture content of corn stover was raised to the desired level by spraying distilled water homogeneously throughout the untreated biomass (40 g in dry weight basis) before transferring it to the reactors. The desired amount of ammonia was loaded from a high pressure vessel located on the top of a balance, which measured the displaced weight of ammonia transferred to the reactors. Immediately after loading ammonia, the reactors were heated to the desired temperature. Set point temperatures were achieved in < 7 min. The top fitting of the reactor was connected to a nitrogen line and the bottom fitting was connected to the extractives collector. The extractives collector was pressurized with nitrogen to equalize the pressure developed in the reactor during the course of pretreatment. After reaching the desired residence time, the valve between the reactor and collector was opened and the extractives were filtered and drained to the collector. Nitrogen overpressure of 1200 psi was applied to the reactor to maintain ammonia in the liquid state during biomass extraction. The valve in the top of the reactor was kept opened to allow a pressure of approximately 1200 psi to be maintained in the system for ~10 min. During this time, nitrogen was allowed to slowly flow through the system by slightly opening the ammonia exhaust valve on the top of the collector. After 10 min, the nitrogen inlet valve was closed and the system was depressurized slowly (~5 min). The pretreated biomass was transferred from the reactor to a tray, which was placed under the hood overnight to remove any

residual ammonia. The biomass was fairly dry after EA pretreatment and this drying procedure was performed to stabilize the biomass with respect to moisture and residual ammonia contents. After collecting the pretreated biomass, the reactor was reconnected to the extractives collector and all the system lines were cleaned with 70 % ethanol and 90 % acetone (both in water) to remove residual extractives from the lines, which were drained to the extractives collector. After drying, the total weight and moisture content of the EA pretreated corn stover (EA-CS) was measured with an analytical balance and moisture analyzer A&D MX-50 (A&D Engineering, Inc., San Jose, CA, USA), respectively. The samples were stored at 4 °C in sealed bags prior to compositional analysis, following NREL protocols NREL/TP-510-42618 and NREL/TP-510-42620, and enzymatic hydrolysis. EA pretreatment conditions used in this work were designed to evaluate the effect of moisture content, temperature, ammonia loading and residence time on enzymatic hydrolysis and lignin extraction performance in this new reactor system, and to compare them with results obtained in the smaller scale reactors in **CHAPTER 4**.

Ammonia Fiber Expansion (AFEX^{TM}) pretreated corn stover (AFEX^{TM}-CS) was provided by Michigan Biotechnology International (MBI). AFEX pretreatment conditions were optimized by MBI to maximize monomeric sugar conversion during enzymatic hydrolysis.

5.3.4. X-ray powder diffraction (XRD)

XRD was performed on an X-ray powder diffractometer with beam parallelized by a Gobel mirror (D8 Advance with Lynxeye detector; Bruker, Bruker AXS Inc., Madison, WI, USA). CuKα radiation (wavelength = 1.5418 Å) was generated at 40 kV and 40 mA. The detector slit was set to 2.000 mm. Sample was analyzed using a coupled 2θ/θ scan type with a continuous PSD fast scan mode; 2θ started at 8.000° and ended at 30.0277° with increments of 0.02151°,

while θ started at 4.0000° and ended at 15.0138° with increments of 0.01075°. Step time was 1.000 sec (i.e., 1025 total steps, effective total time 1157 sec per run). Cellulose samples (approximately 0.5 g) were placed in a specimen holder ring made of PMMA with 25 mm diameter and 8.5 mm height, rotating at 5 degrees per minute during analysis.

5.3.5. Enzymatic hydrolysis for EA pretreatment optimization

Enzymatic hydrolysis was performed at 1 % glucan loading, using 15 mg of enzyme per gram of glucan in 15 mL vials, incubated at 50 ºC, with pH 4.8 for 24 h in an orbital shaking incubator (New Brunswick, USA). The enzymes used in this work were Cellic® CTec2 (138 mg protein/ml, batch No.VCNI0001), Cellic® HTec2 (157 mg protein/ml, batch No.VHN00001), generously provided by Novozymes (Franklinton, NC, USA), and Multifect Pectinase (MP) (72 mg/ml, batch No. 4861295753) a gift from Genencor/Dupont (Palo Alto, CA, USA). The protein concentration of the enzymes was determined using the Kjeldahl nitrogen analysis method (AOAC Method 2001.11, Dairy One Cooperative Inc., Ithaca, NY, USA). The enzyme ratios utilized in this work were 50 % Cellic® CTec2, 25 % Cellic® HTec2 and 25 % MP in a dry protein weight basis. These ratios were previously optimized to maximize total sugar conversion on EA pretreated corn stover. After enzymatic hydrolysis, samples of the hydrolyzate were prepared for glucose and xylose analysis using HPLC equipped with a Bio-Rad Aminex HPX-87H column (Bio-Rad, Hercules, CA, USA) as previously described [88].

5.3.6. Experimental design for high solid loading enzymatic hydrolysis

The impact of variables such as residence time, solids loading and enzyme loading on glucan and xylan conversion was determined using a Box Behnken design of experiments (DOE), for enzymatic hydrolysis on both on EA and AFEX^{TM} pretreated corn stover. The DOE was

performed using Minitab software (Minitab Inc., State College, PA, USA), where 30 experimental points were generated, including duplicates and six center points. The low and high values that defined the boundaries of our design are shown in **Table 5-1** .

Table 5-1 High and low limits defined for the experimental points using Box Benhken design.

Factor	Low	High
Time (h)	24	120
Solid Loading (%)	15	25
Enzyme Loading (mg/g glucan)	5	30

The experimental design used in this work is presented in **Table 5-2**. Glucan and xylan conversions (monomeric and monomeric + oligomeric) were determined for the various enzymatic hydrolysis conditions and used to fit a full quadratic equation containing the factors described in **Table 5-1**. All interaction effects between factors were considered in this analysis and parameters were chosen according to their *P* value and influence on the model prediction (R^2 -predicted and model *P* values). The regression equations were used to predict the responses of the various effects as a function of enzymatic hydrolysis conditions within the boundaries set by the experimental design. Contour plots were used to provide a graphical interpretation of the regression model and compare predicted enzymatic hydrolysis results between EA and AFEX^{TM} pretreated corn stover.

Table 5-2 Enzymatic hydrolysis conditions defined by a Box Benhken DOE.

RunOrder	Time (h)	Solid Loading (wt%)	Enzyme Loading (mg/g glucan)
1	24	15	18.75
2	120	15	18.75
3	24	25	18.75
4	120	25	18.75
5	24	20	7.5
6	120	20	7.5
7	24	20	30
8	120	20	30
9	72	15	7.5
10	72	25	7.5
11	72	15	30
12	72	25	30
13	72	20	18.75
14	72	20	18.75
15	72	20	18.75
16	24	15	18.75
17	120	15	18.75
18	24	25	18.75
19	120	25	18.75
20	24	20	7.5
21	120	20	7.5
22	24	20	30
23	120	20	30
24	72	15	7.5
25	72	25	7.5
26	72	15	30
27	72	25	30
28	72	20	18.75
29	72	20	18.75
30	72	20	18.75

5.3.7. High solids loading enzymatic hydrolysis

Enzymatic hydrolysis was performed in 250 mL Erlenmeyer flasks with 100 mL reaction volume, incubated at 50 ºC, with pH adjusted to 4.8, in an orbital shaking incubator at 250 RPM (New Brunswick, USA). The enzymes used in these experiments were Cellic® CTec2 (138 mg protein/ml, batch No.VCNI0001), Cellic® HTec2 (157 mg protein/ml, batch No.VHN00001), generously provided by Novozymes (Franklinton, NC, USA), and Multifect Pectinase (MP) (72 mg/ml, batch No. 4861295753) a gift from Genencor/Dupont (Palo Alto, CA, USA). The protein concentration for the enzymes was determined using the Kjeldahl nitrogen analysis method (AOAC Method 2001.11, Dairy One Cooperative Inc., Ithaca, NY, USA). The enzyme ratios utilized in this work were 50 % Cellic® CTec2, 25 % Cellic® HTec2 and 25 % MP on a dry protein weight basis for both EA and AFEX^{TM} pretreated corn stover. This relative amounts of the various commercial enzymes was previously optimized and found to maximize total sugar conversion of both feedstocks. The other enzymatic hydrolysis conditions used in this work are defined in **Table 5-2**. After enzymatic hydrolysis, samples of the hydrolyzate were analyzed for glucose and xylose content using HPLC equipped with a Bio-Rad Aminex HPX-87H column (Bio-Rad, Hercules, CA, USA) as previously described [88].

5.4. Results and Discussion

5.4.1. Evaluation of EA pretreatment on corn stover

The EA pretreatment reactor used in this work was developed for larger scale production of EA-CS in order to supply feedstock for experiments that require significant amounts of material, notably high solid loading enzymatic hydrolysis and fermentation. In this new reactor system,

pretreatment conditions already known to maximize sugar yields and lignin extraction (from **CHAPTER 4**) were evaluated in parallel with other unexplored conditions. The major goals were to verify if extended residence times, larger than 30 min, would further improve EA performance and if the results obtained in previous studies could be replicated in the larger EA pretreatment setup. This evaluation was important to define the best EA conditions before expanding our work to high solid loading enzymatic hydrolysis. **Figure 5-2 i)** shows the impact of biomass moisture content on glucose and xylose conversions as well as lignin extraction. From these results is apparent the negative influence of biomass moisture content on glucose conversion. In these experiments, highly digestible cellulose III (CIII) was formed in all cases as was confirmed by XRD analysis [data not shown], however it is possible that the presence of additional water may impact the amount of converted CIII in the sample, as water is known to facilitate reversion of CIII to cellulose I (CI) [80]. XRD of the pretreated material is not sufficient to confirm this hypothesis, because these samples contain different amounts of amorphous material (e.g., hemicelluloses and lignin) and it is impossible to deconvolute the spectra using the technique presented in **CHAPTER 1**. Further work is required to develop methodologies to extract lignin and hemicelluloses from the pretreated biomass without reverting CIII to CI, thereby allowing proper CIII quantification to be performed through XRD or FT-Raman analysis [163, 164]. Xylose conversion seems to be positively affected by the presence of moisture, even though the effects are not large. In the case of lignin extraction, water did not play a major role at this range of conditions, as the highest level of lignin extraction was 36.3 % (10 % moisture) and the lowest was 31.6 % (40 % moisture). From these results, it is possible to conclude that lower moisture contents seem to benefit lignin extraction as well as total sugar conversion and therefore, 10 % moisture was used in the following experiments. **Figure 5-2 ii)**

shows the effect of temperature on EA pretreatment performance. These experiments were performed using biomass with 10 % moisture, 3:1 ammonia:biomass ratio and 60 min residence time. From these results it is clear that temperature positively impacts 24 h glucose conversion in the range between 90 °C and 110 °C, where conversions reached 81.6 % and 93.8 %, respectively. From 110 °C to 120 °C, glucose conversions were maintained practically constant. In the case of xylose conversions, temperature has little impact in the range of conditions tested herein. The results show a slight increase of xylose conversion from 90 °C to 110 °C, reaching 71.1 % and 76.3 %, respectively. This increase was followed by a small decrease to 72.8 % at 120 °C. In the other hand, temperature plays an important role on lignin extraction. From **Figure 5-2 ii)** is clear that % lignin extraction remained practically constant at ~30 % for pretreatment temperatures ranging from 90 °C to 110 °C. However, a sudden increase was observed for EA pretreatment performed at 120 °C, where 36.3 % lignin extraction was achieved. Ammonia-based extraction of lignin is commonly known to be positively affected by temperature [157, 160], however further work is required to evaluate the reasons behind this unexpected sudden increment. One possible hypothesis can be related to the fact that a great portion of the extracted lignin has a Tg (glass transition temperature) of approximately 117 °C (as demonstrated in Appendix from **CHAPTER 6**). Once the Tg is reached, lignin becomes “softer”, and can perhaps be delocalized more easily from the cell wall ultra-structure and solubilized by liquid ammonia.

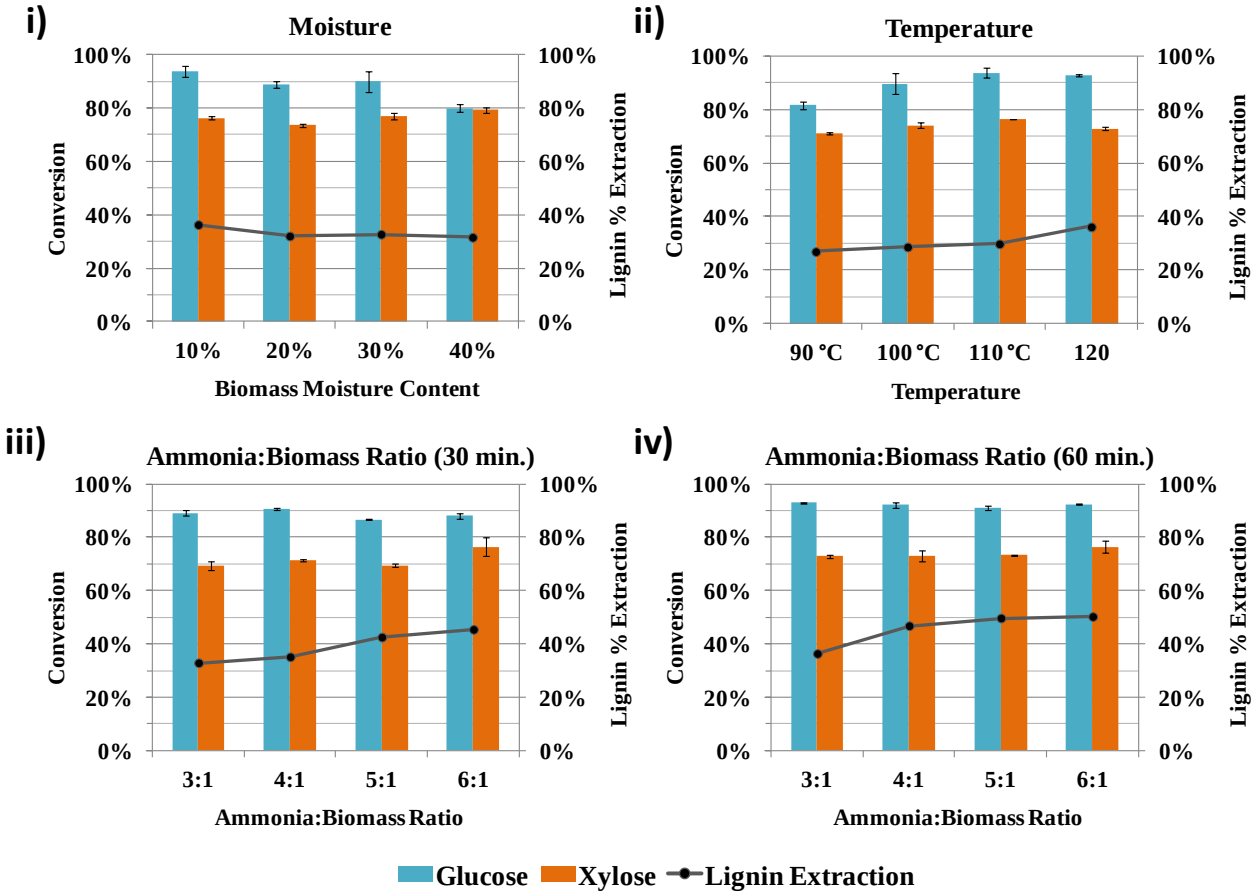

Figure 5-2 i) Effect of moisture content on enzymatic hydrolysis and lignin extraction performances. Experiments were performed at 110 °C for 60 min residence time and 3:1 ammonia loading; ii) Effect of temperature on enzymatic hydrolysis and lignin extraction performances. Experiments were performed with 10 % moisture content, 3:1 ammonia loading and 60 min residence time; iii) Effect of ammonia:biomass ratio at 30 min residence time on enzymatic hydrolysis and lignin performances. Experiments were performed with 10 % moisture content at 120 °C; iv) Effect of ammonia:biomass ratio at 60 min residence time on enzymatic hydrolysis and lignin extraction performances. Experiments were performed with 10 % moisture content at 120 °C. Enzymatic hydrolysis in all cases was performed with an enzyme loading of 15 mg/g glucan for 24 h at 50 °C and 250 RPM.

The effect of the ammonia:biomass ratio on EA performance is shown in **Figure 5-2 iii)**, for a 30 min pretreatment time. The results indicate that glucose conversion does not vary significantly at this range of conditions, where 87-90 % conversion was achieved after 24 h enzymatic hydrolysis at 1% glucan loading. In the other hand, xylan conversion was slightly improved from

69 % to 76 % when ammonia:biomass ratio increased from 5:1 to 6:1. No major differences in xylan conversion were observed from 3:1 to 5:1, where values remained between ~69 and ~70 % conversion. Lignin extraction was significantly improved with increasing ammonia:biomass ratio. This result is in agreement with our early observations that showed the importance of ammonia loading for lignin extraction **CHAPTER 4**. Comparing results from the model generated in **CHAPTER 4** with experimental data presented in **Figure 5-2 iii)**, it is possible to validate that the model has good ability to predict new observations (**Figure 5-3**), even using a larger scale experimental setup. **Figure 5-3** shows that lignin extraction could be predicted well for ammonia:biomass ratios from 4:1 to 6:1, showing residuals ranging from 0.60 % to 1.95 %. At 3:1 ammonia:biomass ratio the residual was largest in absolute terms, as the model underpredicted lignin extraction by 3.81 % compared to the experimental value. From the same figure, it is also possible to compare glucose and xylose conversions with model predictions. The residuals obtained for glucose conversion varied from -3.17 % (3:1) to 6.35 % (5:1), while xylose conversion residuals varied from 0.47 % (6:1) to 5.59 % (5:1). Therefore, experimental results show good agreement with model predictions, even though the data obtained to generate the model was produced with a different experimental setup. Additionally, the enzyme combination used in this study is different from the one used to produce the model, with inclusion of 25 % MP by replacement of 25 % of HTec 2, although both enzyme combinations generate very comparable results at 1 % glucan loading with respect to glucose and xylose conversions [data not shown].

Increasing the pretreatment residence time from 30 min to 60 min did not result in significant improvements both for glucose and xylose conversions (**Figure 5-2 iv)**). However, lignin extraction improved significantly with pretreatment time, especially at 4:1 ammonia:biomass

ratio, where lignin extraction increased from about 35 % to 48 %. Lignin extraction remained constant between 5:1 to 6:1 ammonia:biomass ratio, where about 50% of the lignin from corn stover was extracted. The mathematical model generated in **CHAPTER 4** does not predict observations for pretreatment times above 30 min. Therefore, the comparison between predicted and experimental results could not be performed for these conditions.

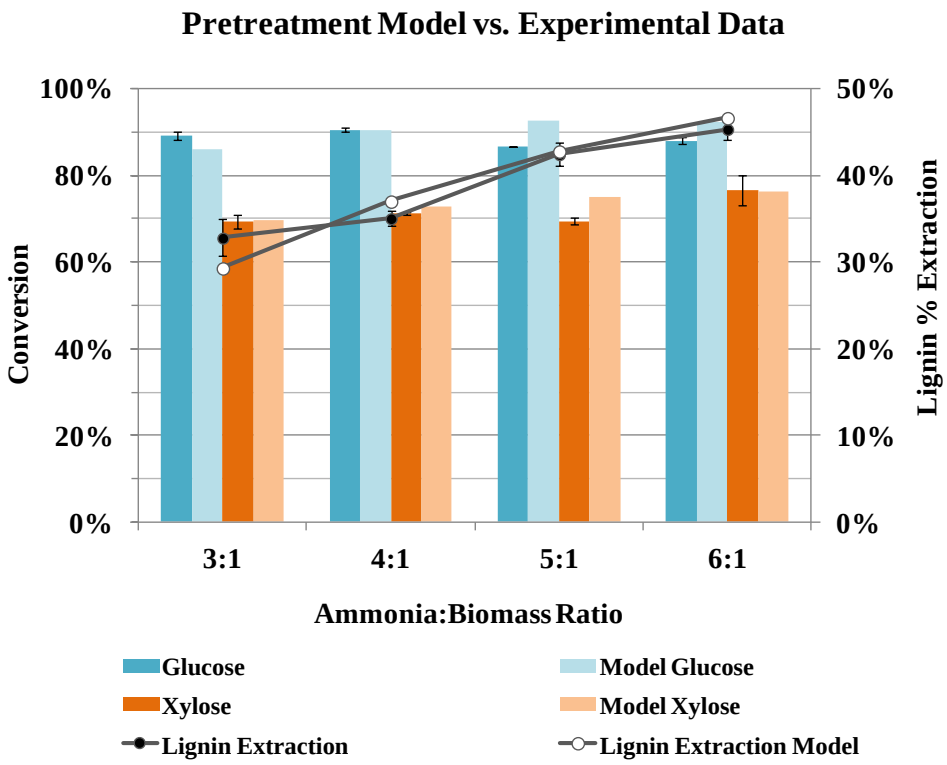

Figure 5-3 Comparison between experimental observations and predicted observations by the model presented in **CHAPTER 4** for glucose, xylose and lignin extraction performances. Pretreatment conditions were performed with a fixed biomass moisture of 10 %, 120 °C and 30 min residence time, varying ammonia:biomass ratio from 3:1 to 6:1.

Using the results presented herein, we defined the EA condition for producing larger quantities of material in order to perform high solid loading enzymatic hydrolysis. The preferred condition

allowed sugar and lignin extraction yields to be close to maximum with minimal energy inputs. Therefore, we chose to use 10 % moisture in biomass, 6:1 ammonia:biomass ratio at 120 °C for 30 min. This choice of pretreatment time had to do with the small improvements obtained by extending the pretreatment to 60 min, as can be observed in **Figure 5-2 iii) & iv)**. The process mass balance with the preferred EA pretreatment condition is shown in **Figure 5-4**. In this work, glucose and xylose conversions ($X_{glucose}$ and X_{xylose}, respectively) will be modeled as a function of enzymatic hydrolysis parameters such as incubation time, solids loading and enzyme loading. The empirical model, based on statistical design of experiments, will provide a useful tool to optimize conditions and perform future techno-economic evaluation studies. Furthermore, it helps us to analyze the effect of the various parameters on enzymatic hydrolysis performance.

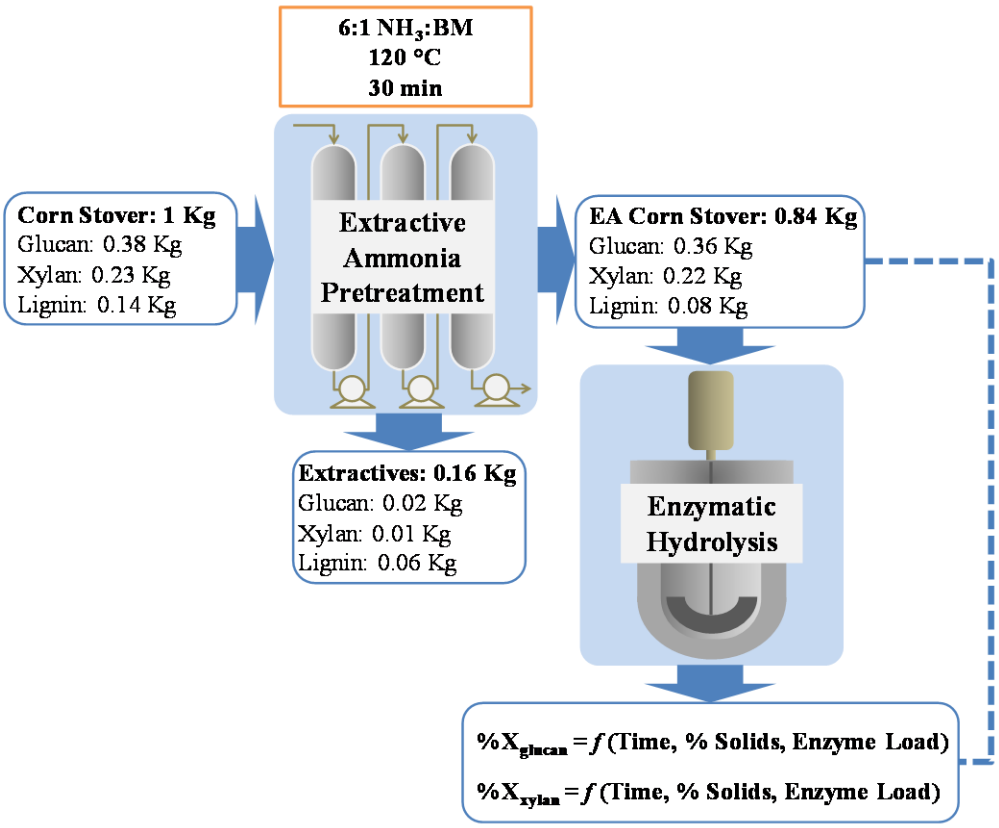

Figure 5-4 Process mass balance for the EA pretreatment condition chosen for this study. Enzymatic hydrolysis conversion (%X) is a function of variables such as time, % solids loading and enzyme loading during enzymatic hydrolysis. Empirical modeling was performed to determine these relationships in this study and complete the material balance around pretreatment and enzymatic hydrolysis.

5.4.2. High solid loading enzymatic hydrolysis of EA corn stover

5.4.2.1. Definition of enzymatic hydrolysis conditions: fixed variables

High solid loading enzymatic hydrolysis was studied using EA-CS pretreated under the conditions determined above. The performance of EA-CS was compared with AFEX^{TM}-CS, as this is an established pretreatment technology that is currently on the path for commercialization. Sugar yields during enzymatic hydrolysis are known to be dependent on various factors that

include, solids loading, enzyme loading and incubation time [170, 172, 173]. Other parameters are also revealed to be important, notably the mixing regime, pH, incubation temperature and enzyme mixture, which is dependent on the lignocellulosic substrate [172, 173]. For this study, incubation temperature was set constant at 50 °C, as enzymes show maximum activity around this temperature according to the literature provided by the enzyme suppliers. Preliminary experiments varying pH from 4.2 to 5.2 revealed a pH between 4.8 and 5.2 maximize sugar conversion of AFEX^{TM}-CS and therefore, a pH of 4.8 was chosen for this study. Other published studies have successfully used this pH, as it is also recommended by enzyme manufacturers [4, 171]. Enzyme cocktail optimization was performed in conical shake flask experiments using 20 % solids and 18.75 mg/g glucan enzyme loading for 72 h incubation time, both for AFEX^{TM}- and EA-CS. Based on our knowledge and experience optimizing enzyme cocktails [22], a set of 6 commercial enzyme combinations known to maximize sugar yields were chosen to determine the optimal mixture. From these experiments the combination of 50 % Ctec2, 25 % Htec2 and 25 % MP maximized total sugar conversion for both AFEX^{TM} and EA pretreated corn stover (in Appendix) at 20% solids. Preliminary experiments were also performed to optimize mixing speed, where 20 % solid loading enzymatic hydrolysis was performed in a shaker incubator for 72 h at optimal pH and temperature. A range of mixing speeds was tested in this preliminary study, from 100 to 300 rpm, demonstrating that 250 rpm is sufficient to maximize sugar conversion [data not shown]. By fixing enzyme mixture, pH, incubation temperature and mixing regime, we will be able to focus our attention on the effects of 1) solid loading, 2) enzyme loading and 3) incubation time on glucose and xylose conversion for EA- and AFEX^{TM}-CS.

5.4.2.2. Empirical modeling of high solid loading enzymatic hydrolysis: AFEX™-CS

For this work, a statistical design of experiments was developed using Minitab software. The Box Benhken design was composed by a total of 30 experiments, including duplicates and six middle points. The experimental results, notably glucose and xylose conversions, were used to develop a regression model composed of a quadratic equation containing the various factors (solid loading, enzyme loading and incubation time) and the respective interaction terms. The coefficients from the terms were considered based on their *P* value (< 0.05), goodness of the regression fit and their effect on the model's ability to predict unknown observations, analyzing statistical parameters such as predicted R^2. These statistical analyses were performed both for enzymatic hydrolysis on AFEX™ and EA pretreated corn stover. From **Figure 5-5 A**, it is possible to observe residual plots from the regression of monomeric glucose conversion as a function of enzymatic hydrolysis parameters for AFEX™-CS. **Figure 5-5 B** shows the coefficients considered for the regression model and respective *P* values. The residual plots show that the residuals are evenly spread through the fitted values, even though there are more experimental points above 50 % conversion (0.5). The residuals varied from -4 % (-0.04) to 4 % (0.04) glucose conversion, however the histogram shows that most residuals waere close to zero. From the normal probability plot, it is also possible to observe that the residuals conform reasonably well to a normal distribution.

A Residual Plots for Monomeric Glucose Conversion (AFEX)

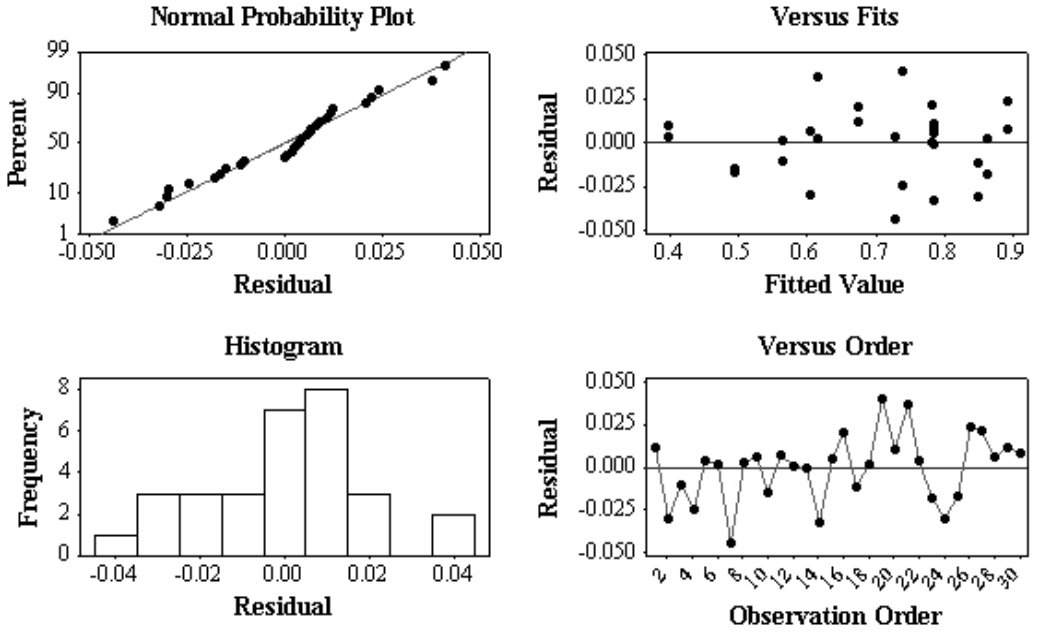

B **Regression Coefficients for Monomeric Glucose Conversion**

Term	Coef	SE Coef	T	P
Constant	-0.034311	0.139759	-0.246	0.808
Time	0.006288	0.000611	10.289	0.000
Solid Loading	0.016447	0.013584	1.211	0.239
Enzyme Loading	0.03727	0.002778	13.416	0.000
Time*Time	-0.000026	0.000004	-7.039	0.000
Solid Loading*Solid Loading	-0.000686	0.000338	-2.028	0.055
Enzyme Load.*Enzyme Load.	-0.000578	0.000067	-8.644	0.000
Time*Solid Loading	-	-	-	-
Time*Enzyme Loading	-0.000039	0.000015	-2.595	0.017
Solid Loading*Enzyme Loading	-	-	-	-

S = 0.0229884 **PRESS** = 0.0231912
R-Sq = 98 % **R-Sq (pred)** = 96.01% **R-Sq (adj)** = 97.36%

Figure 5-5 (A) Residual plots for the regression of glucose conversion on AFEX^{TM}-CS as a function of enzymatic hydrolysis variables (time, solid loading and enzyme loading) and respective interaction terms. Residuals and fitted values are expressed in (glucose conversion). (B) Estimation of regression coefficients and *P* values for the terms affecting glucose conversion. Parameters that determine the goodness of the fit are also shown.

From **Figure 5-5 B**, it is possible to observe that the interaction parameters *Time*Solid Loading* and *Solid Loading*Enzyme Loading* were not considered for the model equation. These two factors had a *P* value higher than 0.05 and had negative impacts on the predictive ability of the model by generating lower predicted R^2 values. Other parameters also have *P* values above 0.05 and were included in the model, as their absence negatively impacted the goodness of the fit and the ability of the model to predict unknown observations, notably by reducing the predicted R^2. The final model presented an R^2 value of 98 %, a predicted R^2 of 96.01 % and an adjusted R^2 of 97.36 %. These three parameters are similar to each other and demonstrate the goodness of the fit and predictability of the model, also suggesting the model is not overfitting the experimental data.

The final equation predicting glucose conversion for AFEX^{TM}-CS as a function of enzymatic hydrolysis parameters was determined as follows:

$$\textit{Glucose Conversion} = (-0.034311) + (0.006288\ X_1) + (0.016447\ X_2) + (0.03727\ X_3) - (0.000026\ X_1X_1) - (0.000686\ X_2X_2) - (0.000578\ X_3X_3) - (0.000039\ X_1X_3) \quad \textbf{5-1}$$

Where,

X_1 = Time (h) [24 to 120]; X_2 = Solid Loading (%) [15 to 25]; X_3 = Enzyme Loading (mg/g glucan) [7.5 to 30].

A Residual Plots for Monomeric Xylose Conversion (AFEX)

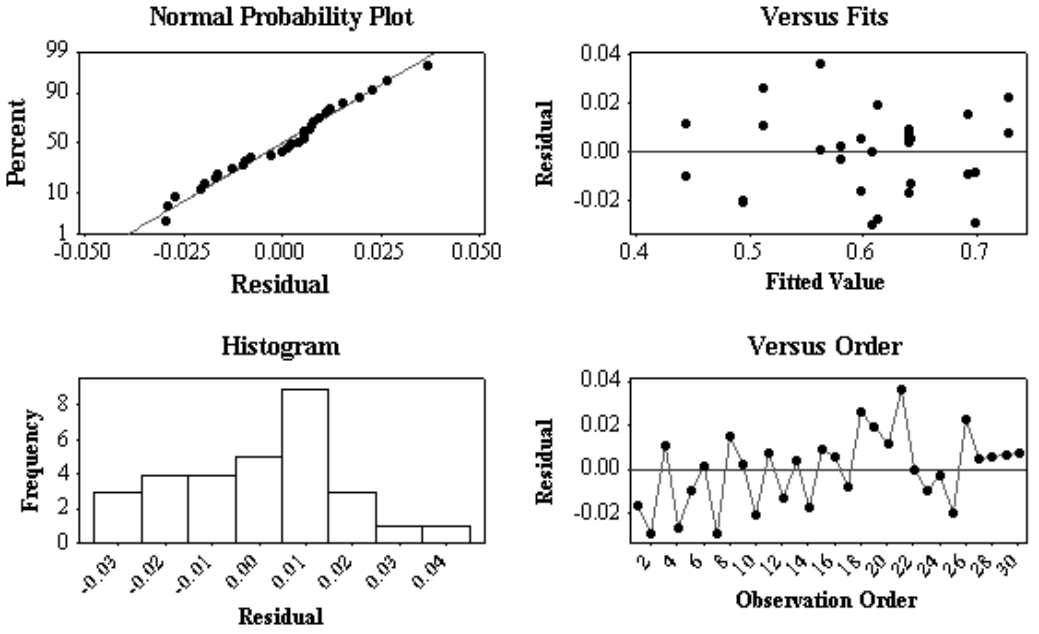

B **Regression Coefficients for Monomeric Xylose Conversion**

Term	Coef	SE Coef	T	P
Constant	0.431136	0.034083	12.65	0.000
Time	0.003516	0.000499	7.041	0.000
Solid Loading	-0.0086	0.000941	-9.139	0.000
Enzyme Loading	0.016491	0.00227	7.266	0.000
Time*Time	-1.5E-05	0.000003	-4.985	0.000
Solid Loading*Solid Loading	-	-	-	-
Enzyme Load.*Enzyme Load.	-0.00023	0.000055	-4.285	0.000
Time*Solid Loading	-	-	-	-
Time*Enzyme Loading	-1.6E-05	0.000012	-1.333	0.196
Solid Loading*Enzyme Loading	-	-	-	-

S = 0.0188255 **PRESS** = 0.0151929
R-Sq = 95.48% **R-Sq (pred)** = 91.58% **R-Sq (adj)** = 94.3%

Figure 5-6 (A) Residual plots for the regression of xylose conversion on AFEX^{TM}-CS as a function of enzymatic hydrolysis variables (time, solid loading and enzyme loading) and respective interaction terms. Residuals and fitted values are expressed in (xylose conversion). (B) Estimation of regression coefficients and *P* values for the terms affecting xylose conversion. Parameters that determine the goodness of the fit are also shown.

Figure 5-6 shows the residual plots and regression parameters for xylose conversion of AFEX^{TM}-CS as a function of enzymatic hydrolysis parameters. In **Figure 5-6 A**, the residuals for this model are randomly distributed throughout the residual plot (versus fit), showing that the model is balanced and does not present systematic lack-of-fit. The histogram and normal distribution plots show that most of the residuals are close to zero, following an approximate bell shape curve ranging from -3 % (0.03) to 4 % (0.04). This observation suggests that the model fits experimental data reasonably well, which can be confirmed by the R^2 value of 95.48 % (**Figure 5-6 B**). The regression coefficients and terms considered for this model are shown in **Figure 5-6 B**. Most of the terms had *P* values below 0.05, showing their significance in explaining the variability of the experimental observations. One exception was the term *Time*Enzyme Loading*, which had a *P* value of 0.196, however, it was included in the final model equation because it positively affected the predictive ability of the model, by increasing the predicted R^2. Since the R^2, predicted R^2 and adjusted R^2 are similar to each other and relatively high (> 90 %), it suggests that the model has good predictive ability, fitting the experimental data reasonably well without overfitting experimental values.

The final equation predicting xylose conversion for AFEX^{TM}-CS as a function of enzymatic hydrolysis parameters was determined as follows:

Xylose Conversion $= (0.431136) + (0.003516\ X_1) - (0.0086\ X_2) + (0.016491\ X_3) -$ **5-2**

$$(1.5\ E\text{-}5\ X_1X_1) - (0.00023\ X_3X_3) - (1.6\ E\text{-}5\ X_1X_3)$$

Where,

X_1 = Time (h) [24 to 120]; X_2 = Solid Loading (%) [15 to 25]; X_3 = Enzyme Loading (mg/g glucan) [7.5 to 30].

5.4.2.3. Empirical modeling of high solid loading enzymatic hydrolysis: EA-CS

A similar analysis was performed for enzymatic hydrolysis of EA-CS, resulting in regression equations for glucose and xylose conversions as a function of incubation time, solid loading and enzyme loading, including their respective interaction terms. **Figure 5-7 A** shows residual plots and histograms for the glucose conversion model. In this model, there is a tendency for the residuals to be negative in the lower and higher extremities of glucose conversion (versus fits plot). The residuals in those regions can go up to -0.07 (-7% conversion). In the intermediate glucose conversions the residuals appear to be randomly distributed and do not show visible evidence of systematic lack-of-fit. It is also important to mention that the experimental observations did not cover a region between ~0.62 and ~0.72 glucose conversion, which can negatively impact the predictive ability of the model. The histogram and normal probability plots show good distribution of the residuals, ranging from -0.07 (-7 %) to 0.04 (4 %), with the majority of the fits having residuals near zero, as preferred. As a consequence of the minor systematic lack-of-fit, the predicted R^2 value for the best fit was 88.73 %, although the R^2 value was 94.16 %. These statistical indicators and the adjusted R^2 (92.3 %) are similar to each other,

which indicate the model does not overfit experimental data. The coefficients considered for the best fit are shown in **Figure 5-7 B** and included all the terms with *P* value below 0.05.

As a result of this analysis, the final equation predicting glucose conversion for EA-CS as a function of enzymatic hydrolysis parameters was determined as follows:

$$\textbf{\textit{Glucose Conversion}} = (0.695671) + (0.004804\ X_1) - (0.02252\ X_2) + (0.02295\ X_3) - (1.2\ E\text{-}5\ X_1X_1) - (0.00051\ X_3X_3) - (9.9\ E\text{-}5\ X_1X_2) - (0.000582\ X_2X_3) \quad \textbf{5-3}$$

Where,

X_1 = Time (h) [24 to 120]; X_2 = Solid Loading (%) [15 to 25]; X_3 = Enzyme Loading (mg/g glucan) [7.5 to 30].

The residual plots and histograms for the xylose conversion model of EA-CS are shown in **Figure 5-8 A**. The plot "versus fits" shows that the residuals are randomly distributed throughout the space of the model. The residual amplitude is also relatively small, ranging from -0.003 (3 %) to 0.024 (2.4 %). The histogram and normal probability plots show that the residuals follow a normal distribution relatively well, with the highest number of residuals being close to zero. Thus the model fits the experimental observations reasonably well and suggests the absence of a systematic lack-of-fit within the space of the model. **Figure 5-8 B** shows that the model has a good predictive ability, with a predicted R^2 value of 93.02 % and fits experimental data reasonably well with an R^2 value of 95.87 %. As the adjusted R^2 value (94.79 %) is similar to

the formerly mentioned R^2 values, there is a strong indication that the model does not overfit experimental data and can be used for predict new observations with good probability of success. The model parameters used for predicting xylose conversion on EA-CS are also shown in **Figure 5-8 B**. The terms of this model were chosen based on their *P* value and their influence on the predictive ability of the model. Terms with *P* values above 0.05 were initially rejected, however the model was negatively impacted by the absence of the terms *Solid Loading* and *Solid Loading*Solid Loading*, due to decrease of predicted R^2 value and increase of *P* value from the F test. Therefore, those two terms were included in the model. As a result, the final equation predicting xylose conversion for EA-CS as a function of enzymatic hydrolysis parameters was determined as follows:

$$\textbf{\textit{Xylose Conversion}} = (0.503478) + (0.001913\ X_1) + (0.00947\ X_2) + (0.01392\ X_3) - (7\ E\text{-}6\ X_1X_1) - (0.00048\ X_2X_2) - (0.00023\ X_3X_3) \quad \textbf{5-4}$$

Where,

X_1 = Time (h) [24 to 120]; X_2 = Solid Loading (%) [15 to 25]; X_3 = Enzyme Loading (mg/g glucan) [7.5 to 30].

A Residual Plots for Monomeric Glucose Conversion (EA)

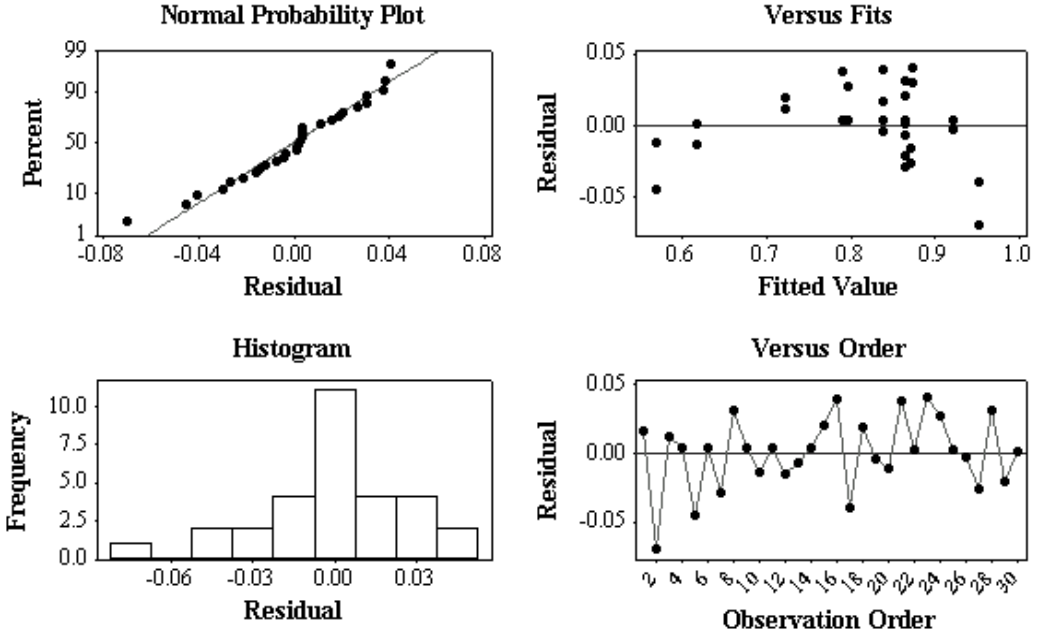

B **Regression Coefficients for Monomeric Glucose Conversion**

Term	Coef	SE Coef	T	P
Constant	0.695671	0.089122	7.806	0.000
Time	0.004804	0.000795	6.04	0.000
Solid Loading	-0.02252	0.003839	-5.865	0.000
Enzyme Loading	0.02295	0.005223	4.394	0.000
Time*Time	-1.2E-05	0.000005	-2.53	0.019
Solid Loading*Solid Loading	-	-	-	-
Enzyme Load.*Enzyme Load.	-0.00051	0.000087	-5.818	0.000
Time*Solid Loading	-9.9E-05	0.00002	-5.06	0.000
Time*Enzyme Loading	-	-	-	-
Solid Loading*Enzyme Loading	0.000582	0.000188	3.09	0.005

S = 0.0299862 **PRESS** = 0.0381324
R-Sq = 94.16% **R-Sq (pred)** = 88.73% **R-Sq (adj)** = 92.3%

Figure 5-7 (A) Residual plots for the regression of glucose conversion on EA-CS as a function of enzymatic hydrolysis variables (time, solid loading and enzyme loading) and respective interaction terms. Residuals and fitted values are expressed in (glucose conversion). (B) Estimation of regression coefficients and *P* values for the terms affecting glucose conversion. Parameters that determine the goodness of the fit are also shown.

A Residual Plots for Monomeric Xylose Conversion (EA)

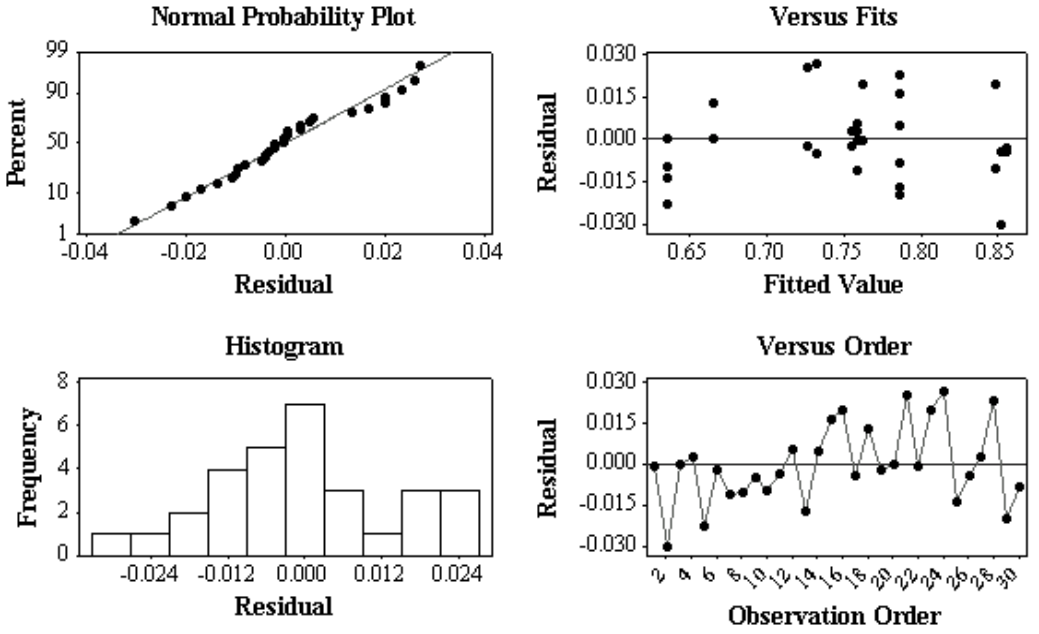

B **Regression Coefficients for Monomeric Xylose Conversion**

Term	Coef	SE Coef	T	P
Constant	0.503478	0.097039	5.188	0.000
Time	0.001913	0.00038	5.028	0.000
Solid Loading	0.00947	0.009533	0.993	0.331
Enzyme Loading	0.013927	0.001795	7.758	0.000
Time*Time	-7E-06	0.000003	-2.618	0.015
Solid Loading*Solid Loading	-0.00048	0.000237	-2.02	0.055
Enzyme Load.*Enzyme Load.	-0.00023	0.000047	-4.812	0.000
Time*Solid Loading	-	-	-	-
Time*Enzyme Loading	-	-	-	-
Solid Loading*Enzyme Loading	-	-	-	-

S = 0.016133 **PRESS** = 0.0101034
R-Sq = 95.87% **R-Sq (pred)** = 93.02% **R-Sq (adj)** = 94.79%

Figure 5-8 (A) Residual plots for the regression of xylose conversion on EA-CS as a function of enzymatic hydrolysis variables (time, solid loading and enzyme loading) and respective interaction terms. Residuals and fitted values are expressed in (xylose conversion). (B) Estimation of regression coefficients and *P* values for the terms affecting xylose conversion. Parameters that determine the goodness of the fit are also shown.

5.4.2.4. Performance of high solid loading enzymatic hydrolysis on EA- and AFEX™-CS

To better evaluate our empirical modeling work, we compared experimental and predicted observations side-by-side, as shown in **Figure 5-9** . The predicted values match reasonably well average glucose (**Figure 5-9 I**) and xylose (**Figure 5-9**) conversions for EA- and AFEX™-CS at the various conditions given by the Box Benhken design (**Figure 5-9 III**). In this figure it is also clear that EA-CS is more digestible than AFEX™-CS for all enzymatic hydrolysis conditions, as reflected by superior glucose and xylose conversions.

To better visualize of the effect of the various enzymatic hydrolysis variables on glucose and xylose conversions, a series of contour plots are presented in **Figure 5-10** and **Figure 5-11**. **Figure 5-10** shows contour plots for glucose A) and xylose B) conversions on AFEX™-CS using "middle point" experimental conditions as fixed variables, i.e., 72 h time, 18.75 mg/g glucan enzyme loading and 20 % solid loading. From the contour plots, it is possible to observe the negative effect of increasing solid loading on both glucan and xylan conversion (plots I and II). This effect, also known as the "solids effect" in the literature, is commonly observed when performing high solid loading enzymatic hydrolysis studies, independently of the pretreatment technology and lignocellulosic substrate applied [170]. As expected, increasing enzyme loading and residence time have a positive effect on enzymatic hydrolysis yields from AFEX™-CS. The effect of time and enzyme loading (within the boundaries of this study) seems to be more impactful to improve glucose conversion than xylose conversion from this substrate as is evident from the range of conversions that can be achieved when controlling these two variables. Using AFEX™-CS, the maximum glucose conversion for "middle point" conditions range from 85 %

to 92 %, achieved using low solid loadings, relatively high enzyme loadings and residence times. The scenario for xylose conversion is significantly different, as maximum xylose conversions range 70 % to 75 % for "middle point" conditions. These significantly lower yields for xylose conversion agree with previous reports in the literature that studied enzymatic hydrolysis on AFEX^{TM}-CS [171]; however the reasons behind these observations are still under investigation.

If we compare these results for AFEX^{TM}-CS with EA-CS (**Figure 5-11**), it is possible to observe significant differences and some similarities. The performance profile and the dependence of the enzymatic hydrolysis variables are similar between the two pretreated substrates. The "solids effect" is still present in EA-CS, especially at lower enzyme loadings and residence times. At higher enzyme loadings the "solids effect" seems to be reduced for glucose conversion as can be observed on **Figure 5-11 A-I**. The major differences between EA-CS and AFEX^{TM}-CS is that EA pretreatment improves glucose and xylose conversions significantly. Maximum glucose conversions of > 92 % and xylose conversions of > 85 % can be achieved for "middle point" conditions on EA-CS in contrast with AFEX^{TM}-CS. Much of this improvement is due to cellulose III conversion [105, 117] and also to lignin removal [157, 165] as discussed in **CHAPTER 4**.

i)

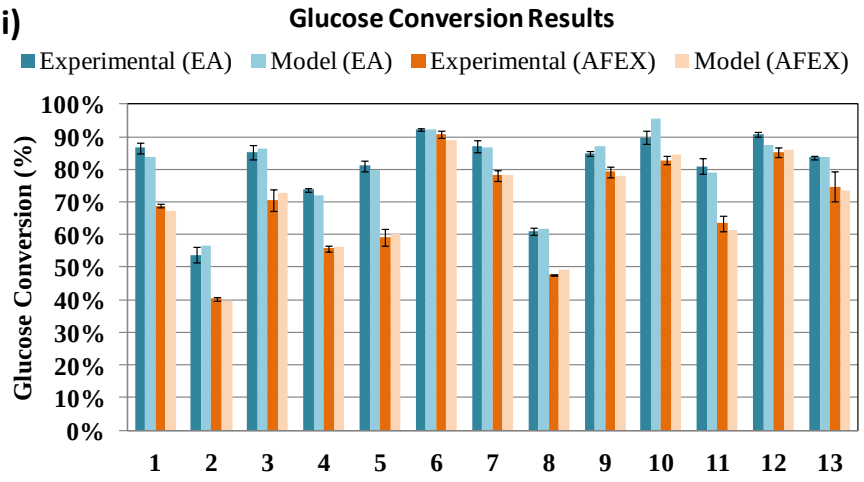

ii)

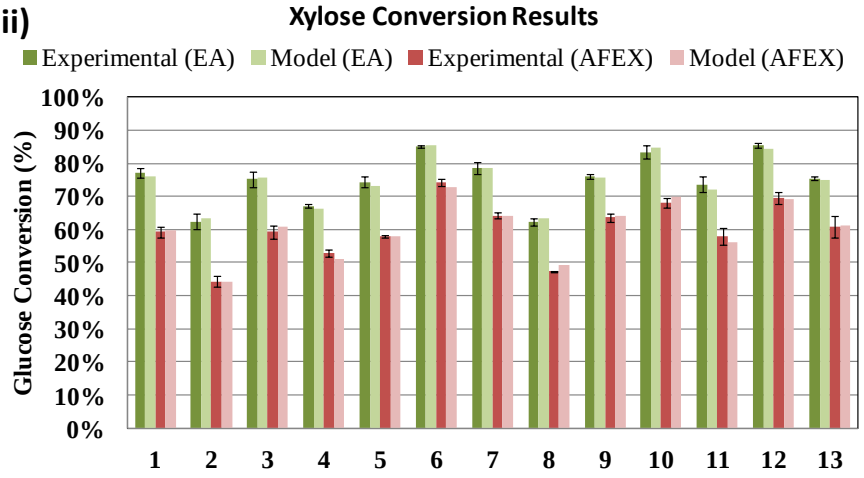

iii)

	Enzymatic Hydrolysis Conditions		
Condition #	**Time (h)**	**Solid Loading (%)**	**Enzyme Loading (mg/g glucan)**
1	24	15	18.75
2	24	20	7.5
3	24	20	30
4	24	25	18.75
5	72	15	7.5
6	72	15	30
7	72	20	18.75
8	72	25	7.5
9	72	25	30
10	120	15	18.75
11	120	20	7.5
12	120	20	30
13	120	25	18.75

Figure 5-9 Comparison of average experimental observations and model predictions for i) glucose conversion and ii) xylose conversion for EA- and AFEX^{TM}-CS. iii) Experimental conditions formulated by the Box Benhken design, which were used for model formulation.

To better observe the benefits of EA pretreatment during high solids loading enzymatic hydrolysis, a few kinetic curves were extracted from the model for two solid loadings (15 % and 20 %) and three enzyme loadings (7.5, 10 and 20 mg/g glucan), which are shown in **Figure 5-12**. As mentioned during the analysis of the contour plots, both residence time and enzyme loading seem of little benefit to xylose conversion. These curves clearly show that in the period between 24 and 120 h, predicted xylose conversions do not improve more than ~10 % for all the enzyme and solid loadings presented. This observation is also independent of the pretreatment type investigated here, as it was observed for both EA and AFEX^{TM}-CS. However, the initial rates of enzymatic hydrolysis are greater for EA-CS than for AFEX^{TM}-CS and that seems to be the key factor for achieving higher xylose conversions. Also, a relatively small improvement (~10 %) in the final xylose conversion is predicted when increasing enzyme loading from 7.5 to 20 mg/g glucan (i.e., 2.7 fold increase enzyme loading). Likewise, increasing solids loading from 15 % to 20 % did not produce considerable effects on the final xylose conversions for the range of enzyme loadings evaluated in **Figure 5-12**.

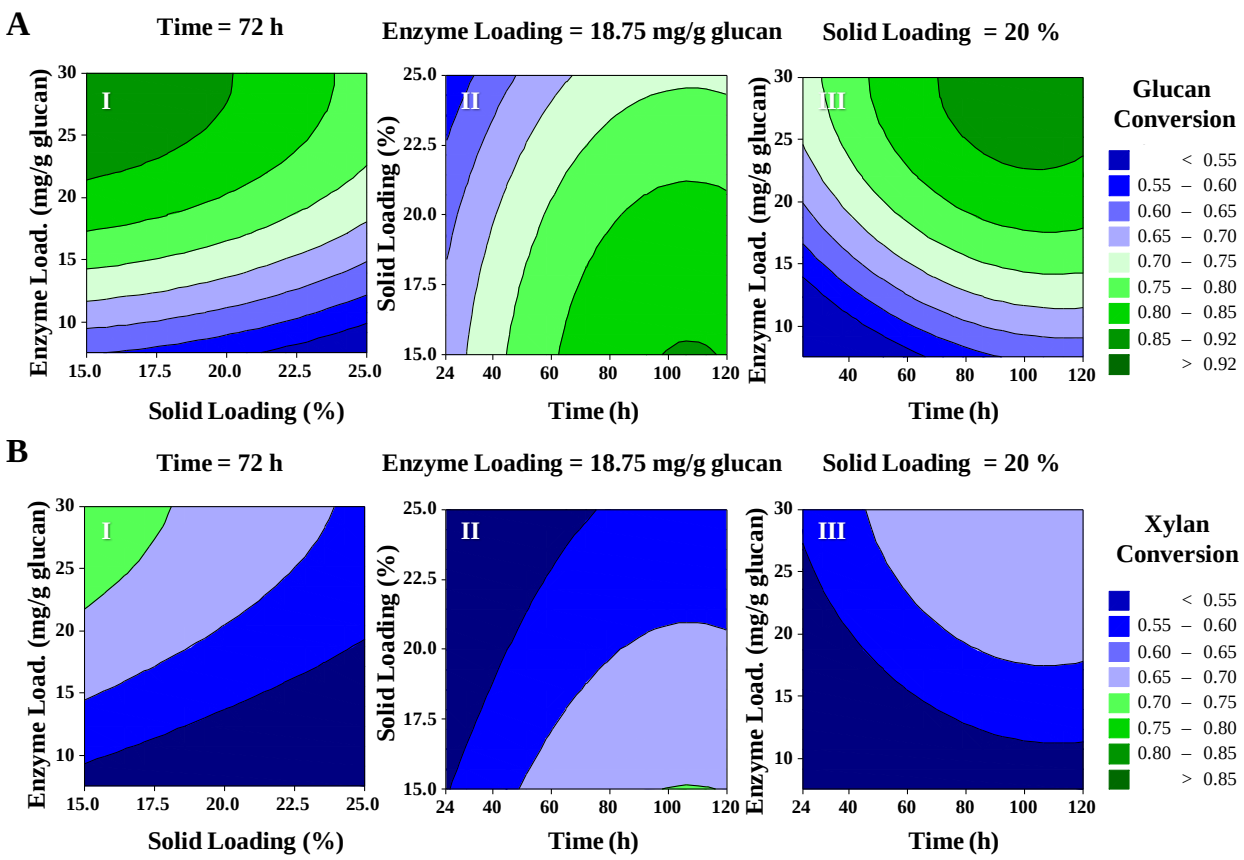

Figure 5-10 Contour plots with model predictions for A) glucose and B) xylose conversion for AFEX^{TM}-CS, as a function of time, enzyme loading and solids loading during enzymatic hydrolysis. Fixed variables were chosen to be at the "middle point" conditions.

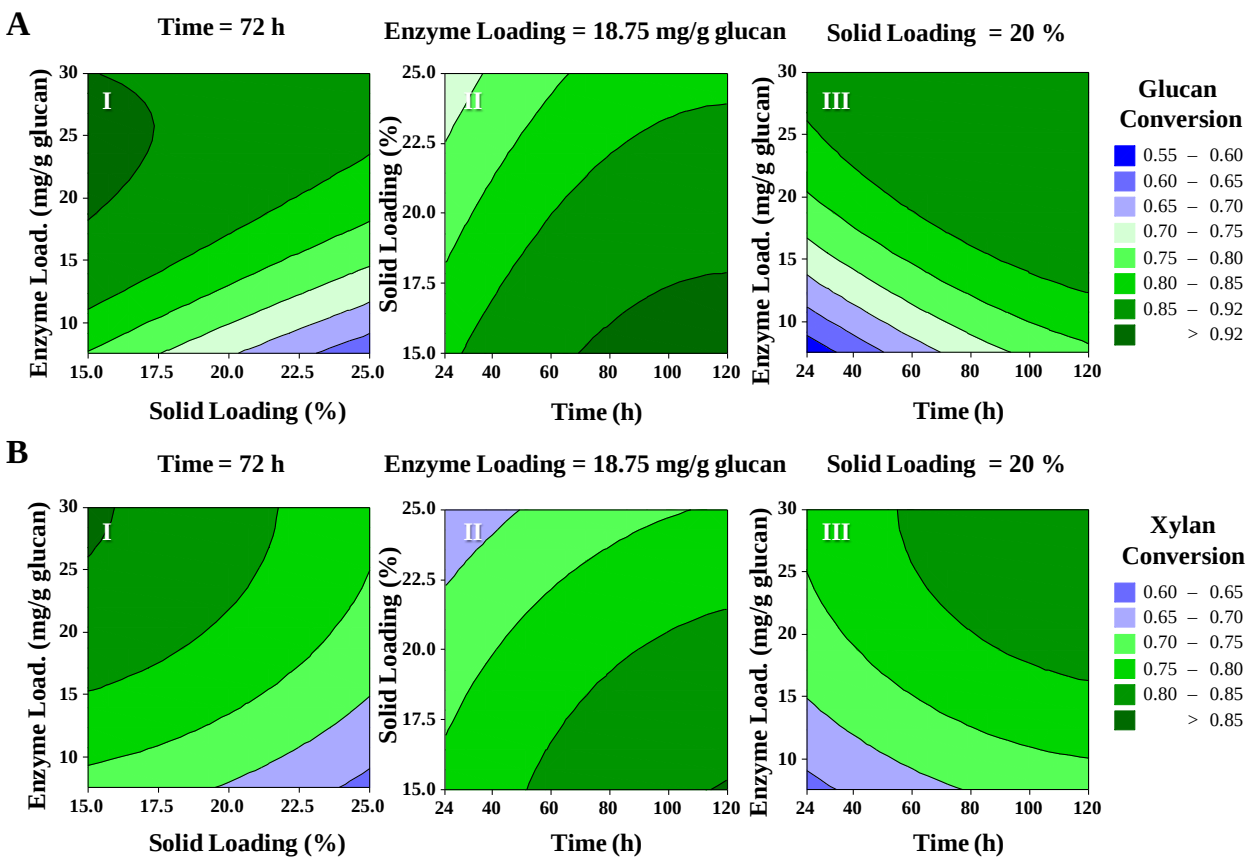

Figure 5-11 Contour plots with model predictions for A) glucose and B) xylose conversion for EA-CS, as a function of time, enzyme loading and solids loading during enzymatic hydrolysis. Fixed variables were chosen to be at the "middle point" conditions.

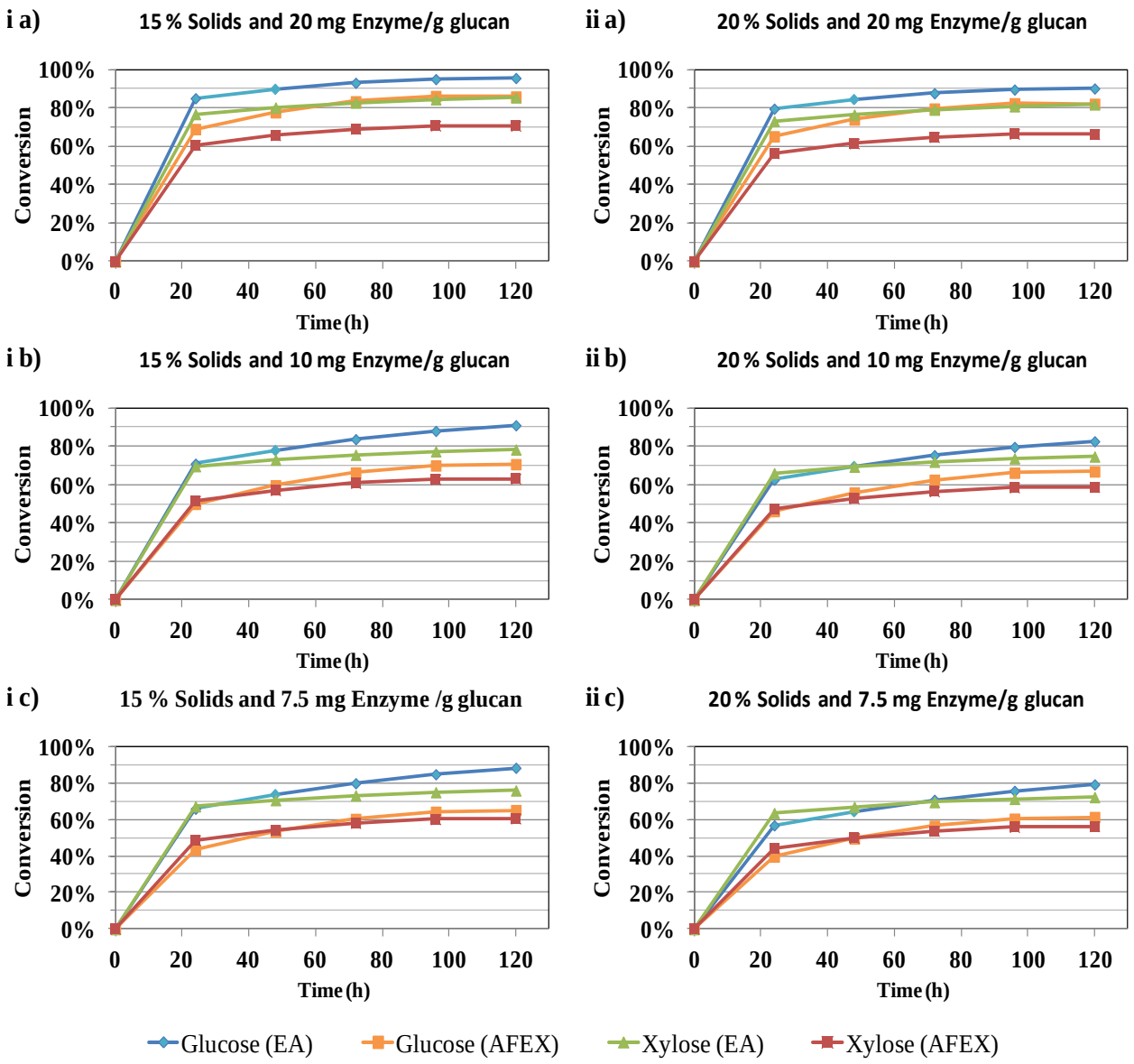

Figure 5-12 Kinetics of enzymatic hydrolysis performed at i) 15 % solids and ii) 20 % solids, for enzyme loadings of a) 20 mg/ g glucan, b) 10 mg/ g glucan and c) 7.5 mg/ g glucan. The kinetics was performed on EA- and AFEX^{TM}-CS and accounts for both glucose and xylose conversion.

Incubation time and enzyme loading seem to be the variables that impact glucose conversion in more than they do xylan conversion. Even though the first 24 h of enzymatic hydrolysis is when most of the glucose is generated from pretreated biomass, the model predicts considerable improvements of glucose conversion in the period from 24 to 120 h incubation time. An additional 15-25 % glucose conversion is predicted in this period for both EA- and AFEX^{TM}-CS and therefore, extended residence times benefit glucose conversions more than xylose conversion. The effect of residence time is very similar for both pretreatment technologies tested in this study and this variable seems to be even more important when operating at lower enzyme loadings. More time is required to achieve terminal glucose conversions at lower enzyme loadings. A major difference between the performance of EA- and AFEX^{TM}-CS under these set of conditions is that glucose conversion of AFEX^{TM}-CS seems to be greatly impacted by decreasing the enzyme loading from 20 to 7.5 mg/g glucan. The drop in glucose conversion by decreasing enzyme loading from 20 to 7.5 mg/glucan is approximately 6 % at 15 % solids and ~11 % at 20 % solids for EA-CS, while for AFEX^{TM}-CS this drop can be as much as ~20 % at both 15 % and 20 % solids (**Figure 5-13 i)**). Comparing EA and AFEX^{TM} pretreatments side-by-side, it is possible to evaluate the absolute improvement in terminal glucose and xylose conversion at 120 h enzymatic hydrolysis. From **Figure 5-13 ii)**, it is clear that the absolute improvement (AI) in terminal glucose conversion is larger as the enzyme loading drops from 20 mg/g glucan to 7.5 mg/g glucan. Also, this difference decreases with increasing solids loading from 10 % to 20 %. This observation suggests that EA pretreatment is more susceptible to the "solids effect", especially at lower enzyme loadings, as the absolute difference drops

significantly with increasing solids loading. However, it is important to notice that for the same solids loading, EA-CS contains higher levels of carbohydrates, which will potentiate higher concentrations of sugars for similar sugar conversion levels. This fact will negatively impact enzymatic activity due to sugar inhibition at lower sugar conversions and therefore, the "solids effect" between these two pretreated feedstocks cannot be compared under the same terms. Interestingly, the AI value for xylose conversion was not affected by enzyme loading or solid loading, which was maintained constant at approximately 15 % conversion. In a different type of analysis, it is possible to determine the relative improvement (RI) with respect to AFEX^{TM} conversion (**Figure 5-13 iii)**). From this perspective, it is also possible to have a better idea of the predicted impact of EA pretreatment as a function of enzymatic hydrolysis conditions. For example, glucose conversion improvements at high enzyme loading (i.e., 20 mg/g glucan) represent ~10 % of the final conversion for AFEX^{TM}-CS. This RI value is similar for both at 15 and 20 % solids loading enzymatic hydrolysis. However, if we decrease the enzyme loading by half (i.e., to 10 mg/g glucan), we can practically increase the RI for glucose conversion up to ~3 fold for 15 % solids loading and ~2.5 fold for 20 % solids enzymatic hydrolysis. This RI value can increase up to ~35 % for 15 % solids and ~29 % for 20 % solids as we reduce the enzyme loading down to 7.5 mg/g glucan. A similar trend is observed for xylose conversion, however a major difference is that increasing solids loading from 10 to 15 % benefits the xylose RI value in contrast to the glucose conversion RI. In summary, this analysis helped us to determine the impact of EA pretreatment with respect to a leading ammonia-based pretreatment technology such as AFEX^{TM}. From these results, it is clear that EA pretreatment is more beneficial for enzymatic hydrolysis performed at lower enzyme loadings and lower solid loadings. These

results were expected, since at high enzyme loading the final sugar conversion is very close to 100 % for AFEX^{TM}-CS, leaving little room for terminal conversion improvements. However, the initial rate of enzymatic hydrolysis at high enzyme loading was still considerably higher for EA-CS, which means that the benefit of using EA pretreatment and high enzyme loading may be better observed for residence times below 24 h. At higher solids loading, the impact of EA pretreatment seems to be slightly decreased, since effects such as sugar inhibition [174] start playing an important role on terminal enzymatic hydrolysis conversion.

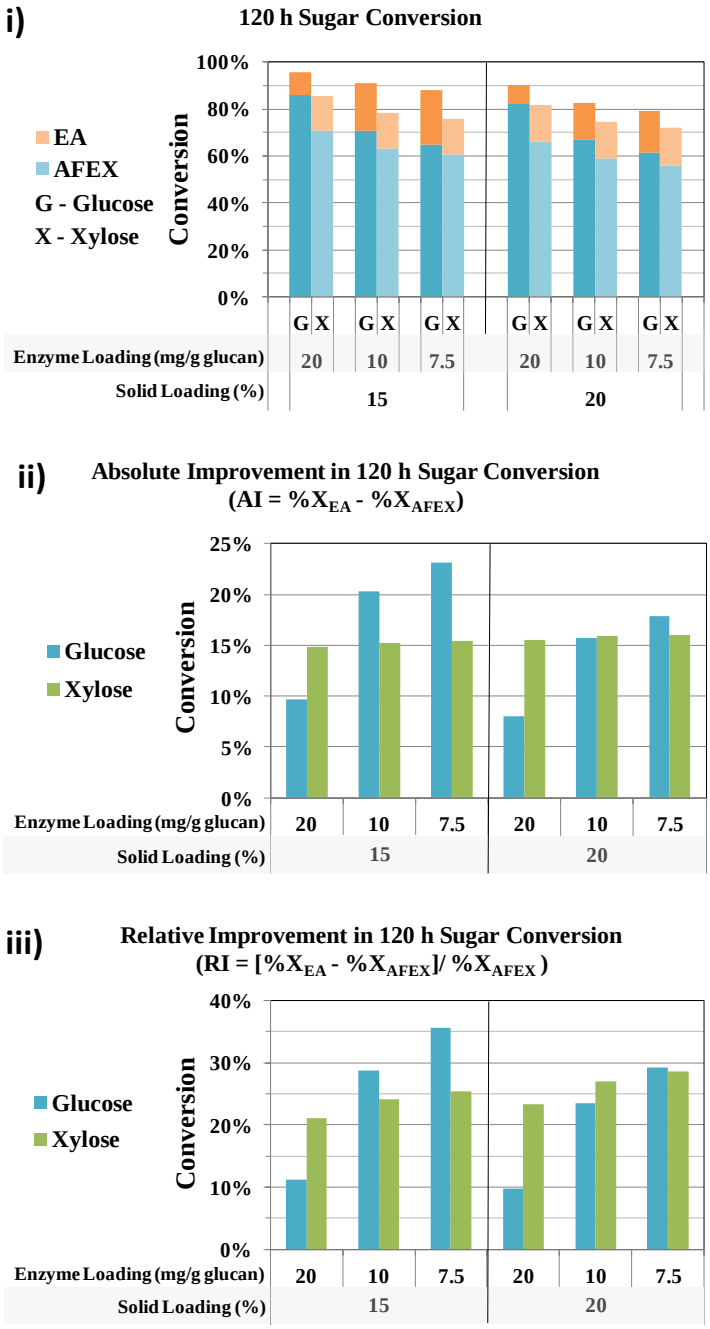

Figure 5-13 i) Terminal (120 h) glucose and xylose conversion as a function of solids loading and enzyme loading; ii) Absolute improvement (AI) in glucose and xylose conversion observed for EA-CS with respect to AFEX^{TM}-CS; iii) Relative improvement (RI)

5.5. Conclusion

A larger scale EA pretreatment system, capable of pretreating 3 x 40 g of biomass per run, was developed to produce enough feedstock for studying high solid loadings enzymatic hydrolysis. The experimental values obtained for this larger EA system are in agreement with predicted values from the model developed in **CHAPTER 4** for glucose and xylose conversions, as well as lignin extraction. As this model was developed using experimental data obtained from the small scale high-throughput EA system, these observations suggest that this pretreatment technology is scalable without having to perform new optimization protocols. The effects of moisture, and residence time were evaluated beyond the workspace of the earlier model (see **CHAPTER 4**). By increasing the moisture content of the biomass up to 40 %, it was possible to observe a gradual decrease in glucan conversion and a very marginal increase in xylan conversion. As moisture reduces cellulose III (CIII) formation, this observation may be a result of lower CIII content of biomass samples treated under higher moisture conditions. Although XRD analysis revealed CIII formation under every condition, this methodology revealed limitations to quantify CIII conversion in lignocellulosic biomass and therefore, further work is required to develop methods that allow determination of ratios between CIII, CI and amorphous cellulose in EA-CS. Extending residence time from 30 to 60 min during pretreatment impacted lignin extraction more than sugar conversion, especially at lower ammonia loadings. At high ammonia loading, i.e., 6:1 ammonia:biomass ratio, the increase in residence time had marginal effects on EA pretreatment performance, and therefore the EA condition used for enzymatic hydrolysis studies was 6:1 ammonia:biomass ratio, 10 % moisture, 30 min residence time and 120 °C. Under these conditions, glucan and xylan extraction during EA pretreatment reached 4.7 % and 5.2 % respectively, while lignin extraction reached 45.3 %.

The performance of EA pretreatment was compared with AFEX^{TM} during high solid loading enzymatic hydrolysis, where the effects of 1) enzyme loading, 2) solids loading and 3) residence time were evaluated. For this purpose, a statistical design of experiments was implemented, allowing the formulation of mathematical models for predicting glucose and xylose conversions as a function of the variables mentioned above, for both pretreated substrates. The resulting models were statistically robust with good predictive ability within their workspace, reflected by predicted R^2 values higher than 88.73 %. Using model predictions, it was possible to conclude that the initial rates of enzymatic hydrolysis are greater for EA-CS than for AFEX^{TM}-CS. Initial rates seem to be a determining factor for maximizing sugar yields at 120 h incubation time. For example, little improvement in xylose conversion was observed after 24 h enzymatic hydrolysis, independently of the enzyme loading and solid loading, showing the importance of the initial rates of hydrolysis to xylose conversion. Glucose conversion required longer times to reach high levels; however, most of the terminal conversion was obtained within the first 24 h of hydrolysis. More importantly, EA pretreatment offers greater benefits to enzymatic hydrolysis at lower enzyme loading when compared with AFEX^{TM}. At high enzyme loadings the benefits of CIII conversion and lignin extraction are diluted by the fact that enzymes are non-limiting, even though initial and final conversions on EA-CS are still higher compared to AFEX^{TM}-CS. At high solid loadings, the impact of EA pretreatment on glucose conversion seems to be reduced with respect to AFEX^{TM} pretreatment. Perhaps factors such as sugar inhibition start playing important roles on the performance of cellulases, especially because sugar conversions can reach very high values within the first 24 h of enzymatic hydrolysis for EA-CS. Also, for the same

solids loading, EA-CS presents higher carbohydrate content due to lignin removal during the pretreatment process. Therefore, the solids loading effect for pretreated feedstocks with distinct compositions cannot be compared on the same terms. Although glucose conversion improvements decrease with increasing solid loadings, EA-CS is still able to achieve approximately 10 to 30 % higher glucose conversion with respect to AFEX^{TM} at 20 % solids. In the other hand, the beneficial effect of EA pretreatment on xylose conversion improved with higher solid loadings, in contrast with what was observed for glucose conversion. Understanding these phenomena requires detailed studies beyond the scope of this work. In that regard, it is important to determine the contributions of sugar inhibition, lignin inhibition and CIII reversion during enzymatic hydrolysis for individual cellulases and xylanases. Those studies will help unveil factors that should be improved for enzyme technology and pretreatment technology in order to reduce enzyme loading during enzymatic hydrolysis operations at high solid loadings.

From the analysis presented herein, EA pretreatment decreases required enzyme loading by up to 2.7 fold (from 20 to 7.5 mg/g glucan) compared to AFEX^{TM}, at both 15 % and 20 % solids, without reducing performance in sugar conversion. This reduction of enzyme loading will certainly impact process economics. However, as EA pretreatment operates at higher pressures and is energy intensive, process economic studies are required to determine whether this enzyme loading reduction (along with lignin valorization) can offset the increase in pretreatment capital cost and operating cost.

APPENDIX

Table 5-3 Enzyme mixtures used during enzyme cocktail optimization for EA and AFEX™-CS

	Ctec 2	Htec 2	MP
Mix 1	100	0	0
Mix 2	70	15	15
Mix 3	50	25	25
Mix 4	25	50	25
Mix 5	25	25	50
Mix 6	33.33	33.33	33.33

Table 5-4 Enzyme optimization results for EA and AFEX-CS using enzyme mixtures 1 to 6. Glucose (Glc), xylose, (Xyl) and arabinose (Ara) concentrations are presented here as a measure of each enzyme cocktail performance after 72 h enzymatic hydrolysis. Highlighted in bold letters is the enzyme mixture used for this study.

	EA			AFEX		
	Glc (g/L)	**Xyl (g/L)**	**Ara (g/L)**	**Glc (g/L)**	**Xyl (g/L)**	**Ara (g/L)**
Mix 1	87.17	39.75	4.89	63.86	29.03	3.38
Mix 2	89.53	43.97	6.17	66.17	32.76	4.77
Mix 3	**89.86**	**45.60**	**6.28**	**68.05**	**36.12**	**5.22**
Mix 4	89.46	45.38	6.32	66.38	35.01	5.04
Mix 5	88.82	47.30	6.53	62.56	35.60	5.19
Mix 6	89.25	45.83	6.34	67.36	34.56	5.02

CHAPTER 6 - ISOLATION AND CHARACTERIZATION OF LIGNIN DERIVED FROM THE NOVEL EXTRACTIVE AMMONIA (EA) PRETREATMENT.

6.1. Abstract

With the increasing interest in sustainable lignocellulosic biofuels, and the demand for an economic conversion process, several authors have begun to look at lignin as a potential revenue source for the biorefinery. Until recently, ethanol was seen as the only revenue source for the biorefinery, where lignin-rich residues were envisioned as combustion fuel to generate electricity and heat to the process. However, these energy forms can be supplied by other kinds of alternative sources and lignin could be potentially used for further upgrade to liquid fuels or valuable chemicals. In this context, Extractive Ammonia (EA) is a pretreatment technology of lignocellulosic biomass that uses anhydrous ammonia in the absence of water to extract lignin and convert native cellulose I to highly digestible cellulose III by cellulolytic enzymes. Due to the higher ammonia loadings used in this process, would be important to use the lignin-rich streams to improve the economics of the process. One of the challenges for lignin utilization is related with the level of impurities and structural modifications that usually occur during pretreatment processes. Such factors limit the potential of the lignin as an economic material to produce bio-based fuels and chemicals. For this reason, a detailed characterization of the various lignin streams generated by the EA-based biorefinery was performed and discussed herein. Process mass balances, compositional analysis, structural determination by NMR, elemental analysis by ICP, molecular weight determination by GPC) and thermogravimetric analysis (TGA) were performed and discussed in this work to provide a comprehensive understanding of the potential of EA lignins for commercial applications.

6.2. Introduction

Recent advances on ammonia-based pretreatment technologies have demonstrated the importance of transforming the naturally occurring crystalline allomorph of cellulose I to III_I [105, 117]. This rearrangement is responsible for improved enzymatic hydrolysis rates up to 2-folds in pure cellulose, thereby allowing a reduction of the enzyme loading to achieve equivalent glucose release compared to native cellulose [105]. Efficient conversion to this crystalline structure is allowed by contacting liquid anhydrous ammonia at elevated liquid-to-solid ratios (> 3:1, w/w) for relatively short residence times (> 10 min). The utilization of such conditions during pretreatment of lignocellulosic biomass also enables partial solubilization of plant cell wall components, which include lignin, monomeric and oligomeric carbohydrates, proteins, lipids, minerals, etc. The presence of lignin has been considered one of the most detrimental factors for achieving efficient biomass conversion, due to its role on inhibition of both cellulolytic enzymes and microorganisms [29, 30]. Therefore, the possibility of efficient lignin solubilization and subsequent extraction from the carbohydrate polymers is desirable to enhance enzymatic hydrolysis and fermentation performances downstream. In this context, we developed a novel Extractive Ammonia (EA) pretreatment process that is able to selectively remove lignin from corn stover (up to ~50 %), with minimal carbohydrate loss, being simultaneously able to convert cellulose I_β to the highly digestible cellulose III_I (**CHAPTER 4**). While most of the reports found in the literature describe the utilization of aqueous ammonia to improve biomass delignification, EA pretreatment process utilizes concentrated anhydrous ammonia at mild temperatures (< 120 ºC) and relatively short residence times (15-60 min). Variations on this pretreatment method can also be implemented with the utilization of organic solvent systems in

combination with ammonia, allowing the reduction of operation pressure while extracting lignin and converting cellulose I_β to III_I (**CHAPTER 3** & **CHAPTER 4**).

Special attention has been recently dedicated to lignin as a possible bio-based precursor of aromatic building blocks that are currently obtained through petroleum refining (e.g. BTX chemicals and phenol) [26]. Lignin represents about 10-40 % of the lignocellulosic biomass content, depending on the type of plant and variety within the same species, as well as on the growth conditions of the plant [175]. Several methods have been developed to depolymerize lignin and further convert it to simpler monomeric aromatic compounds. These methods comprise catalytic cracking and hydrolysis, catalytic and electrocatalytic reductions and oxidations, among other methods [26]. In most of these processes, the preservation of lignin functionalities, such as β-O-4 aryl ether linkages, are desirable for efficient conversion to value added products [26]. Lignin isolation methods often affect these functionalities, possibly resulting in condensation reactions by the formation of chemical resistant C-C bonds that will require extra energy and controlled chemistry for selective cleavage [176, 177]. Therefore, utilization of lignin isolation methods that minimize lignin decomposition, providing lignin streams closer to its "native" form, are preferable to facilitate depolymerisation chemistry with high selectivity at acceptable yields. In this work, we present a methodology to fractionate and isolate lignin from EA pretreatment of corn stover. Further characterization of EA lignin fractions was performed by composition analysis, NMR, GPC, TGA, DSC and ICP analysis.

6.3. Experimental

6.3.1. Untreated corn stover

Corn stover (Pioneer 36H56) was harvested in September 2009 in Wisconsin (USA) and oven dried at 60 ºC for approximately 2 weeks. The biomass was further passed through a 5 mm screen installed in a Christy hammer mill (Christison Scientific LTD, England) and stored at 4 ºC in heat sealed bags prior to utilization. The moisture content of the dried and milled corn stover was approximately 6 % on a wet weight basis. The biomass composition analysis was performed using NREL protocols NREL/TP-510-42618 and NREL/TP-510-42620. On a dry weight basis, the untreated corn stover contained approximately 38 % glucan, 23 % xylan, 1 % galactan, 3 % arabinan, 14 % Klason lignin, 2 % acid soluble lignin, 5 % ash and 15 % extractives (i.e. ethanol and water soluble compounds).

6.3.2. Extractive Ammonia (EA) pretreatment of corn stover

EA pretreatment was conducted in a high pressure, stainless steel tubular reactors, equipped with individual heating mantles, temperature and pressure gauges. The reactors were connected to a temperature controlled, high pressure flash tank to allow separation of ammonia from the extractives by evaporation (**Figure 6-1**). In each reactor, 40 grams of corn stover (dry weight basis), containing 10 % moisture (wet weight basis) reacted with 240 g of ammonia for 30 min at 120 ºC. Set point temperature was achieved in the first 7 min of reaction, allowing the pressure to reach 83 bar. The pressure in the flash tank was equilibrated with nitrogen to the same pressure observed in the reactor during pretreatment. Upon reaction completion, the bottom valve in the reactor was open, allowing liquid ammonia and soluble extractives to pass through a stainless steel filter of 50 μm pore size. The ammonia gas was then allowed to be released from the top of

the flash tank while pressure was maintained in the reactor at 83 bar using nitrogen for 10 min. This procedure was designed to maintain ammonia in the liquid state during extraction and allow residual ammonia to be efficiently released from the biomass. After extraction, the reactor and flash tank pressures were equalized to ambient pressure by releasing the ammonia and nitrogen gas from the top of the flash tank. During evaporation, the liquid extractives precipitated in the bottom of the flash tank.

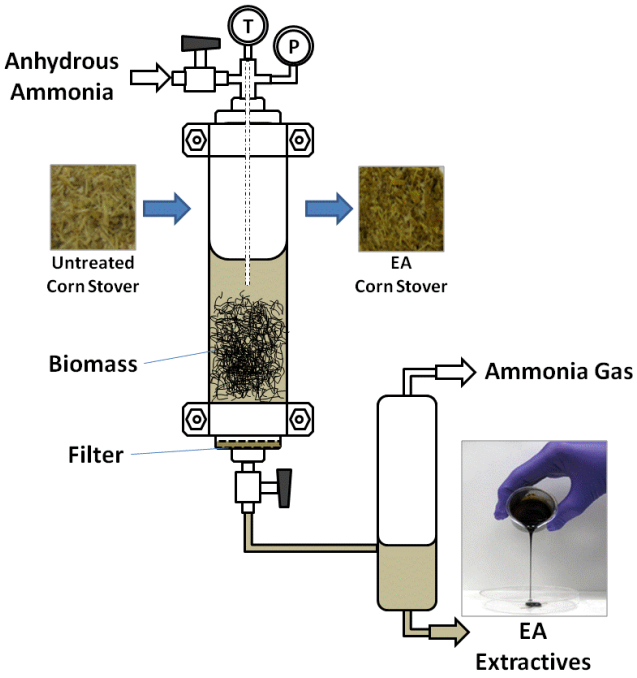

Figure 6-1 Schematic illustration of the EA pretreatment apparatus and process streams.

The biomass was then removed from the tubular reactors and allowed to dry overnight in the hood. The system lines were further cleaned with 70 % ethanol and 90 % acetone (both in water) to remove residual extractives from the lines, which were collected in the flash tank. All the EA extractives were then drained from the flash tank, collected in a 1 L round bottom flask and further concentrated in vacuum using a rotary evaporator (BUCHI Labortechnik AG,

Switzerland) set at 70 ºC. The EA extractives were then dried using a freeze drier (Labconco, Kansas City, MO, USA). The dry weight of the extractives and EA pretreated biomass was further recorded for mass balance purposes. The dried samples were stored at 4 ºC in sealed containers to avoid major moisture exposure.

6.3.3. EA extractives fractionation and production of lignin rich streams from EA process

Freeze dried EA extractives were solubilized in 100 % ethanol using 1:20 (w/v) extractives-to-solvent ratio for 30 min at continuous mixing conditions. The ethanol insoluble fraction was filtered using a fiberglass filter installed in a Millipore vacuum filter holder (EMD Millipore, Billerica, MA, USA). The filtrate was further washed with fresh 100 % ethanol to remove residual ethanol-soluble components adsorbed to the solid fraction. The solid fraction was air dried for 2 h in the hood to evaporate residual ethanol in the sample. The dried ethanol insoluble sample was weighed and placed in a beaker containing distilled water in a 1:30 (w/v) extractives-to-water ratio and stirred for 30 min. The resulting suspension was vacuum filtered using a fiberglass filter and the filtrate washed with water to remove residual water soluble components. The water insoluble fraction resulting from this separation was transferred to a pre-weighed container and dried using a freeze dried (Labconco, Kansas City, MO, USA). The dried sample was weighed for mass balance purposes and labeled as Fraction 1 (F1). The water soluble fraction was collected in a round bottom flask and concentrated using a rotary evaporator (BUCHI, Labortechnik AG, Switzerland) under vacuum, while not allowing it to reach dryness. The sample was then transferred to a pre-weighed container and freeze dried. The dried sample was weighed for mass balance purposes and labeled as Fraction 2 (F2).

The ethanol soluble fraction was transferred to a pre-weighed round bottom flask and dried using a rotary evaporator at 60 ºC under vacuum. Distilled water in a 1:30 (w/v) extractives-to-water ratio was added to the dried ethanol soluble fraction and mixed for 30 min to solubilize water soluble extractives. The suspension was vacuum-filtered and washed with distilled water to remove additional water soluble components adsorbed to the water insoluble fraction. The water insoluble fraction was transferred to a pre-weighed container and freeze dried. The dry weight of the sample was recorded for mass balance purposes and labeled as Fraction 3 (F3). The filtered water soluble fraction was further concentrated using a rotary evaporator under vacuum at 80 ºC, while not allowing it to reach dryness. The concentrated fraction was transferred to a pre-weighed container and freeze dried. The dried sample was weighed for mass balance purposes and labeled as Fraction 4 (F4). All freeze dried samples were stored in the fridge at 4 ºC in sealed plastic containers prior to utilization to avoid moisture exposure.

6.3.4. Enzymatic hydrolysis (EH) of EA pretreated corn stover

Enzymatic hydrolysis (EH) was performed at 6 % glucan loading, using 15 mg of enzyme per gram of glucan in a 5 L bioreactor set to control mixing speed at 120 RPM, temperature of 50 ºC and pH 4.8 for 72 h. The enzymes utilized in this work were Cellic® CTec2 (138 mg protein/ml, batch No.VCNI0001) and Cellic® HTec2 (157 mg protein/ml, batch No.VHN00001), generously provided by Novozymes (Franklinton, NC, USA). The enzymatic cocktail was also supplemented with Multifect Pectinase (MP) (72 mg protein/ml, batch No. 4861295753), a gift from Genencor (Pala Alto, CA, USA). The protein concentration for the enzymes was determined using the Kjeldahl nitrogen analysis method (AOAC Method 2001.11, Dairy One

Cooperative Inc., Ithaca, NY, USA). The enzyme ratios utilized in this work was 50 % Cellic® CTec2, 25 % Cellic® HTec2 and 25 % MP in a dry protein weight basis.

After EH, the resulting suspension was centrifuged at 8,000 RPM for 30 min in a Beckman Coulter Avanti J-26XP centrifuge, equipped with a rotor model JLA 8.1000 (Beckman Coulter, Inc., Brea, CA, USA), to separate the unhydrolyzed solids (UHS) from the liquid hydolyzate. The liquid hydrolyzate was decanted to a volumetric cylinder and the volume was recorded for mass balance purposes. The UHS were washed twice with the distilled water. In each washing step, the volume of distilled water used was equal to the volume of hydrolyzate generated during EH. This washing step was performed by sequential re-suspension of the solids, centrifugation and decantation. The solution resulting from the washing steps was transferred to a volumetric cylinder and the volumes were recorded for mass balance purposes. Samples of the hydrolyzate and water washing solutions were prepared for glucose and xylose analysis using HPLC equipped with a Bio-Rad Aminex HPX-87H column (Bio-Rad, Hercules, CA, USA) as previously described [88].

6.4. Lignin mass balance

Mass balance on lignin was performed around the EA pretreatment, EA extractives fractionation and enzymatic hydrolysis. The dry weight loss observed during pretreatment of corn stover was calculated by measuring the weight of the biomass before and after pretreatment, along with the moisture content using a moisture analyzer A&D MX-50 (A&D Engineering, Inc., San Jose, CA, USA). Composition analysis was performed on corn stover before and after EA pretreatment using the standard NREL protocols NREL/TP-510-42618 and NREL/TP-510-42620. Nitrogen analysis was performed using a nitrogen analyzer (Skalar PrimacsSNC, Breda, The Netherlands).

Lignin extraction yield was calculated by the difference in total lignin weight before and after pretreatment, divided by the total lignin weight of the untreated sample. The percent recovery of each fraction was normalized with respect to the total lignin present in corn stover and total extracted lignin during EA pretreatment.

6.4.1. Characterization of EA extractives fractions

6.4.1.1. Lignin characterization by NMR

6.4.1.1.1. 2D-HSQC NMR analysis

Nuclear magnetic resonance (NMR) spectra of samples in DMSO-*d6*/pyridine-*d5* (4:1, v/v) were acquired in University of Wisconsin, Madison, using a Bruker Biospin (Billerica, MA, USA) AVANCE 500 (500 MHz) spectrometer fitted with a cryogenically-cooled 5 mm TCI gradient probe with inverse geometry (proton coils closest to the sample) and spectral processing used Bruker's Topspin 3.1 (Mac) software. The central DMSO solvent peaks were used as internal reference (δ_H/δ_C: 2.50/39.51).

6.4.1.1.2. ^{13}C-NMR and ^{31}P-NMR analysis

Lignin was isolated from corn stover and UHS by ball milling and organic-solvent extraction. Ball milled lignin (BML) samples of corn stover and UHS were prepared according to the procedures described by Guerra et al. [178] and Holtman et al. [179]. Lignin isolation of EA extractive fractions was performed according to the same procedures as corn stover and UHS, excluding ball milling.

Isolated lignin samples (~100 mg) were dissolved in DMSO-d6 (500 mg) and analyzed by quantitative ^{13}C NMR using a Bruker Avance-400 MHz spectrometer at a frequency of 100.59 MHz with an inverse gated decoupling pulse sequence using a 12 s pulse delay and 10K scans. Quantitative ^{31}P NMR analysis of BML (~25 mg) was accomplished by using a pyridine/CDCl3 (1.6:1, v/v) solvent, cyclohexanol as an internal standard and 2-chloro-4,4,5,5-tetramethyl-1,3,2-dioxaphospholane (TMDP) as the derivatization agent following literature methods [180]. The ^{31}P NMR spectra were acquired using an inverse gated decoupling pulse sequence with a 25 s pulse delay and 128 scans.

6.4.1.2. Gel permeation chromatography (GPC)

The isolated lignin samples (100.00 mg) were treated with a mixture of pyridine and acetic anhydride (1:1, v/v, 4.00 mL) with stirring at room temperature for 24-36 h. The reaction mixture was diluted with ethanol (30.00 mL) and stirred for 30 min and then concentrated under lower pressure. The acetylated lignin samples were dissolved in chloroform (2.00 mL) and added dropwise into diethyl ether (100.00 mL) to precipitate the sample followed by centrifugation. The precipitate was washed with diethyl ether and centrifuged three times. After air drying, the acetylated samples were dried for 24 h in a vacuum oven at 40 °C prior to GPC analysis.

Molecular weight determination was conducted using a Polymer Standards Service (PSS) GPC Security 1200 system equipped with four Waters Styragel columns (HR0.5, HR2, HR4, HR6) at 30 ºC, Agilent isocratic pump, Agilent auto-sampler, Agilent degasser, Agilent refractive index (RI) detector and Agilent UV detector (270 nm) using THF as the mobile phase (1.0 mL/min) with injection volumes of 20 μL.

The weight average molecular weight (M_w) values of the derivatized lignin samples were acquired by using an relative calibration curve and this relative calibration curve was created by fitting a third order polynomial equation to the retention volumes obtained from a series of narrow molecular weight distribution polystyrene standards (1.36×10^6, 5.38×10^5, 3.14×10^4, 7.21×10^3, 4.43×10^3, 5.80×10^2 g/mol). The curve fit had an R^2 value of 0.9984.

6.4.1.3. Elemental analysis

The inorganic elements in the samples were determined by Inductively Coupled Plasma Emission Spectroscopy (ICP) according to methodology previously employed by Allison et al. [181]. Nitrogen, Carbon, Hydrogen and Oxygen analysis in fraction F3 were performed by Galbraith Laboratories, Inc., Noxville, TN, USA.

6.4.1.4. Thermogravimetric analysis (TGA) and differential scanning calorimetry (DSC) analysis

Thermal gravimetric analysis (TGA) data were obtained using PerkinElmer Simultaneous Thermal Analyzer (STA) 6000. Samples were put into a ceramic crucible with a lid. The ramp rate was 10 ºC/min from 25 to 600 ºC. When the temperature reached 600 ºC, it was held under isothermal condition for 2 minutes. Nitrogen was used as the flushing gas set at a flow rate of 50 mL/min throughout the test.

Differential scanning calorimeter (DSC) data were obtained using a Q20 TA Instruments V24.7 Build 119. Samples were put into an aluminum pan with a lid and underwent a heat-cool-heat cycle at a ramp rate of 10 ºC/min, including 25 to 400 ºC, 400 to 100 ºC and 100 to 400 ºC. As a reference, an identical empty aluminum pan with a lid was used. Nitrogen was used as the flushing gas set at 50 mL/min.

6.5. Results and Discussion

6.5.1. EA pretreatment process and lignin mass balance

EA pretreatment conditions that produce high lignin removal, while allowing simultaneous conversion of cellulose I_β to III_I, provided the pressure limit for operation of the EA reactors (~1200 psi). Enzymatic hydrolysis results at 6 % glucan loading demonstrates a superior digestibility of EA pretreated corn stover (EA CS) when compared to AFEX^{TM} pretreated corn stover (AFEX^{TM} CS), which is a leading pretreatment technology, based on ammonia, that performs particularly well on grasses [182]. From **Figure 6-2**, it is possible to observe a maximum glucan and xylan conversions of ~90 % for EA pretreated corn stover, obtained during the first 24 hours of incubation, while for AFEX^{TM} CS was only possible to observe similar conversions after 72 hours of incubation. These experimental results confirm the point that EA pretreatment, while removing lignin and converting cellulose I to III (**CHAPTER 4**) is able to significantly decrease biomass recalcitrance to enzymatic digestion.

The ammonia-soluble EA fraction, which was recovered after extraction and evaporation of ammonia, is a black viscous fluid that contains approximately 44 % of the total lignin from untreated corn stover (F0 in **Figure 6-3**). This black liquor was further fractionated by sequential precipitation using 100% ethanol and water, as demonstrated in **Figure 6-3**. The choice of solvents was based on their cost and availability in the ethanol biorefinery, keeping in mind the goal to pursue the most economic and sustainable fractionation process. In this context, ethanol will certainly be one of the cheapest solvents available once the lignocellulosic bioeconomy becomes a reality and will be readily available in the biorefinery.

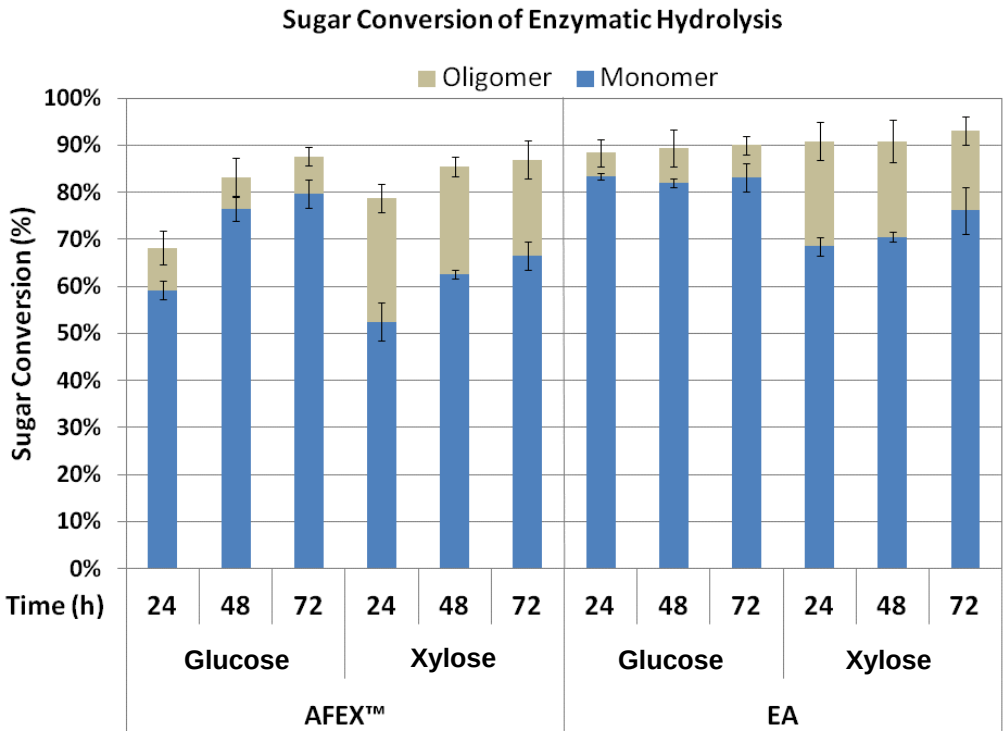

Figure 6-2 Sugar conversion based on monomeric + oligomeric glucose and xylose during enzymatic hydrolysis of AFEX™ and EA pretreated corn stover.

Using this methodology, it was possible to fractionate EA lignin extractives into four different streams (F1-F4 in **Figure 6-3**). The ethanol insoluble/water insoluble fraction (F1) represents approximately 1.5 % (dry weight) of the untreated biomass and contains approximately 1% of the lignin present in untreated corn stover. This fraction contains approximately 69 wt% of lignin and relatively low levels of carbohydrates and ash, as demonstrated in **Table 6-1**. Fraction 2 (F2) is ethanol insoluble and water soluble, containing approximately 3 % of the initial lignin present in untreated corn stover. Composition analysis results show that this stream is abundant in water soluble carbohydrates (~28 %), ash (~4 %) and water soluble lignin (~14 %). The ethanol soluble fractions (F3 & F4) contain most of the lignin extracted during EA pretreatment (F0), representing approximately 40% of the lignin present in untreated corn stover. After adding

water to the ethanol soluble extracts, it was possible to observe the creation of lignin aggregates, beige in color, while the darker brown extracts were solubilized by the added water. Mass balance and composition analysis showed that about 32 % of the lignin present in untreated corn stover is present in water insoluble fraction F3 while the remaining 8% is water soluble (F4). More importantly, this methodology allowed the isolation of a fraction that contained 92.35 % of lignin in its composition (i.e., F3).

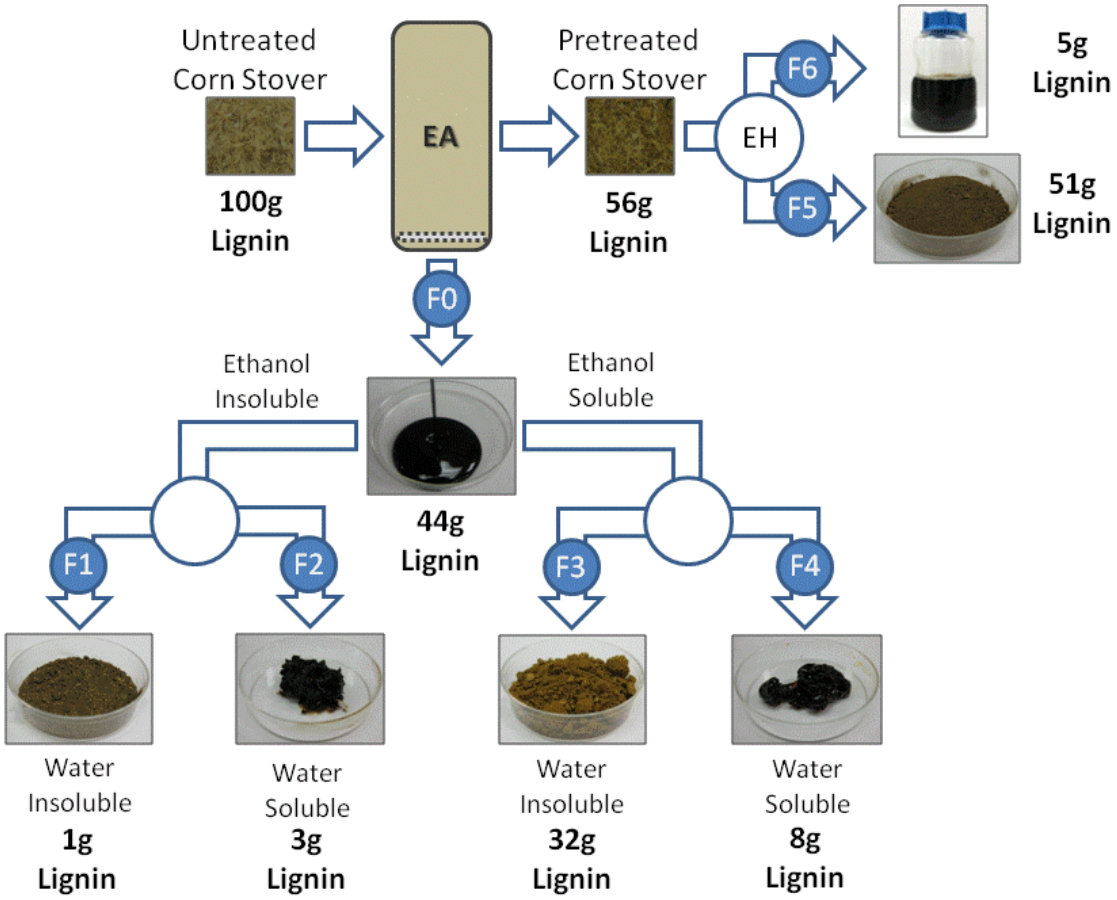

Figure 6-3 Illustration of EA lignin processing and mass balance. Fraction F6 is the enzymatic hydrolyzate, rich in glucose and xylose, which is usually fermented to ethanol in a lignocellulosic ethanol biorefinery. Fractions F1-5 may be utilized for value addition within the biorefinery, with special attention to fraction F3 and F5 that contain 32% and 51% of the lignin originally present in untreated corn stover, respectively.

From the EA CS that was hydrolyzed to fermentable sugars, it was possible to obtain a solid (F5) and a liquid (F6) stream. The liquid stream (F6) contains mostly the sugars that will be fermented to ethanol, while F5 is in great part composed by lignin (42.90 %) and recalcitrant carbohydrates (25.78 % total) that could not be solubilized in water.

Table 6-1 Compositional analysis of fractions F1 to F5.

	F1	F2	F3	F4	F5
Glucan	0.45%	13.29%	0.04%	4.43%	18.97%
Xylan	0.16%	11.72%	0.01%	1.28%	5.54%
Arabinan	0.03%	3.21%	0.00%	0.53%	1.27%
Acetyl	0.39%	1.24%	0.35%	27.28%	0.36%
Lignin	69.12%	14.44%	92.35%	13.49%	42.90%
Ash	1.43%	4.01%	0.18%	2.35%	4.05%

Further work will be required to identify the remaining unknown components of fractions F1-F5. However, fractions F1, F2 and F4 do not show great potential from the perspective of lignin utilization, since they only carry 1%, 3% and 8%, respectively, of the total lignin in untreated corn stover, respectively. In this regard, fractions F3 and F5 are highly enriched in lignin and therefore, these fractions may provide a good source of aromatic precursors for advanced fuels and chemicals in an EA-based biorefinery. To evaluate the potential of these lignin streams, a detailed characterization was performed and will be further discussed herein.

6.5.2. NMR characterization of EA extractives fractions from corn stover

6.5.2.1. ^{13}C NMR and 2D NMR analysis of lignin derived from EA pretreated corn stover

Quantitative ^{13}C NMR was performed in isolated lignin from fractions F1, F3 and F5 derived from EA pretreatment process. These are the samples that had the highest content of lignin and, therefore, are the most representative to perform this analysis. Due to the complexity of these samples, quantification requires a number of conditions to be fulfilled, which include having a sample as free of contaminants as possible (e.g. proteins, fatty acids, carbohydrates, etc.) and having a highly concentrated sample to maximize signal-to-noise ratio during analysis. Therefore, NMR was performed on isolated lignins by the methods described above. Lignin, usually defined as a complex polymer composed of *p*-coumaryl alcohol (H), coniferyl alcohol (G), and sinapyl alcohol (S), also intercalates *p*-coumaric acid and ferulic acid units in grasses (e.g. maize) [152, 153, 183]. These two monomers are typically ester and ether-linked to the lignin backbone and ferulic acid can also participate in lignin-carbohydrate complex (LCC) cross-links with arabinoxylans [96, 152, 153]. In **Table 6-2**, it is possible to observe some lignin-specific NMR assignments and the relative signal intensities with respect to the aromatic contents (Ar) of fractions F1, F3 and F5. The Ar content was determined by integrating the signal intensity between 162.0 and 103 ppm and subtracting the integration value for the two vinyl carbons of ferulate and *p*-coumarate.This table shows the assignments for conjugated COOR and $CONH_2$, corresponding to the C_γ carbon signal from both *p*-coumaric and ferulic acids and the respective amides (169-166 ppm). Also, it is possible to identify the C_4 carbon of *p*-coumaric acid from NMR signals at 163-157 ppm. These signals are very similar between the

ammonia extracted samples (F1 and F3) and F5. By subtracting the 163-157 ppm integration from the 169-166 ppm, it is possible to obtain the ferulic content in these fractions (both amide and acid forms). Using this methodology we can observe that the F5 fraction has the highest ferulic (0.08 per Ar) content, but the lowest coumaric (0.19 per Ar) content. However, no major differences can be found between the integration values of all the fractions analyzed here concerning both coumaric and ferulic contents. The release of ferulic acid and amides during ammonia pretreatment of corn stover has been reported in literature [23, 97]. As mentioned before, some of these phenolic residues are often present in the plant cell wall of C4 plants connected by ester linkages. These linkages are easily disrupted in aqueous ammonia through hydrolysis or ammonolysis reactions [23, 95, 99], releasing the respective phenolic acids or amides, which were further extracted by the liquid phase during EA pretreatment. Further evidence of the formation of amides is revealed by 2D NMR (e.g. *p*CM – *p*-coumaroyl amide) from F1-F4, as can be observed in **Figure 6-4**. As suggested earlier, it is possible that most of the ferulic and coumaric content of the biomass was extracted during EA pretreatment, under the conditions applied in this study (**CHAPTER 4**). However, both these phenolic acids and amides are water and ethanol soluble and therefore, they should be present in greater levels in sample F4 after ammonia extraction and fractionation.

The amount of guaiacyl (G) units for the lignin from F1, F3 and F5 can be calculated from the integration values of the peaks between 123 and 117 ppm, subtracting the values calculated for ferulic acid (**Table 6-2)**. This methodology suggests that the G content of F1, F3 and F5 is 0.3, 0.23 and 0.3 units per aromatic ring, respectively. Concerning the syringyl content (S), it can be calculated from half of the integration value of the peak in the 109-103 ppm interval. The values obtained from this calculation were 0.55, 0.40 and 0.51 S units per Ar, for F1, F3 and F5,

respectively. From the S and G content, it is possible to perform S/G ratio calculations, which resulted in 1.83, 1.77 and 1.72 for F1, F3 and F5, respectively. The S/G ratio can vary substantially in maize depending on the type of hybrid, cell type and location of the internode (from bottom to top) of the plant. However, in the literature is possible to observe variations from 0.69 to 1.47 measured by thioacidolysis of various hybrids [184, 185]. Therefore, the numbers calculated in this study for the various lignin fractions are at the high end of what has been normally reported in the literature for maize lignin.

One of the most important linkages in lignin is the β-O-4 ether bond, which is usually cleaved by most alkaline or acidic pretreatments, often leading to further condensation reactions and the formation of C-C bonds [177]. In the context of lignin valorization, it is important to preserve these β-aryl ether bonds, which could potentially be oxidized or reduced during catalytic reactions to valuable products [26].

From **Figure 6-4**, it is possible to observe that the β-O-4 linkages (in light blue) are still present in fractions F1-F4, which resulted from ammonia extraction of corn stover. Quantification of these linkages can be performed by ^{13}C NMR integrating the peak at 61-57 ppm, correspondent the C_γ in β-O-4 without α carbonyl structures. The results obtained from this measurement indicate that these linkages are more abundant in F1 (0.26/Ar), followed by F3 (0.17/Ar) and F5 (0.11/Ar). Therefore, these results suggest that these lignins could offer good potential for conversion to fuels, chemicals or polymers, with special interest in the highly abundant F3, that is ethanol soluble and F5 that contains high molecular weight and could potentially be of interest to the polymer industry.

Table 6-2 Assignments and integration value of quantitative ^{13}C NMR spectra of fractionated lignin from EA pretreated corn stover [186].

		Amount/Ar[b]		
Chemical Shift (ppm)	**Assignments**	**F1**	**F3**	**F5**
184-180	C=O in spirodienone unit	0.08	0.04	0.07
176-169	Aliphatic COOR	0.40	0.42	1.03
169-166	Conjugated COOR	0.30	0.27	0.27
163-157	C_4 of *p*-coumaric acid	0.25	0.21	0.19
156-142	C_3/C'$_3$ in 5-5' biphenyl and C_3/C_4 in G units, C_3/C_5 in S units	1.79	1.60	1.98
142-124	C_1 G units, C_5/C_5' in etherified 5-5 units	1.97	2.42	2.07
123-117	C_6 in G units	0.34	0.28	0.38
117-113	C_5 in G units	0.96	1.01	0.72
113-109	C_2 in G units	0.15	0.20	0.17
109-103	C_2/C_6 in S units	1.11	0.80	1.02
90-78	C_β in β-O-4, Cα in β-5 and β-β	0.84	0.50	0.51
65-62	C_γ in β-5 and β-O-4 with α-carbonyl structures (G and S units)	1.28	1.31	1.23
61-57	C_γ in β-O-4 without α carbonyl structures (G and S units)	0.26	0.17	0.11
58-55	Methoxy CH_3	0.66	0.36	0.56
53-51	C_β in β-β and β-5 structures	0.02	0.04	0.04
22-20	Acetyl CH_3	0.00	0.36	1.03
S/G ratio $(I^a_{108\text{-}103}/2)/I_{114\text{-}108}$ [187]		1.83	1.77	1.72

[a] I – Integration value, [b] Ar – Aromatic ring

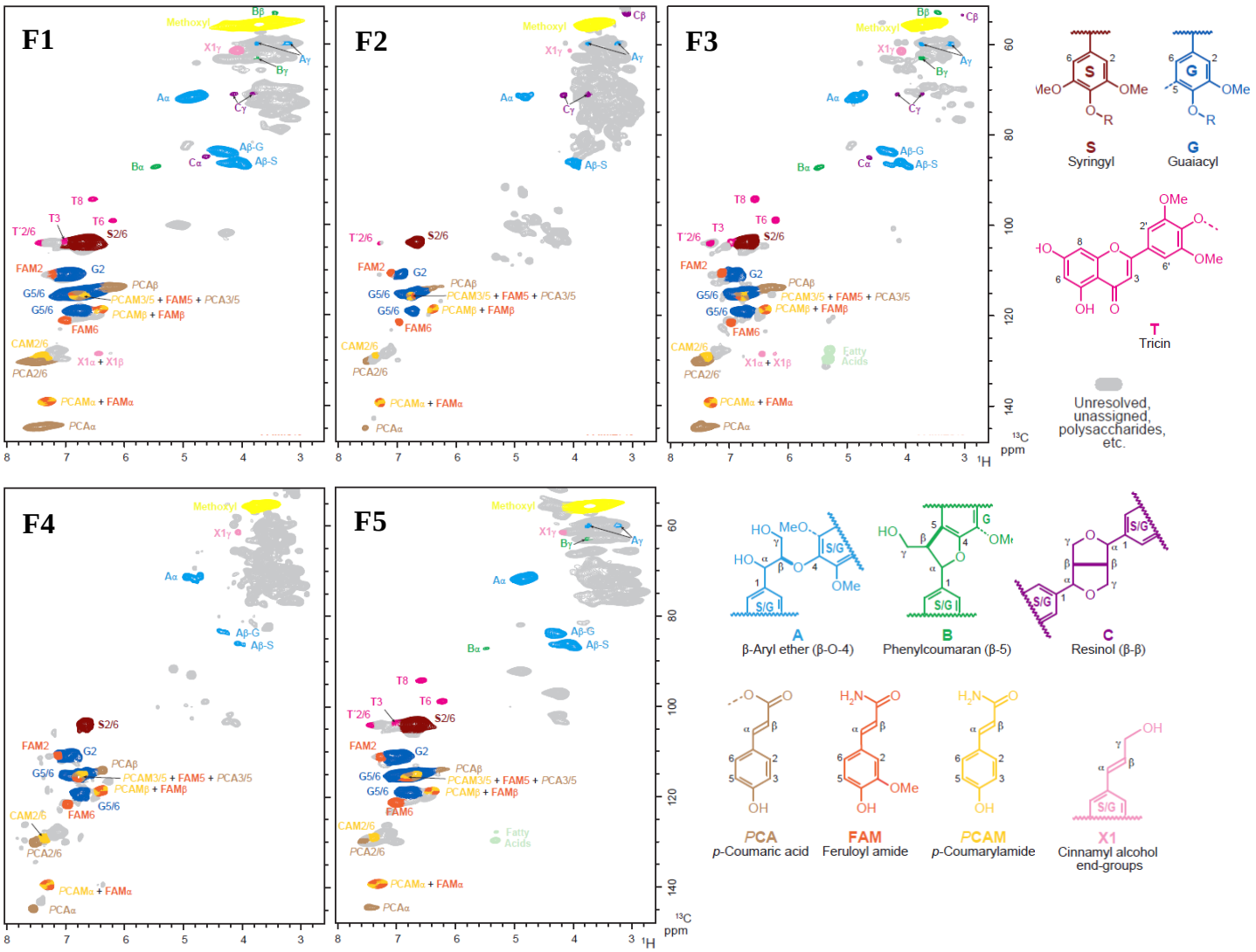

Figure 6-4 2D-HSQC NMR of fractions derived from EA pretreated corn stover.

6.5.2.2. ^{31}P NMR analysis of lignin derived from EA pretreatment of corn stover

To evaluate the relative distribution of the hydroxyl groups of the various fractions F1-F5, quantitative ^{31}P NMR was performed. This technique uses TMDP derivatization, which attacks all of the exposed hydroxyl groups present in lignin, allowing the analysis by ^{31}P NMR. **Table 6-3** summarizes the results based on the integration of the peaks associated with the different assignments. The relative abundance of each type of hydroxyl group was calculated dividing the peak area of each assignment by the sum of the areas of all the peak assignments. From these results, it is possible to rapidly observe that the aliphatic hydroxyl groups are the most abundant peaks in all the lignins analyzed in this study. This result is often observed in the literature as it has been reported by several authors for biomass materials that include wheat straw [188], switchgrass [189] and poplar [190]. One other important observation is that the most hydrophilic lignins, i.e., F2 and F4, have more hydroxyl groups, with a total of 9.39 mmol/g and 11.60 mmol/g, respectively. The water insoluble lignins contain very similar amounts of hydroxyl groups, ranging between 4.87 and 5.08 mmol/g. Also, the relative level of hydroxyl groups from carboxylic acids is higher for ethanol soluble fractions F3 and F4, with values of 18.59% and 36.59%, respectively. The differences in hydroxyl content and in the percentage of the various types of hydroxyl groups can provide a great insight about the chemical diversity among the lignins that were fractionated from corn stover by EA pretreatment. This data, along with ^{13}C NMR and 2D NMR analysis presented here, can provide good chemical information to researchers that are interested of using these streams, especially the abundant F3 and F5, to convert to fuels and chemicals.

Table 6-3 Abundance of assigned hydroxyl groups of fractionated EA extractives from corn stover, determined by ^{31}P NMR [189].

	Percentage of Total -OH				
Assignments	**F1**	**F2**	**F3**	**F4**	**F5**
Aliphatic -OH	61.89%	84.28%	47.28%	51.53%	73.79%
C5 + C3 Substituted -OH	6.82%	2.99%	8.17%	1.37%	6.85%
C3 Substituted, *p*-Coumaryl and *p*-Hydroxyphenyl -OH	22.39%	4.38%	25.96%	10.51%	11.57%
Carboxylic acid -OH	8.90%	8.34%	18.59%	36.59%	7.79%
Total OH (mmol/g of lignin)	5.08	9.39	4.94	11.60	4.87

6.5.3.Gel Permeation Chromatography (GPC)

The weight average molecular weights (M_w) of the acetylated lignins, isolated from the various fractions (F1-F5), were measured by GPC (**Figure 6-5**). These values were calculated in reference to polystyrene standards, which are not representative of lignin in its shape or chemistry. Therefore, the M_w values presented in this work cannot be interpreted as being absolute, but can help us have a relative comparison between the average sizes of the lignin molecules present in the various fractions and also compare with other literature values derived by this technique [186].

The chromatograms show that the lignin molecular weights decrease between F1 to F4, as the M_w value decreases from 3314 g/mol to 416 g/mol. This result was expected, as the ethanol insoluble fractions should contain higher molecular weight polymers in comparison to the ethanol soluble fractions. It is also possible to observe that from the ethanol insoluble fractions, F2 has a greater range of molecular weights compared to F1, as it shows a larger number of

peaks in the lower molecular weight region of the chromatogram. These lower molecular weight components could be associated with highly polar compounds that are not ethanol soluble, but can be solubilized by water. From the ^{31}P NMR results discussed above, it is clear that F2 lignin is highly rich in aliphatic OH groups, which provide hydrophilic properties to the lignin molecules.

Similarly to F1, the ethanol soluble lignins from F3 and F4 show relatively narrow molecular weight distributions compared to F2. However, the most important fraction derived from the EA extractives, i.e. F3, presents an Mw value of 1470 g/mol, which is relatively low compared to F1 and F2 (**Figure 6-5**) and significantly lower than the Mw from dioxane-extracted lignin from corn stover (3400-3900 g/mol) [191].The polydispersity of the lignin from F3 was calculated to be approximately 2. The lowest molecular weight lignin is found in F4, however it is important to mention that the highest peak shown in the chromatogram of F4 represents the sum of the low molecular weight molecules, which could not be resolved by the column during analysis. Therefore, due to this limitation, the M_w value presented in **Figure 6-5** (F4) is overestimated.

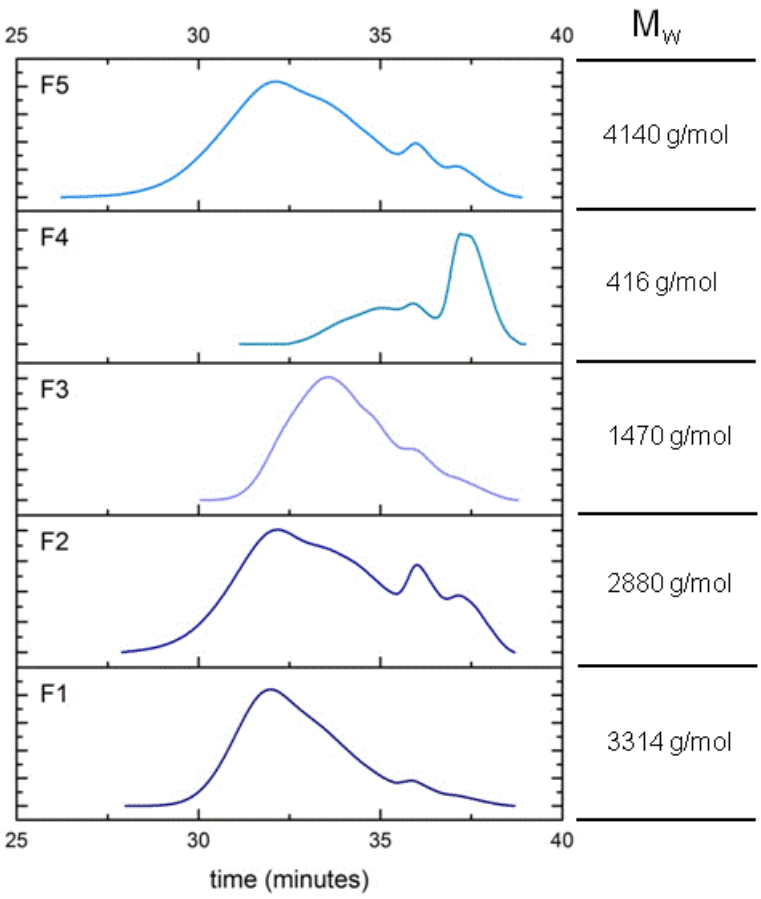

Figure 6-5 Gel permeation chromatograms of fractions F1-F5. Weight average molecular weight (M_w) was calculated based on polystyrene standards.

The highest molecular weight lignin from the fractions obtained in this study is present in F5. This lignin was not solubilized by ammonia during EA pretreatment and remained water insoluble after enzymatic hydrolysis. Due to its abundance, this lignin stream can be potentially used in chemical conversion, especially in processes that prefer higher molecular weight lignin polymers. The M_w value obtained by GPC was approximately 4140 g/mol and is slightly higher than literature values from lignin isolated directly from corn stover (3400-3900 g/mol) by dioxane or acidic dioxane extraction [191]. This result is expected, as the fractionation process

eliminated part of the lower molecular weight lignin from F5, resulting in a higher M_w value. The polydispersity of the lignin from F5 was also calculated and determined as approximately 4.38, which is considerably higher than the values that are usually observed in dioxane extracted lignin (i.e. 2.2 to 2.5) [191]. From this fact we may infer that the lignin might have been subjected to some structural modifications during pretreatment and enzymatic hydrolysis that made the lignin polymer more heterogeneous in size, even though the average degree of polymerization was increased by the nature of the fractionation process. However, more studies are required to evaluate the nature of such structural modifications and the chemistry involved.

6.5.4. Elemental analysis

Elemental analysis of the fractions F1-F5 was performed by ICP and the results are found in **Table** 6-4. If we compare the minerals present in F5 with the remaining fractions, we can depict that the most abundant minerals extracted from corn stover by ammonia include: calcium (Ca), copper (Cu), iron (Fe), potassium (K), magnesium (Mg), phosphorous (P), sulfur (S) and silicon (Si). However, in F5 we can still observe relatively high levels of aluminum (Al), Ca, Fe, K, Mg, sodium (Na), P, S, Si and zinc (Zn) that remained insoluble after pretreatment and enzymatic hydrolysis.

Most of the ammonia-extracted minerals (F1-F4) were precipitated by the addition of ethanol and are present in the fractions F1 and F2. As a result, these fractions contain relatively higher content of mineral elements compared to the ethanol soluble fractions (F3 and F4), notably the content of K that was exceeded by two orders of magnitude. The addition of water to the ethanol insoluble extractives was able to enrich mostly K, P and S in F2.

From the ethanol soluble minerals, which are present in F3 and F4, P and S are the most abundant. From these results, it is visible that the early ethanol extraction could deplete these two fractions from most of the mineral elements. One of the important reasons for this fractionation process, apart from enriching the EA-extracted lignin, was to remove possible mineral elements that could potentially interfere with catalytic processes during lignin valorization to fuels and chemicals. With this respect, this strategy could remove most of the minerals from F3 (the most important lignin rich fraction), except P (209.7 mg/Kg) and S (1310.0 mg/Kg) that are present in reasonable amounts. Other strategies could be studied to further remove these residual levels of inorganic elements, if processing limitations require their total absence. In the other hand, process streams that are rich in minerals could be potentially used in soil amendment, to improve the sustainability of the bioeconomy.

In the perspective of lignin processing, the most relevant fraction (F3) was further analyzed by CHNO analysis. The results show that this sample contains approximately 67 % of carbon (C), 8.2 % of hydrogen (H), 2.3 % of nitrogen (N) and 22.5 % of oxygen (O). Apart from the presence of relatively high N content, this element composition is very similar to the ones typically observed in commercial lignins [192]. Nitrogen values are typically below 1% for most commercial lignins, however F3 lignin was subjected to ammonia treatment which may likely have functionalized some of the lignin compounds with nitrogen-based groups, such as amides or amines. Also, is possible that some lipids may be part of the remaining 7.65% that compose the F3 sample, which contains approximately 92.35% of lignin. The ester linkages present in triglycerides can react with ammonia during ammonolysis reactions, potentially forming amides, which may be present in F3 [193]. Moreover, it is also possible that some proteins derived from corn stover are still present in F3, contributing to the nitrogen content in this sample. The high

levels of nitrogen are not only present in F3, but also in the remaining samples from F1 to F4. As mentioned above, in F4 there is high abundance of coumarates and ferulates that were cleaved from the plant cell wall structure by hydrolysis and ammonolysis reactions during EA pretreatment. Ammonolysis reactions formed coumaroyl amide and feruloyl amide that will highly contribute to the nitrogen abundance of this sample (~13.24 %).

Table 6-4 Mineral inorganic elements and CHNO analysis of fractions derived from the EA process.

	Composition (mg/kg of Fraction)				
Element	**F1**	**F2**	**F3**	**F4**	**F5**
Al	12.5	11.7	3.0	2.1	390.1
B	0.4	11.4	< 0.3	< 0.3	3.2
Ba	2.5	3.3	1.3	1.0	29.0
Be	< 0.0	< 0.0	< 0.0	< 0.0	< 0.0
Ca	361.7	288.6	27.6	24.5	2714.0
Cd	< 0.5	< 0.5	< 0.5	< 0.4	< 0.5
Co	< 0.7	< 0.7	0.7	1.0	< 0.7
Cr	4.8	2.7	0.9	4.6	14.6
Cu	134.0	36.6	33.2	51.7	59.2
Fe	248.5	63.6	11.5	17.5	750.3
K	3830.0	26643.4	131.2	75.6	845.9
Mg	1120.0	496.8	11.2	7.5	345.3
Mn	34.6	20.9	2.1	1.0	28.7
Mo	< 1.6	4.3	1.6	3.2	3.0
Na	40.3	388.5	39.6	12.3	187.9
Ni	3.7	2.5	1.5	10.2	9.8
P	898.9	2573.3	209.7	1033.1	754.9
S	1340.0	2305.0	1310.0	911.6	1860.0
Sb	< 5.1	< 5.1	< 5.1	< 4.6	< 5.1
Se	< 11.3	< 11.3	< 11.3	< 10.1	< 11.4
Si	100.9	242.9	53.5	100.0	162.6
Sn	6.3	8.3	7.4	6.5	4.7
Sr	1.2	1.0	0.1	0.1	7.4

Table 6-4 (Cont'd)

Ti	0.8	1.4	0.5	0.1	13.2
V	< 0.2	< 0.2	< 0.2	< 0.2	1.6
Zn	62.5	59.7	30.1	16.5	99.1
C	ND[a]	ND	67.0 %	ND	ND
H	ND	ND	8.2 %	ND	ND
N	3.67 %	2.74 %	2.3 %	13.24 %	ND
O	ND	ND	22.5 %	ND	ND

[a]ND – Not determined

6.5.5.Thermogravimetric analysis (TGA) of the EA fractions

The thermal stability of the various fractions obtained in this study (i.e., F1-F5) was measured by TGA as shown in **Figure 6-6**. Thermal decompositions were measured in a temperature range between 100 °C and 600 °C at a heating ramp of 10 °C/min. This figure shows very distinct curve profiles associated with the thermal decomposition of the different fractions. For all the samples, a substantial mass loss was recorded at a temperature range between 100 and 450 °C, after which no major decomposition was observed. The water soluble fractions (F2 and F4) showed significant thermal decomposition at temperatures ranging 100 to 200 °C, which was not observed in the remaining water insoluble fractions (F1, F3 and F5). This observation may be associated to the fact that these samples are rich in water soluble carbohydrates, most likely monomeric and small oligomeric sugars that can be thermally decomposed at these temperature ranges [194, 195]. For example, literature reports show that glucose can be decomposed at onset temperatures ranging 146-158 °C, xylose at 153-156 °C and fructose can be decomposed at onset temperatures ranging from 102-132 °C [195, 196]. Also, some of the initial mass loss may be derived from water evaporation, as these water soluble samples are highly hygroscopic. One other consideration is that samples F1 and especially F4 contain high levels of acetic acid as can

be observed in **Table 6-1**, which can be evaporated at temperatures of 118 °C. All these factors have contributed to some extent to the weight loss due to thermal decomposition of these two samples, which resulted in approximately 70 % weight loss for F4 at temperatures below 300 °C and 50 % weight loss for F2 at temperatures below 350 °C.

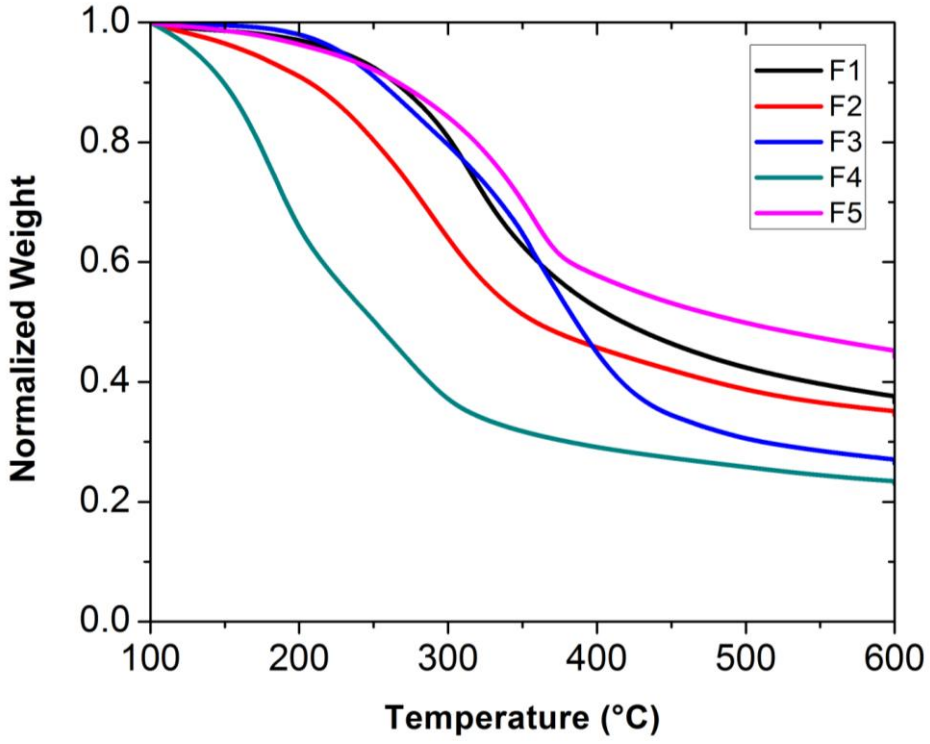

Figure 6-6 Thermogravimetric curves for the various biomass fractions (F1-F5) derived from the EA pretreatment of corn stover. The heating ramps for all the samples were set at 10 °C/min.

Water insoluble fractions, F1 and F3, show a significantly higher thermal stability compared to the water soluble samples. Sample F1 is slightly decomposed (~5 % weight loss) at temperatures below 250 °C followed by an abrupt decrease in weight (~40 %) before reaching temperatures around 375 °C. This fraction (F1) produced higher levels of solid products of decomposition than the water soluble fractions, as it was only possible to evaporate about 60 % of its total weight.

On the other hand, F3 showed an unusual decomposition pattern for a sample that contains approximately 92 % lignin. The initial thermal stability in relation to the other samples is explained by the absence of major carbohydrate content as well as the low presence of volatile organic compounds. The onset temperature of ~220 °C was followed by a rapid decrease in mass loss before reaching ~420 °C, resulting in a mass loss of approximately 70% in F3. For example, at 10 °C/min, organosolv lignin behaves quite differently, as it is possible to observe an onset temperature around 350 °C (~130 °C higher than F3) followed by a very slow decrease in mass weight [197]. At temperatures around 420 °C, only about 30 wt% of the organosolv lignin was lost in TGA (as opposed to 70% in F3) [197]. It is also evident that sample F3 leaves behind very little solid intermediates after pyrolysis, as only 26 wt% of the sample remained in the TGA tray at 600 °C. At these temperatures, only about 50 % of the organosolv lignin was pyrolyzed to gases while the remaining 50% required higher temperatures to continue thermal decomposition [197]. DSC analysis on F3 (in Appendix) also showed that the glass transition temperature (Tg) value for this sample is approximately 117 °C, which helps explain the reason why EA lignin extraction yields can increase significantly after reaching temperatures ranging 115 to 120 °C (**CHAPTER 4**).

Sample F5, in the other hand contains high levels of recalcitrant carbohydrates. Cellulose and hemicellulose decomposition occurs at 315-400 °C and 220-315 °C, respectively, while lignin decomposes at a temperature range from 130-1000 °C, depending on the lignin origin. Therefore the thermal decomposition occurring between 220 °C and 375°C should be mostly associated with cellulose and hemicellulose present in F5. Lignin decomposition should occur in great part after 375 °C, where is possible to see a very small weight loss with increasing temperature. A

similar TGA profile is possible to observe in maplewood, as described by Joungmo Cho et al. (2012) [197].

6.6. Conclusion

A comprehensive characterization of various lignin-rich streams generated during the processing of corn stover in an EA-based biorefinery was performed and reported here. By treating corn stover exclusively with anhydrous ammonia, using 6:1 ammonia to biomass ratio and 120 °C for 30 min, it was possible to extract approximately 44% of the lignin from corn stover, which was further fractionated into four streams (F1-F4) by sequential ethanol and water precipitation. In one of these fractions (i.e., F3), it was possible to recover approximately 32 % of the lignin content in untreated corn stover. F3 contained about 92% lignin and was practically carbohydrate free. Another important lignin rich stream was a solid residue that resulted from enzymatic hydrolysis of EA pretreated biomass. This fraction (F5) contained about 51 % of the lignin originally present in the untreated corn stover, however it was composed of only about 43% lignin.

NMR characterization of the various fractions showed that these lignins contain a high S/G ratio, ranging from 1.72 to 1.83 and still retain a good level of β-O-4 linkages, which were not cleaved by the ammonia treatment. The preservation of these linkages is of great importance to some chemical processes that target ether bonds during conversion of lignin aromatics to valuable products. ^{31}P NMR also showed that the water soluble fractions of EA lignin (F2 and F4) contain a considerably higher amount of hydroxyl groups compared to the water insoluble lignins (F1, F3 and F5), which makes them more hydrophilic, allowing the water fractionation process to be possible. The weight average molecular weight of these lignins range from 4140

g/mol to <416 g/mol according to GPC, against polystyrene standards. The highest molecular weight was observed in F5, which is comparable to the lignins from various grasses (e.g. switchgrass) [186] and the lowest was observed in F4. The weight average molecular weight of F3 was considerably lower than what is usually observed for grasses, with a value of 1470 g/mol. Therefore, we can conclude that we have produced of a very unique lignin stream in F3, one which is highly abundant, with low molecular weight, ethanol soluble, with 92% lignin content, and that maintained most of the native chemistry practically intact. One other feature of this lignin stream was highlighted by the TGA results, where F3 showed a relatively low decomposition temperature for lignin, with the formation of very low levels of solid decomposition products (i.e., ~30 wt%). Furthermore, F3 contains reduced levels of inorganic elements, which can potentially benefit catalytic processes by avoiding catalyst poisoning. The lignin from F5, also abundant in the EA-based biorefinery, shows good chemical properties with the preservation of functionalities such as β-aryl ether bonds and high molecular weight. However this lignin stream requires some further processing to eliminate the carbohydrate content and thereby improve its quality for future usage.

One of the important goals of this process is also to provide good quality lignin, so it can be used as a starting material for its valorization and help to reduce biofuel price, contributing to the economy of the EA pretreatment. With this regard, is expected that the F3 lignin, as well as F5, can provide good starting materials for lignin-based conversion to fuels and chemicals. Within the scope of this work, was possible to provide a summary of the most important properties of these lignin streams, so they can be used in research related to lignin valorization in the future.

APPENDIX

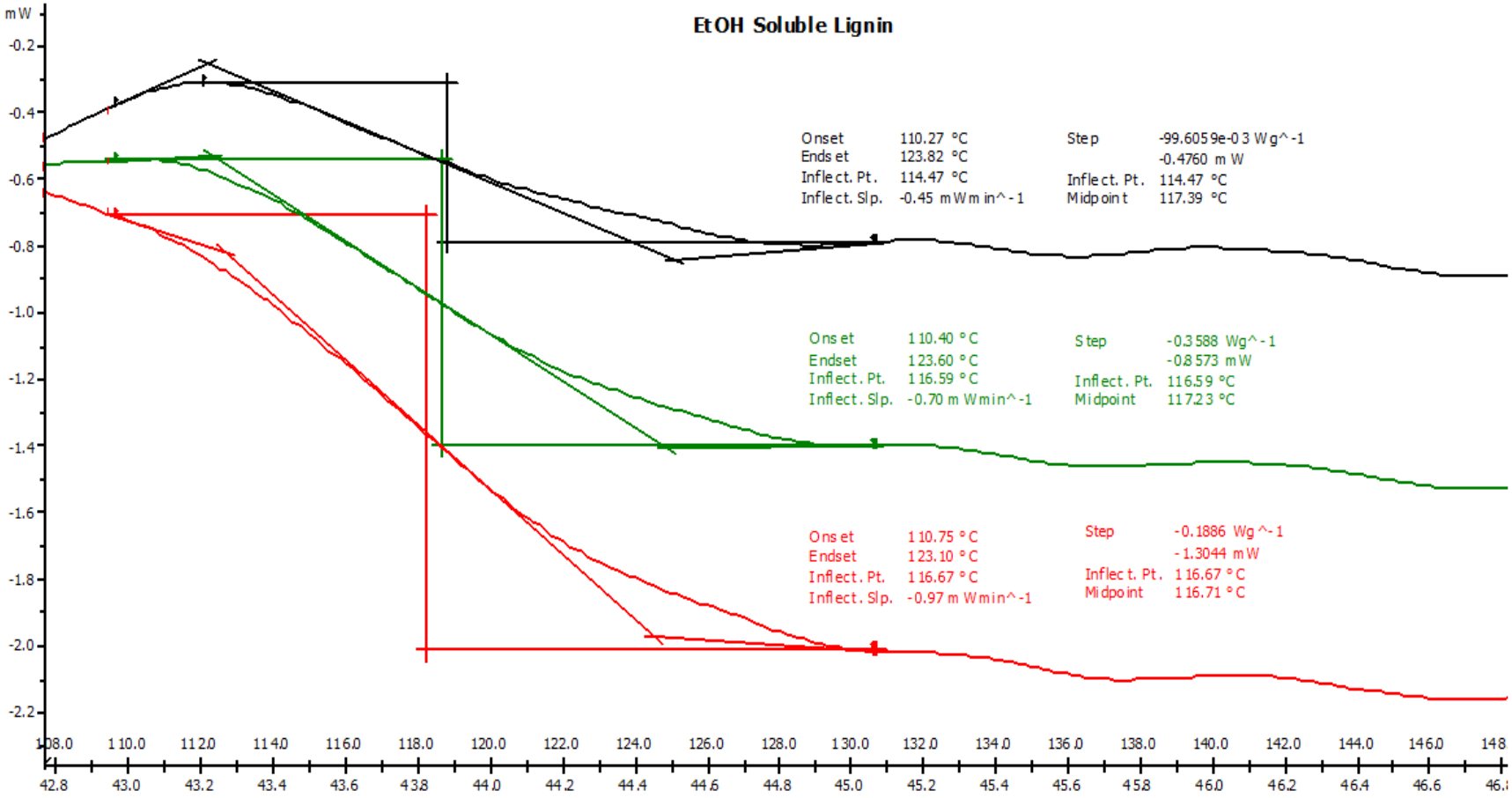

Figure 6-7 DSC of F3 lignin showing the glass transition temperature at approximately 117°C. Black and red curves (top and bottom) are sample replicates, while the green curve (middle) is the average of the two replicates.

CHAPTER 7 – CONVERSION OF EXTRACTIVE AMMONIA PRETREATED CORN STOVER TO ETHANOL BY RaBIT PROCESS.

7.1. Abstract

Rapid Bioconversion with Integrated Enzyme Recycling Technology (RaBIT) has been shown as a very promising process on ammonia fiber expansion (AFEX^{TM}) pretreated corn stover (CS) in terms of enzyme loading reduction and ethanol productivity enhancement. The present study applied RaBIT on EA (Extractive Ammonia) pretreated corn stover, enzyme loadings were optimized and the results were compared to conventional SHF process. The RaBIT on EA pretreated corn stover applied the enzyme loading as low as 8.4 mg protein per g glucan, however, reached a glucan conversion and a xylan conversion as high as 97.7% and 98.0%, respectively. The overall ethanol yield was 227 g ethanol/ kg EA-CS (191 g ethanol/ kg untreated CS). Compared to conventional SHF, enzyme loading was 30% less and ethanol productivity was two times higher with greater sugar conversions.

7.2. Introduction

The advances in ammonia pretreatment of lignocellulosic biomass and the understanding of how the plant cell wall chemistry can be modified to facilitate enzyme action towards improved sugars conversion enabled us to introduce the novel Extractive Ammonia (EA) pretreatment technology. This technology allies the disruption of lignin-carbohydrate complex (LCC) bonds to the high selectivity of ammonia for extracting lignin and phenolic compounds, thereby allowing the removal of these components from the plant cell wall, which are inhibitory to microbes and enzymes, leaving the desired carbohydrate polymers behind. Additionally, EA pretreatment uses

high ammonia-to-biomass ratios (from 3:1 to 6:1) without addition of water, which enables a rewiring of the hydrogen bonding from native cellulose, yielding cellulose III_I (**CHAPTER 4**) This non-native cellulose crystal structure has been identified as being more vulnerable to cellulase degradation [105, 117]. From these results, initial rates of enzymatic hydrolysis can be enhanced more than two fold as compared to native cellulose I, which can drive a significant reduction of enzyme loading for processes that promote this cellulose crystal modification. Our work has already confirmed the processing advantages of cellulose III conversion allied with removal of lignin from the plant cell wall. However, the performance of EA-CS hydrolyzates has not yet been evaluated with current fermentation technology.

New advances in the bioprocessing methodology to convert lignocellulosic biomass to ethanol have been also investigated with great success. For example, adding to the traditional Separate Hydrolysis and Fermentation (SHF) and Simultaneous Saccharification and Fermentation (SSF) a new approach was developed by Mingjie Jin and co-authors [4], denominated by Rapid Bioconversion with Enzyme Recycling Tehcnology (RaBIT). These processes take advantage of the fact that the least recalcitrant portion of the biomass consists of nearly 80 % of the total sugars of the plant cell wall and can be hydrolyzed in the first 24 h of enzymatic hydrolysis. The resulting hydrolysate is fermented to fuels while the unhydrolyzed solids remaining after the first 24 h are transferred to another vessel where fresh biomass is added along with make-up enzymes to start another fermentation cycle. This process can be carried on for multiple cycles with consistent process efficiency. A major advantage of this process is that cellulases and hemicellulases can be recycled from cycle to cycle, as they are adsorbed to the surface of the recalcitrant biomass that is transferred to the multiple cycles. This feature allowed 30% enzyme

reduction using AFEX^{TM} CS as the substrate, when compared to the traditional SHF and SSF [4]. Additionally, this process could improve ethanol productivity up to approximately four fold from 0.13 g/L/h to 0.5 g/L/h [4] . To further reduce enzyme usage in the biorefinery process, we evaluated the integration of EA pretreatment with the RaBIT process. Some of the benefits and limitations of these two state-of-the-art technologies developed in BCRL, at Michigan State University, integrated in a full biorefinery concept will be presented and discussed here and compared with the traditional AFEX^{TM} and SHF processes.

7.3. Experimental

7.3.1. EA pretreated corn stover

EA pretreatment method was performed on GLBRC 2009 corn stover as described **CHAPTER 5**. Pretreatment conditions applied were ammonia loading: 6.0 g/g dry biomass, 10% moisture content, 120 °C, 1300 psi, and pretreated for 1 h. The composition of EA-CS includes glucan content: 43.3%, xylan content: 26.7%, arabinan content: 4.0%, acid insoluble lignin content: 9.0% and acetyl content: 1.1%.

7.3.2. Microorganisms and seed culture preparation

Saccharomyces cerevisiae 424A(LNH-ST) [198] was obtained from Prof. Nancy W. Y. Ho, Purdue University and used for fermenting both glucose and xylose in the EA-CS hydrolysate. The seed culture was prepared in a 250 ml Erlenmeyer flask with 100 ml YEP medium (10 g/L yeast extract, 20 g/L peptone, 75 g/L glucose and 20 g/L xylose). A frozen glycerol stock stored at -80 °C was used for seed culture inoculation with a final optical density (OD_{600}) of 0.1. Seed

cultures were cultivated at 30 °C and 150 rpm under micro-aerobic conditions for 24 h. Then the seed culture was centrifuged at 4400 rpm for 6 min and the cell pellets were used for fermentation inoculation.

7.3.3. Conventional separate enzymatic hydrolysis (EH) and fermentation (SHF)

Conventional separate hydrolysis and fermentation was carried out using 96 h enzymatic hydrolysis followed by 96 h fermentation. Enzymatic hydrolysis was performed using a commercial enzyme mixture with a total protein loading of 12 mg protein/g glucan, which included 66.7% Ctec2 (Novozymes, USA), 16.7% Htec2 (Novozymes, USA) and 16.7% Multifect pectinase (Dupont, former Genencor Inc., USA). Pretreated biomass solids loading used in this study was 7.5% (w/w) glucan loading, which corresponding to 17.3% (w/w) total solids loading. The Enzymatic hydrolysis reaction was carried out in a 250 ml baffled flask with a total mixture weight of 100 g at 50 °C, 250 rpm and pH around 5.0. After 96 h, the hydrolysate was centrifuged at 10,000 rpm for 30 min. The supernatant was used for fermentation. Fermentation was performed at 150 rpm, 30 °C and pH 5.5 with an initial OD_{600} of 2.0.

A mass balance was performed around the enzymatic hydrolysis step as previously described in the literature [4, 78]. Total ethanol yield was calculated based on the sugar yield during enzymatic hydrolysis and the sugar consumption and ethanol metabolic yield during fermentation. Ethanol metabolic yield (%) was calculated based on the consumed sugars and the maximum ethanol metabolic yield of 0.51 g ethanol per gram of glucose/xylose consumed.

7.3.4. Rapid Bioconversion with Integrated Enzyme Recycling Technology (RaBIT)

The RaBIT process is shown in **Figure 7-1**, adapted from the work of Jin, Mingjie et al., 2012 [4]. Enzymatic hydrolysis was conducted under the same conditions as the conventional enzymatic hydrolysis except that it only proceeded for 24 h. The same amount of pretreated biomass and water were added for enzymatic hydrolysis of each cycle. After 24 h hydrolysis, the liquid hydrolysate was separated from the unhydrolyzed biomass solids (solid residue) by centrifugation in 50 ml falcon tubes at 5300 rpm for 20 min. The solid residue was then recycled and fed to the next cycle of enzymatic hydrolysis. The liquid hydrolysate was fermented with a high initial yeast cell density (an initial OD_{600} of 20) at pH 5.5 and 32 °C for 24 h. After fermentation, the broth was centrifuged and the yeast cells were reused for the next cycle fermentation. Since the unhydrolyzed solid biomass was recycled with some enzymes absorbed on it, the enzyme loadings for cycles other than the first cycle were reduced and optimized. We performed five cycles in total for this study. The last step was carried out with the addition of water but no fresh biomass input. However, the enzyme loading for the last step was calculated based on the assumption that the same amount of fresh biomass was added as previous cycles. After 24 h enzymatic hydrolysis of the last step, the hydrolysate pH was adjusted to 5.5 and yeast cells were directly added without solids-liquid separation. The last fermentation step also lasted for 24 h.

Concentrations of glucose, xylose and ethanol were analyzed using an HPLC equipped with a Biorad Aminex HPX-87H column as described previously [4].

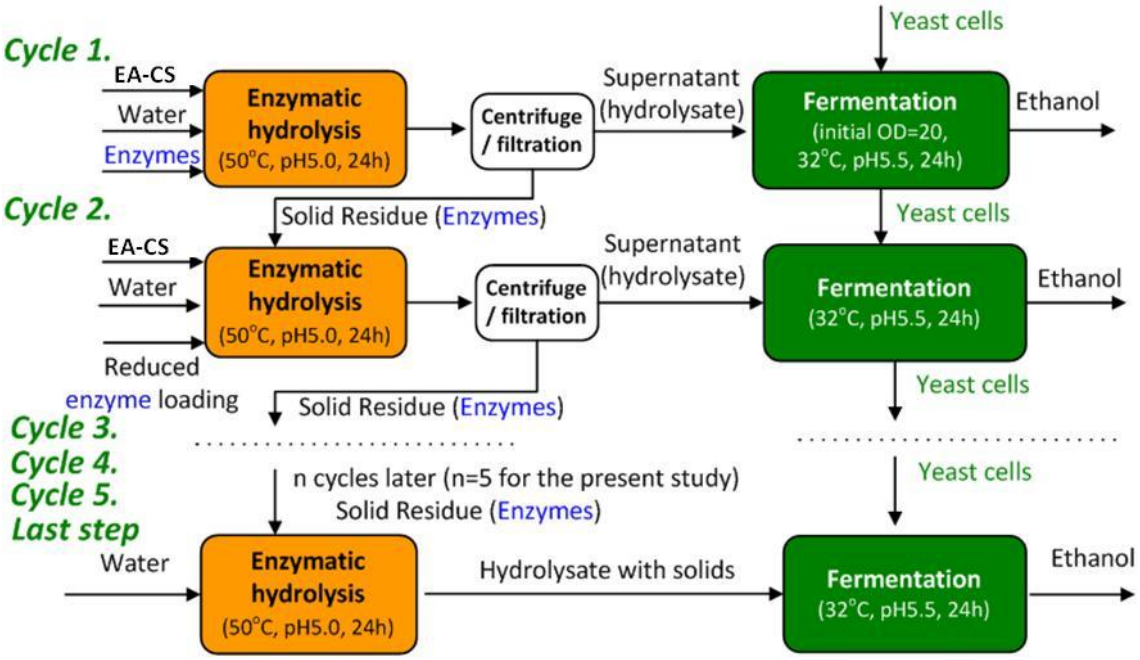

Figure 7-1 Diagram of the RaBIT process (adapted from Jin, M. et al. (2012) [4])

7.4. Results and Discussion

7.4.1. Conventional SHF

Conventional enzymatic hydrolysis of EA-CS resulted in approximately 75% total glucan conversion and 91% total xylan conversion in the first 24 h (**Figure 7-2a**). However, it took another 72 h to reach 91% glucan conversion. Rapid hydrolysis at the beginning of enzymatic hydrolysis and then a reduced rater was typically observed during high solids loading hydrolysis [199]. The rate reduction is due to several factors including sugar inhibition [174], enzyme de-activation [200] and reduction of substrate availability [172, 173]. Nevertheless, high sugar conversions (91% for both glucan and xylan) were achieved for EA-CS after 96 h hydrolysis with a low enzyme loading of 12 mg/g glucan.

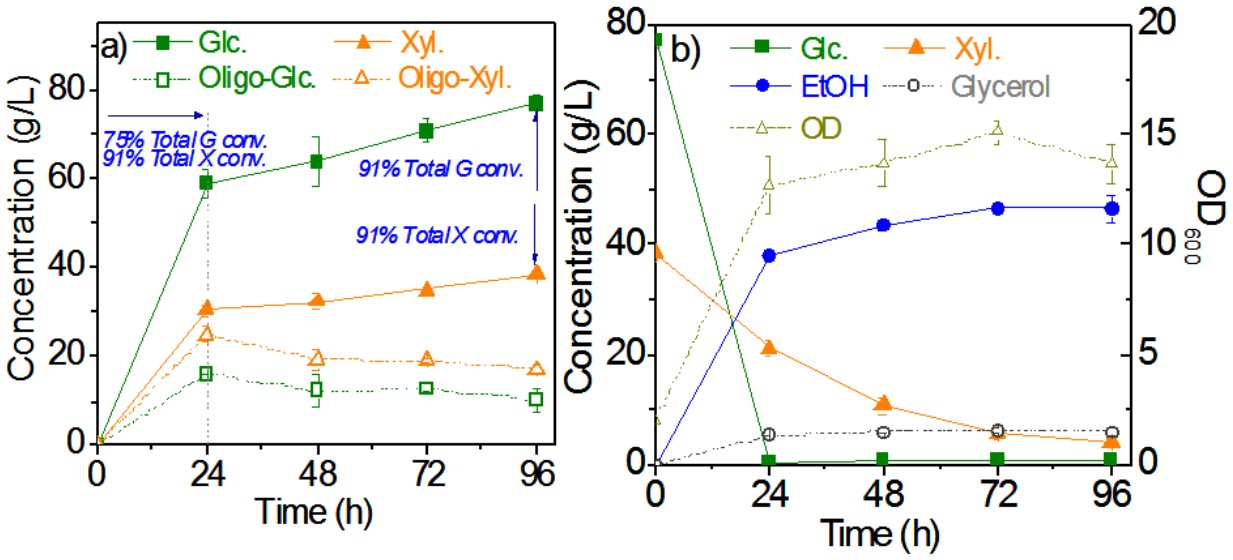

Figure 7-2 Enzymatic hydrolysis (a) and fermentation (b) performance of conventional SHF on EA pretreated corn stover.

Hydrolysate fermentation began with glucose and xylose concentrations of 77.4 and 38.5 g/L, respectively. There were also 10.1 and 17.2 g/L oligomeric glucose and oligomeric xylose, respectively in the hydrolysate (**Figure 7-2a**), which cannot be fermented by *Saccharomyces cerevisiae* 424A(LNH-ST) . Glucose was rapidly converted to ethanol and yeast cell biomass as expected (**Figure 7-2b**). Xylose was consumed to a concentration of 5.9 and 4.2 g/L after 72 h and 96 h fermentation, respectively. The ethanol concentration was 46.8 g/L for both 72 and 96 h. Therefore, 72 h fermentation results were used for further mass balance and ethanol productivity calculations. The ethanol metabolic yield in the fermentation of EA corn stover hydrolysate was approximately 84%, which is lower compared to AFEX^{TM} hydrolysate fermentations that can typically achieve ~90% metabolic yield [78]. Currently, the reasons for this result are still unclear; however, it is possible that removal of cell growth inhibitors during pretreatment favor carbon flux toward cell growth, resulting in lower ethanol production. This

hypothesis is supported by the fact that the OD_{600} for EA hydrolyzate is slightly higher that for AFEX^{TM} hydrolyzate (15 compared to 11, respectively) [78]. Another hypothesis is that some of the nutrients present in corn stover are removed from the biomass during EA pretreatment, resulting in lower ethanol yields comparing with AFEX^{TM} hydrolyzate.

7.4.2. Optimization of enzyme loadings for the cycle 2 and the last step of RaBIT

Enzyme loading for cycle 1 was performed based on the work described in **CHAPTER 5**. However, after enzyme recycling, the make-up enzyme must be optimized to obtain constant sugar yields in all the cycles. For this purpose, an enzyme optimization experiment was performed as described in **Table 7-1**.

Table 7-1 Design for the optimization of enzyme loadings (EL) for the Cycle 2 and the last step.

	Total EL (mg protein/g glucan)	**% Ctec2**	**% Htec2**	**% Pectinase**
Cycle 1	12	66.7%	16.7%	16.7%
Optimization of enzyme loadings for the Cycle 2				
EL1	**0**	0	0	0
EL2	**7.5**	66.7%	16.7%	16.7%
EL3	**7.5**	50%	25%	25%
EL4	**7.5**	80%	12%	8%
EL5	**6**	66.7%	16.7%	16.7%
Optimization of enzyme loadings for the last step[a]				
EL*a*	**3.75**	80%	10%	10%
EL*b*	**4.5**	66.7%	16.7%	16.7%
EL*c*	**6**	66.7%	16.7%	16.7%

[a] In the experiment of optimizing the enzyme loadings for the last step, the enzyme loadings for the Cycle 2 was 7.5 mg/g protein and was 6 mg/g protein for the Cycle 3-5. The enzyme combinations were all 66.7% Ctec2, 16.7% Htec2 and 16.7% Multifect Pectinase.

Jin, Mingjie et al., (2012) showed that by implementing the RaBIT process on AFEX^{TM} pretreated corn stover, it is possible to reduce external enzyme addition from cycle 2 to 5 by 40-50% of the enzyme added in cycle 1, while achieving the same sugar concentrations [4]. EA pretreatment converts cellulose I to cellulose III (unlike AFEX^{TM}), which has a lower binding affinity to cellulases [118]. Therefore, when the unhydrolyzed solid biomass is recycled, less number of cellulase enzymes will be adsorbed to it which could negatively affect enzyme recycling. In other words, enzyme loading reduction for cycles 2 to 5 on EA CS was expected to be lower than for AFEX^{TM} CS. However, also EA removes around 44% of the lignin, which reduces the non-productive binding of the enzymes to lignin and thereby improves the quality of the recycled enzymes. Our results on EA CS (**Figure 7-3a**) showed that with no freshly added enzymes in the cycle 2, it was possible to produce 30 g/L glucose and 18 g/L xylose after 24 h hydrolysis, which was lower than the results obtained with AFEX^{TM} CS (around 40 g/L glucose and 20 g/L xylose) [4]. Nevertheless, with an enzyme loading of 7.5 mg protein/ g glucan in cycle 2 (62.5% of the cycle 1 enzyme loading), it was possible to achieve almost the same sugar concentrations as in cycle 1 (around 60 g/L glucose and 30 g/L xylose). Thus, under these conditions, the enzyme loading reduction on EA CS for cycle 2 was similar to that for AFEX^{TM} CS.

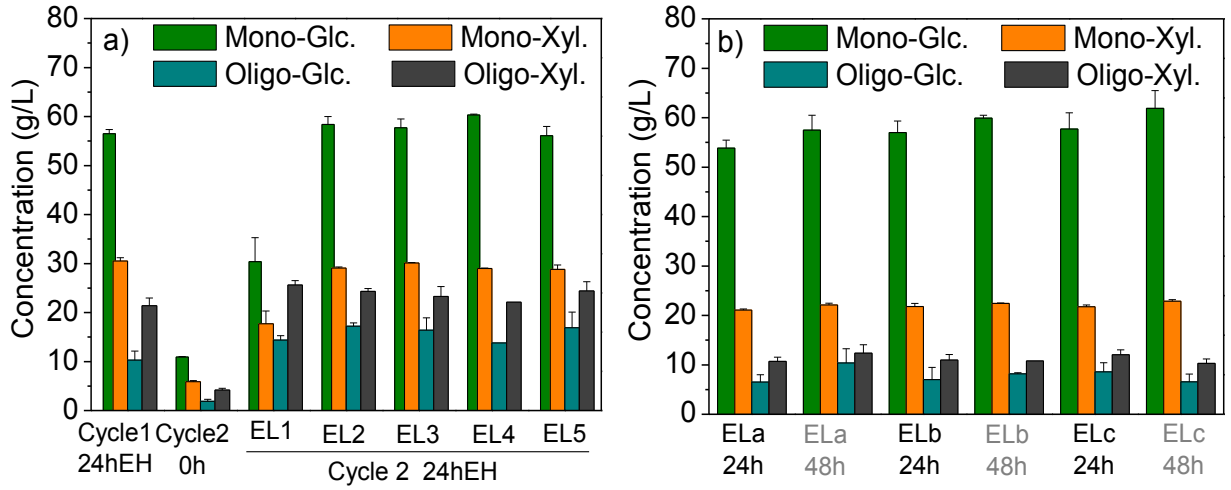

Figure 7-3 Optimization of the enzyme loadings (EL) for the Cycle 2 (a) and the last step (b) during RaBIT process on EA CS. Experiment design was shown in **Table 7-1**.

Our previous study of RaBIT on AFEX^{TM} CS indicated that less xylanases were recycled with solids compared to cellulases [4]. One possible explanation for this fact is that hemicellulose was hydrolyzed faster compared to cellulose and hence, less substrate remained for binding xylanases after 24 h hydrolysis, although considerable oligomeric xylose was generated. This same trend is observed during RaBIT on EA CS (**Figure 7-2a** & **Figure 7-3a**), where hemicellulose is mostly solubilized in the first 24 h of enzymatic hydrolysis. However, since cellulases present in commercial cocktails have lower binding affinity to cellulose III from EA CS, it may lead to less number of cellulases recycled with solids compared to AFEX^{TM} CS as well. Under this hypothesis we investigated various combinations of cellulases and hemicellulases to minimize enzyme loading while maximizing enzyme performance (**Figure 7-3a**, EL2-4). Surprisingly, the results obtained show that increasing the hemicellulases ratio (EL 3) or increasing the cellulases ratio (EL 4) does not affect significantly the enzymatic hydrolysis performance, as the sugar concentrations were almost unchanged. The reasons for this observation remain unclear;

however, is possible that by increasing the amount of hemicellulases, cellulases could be more efficient performing hydrolysis of cellulose and vice-versa. From this result we concluded that the original enzyme combination (66.7% Ctec2+16.7% Htec2+16.7% Multifect pectinase) did not need to be readjusted and therefore, it was also used for Cycles 2-5 of enzymatic hydrolysis. Also similarly to Cycle 1, the enzyme loading of Cycle 2 remained as 7.5 mg protein /g glucan, however as the number of enzyme transfer cycles increased we observed more potential to reduce make-up enzymes and therefore, an enzyme loading of 6.0 mg protein /g glucan was used for Cycles 3-5. An enzyme loading of 6.0 mg protein /g glucan was also tested in Cycle 2 (**Figure 7-3a**, EL5), but sugar concentrations were slightly lower compared to the first cycle. However, this lower make-up enzyme loading was adequate for Cycles 3-5, as demonstrated in **Figure 7-4a**.

The enzyme loading of the last step was also optimized (**Figure 7-3b**). Three enzyme loadings and two time points (24 & 48 h) were tested. In this step there was no addition of fresh biomass and therefore, this step deals with the hydrolysis of the accumulated biomass from the previous cycles. This results in the presence of a highly recalcitrant substrate in the last step, and because of that, the sugar concentrations were relatively low without the addition of make-up enzymes [201-203]. With the addition of an enzyme loading of 4.5 mg protein /g glucan (EL*b*) (**Figure 7-3b**), the glucose and xylose concentrations reached 57 and 22 g/L, respectively, after 24 h. Since most of the xylan was hydrolyzed in previous cycles and the leftover xylan was recalcitrant, the resulting xylose concentration was lower than in Cycles 1-5. Increasing the enzyme loading to 6 mg protein/g glucan (same as Cycle 3-5) did not result in the expected improvement in sugar yield. Further attempts were made to reduce the enzyme loading by keeping the same levels of Ctec 2 loading (3 mg protein /g glucan) as EL*b* but reduce the Htec 2

and Multifect Pectinase usage, since the available xylan in the last step was lower than in previous cycles (EL*a*). However, this enzyme addition reduced the sugar concentration in comparison to the other conditions evaluated here. It may be that that the recalcitrant biomass used in the last step contains more branched polymers which could possibly require accessory enzymes present in hemicellulase cocktails, allowing a greater synergy with cellulases during enzymatic hydrolysis. However, further work is required to understand and explain this phenomenon at the molecular level. We also evaluated the effect of extending hydrolysis time to 48 h. However, the increase of hydrolysis time did not show significant improvement of sugar concentrations (solely 3-4 g/L). Therefore, EL*b* (4.5 mg protein /g glucan) and 24 h enzymatic hydrolysis time was used for the last step of the study that will now be discussed.

7.4.3. Performance of RaBIT

Based on the results and discussion of enzyme loading for Cycle 2 and the last step, the following enzyme loadings were applied for the process: 12 mg protein/g glucan for Cycle 1, 7.5 mg protein/g glucan for the Cycle 2, 6 mg protein/g glucan for Cycles 3-5, and 4.5 mg protein /g glucan for the last step. The average enzyme loading of the process was 8.4 mg protein/ g glucan. Cycle 1-5 enzymatic hydrolysis yielded similar glucose and xylose concentrations (around 60 g/L and 30 g/L, respectively), which are enough for producing >40 g/L ethanol if the ethanol metabolic yield is above 90%. The sugar concentrations were slightly lower after the last cycle of enzymatic hydrolysis (approximately 55 g/L glucose and 20 g/L xylose). The last cycle of fermentation is performed without solid-liquid separation, using simultaneous saccharification and co-fermentation (SSCF) mode, where enzymes are still breaking down the unhydrolyzed glucan and xylan during fermentation. Therefore, it is possible that the last step fermentation also

generates around 40 g/L ethanol, which is a common threshold for economic distillation [166]. The large amount of oligomeric sugars (10-25 g/L oligomeric glucose and 10-30 g/L oligomeric xylose) generated during enzymatic hydrolysis was the major source of sugar loss since the *S. cerevisiae* does not consume those sugars.

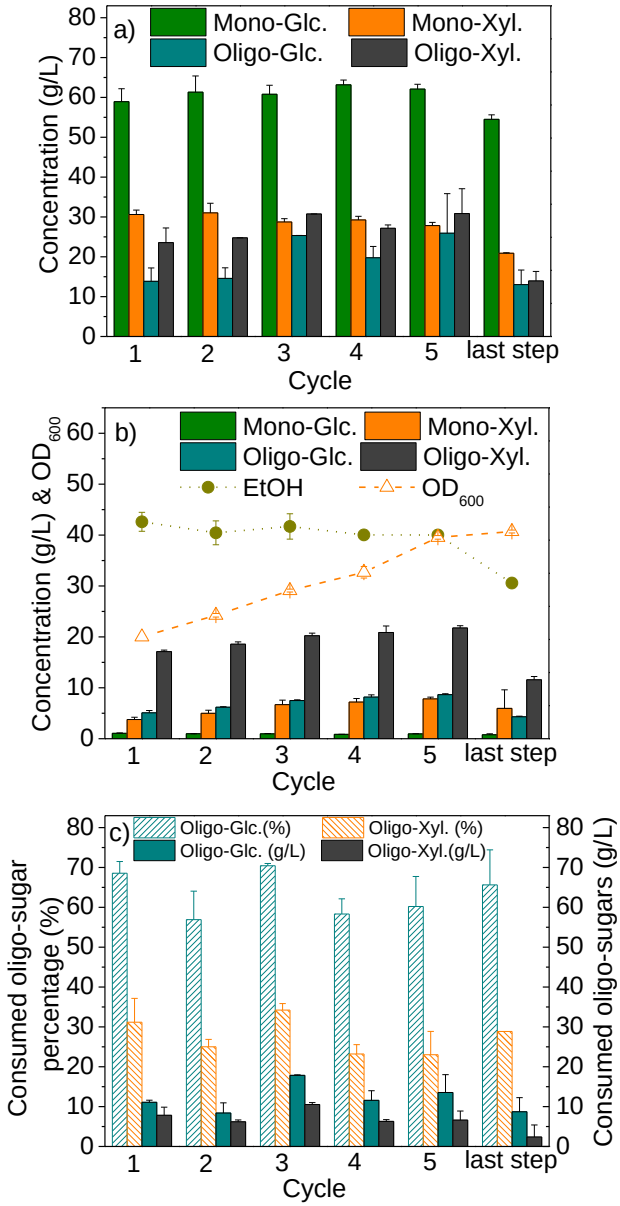

Figure 7-4 Enzymatic hydrolysis performance (a), fermentation performance (b) and oligomeric sugars hydrolyzed and consumed during fermentation (c) using the RaBIT process.

Fermentation for each cycle also proceeded for only 24 h with a high initial OD_{600} of 20. Most of the monomeric glucose and xylose was consumed leaving only 3-7 g/L xylose in the fermentation broth (**Figure 7-4b**). It should be noted that the HPLC column used cannot resolve xylose and arabinose peaks. Since arabinose cannot be utilized by *Saccharomyces cerevisiae* 424A(LNH-ST), is possible that great part of the leftover sugar (here designated as xylose) is in reality unfermented arabinose. Therefore, the real leftover xylose concentration is lower than what is shown in **Figure 7-4**. The oligomeric sugar concentrations were also reduced after each fermentation cycle. The enzymes that did not adsorb on unhydrolyzed solids, notably β-glucosidase and β-xylosidase, stayed in the liquid hydrolysate, which was recovered from enzymatic hydrolysis reactor and used for fermentation. Due to short period of enzymatic hydrolysis (24 h), these enzymes were still active during fermentation of the liquid hydrolysate and hence still could hydrolyze soluble oligomeric sugars to fermentable glucose and xylose. This activity on soluble oligomeric sugars could be further facilitated by the fact that fermentation removed monomeric sugars rapidly, thereby decreasing sugar inhibition of those enzymes. Around 55%-70% of the oligomeric glucose and 22%-35% of the oligomeric xylose in the liquid hydrolysate were hydrolyzed to monomeric glucose and xylose, which were further consumed by the yeast during fermentation (**Figure 7-4c**). The observed lower reduction of oligomeric xylose during fermentation in comparison to oligomeric glucose was partly due to the fermentation profile of this yeast strain. Xylose is typically consumed after glucose is depleted from the media, which allowed the oligomeric glucose to be efficiently hydrolyzed first. However, when xylose starts being consumed by the yeast, the ethanol concentration has already reached inhibitory levels for xylanases, even though xylose inhibition is reduced during

fermentation. Consequently, 10-20 g/L of oligomeric xylose were still unutilized from each cycle.

Using this processing setup, approximately 40 g/L of ethanol were consistently produced in Cycles 1-5, while in the last step only 31 g/L of ethanol could be generated. The ethanol metabolic yield for each cycle varied from 74%-80%, which was significantly lower than AFEX^{TM} hydrolysate fermentation (>90%) and also slightly lower than conventional SHF fermentation (~84%). Lower ethanol metabolic yield of RaBIT compared to SHF was not observed on AFEX^{TM} pretreated corn stover. *Zymomonas mobilis*, which utilizes Enter-Doudoroff pathway for fermentation, may be a better choice for enhancing ethanol metabolic yield in the EA process platform [204]. The cell density (OD_{600}) increased from cycle to cycle, which guaranteed rapid fermentation of sugars. Recently, a native yeast strain *Spathaspora passalidarum* was found able to efficiently ferment glucose and xylose to ethanol [205]. If this strain is applied for fermentation, it could generate another revenue source from hydrolysate fermentation because the wild-type yeast residues could be used as animal feed.

7.4.4. Comparison of RaBIT and conventional SHF

The RaBIT process works on the concept that the less recalcitrant portion of the cell wall can be rapidly hydrolyzed in the first 24h, generating high concentration of sugars that can be readily fermented to ethanol. Also, this process provides more time for the recalcitrant biomass to be hydrolyzed by recycling the unhydrolyzed solids to the following cycle of enzymatic hydrolysis. Using RaBIT process, 97.7% total glucan and 98.0% total xylan conversions during enzymatic hydrolysis were achieved, which are higher compared to the ones reached by conventional SHF

(90.7% and 91%, respectively, **Figure 7-5a**). However, the monomeric glucose and monomeric xylose conversions were slightly lower for RaBIT compared to SHF. The major reason for this result is that in RaBIT, enzymatic hydrolysis was only performed in 24 h while SHF enzymatic hydrolysis was carried out for 96h. A significant amount of oligomeric sugars was generated during the early stages of enzymatic hydrolysis and then were slowly degraded to monomeric sugars in the later stages (**Figure 7-2a**). Nevertheless, most of the oligomeric sugars were still converted to monomeric sugars during RaBIT fermentation, which was not observed during conventional SHF fermentation, most likely because the enzyme activities were very low after 96 h enzymatic hydrolysis. Therefore, higher glucan-to-ethanol conversion and higher total sugar-to-ethanol conversions were observed for RaBIT process when compared to SHF (**Figure 7-5b**). The xylan-to-ethanol conversion followed a similar trend and was much lower than glucan-to-ethanol conversion. Higher concentrations of oligomeric xylose are present in the hydrolysate (**Figure 7-2a** & **Figure 7-4b**), and cannot be utilized by this fermentation yeast. This is the major cause for low xylan-to-ethanol conversion. A similar observation was elaborated in previous study on AFEX^{TM} pretreated corn stover [109].

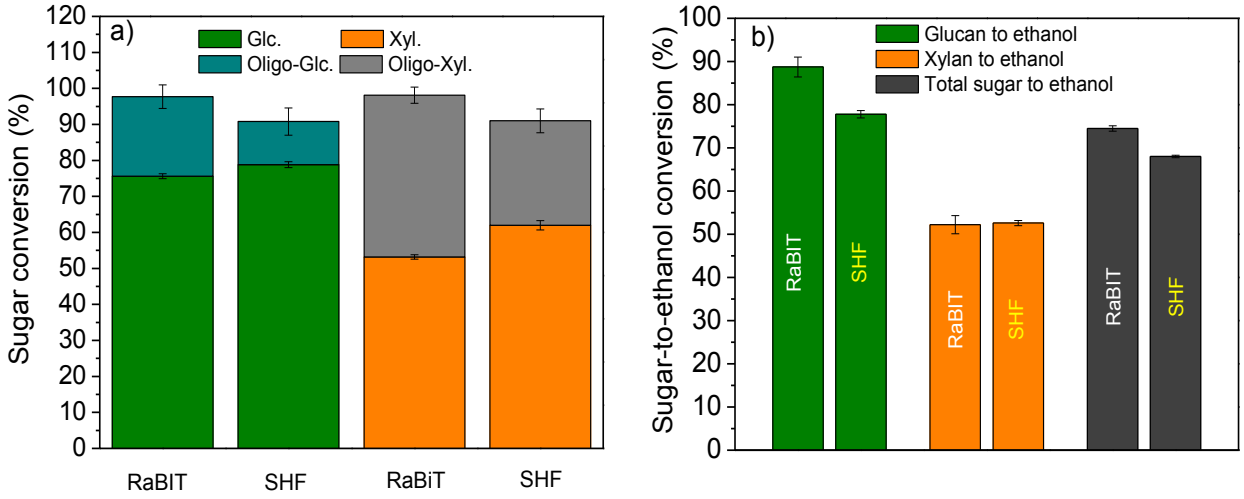

Figure 7-5 Sugar conversions during enzymatic hydrolysis (a) and sugar-to-ethanol conversions (b) for the processes of RaBIT and conventional SHF.

Even though RaBIT showed higher sugar-to-ethanol conversion, the ethanol yield was the same as the conventional SHF process (227 g ethanol per kg EA CS) because of a lower ethanol metabolic yield (**Figure 7-6a**). However, the process ethanol productivity was around 2 times higher than the conventional SHF (0.58 vs. 0.28 $g \cdot L^{-1} \cdot h^{-1}$, **Figure 7-6b**) and the enzyme loading was 30% lower (8.4 mg protein/ g glucan vs. 12 mg protein/g glucan). Higher productivity was mostly due to less time needed for the RaBIT process (**Figure 7-6c**).

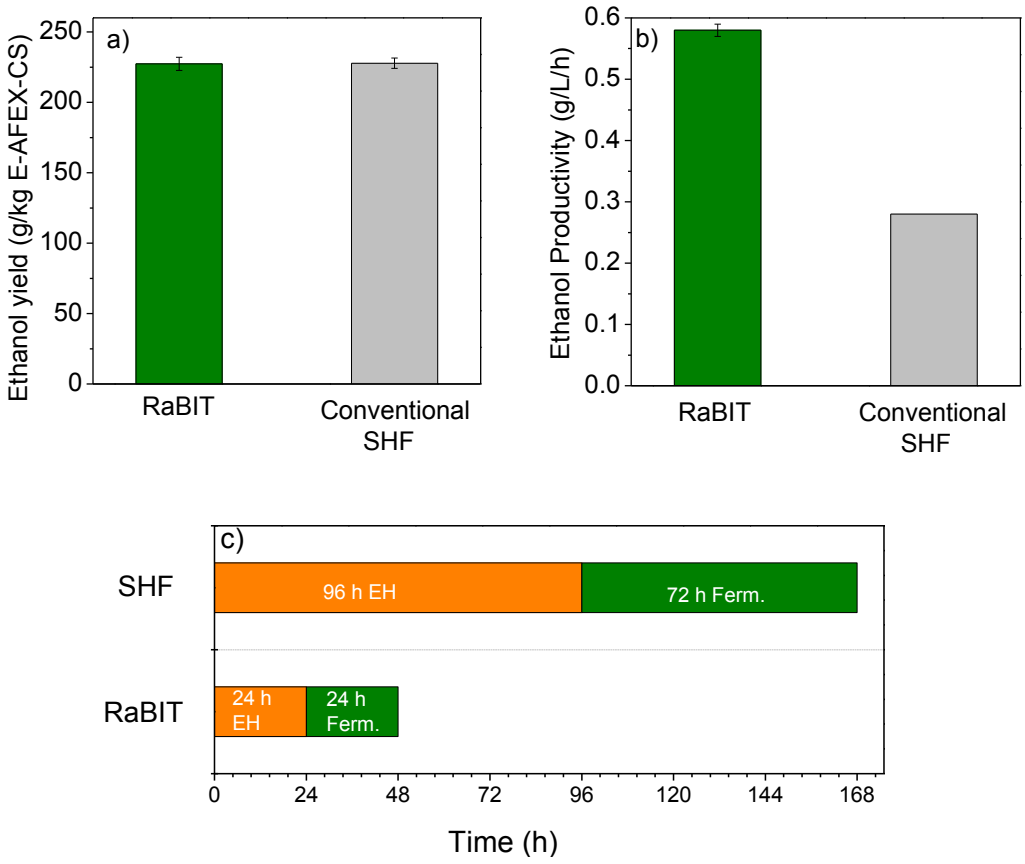

Figure 7-6 Comparison of ethanol yield (a), ethanol productivity (b) and timelines (c) for RaBIT and conventional SHF processes. Ethanol productivity was calculated based on enzymatic hydrolysis plus fermentation.

Based on 1 kg of untreated corn stover, 840 g of EA pretreated corn stover were obtained after pretreatment, which contained 401.3 g of glucose equivalent glucan and 254.8 g of xylose equivalent xylan (**Figure 7-7**). The maximum ethanol yield from this amount of sugar is approximately 334.6 g. Both the RaBIT process and the conventional SHF yielded around 190 g of ethanol from 1 Kg of untreated corn stover. However, the enzyme addition per kilogram of untreated corn stover was 3.0 g for the RaBIT process versus 4.3 g for the conventional SHF process. In the RaBIT process, around 2% and 23.3% of the total sugars were lost in the solid unhydrolyzed biomass and in the liquid fermentation broth, respectively, which corresponded to

a maximum loss of 85 g ethanol. This result means that 74.5% of the total sugars (488.8 g) could be converted to ethanol, yielding 249.3 g of ethanol considering for 100% metabolic yield. This amount is considerably higher than what has been reported in the literature [4]. However, the ethanol metabolic yield of the fermentation was low (around 76.6% of the theoretical maximum). This problem can probably be solved with some stain development and adaptation, to direct the carbon flux towards ethanol production instead of cell mass production. Nevertheless, we still achieved the same ethanol yield (191 g ethanol/kg CS) as reported for AFEX^{TM} CS [78] due to higher sugar-to-ethanol conversion. However, this result was obtained with much lower enzyme loading and higher ethanol productivity. If the ethanol metabolic yield issue can be solved in the future by achieving values near 90%, it will be possible to generate 224 g of ethanol from 1 kg CS combining the RaBIT process and EA pretreatment technology.

As a side product, 29.3 g and 25.8 g glycerol per Kg untreated corn stover was produced from RaBIT and SHF processes, respectively (**Figure 7-7**). Glycerol production could alleviate the redox imbalance caused during xylose metabolism through xylose reductase and xylitol dehydrogenase. Another side product is the unhydrolyzed solids, which compositions are showed in the **Table 7-2**. Currently, the unhydrolyzed solids are considered to supply heat/electricity for the biorefinery.

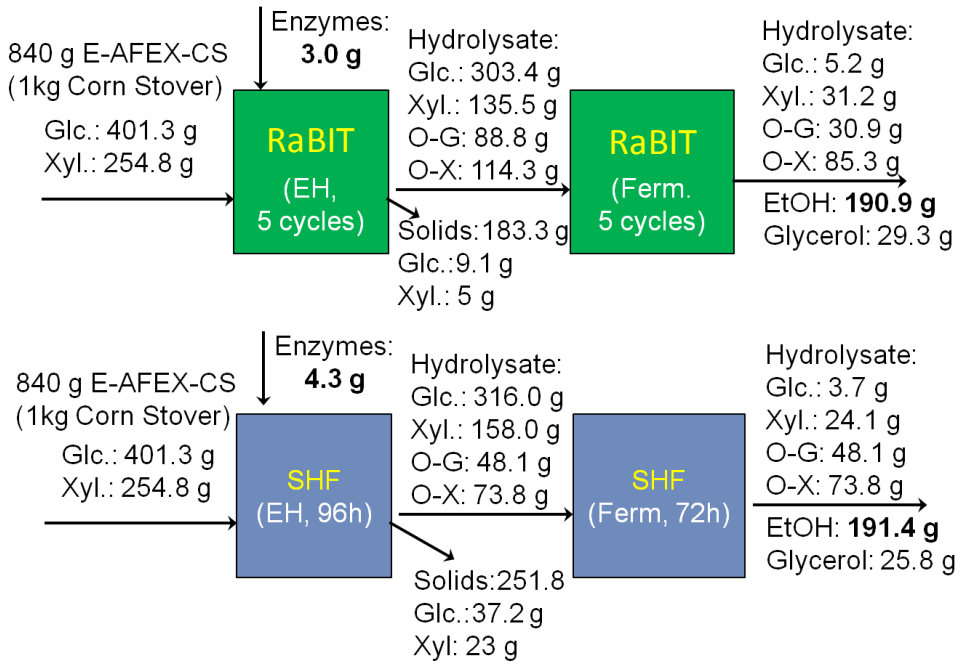

Figure 7-7 Mass balance comparison of RaBIT and conventional SHF processes.

Table 7-2 Compositions of unhydrolyzed solids from RaBIT and conventional SHF processes.

Process	% Glucan	% Xylan	% Arabinan	% Klason Lignin	% Ash
RaBIT	11.6% ±0.8%	6.1% ±0.3%	0.9% ±0.1%	47.4% ±0.3%	11.4% ±0.1%
SHF	18.1% ± 2.4%	7.2% ± 1.1%	1.4% ± 0.1%	43.7% ± 0.4%	9.3% ± 0.8%

7.5. Conclusion

The integration of the novel EA pretreatment with state-of–the-art bioprocessing technologies, such as RaBIT, further reduced the enzyme loading by 30% (from 12 mg/g to 7.5 mg/g glucan) compared with the conventional SHF process. It was demonstrated that processing engineering innovations allied with novel pretreatment strategies can decrease enzyme usage in the biorefinery and reduce processing time and capital costs. It is also important to mention that

conventional AFEX^{TM} technology uses approximately 20 mg/g glucan for optimal results in a traditional SHF process, as reported in **CHAPTER 5**. Therefore, this technology advancement and, in particular, the integration of EA pretreatment with the RaBIT process, allowed a very substantial decrease in enzyme loading. Furthermore, RaBIT process enhanced ethanol productivity by 2 fold and allowed higher sugar conversions compared to SHF process on EA CS.

While continuing to develop incremental improvements to this novel biomass processing strategy, it is also important to generate appropriate enzymes and microorganisms that are adapted to the properties of these new substrates. For example, developing novel strains that can generate higher ethanol metabolic yields is important to continue decreasing enzyme loading and improve process yields. Also, advances in enzyme technology can provide novel engineered cellulases with higher binding affinity to cellulose III, which will not only allow improvements in glucan conversion rates but also more efficient cellulase recycling, which is currently not possible with wild-type cellulases.

CHAPTER 8 – EXTRACTIVE AMMONIA (EA) PRETREATMENT PROCESS DESIGN, PRELIMINARY ECONOMICS AND FINAL CONSIDERATIONS.

8.1. Abstract

The novel Extractive Ammonia (EA) pretreatment of lignocellulosic biomass has been studied on various fronts that include the three most important units of the biorefinery: pretreatment, enzymatic hydrolysis and fermentation. Even though this pretreatment technology presents good downstream processing performance, the most important aspect to consider is the overall economics of the EA-based biorefinery. Therefore, this study aimes to evaluate EA pretreatment economics, by determining capital and operating costs. These were adapted to the existing downstream operations described by the NREL economic model for lignocellulosic ethanol production. By coupling the economic model with enzymatic hydrolysis and fermentation performance results, a techno-economic evaluation of the EA biorefinery was performed. For the base case pretreatment conditions (6:1 ammonia to biomass ratio, 30 min residence time and 120 °C), the minimum ethanol selling price (MESP) at an internal rate of return (IRR) of 10 % was $2.36 per gallon of ethanol. Compared with an AFEX™ biorefinery, this value is slightly higher (about 8 cents per gallon of ethanol); however, there is great room for improvements as this result represents a preliminary level of optimization on the pretreatment conditions and process design. From sensitivity analysis is clear that the heat duty during ammonia-water separation can highly impact the economy of the EA biorefinery. Also, the lignin selling price is a very important factor that can dictate the viability of the EA process. These and other considerations will be evaluated in detail in this work.

8.2. Introduction

The development and study of Extractive Ammonia (EA) pretreatment has provided understanding on how plant cell wall modifications can improve enzymatic hydrolysis yields and potentiate reduce enzyme loadings during biorefinery operations. However, besides the scientific knowledge that has been presented in the previous chapters of this dissertation, is also important to provide techno-economic information and thereby determine the most important areas for scientific and technological development. In 2011, the National Renewable Energy Research Laboratory (NREL) published a new technical report and respective model tools to simulate biorefinery conditions based on dilute acid (DA) pretreatment. This report provides the most updated and detailed economics information on the literature [206]. From the report, a minimum ethanol selling price (MESP) of approximately $2.15 per gallon ethanol ($3.27/gal gasoline energy equivalent) was determined for a DA-based biorefinery. Based on this study, this work will focus on determining the impact of EA pretreatment on the overall economics of the biorefinery. The base case pretreatment conditions for EA will be considered as 6:1 ammonia to biomass ratio, 30 min residence time and 120 °C. These conditions are not optimized for achieving the lowest ethanol price, but will serve as a benchmark for future improvements of this technology. For this base case, EA process design will be simulated to generate material and energy balances for processing 2000 ton/day of biomass, which will be further used for sizing of equipment and determination of energy requirements. From this information, capital and operational costs of EA pretreatment will be determined and incorporated into the NREL economic model [206], replacing the existing DA pretreatment. Downstream conditions will be optimized using the enzymatic hydrolysis performance models generated for corn stover in

CHAPTER 5, which will generate the most profitable biorefinery operation for the EA base case scenario. The MESP will be determined for the base case EA biorefinery and compared with an AFEX^{TM} biorefinery. Further sensitivity analysis will be used to provide technical recommendations for research and development of new processing conditions of EA pretreatment, always aiming to improve the profitability of the process.

8.3. Experimental

8.3.1. EA pretreatment process flow diagram (PFD)

The EA process was scaled based on the batch design presented in **CHAPTER 4** to pretreat 2000 tons of dry biomass per day. The process flow diagram is presented in **Figure 8-5**, and consists of two reactors that operate intermittently in what we called a "reactor system". After pretreatment, the ammonia from one reactor is always recycled to the other reactor belonging to the same system. The pretreatment unit operation for 2000 ton per day is composed of five reactor systems with two pretreatment reactors each, in a total of ten reactors. For this operation, two ammonia recycling systems comprised of one distillation column, a compressor, a pump and a flash evaporator, operate continuously throughout the production of EA pretreated biomass, following the schedule in **Figure 8-6**. For this analysis, approximately 13.9 tons of dry biomass were added to each batch reactor (streams 1), along with 1.39 tons of water and 83.4 tons of ammonia (6:1 ammonia to biomass ratio) in our base case (streams 2). The reactor operates at 1200 psi of pressure and 120 °C for 30 min residence time. The liquid ammonia is filtered through the bottom of the reactor and flows (streams 7) to a distillation column that operates under 200 psi pressure. The top stream of the distillation column (stream 9) is fully condensed to

liquid and is pumped to a new reactor that has been freshly loaded with biomass. The bottoms of the distillation column contain lignin rich extractives, which can be used as a valuable by-product for the biorefinery (stream 8). The EA pretreated biomass is further transferred to a flash evaporator column (stream 3) where heat is applied to recover the ammonia adsorbed on the biomass surface and inside the pores. The evaporated ammonia (stream 5) is further compressed to the ammonia tank (stream 6) and reused in the pretreatment system. For all the ten reactors that compose the pretreatment operation, two evaporators and two compressors are used continuously during ammonia recycling.

8.3.2. Material and energy balances around EA pretreatment

Material and energy balance calculations around ammonia-water system were performed using Aspen Plus software (Aspen Tech, Burlington, MA, USA). Biomass energy balance calculations were added based on heat capacity and enthalpy values, which were determined through regression of experimental numbers obtained for lignin [207] and cellulose [208]. Thermodynamic parameters for hemicellulose and the remaining unknown components of the biomass were assumed to be the same as those for amorphous cellulose [208].

The reactor was modeled based on flash calculations at constant pressure (1200 psi) and temperature (120 °C) for the ammonia-water system, entering at 25 °C and 150 psi. All thermodynamic calculations were determined using the Non-Random Two-Liquid (NRTL) electrolyte model with default parameters provided by Aspen Plus software. The heat required to increase biomass temperature from 25 to 120 °C during reaction was added to the heat duty calculations. Heat of mixing of ammonia with water and heat of adsorption of ammonia/water to the biomass were not accounted to simplify these calculations. This assumption was made based

on the fact that ammonia loadings during EA pretreatment are about sixty times higher than water loadings and also because the amounts of ammonia/water adsorbed on the biomass is considerably smaller than the free ammonia in the bulk phase. Mass balance on the reactor was performed experimentally as described in **CHAPTER 4**. In this study, ammonia reactions with biomass were considered to result in 0.5 wt% ammonia loss (from the total ammonia added to pretreatment) [95], where ammonia is chemically bound to the biomass. This assumption is based on information provided by Michigan Biotechnology International (MBI), who is performing ammonia recycling tests during AFEX pretreatment. The chemistry of AFEX is similar to EA pretreatment and therefore, we assumed the ammonia loss per amount of pretreated biomass to be the same.

The energy balance for the evaporator was simulated based on flash calculations for ammonia, which was allowed to reach a vapor fraction of 1.0 at ambient pressure, assuming an input of ammonia in liquid state (pressure of 150 psi) at ambient temperature. The enthalpy of desorption of ammonia from the biomass (33 kJ/mol adsorbed ammonia) [209] and the enthalpy associated with biomass temperature variations was accounted for during heat duty calculations for the evaporator. Mass and energy balances for distillation were modeled based on ammonia-water mixture with RadFrac simulation tool from Aspen software. Extractives composition and mass balances were not accounted for during distillation calculations. However, the heat duty required to increase the extractives temperature in the reboiler was accounted for the heat requirements of the distillation process. The extractives were assumed to be recovered on the bottom of the distillation column with most of the water entering in the front of the process.

8.3.3. Equipment sizing and cost

All equipment, with the exception of the reactor and ammonia evaporator, were sized and cost estimated using Aspen Capital Cost Estimator software (Aspen Tech, Burlington, MA, USA). The reactor volume was sized based on the experimentally measured capacity of 1L for every 100 g of dry biomass input. The ammonia evaporator was sized assuming that the biomass volume occupies 1/3 of the evaporator volume. Capital cost estimations for these two pieces of equipment were performed according to tabulated values for high and low pressure vessels in the literature [210-213].

8.3.4. Techno-economic analysis

A biorefinery designed to process 2000 ton biomass/day was evaluated for 30 years of operation based on the NREL economic model for biochemical conversion of lignocellulosic biomass to ethanol [206]. The capital and utility costs for EA pretreatment were calculated in this work and added to the NREL economic model in replacement of the dilute acid pretreatment. The base case conditions for EA pretreatment was defined as 6:1 ammonia to biomass ratio, 120 °C and 30 min residence time. On Table 8-12, the capital cost for EA pretreatment and utility costs assumed for economic analysis are given. The cost of delivered biomass at the biorefinery was assumed to be $60 per dry ton (similarly to the NREL model) and ammonia price was assumed to be $600 per ton [214] in the base case. Revenues from lignin were also accounted with a selling price of 10 cents/lb [215]. Economic evaluation was performed without in-house power production from unhydrolyzed solids that are released after enzymatic hydrolysis and fermentation because they are assumed to be used as feedstock for lignin valorization. Instead, electricity is bought from the grid at cost of 5.72 cents/kWh.

The MESP was calculated based on an internal rate of return of 10% for different processing conditions of enzymatic hydrolysis using a cellulase cost of $3600/ton and hemicellulase cost of $4500/ton, as the base case scenario, which results in a similar average value to the NREL model [206]. These conditions were the same as used on the Box-Benhken design from **CHAPTER 5**, with variable solid loadings, enzyme loadings and incubation times. Experimental values of enzymatic hydrolysis were obtained from the work presented in **CHAPTER 5.** Fermentation metabolic yields were fixed constant at 90% of theoretical. This fermentation performance was assumed based on the yields obtained for AFEX^{TM} treated corn stover (AFEX^{TM}-CS) hydrolysates [78]. The calculated MESPs for each enzymatic hydrolysis condition of EA-CS were used to produce an empirical, full quadratic regression model that relates MESP ($ gallon EtOH) with processing variables during enzymatic hydrolysis. This model, produced with Minitab software (Minitab Inc., State College, PA, USA), was used to further optimize the enzymatic hydrolysis conditions that generate the lowest MESP. This lowest MESP value for the EA biorefinery was further compared with the lowest MESP obtained for an AFEX^{TM}-based biorefinery, also using the same methodology as described for EA-CS, with experimental values from **CHAPTER 5**. For the AFEX^{TM}-based economic model, the pretreatment was not included in the biorefinery. Instead, AFEX^{TM}-CS pellets were assumed to be delivered at the door of the biorefinery from regional biomass processing depots (RBPDs) [216]. The cost of AFEX^{TM}-CS pellets was assumed to be $120 per ton (dry weight), as estimated by Michigan Biotechnology Institute (MBI). Sensitivity analysis on the MESP was performed for enzyme cost, biomass cost, lignin price, utility cost and capital cost of EA pretreatment.

8.4. Results and Discussion

8.4.1. Material and energy balances for the EA pretreatment model

The preliminary EA pretreatment configuration presented herein (**Appendix Figure 8-5**) is composed of a set of five reactor systems, with two reactors each, and two ammonia recycling systems containing by a pump, a distillation column, an evaporator and a compressor each. While the pretreatment reactors are operating in batch mode, ammonia recycling is operated continuously to fulfill the demand of the ten reactors that compose this unit operation (see schedule on **Appendix Figure 8-6**). Mass and energy balance calculations were performed assuming the base case EA conditions of 6:1 ammonia-to-biomass ratio, 120 °C and 30 min residence time. From the material balances around EA pretreatment, presented in **Appendix Table 8-4,** it is possible to predict loss of ammonia from the bottom of the distillation column. This loss represents 0.12% of the ammonia input during pretreatment. The major ammonia loss represents 0.5% of the ammonia loaded during pretreatment, which is chemically bound to the biomass. This assumption was based on previously quantified ammonolysis products and Millard reaction products formed during AFEX pretreatment [23, 95, 97], which was assumed to be similar for EA pretreatment. More detailed ammonia mass balance should be performed experimentally to verify the validity of this assumption for a more detailed economic evaluation. The mass balance around the biomass was determined experimentally from **CHAPTER 4** and **CHAPTER 5** where about 45 % of the lignin present in the biomass was extracted during the process. Energy balances on the biomass streams were evaluated based on heat capacities from literature associated with crystalline and amorphous cellulose and lignin [207, 208]. Hemicellulose heat capacities and enthalpies were assumed to be the same as amorphous

cellulose. From those literature values it was possible to account for changes in composition during energy balance calculations for every stream, which are presented in **Appendix Table 8-4**. Biomass composition changes for the various pretreatment streams were determined experimentally and are presented in **CHAPTER 5**. Regarding the water mass balance, some water cannot be efficiently removed from the system, causing water build up. The optimum moisture content during EA pretreatment is 10 % in a dry weight basis. To avoid water build up in the system and maintain the pretreatment operating at steady state, the biomass should contain about 7% moisture when added to the EA pretreatment system, because the remaining 3% moisture is already present in the ammonia recycling system.

The energy requirements of each unit operation involved on EA pretreatment are shown in **Appendix Table 8-5**. From this table, it is possible to observe that EA process is energy intensive, especially during ammonia recovery. Simulation values for total heat requirements of EA pretreatment are 9.08 GJ/ ton biomass and electricity requirements are 89.59 kWh/ ton biomass. The energy requirement for the EA pretreatment operation represents about 50 % of the HHV of the corn stover input. Analyzing the distribution of these energy requirements by the various equipments is possible to observe that the distillation is the most energy demanding operation, covering about 73 % of the total heat duty of EA pretreatment, followed by the reactors (20.59 %) and evaporator (6.21 %) (**Figure 8-1**). The electricity duty is shared by the pump and compressor, where the later represents about 92.43 % of the total electricity consumption and the former represents 7.57 % (**Figure 8-2**).

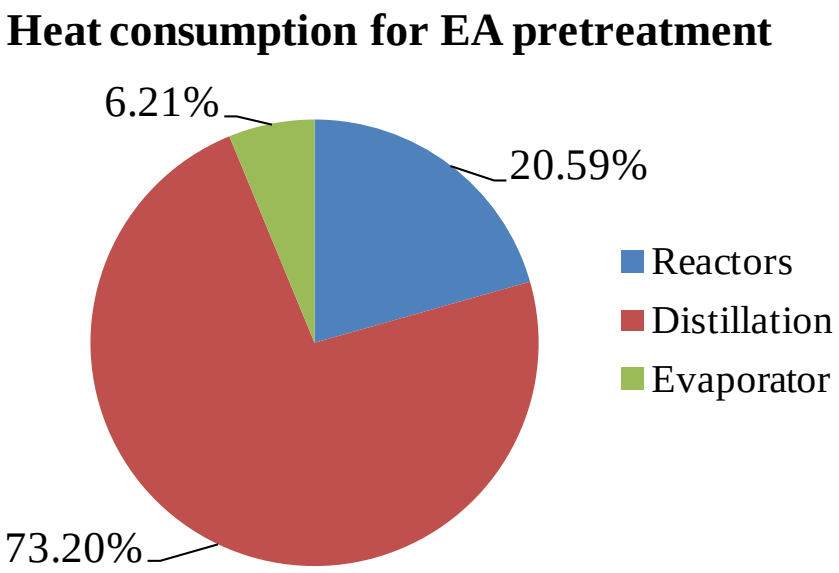

Figure 8-1 Pie chart describing the heat consumption of the various unit operations during EA pretreatment. The total heat duty is 9.08 GJ/ ton biomass.

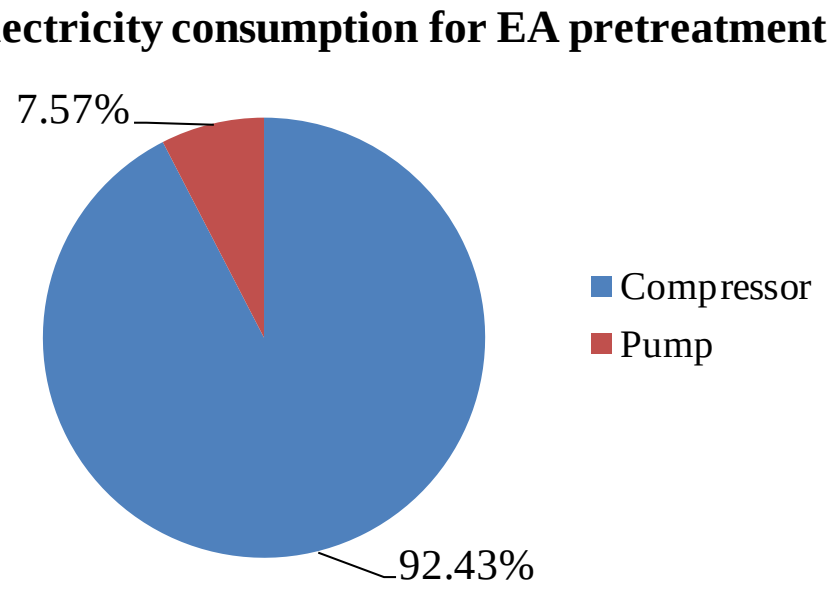

Figure 8-2 Pie chart describing the heat consumption of the various unit operations during EA pretreatment. The total electricity consumption is 89.59 kWh/ ton biomass.

8.4.2. Capital cost of EA pretreatment

EA pretreatment equipment was sized based on Aspen Plus simulations and on experimental information. In Appendix **Table 8-6** to **Table 8-11**, the various pieces of equipment used in the EA pretreatment system are described. The cost estimation was performed with Aspen Capital Cost Estimator for most of the equipment except the reactor vessel and the evaporator, which were estimated based on literature information [211-213]. **Table 8-1** summarizes the equipment used for a 2000 ton/day of biomass processing capacity with respective unit cost, number of units and total cost. Analyzing this information, is clear that the pretreatment reactors represent the highest expenditure on the EA capital cost ($17,447,100.00), followed by the distillation columns ($12,789,984.00) and the compressors ($7,298,000.00). The other unit operations are relatively cheaper and do not impact capital cost significantly. The total capital cost estimated for the EA pretreatment system was $51,907,471.20 for the base case scenario. Compared with the DA pretreatment operation for the same size biorefinery, EA pretreatment is more capital intensive, as DA pretreatment unit was estimated to be purchased under MM$30 [206]. Thus EA pretreatment would benefit more from being implemented at a very large scale in centralized biorefineries.

Table 8-1 Summary of equipment and capital cost for EA pretreatment.

Name	Unit Cost ($)	# Units	Total cost ($)
Reactor	1,744,710.00	10	17,447,100.00
Distillation Column	6,394,992.00	2	12,789,984.00
Evaporator	360,910.00	2	721,820.00
Compressor	3,649,000.00	2	7,298,000.00
Pump	354,775.00	2	709,550.00
Ammonia Tank	320,790.00	3	962,370.00
	Installation factor		1.3
	Total installed cost ($)		**51,907,471.20**

8.4.3. Material balance for enzymatic hydrolysis and fermentation and MESP calculation

To evaluate enzymatic hydrolysis conditions that produce the optimal MESP, a Box Benhken design of experiments was implemented with the same enzymatic hydrolysis parameters as described in **CHAPTER 5**. The sugar yields obtained for EA-CS as a function of pretreatment conditions were presented in **CHAPTER 5** and were used in this work for determination of the economic optimal conditions. For this purpose, enzymatic hydrolysis conditions and respective sugar yields were added to the modified NREL economic model. This model was built based on the NREL economic model for Dilute Acid (DA) pretreatment, where EA pretreatment data (both fixed and variable costs) were introduced in replacement of DA pretreatment parameters. The MESP was calculated for the various enzymatic hydrolysis conditions for a 30 year plant operation, with 2000 ton/ day of dry biomass capacity, using an internal rate of return of 10%. Fermentation performance was assumed to be constant at 90 % of the theoretical metabolic yield from the sugar produced during enzymatic hydrolysis. The costs associated with pretreatment are defined in **Appendix Table 8-12**. For the economic model, both the EA extracted lignin and the lignin from unhydrolysed solids were considered as revenue for the biorefinery, with an average selling price of $220 per ton of lignin. The lignin market is currently occupied by kraft lignin, ligno-sulphonates or organosolv lignin. The Chinese market for lignin seems to be the most competitive, with prices ranging 200 to 600 US dollars per metric ton (FOB), depending on the type and quality of the lignin [215].

The calculated MESP values after running the economic model were further processed using Minitab software to fit a full quadratic equation as a function of enzymatic hydrolysis parameters (i.e., incubation time, solids loading and enzyme loading). The residuals and coefficients obtained for this model are presented in **Appendix Figure 8-7** and **Appendix Table 8-13**,

respectively. From the residual plots, it is possible to observe that the residual values are reasonably dispersed throughout the MESP range and do not denote any systematic deviation. The histogram also presents a reasonably normal distribution with the highest number of residuals being similar to zero, as expected. From the coefficient table, it is possible to observe a *P* value above 0.05 for the terms *Enzyme Loading* and *Solid Loading*Solid Loading*. These terms were considered in the model equation because their absence impacted negatively the predictive ability of the model (predicted R^2) and the goodness of the fit. Using this model along with the optimization tool from Minitab software, the minimum MESP was determined along with the enzymatic hydrolysis conditions (time, enzyme loading and solids loading) that provide this ethanol price. **Appendix Figure 8-8** shows the optimization plots obtained in this study, with a predicted MESP of $2.37 per gallon of ethanol. The enzymatic hydrolysis conditions and predicted glucose and xylose yields are also shown. The optimal enzymatic hydrolysis condition that projects the lowest MESP for EA-CS is 93.7 h incubation time, 21.44% solid loading and 7.5 mg enzyme/g glucan. At these conditions, the regression model predicts a monomeric glucose conversion of 72.46 % and monomeric xylose conversion of 69.77 %. When introducing these predicted enzymatic hydrolysis results and processing conditions into the modified NREL economic model for EA pretreatment, it was possible to recalculate the MESP and compare with the regression model prediction. The value given by the modified NREL economic model for these enzymatic hydrolysis conditions was $2.36 per gallon of ethanol, which means the MESP prediction from the regression model was $0.01 higher than the value calculated by the modified NREL model for that processing condition.

Table 8-2 shows the ethanol yields on a mass and volume basis, per ton of biomass and per year, using the optimal conditions of enzymatic hydrolysis for the base case EA pretreatment condition. From this table, it is possible to observe that for each ton of untreated biomass entering the biorefinery about 61.8 gallons of ethanol are produced, which results in an annual production of 47.74 million gallons of ethanol. The ethanol titer after fermentation was projected to be 6 %, based on a fermentation yield of 90 % of theoretical maximum. Extracted lignin from the EA process is about 63 Kg lignin/ton of biomass, while about 77 Kg lignin/ton of biomass are recovered from the unhydrolyzed solids after enzymatic hydrolysis and fermentation.

For the overall EA biorefinery economics in the base case scenario, the total capital investment was approximately MM$292.10 (**Table 8-3**). The MESP of $2.36 per gallon of ethanol was calculated based on an IRR of 10 %. For this process, the enzyme cost per gallon of produced ethanol is approximately $0.16, which is considerably lower than the one obtained by the AFEX-based biorefinery ($0.43). This result is a direct consequence of the lower enzyme loading used in the EA biorefinery during enzymatic hydrolysis, due to the high digestibility of EA-CS.

Table 8-2 Ethanol and lignin yields for the optimized base case scenario of an EA biorefinery.

Ethanol yield (kg/ton BM)	242.20
Ethanol yield (gal/ton BM)	61.80
Ethanol volume (MMgal/yr)	47.74
Ethanol titer (w/w)%	0.06
Extracted lignin (kg/ton BM)	63.00
Lignin from solids (Kg/ton BM)	77.00

Table 8-3 Economic considerations for the base case EA biorefinery (2007 US$).

Fixed Capital Investment (MM$)	292.10
TCI/Annual gallon Ethanol ($/gal EtOH)	6.46
Ethanol Selling Price ($/gal EtOH)	2.36
IRR	0.10
Enzyme Cost ($/gal EtOH)	0.16
Fixed Costs ($/gal EtOH)	0.19
Other Operation Costs ($/gal EtOH)	0.53

8.4.4. Performance of EA-based biorefinery

A comparative study was also performed to evaluate the performance of the EA biorefinery and the base case scenario presented here. **Figure 8-3** shows the MESP values for biorefineries based on two different ammonia pretreatment technologies, notably AFEX^{TM} and EA (base case). The AFEX^{TM} biorefinery was also modeled based on NREL economic model for all unit operations with the exception of pretreatment. The scenario evaluated for AFEX^{TM} was based on the depot system, with a delivered cost of pretreated AFEX^{TM}-CS pellets to the biorefinery of $120/ton on dry weight basis. Enzyme cost was assumed to be the same as for the EA biorefinery. The enzymatic hydrolysis data were generated from **CHAPTER 5** and used in this work to project the AFEX^{TM} biorefinery MESP. The AFEX^{TM}–based biorefinery was evaluated considering internal power generation by combustion of the unhydrolysed solids. Excess electricity production was assumed to be revenue to the biorefinery. For the EA biorefinery, lignin was assumed to be a valuable raw material with good potential for future valorization, according to

the physico-chemical characterization presented in **CHAPTER 6**. Therefore, lignin was assumed to be a source of revenue to offset the high energy demand of EA pretreatment.

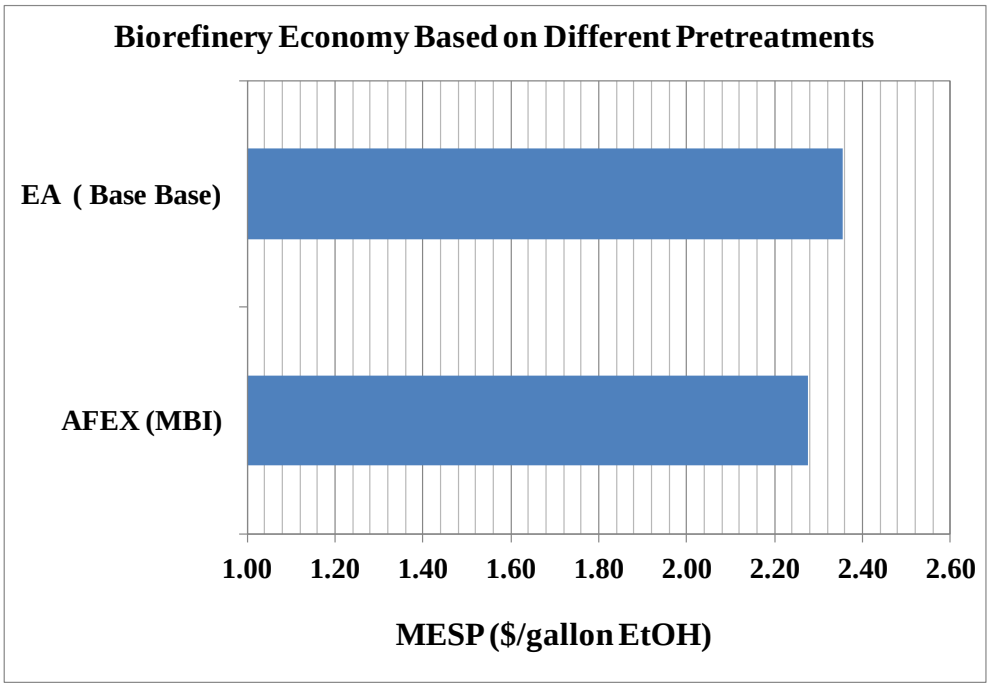

Figure 8-3 MESP values for biorefineries based on different pretreatment technologies.

From **Figure 8-3**, it is possible to conclude that the base case EA biorefinery shows a higher MESP compared to an AFEX^{TM} biorefinery, with a value of $2.36 per gallon of ethanol compared with $2.28. However, the base case scenario represents the starting point for the development of this technology. Besides being important to evolve on developing technologies to better separate lignin from plant biomass, generating important revenue to the sustainability of an EA biorefinery, is also imperative to find processing conditions that minimize energy input to the EA pretreatment. From **Figure 8-4**, is clear that heat usage in EA pretreatment is the factor that most affects the economy of the biorefinery, followed by biomass cost. As mentioned above

and observed in **Figure 8-1**, the distillation unit used for separating ammonia and water is the most energy demanding operation in the EA pretreatment process.The temperature requirement for the distillation is 290 °C for the reboiler and 110 °C for the condenser. It is highly probable that the 6:1 ammonia-to-biomass ratio condition used here as a base case is not the most economical for the EA biorefinery. Analyzing the sensitivity chart in **Figure 8-4**, it is clear that reduction in the ammonia loading and heat duty by 30% could have significant impact on the MESP of EA biorefinery. Besides heat integration and process optimization, this is possible to achieve by reducing the ammonia loading between 3:1 and 4:1, or possibly by directly reusing the liquid ammonia with the additional water for one more pretreatment cycle before separating the ammonia from the water by distillation. The former strategy would not have significant impact on the enzymatic hydrolysis yields but would impact lignin extraction, unless the pretreatment time is extended to 60 min (**Figure 5-2 iv)**. This extension of residence time would practically duplicate the capital investment of EA pretreatment, which does not significantly impact the projected MESP from the sensitivity chart. Therefore, doing pretreatment at 4:1 ammonia-to-biomass ratio would possibly benefit the economics of the EA biorefinery. In the case of liquid ammonia reuse before distillation, the major downfall is that it will cause some temporary water build up in the system, which may have some negative impact on the sugar yields, although it should not be very significant by analyzing the results shown in **Figure 5-2 i)**. However, the impact in lignin extraction should be determined experimentally using this method.

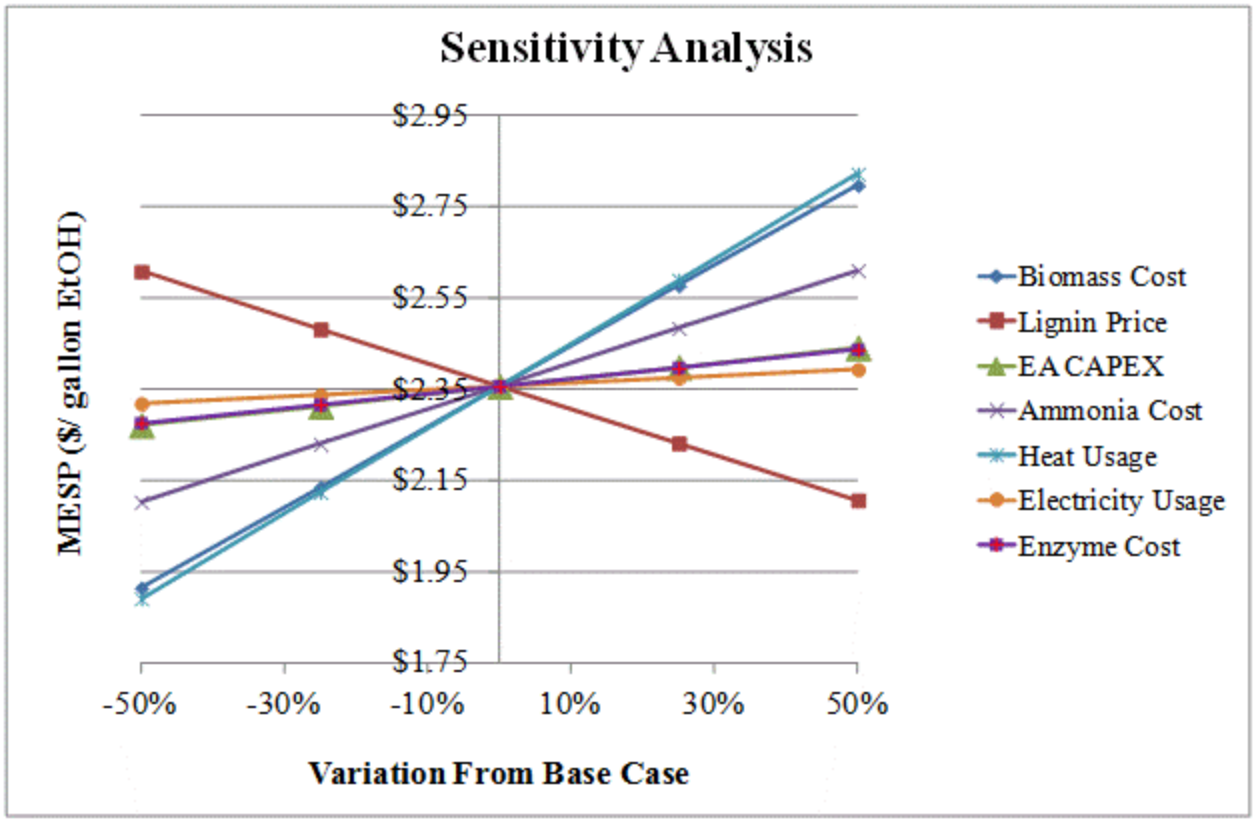

Figure 8-4 Sensitivity analysis chart for measuring the impact of variations in utility and capital cost of EA pretreatment on the MESP. The impact of enzyme cost and lignin selling price on the MESP are also presented.

Another important aspect to note about the EA technology is that it reduced the impact of enzyme cost on the overall biorefinery economics, as shown in the sensitivity analysis chart. This effect is a direct consequence of the reduced enzyme loading (7.5mg/g glucan) during efficient enzymatic hydrolysis of EA-CS. Even though we could achieve this reduction on enzyme loading effect on the economics of the biorefinery, the EA process is highly dependent of the lignin value generated as a by-product from the biorefinery. Therefore, creating value addition to EA-derived lignin is a major area that will determine the success of this technology. Moving forward on the development and improvement of the EA biorefinery, it is critical to expand our research on developing technologies for converting EA lignin to value added products.

A final consideration is the operating pressure of EA pretreatment in the base case scenario (1200 psi). For industrial processes, high pressure has significant impact on capital cost, but also on process safety and social acceptance of the industrial activity. Therefore, decreasing operating pressure is also an important area that deserves attention moving forward during development of the EA technology. A possible strategy is to use co-solvents of higher boiling point that can interact with ammonia and further reduce operating pressure at higher temperatures. Preferentially, solvents that can be produced within the biorefinery, such as ethanol, which present good properties for selectively dissolving lignin and that do not impact cellulose III conversion (**CHAPTER 1**). The impact of these solvent systems on EA pretreatment effectiveness and process economics should be evaluated in future research.

8.5. Conclusion

EA pretreatment process optimization was performed in this study and compared with a leading ammonia pretreatment technology, i.e., AFEX^{TM}. From optimization studies, it was possible to observe that EA pretreatment minimizes enzyme utilization (7.5 mg/g glucan) during enzymatic hydrolysis at high solids loading (21.44 % solids), while being able to achieve about 72.5 % and 69.8 % glucose and xylose conversions, respectively. Oligomeric glucan and xylan predicted for these conditions were 8.2 % and 25.5 %, respectively. These projected results allow the biorefinery to produce an ethanol titer of 6 wt% and a process yield of 242.20 Kg ethanol/ton untreated biomass, assuming 90 % of theoretical maximum ethanol yield during fermentation. Under these conditions, the predicted MESP was $2.36 per gallon of ethanol ($3.59/gal gasoline equivalent), assuming an IRR of 10%. This value was obtained by assuming that the lignin produced during EA is a source of revenue to the biorefinery (10 cents/lb lignin) and electricity

was externally purchased. Using these base case assumptions, the EA economic performance is slightly worse than AFEX™ ($2.28/gal ethanol). However, this technology is still taing its first steps and offers great room for improvement from the base case scenario, as pretreatment conditions were not optimized for producing the lowest possible MESP.

From the sensitivity analysis results, the heat consumption during EA pretreatment has the highest impact on the overall economics of the biorefinery. Also, most of the heat consumption is associated with distillation activities during ammonia recycling. Therefore, it is important to focus attention on the development of less heat intensive conditions for EA, possibly by better heat integration and process optimization, as well as by decreasing ammonia loading or the number of cycles of distillation. Capital cost and enzyme cost seem to have significantly lower impact on the economics of the EA biorefinery, and therefore, the ~M$52 capital cost predicted for the EA unit operation did not affect the MESP to a large extent. In the other hand, the lignin price had a great impact on the MESP and can significantly affect the economies of the EA biorefinery. Therefore, it is important to create a large market for lignin in the future in order to make this process economically viable. From this perspective, future research on EA technology should also be focused on creating value addition to EA lignin streams and provide diverse market opportunities for lignin in the future.

Future developments should also include the decrease of operating pressure during EA pretreatment. Although pretreatment capital costs do not significantly affect the economics of the biorefinery, handling substantial amounts of ammonia at 1200 psi can constitute a liability issue and therefore, social acceptance of the process may be jeopardized. This goal can be achieved by various strategies that include the utilization of co-solvents along with ammonia that could

potentially improve lignin extraction without compromising cellulose III conversion. For example, ethanol is used for efficient extraction of lignin in other processes and its usage along with ammonia would decrease the operating pressure of EA pretreatment, as well as ammonia usage. In **CHAPTER 3** we showed that it is possible to convert cellulose I to cellulose III while operating at a under 2.4:1 ammonia to cellulose ratio if we use a solution of 60 wt% ammonia in ethanol. This could potentially decrease the pressure below 800 psi. Other solvents of higher boiling point could be considered in the future research. However, is important to focus attention on inexpensive solvents, preferably produced within the biorefinery system.

APPENDIX

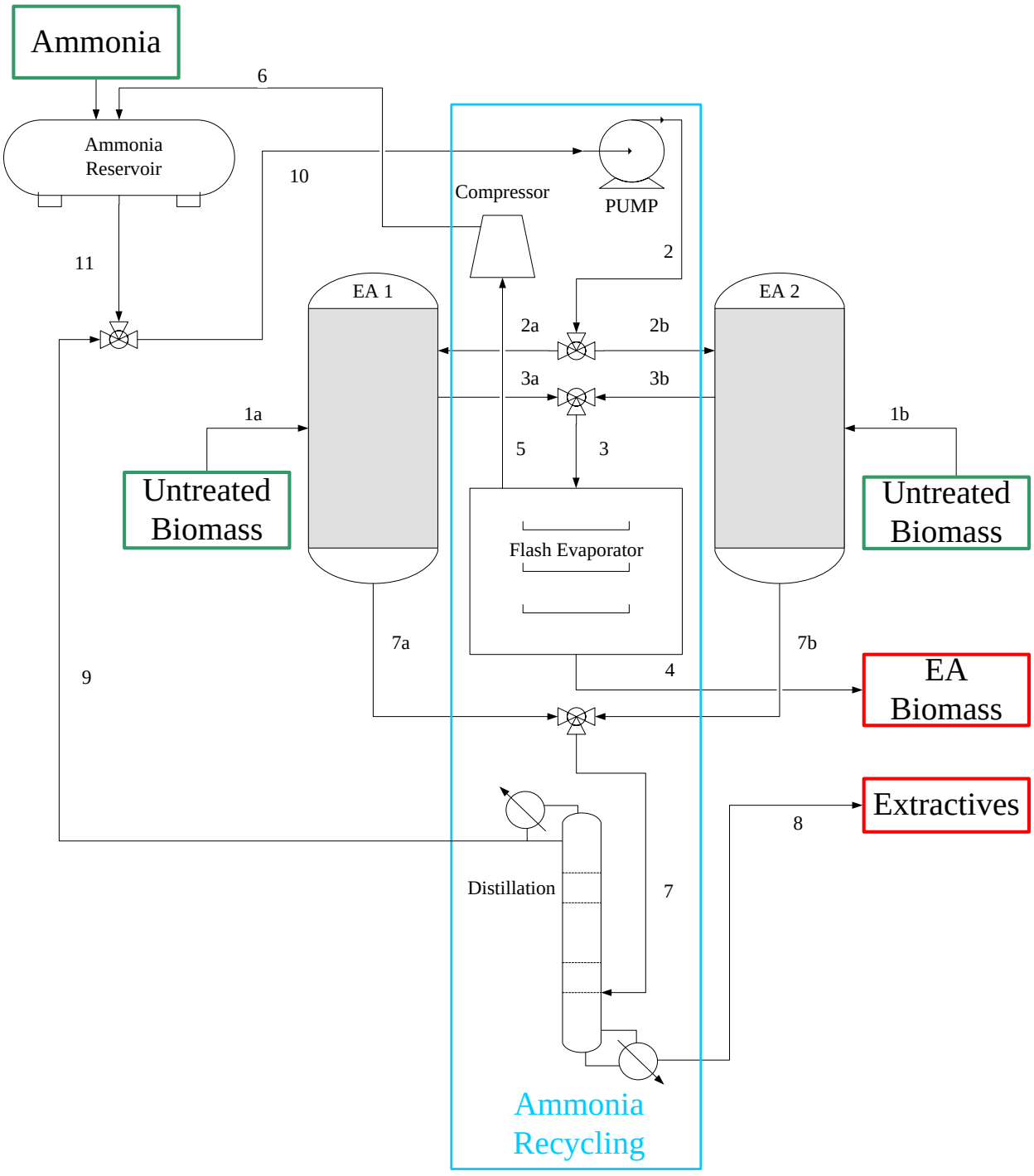

Figure 8-5 EA pretreatment process flow diagram. EA1 and EA2 work intermittently one after the other, sharing the equipment used for ammonia recovery (highlighted in blue). This system of two reactors (EA1 and EA2) is replicated five times to compose the full biorefinery, scaled for processing 2000 tons/day of untreated corn stover. The ammonia recycling system duplicated to be shared among the 10 reactors that are synchronized during operation.

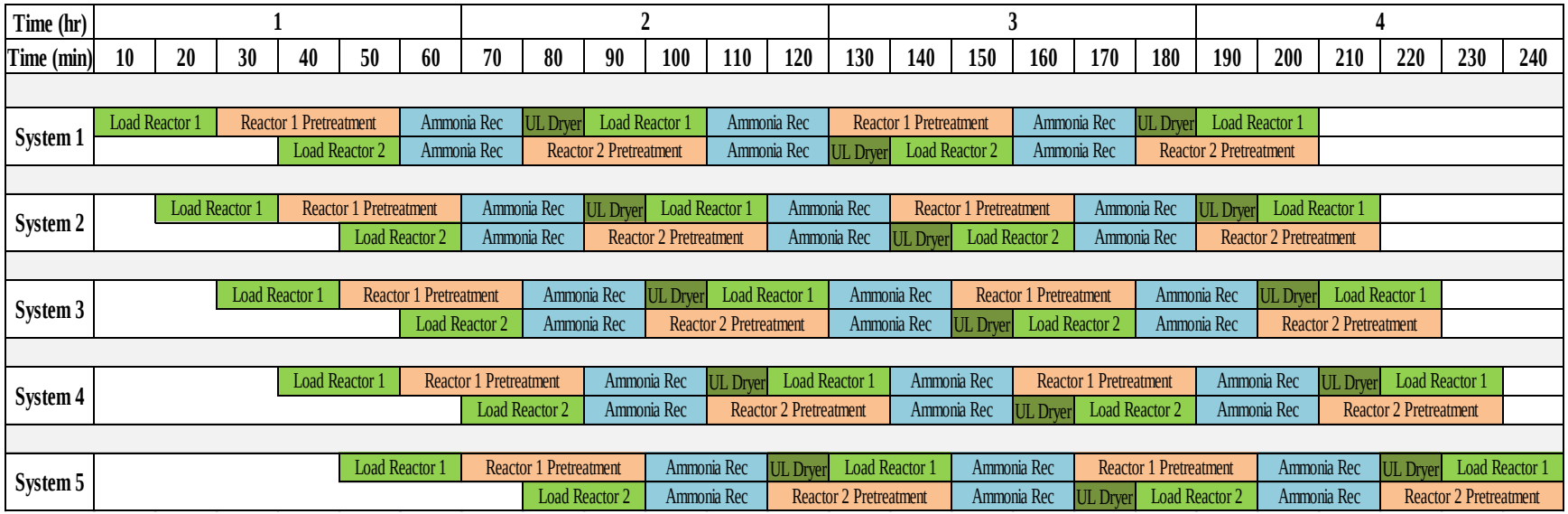

Figure 8-6 Schedule for EA pretreatment operation in the biorefinery. The pretreatment unit is composed by five systems of two reactors that load and unload (UL) intermittently. While pretreatment reactors requires the utilization of five systems of two reactors, ammonia recycling can be operated with two systems, each of them composed by a distillation column, an ammonia evaporator, a compressor and a pump.

Table 8-4 Stream table for EA pretreatment process.

Stream	Temperature (°C)	Temperature (K)	Pressure (Psi)	Flow Rate (kg/min)			H (GJ/hr)	Phase
				Biomass	Ammonia	Water		
1a/1b	25.00	298.15	14.70	1388.89	0.00	78.76	-47.04	Solid
2/2a/2b	99.60	372.75	1200.00	0.00	8333.40	60.12	-1627.30	Liquid
3a/3b/3	25.00	298.15	150.00	1166.67	1679.54	0.27	-373.74	Solid/Vapor
4	-33.40	239.75	14.70	1166.67	41.67	0.27	-0.66	Solid/Liquid
5	-33.40	239.75	14.70	0.00	839.77	0.00	-210.83	Vapor
6	195.70	468.85	150.00	0.00	839.77	0.00	-117.17	Liquid
7a/7b/7	120.00	393.15	1200.00	222.22	7493.56	138.614	-1297.83	Liquid
8	278.00	551.15	200.00	222.22	10.35	78.492	-43.28	Liquid
9	105.10	378.25	200.00	0.00	7483.21	60.122	-1145.10	Vapor
10	99.20	372.35	1000.00	0.00	8333.40	60.122	-1629.56	Liquid
11	25.00	298.15	150.00	0.00	850.19	0.00	-196.97	Liquid

Table 8-5 Total energy duty of EA pretreatment.

Name	Heat duty (GJ/h)	Electricity (kW)	Heat duty (GJ/Ton BM)	Electricity (kWh/Ton BM)
Reactor	155.76	-	1.87	-
Distillation Column	553.84	-	6.65	-
Evaporator	46.97	-	0.56	-
Compressor	-	6901.04	-	82.81
Pump	-	565.08	-	6.78
Ammonia Tank	-		-	
	Total Energy Spending		**9.08**	**89.59**

Table 8-6 EA reactor specifications and cost.

Reactor	
Volume (gallon)	31,530.68
Material of construction	Stainless steel
Design temperature (°C)	147.78
Design pressure (psig)	1318.05
Heat duty (GJ/h)	155.76
Unit cost ($)	1,744,710.00
Number of systems	10.00
Total cost ($)	17,447,100.00

Table 8-7 Ammonia storage tank specifications and cost.

Ammonia tank	
Volume (gallon)	82,187
Material of construction	Stainless steel
Design temperature (°C)	70
Design pressure (psig)	160.30
Unit cost ($)	320,790.00
Number of systems	3
Total cost ($)	962,370

Table 8-8 Ammonia evaporation column specifications and cost for ammonia recycling system.

Evaporation column	
Volume (gallon)	94,591.98
Material of construction	Stainless steel
Design temperature (°C)	70
Design pressure (psig)	160.30
Heat duty (GJ/h)	23.49
Unit cost ($)	360,910.00
Number of systems	2
Total cost ($)	721,820.00

Table 8-9 Distillation equipment specifications and cost for ammonia recycling system of EA pretreatment.

Distillation	
Tower	
Column diameter (ft)	14
Number of stages	13
Feed stage	3
Distillate to feed ratio	1
Reflux ratio	1
Tray type	Sieve
Tray spacing (ft)	2
Design Pressure (psig)	1,035.30
Design Temperature (°C)	306.00
Condenser	
Heat transfer area (sqft)	4,304.79
Tube design temperature (°C)	132.87
Operating Temperature (°C)	110.86
Tube design pressure (psig)	1,035.30
Reflux pump efficiency	0.70
Heat duty (GJ/h)	-161.45
Reboiler	
Heat transfer area (sqft)	31,917.26
Tube design temperature (°C)	343.33
Operating Temperature (°C)	290.03
Tube design pressure (psig)	1,035.00
Shell design temperature (°C)	343.00
Shell design pressure (psig)	685.30
Heat duty (GJ/h)	114.82
Unit cost ($)	6,394,992.00
Number of systems	2.00
Total cost ($)	12,789,984.00

Table 8-10 Pump specifications and cost for ammonia recycling system of EA pretreatment.

Pump	
Pump type	centrifugal
Flow rate (gpm)	2,643.66
Fluid head (ft)	1,008.73
Design pressure (psig)	1,245.30
Design temperature (°C)	127.38
Pump efficiency	0.74
Power (kW)	282.54
Unit cost ($)	354,775.00
Number of systems	2.00
Total cost ($)	709,550.00

Table 8-11 Compressor specifications and cost for ammonia recycling system of EA pretreatment.

Compressor	
Actual gas flow rate (CFM)	14,691.30
Design pressure inlet (psig)	0.30
Design pressure outlet (psig)	160.30
Compressibility factor inlet	0.99
Compressibility factor outlet	0.98
Driver power (kW)	2,998.63
Unit cost ($)	3,649,000.00
Number of systems	2.00
Total cost ($)	7,298,000.00

Table 8-12 Utility costs and pretreatment capital cost assumed for economic model of biorefinery[a]

Pretreatment installed cost	51.907	Million $
Thermal energy use	9.08	GJ/ton biomass
Electricity use	89.59	kWh/ton biomass
Ammonia use	0.0375	kg/kg biomass
Ammonia price	600	$/ton
Biomass price	60	$/ton
Electricity price	5.72	Cents/kWh
Lignin price	10	Cents/lb
Cellulase price	3600	$/ton
Hemicellulase price	4500	$/ton

[a] Other variable costs were assumed to be as defined by the economic model from NREL [206].

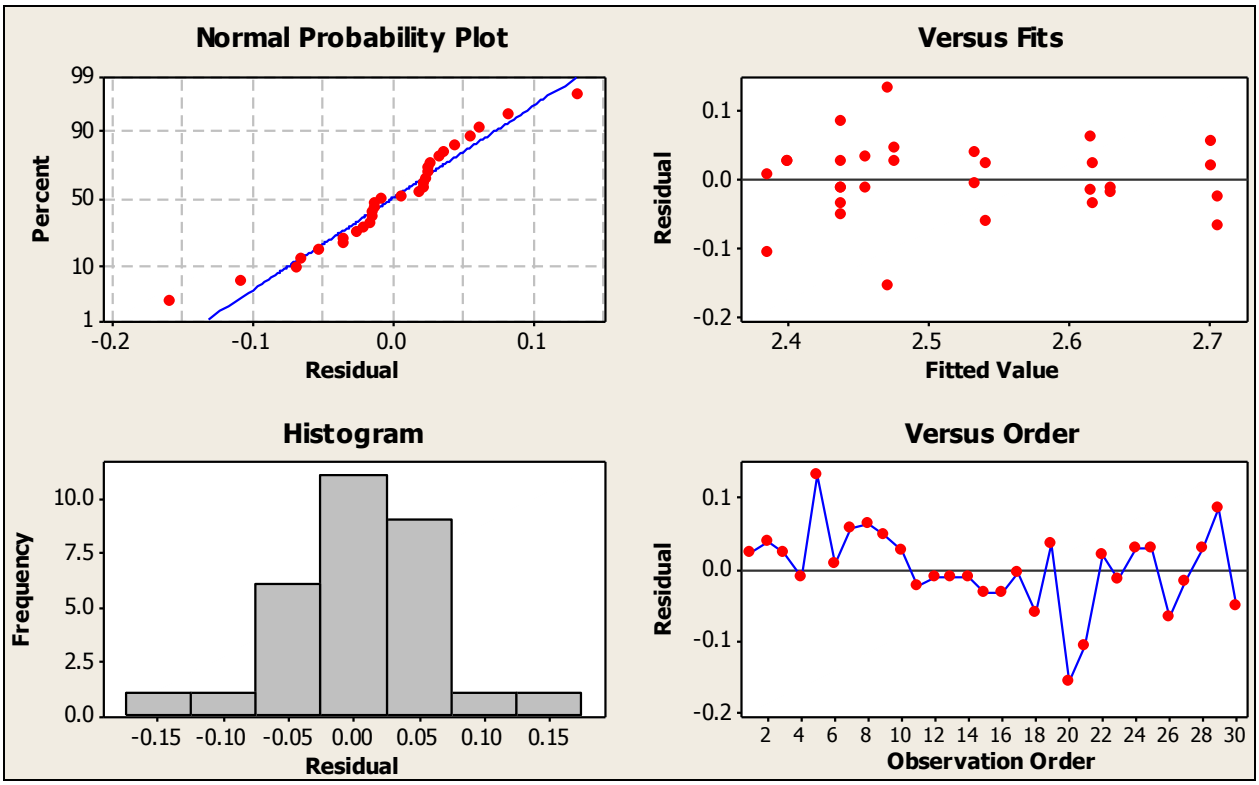

Figure 8-7 Residual plots and histograms for MESP prediction as a function of enzymatic hydrolysis conditions (enzyme loading, solid loading and incubation time) for base case EA pretreated corn stover.

Table 8-13 Regression coefficients for MESP prediction as a function of enzymatic hydrolysis conditions for base case EA pretreated corn stover.

Term	Coef	SE Coef	T	P
Constant	3.60571	0.382689	9.422	0
Time	-0.00373	0.0015	-2.485	0.021
Solid Loading	-0.09476	0.037595	-2.521	0.019
Enzyme Loading	-0.00788	0.00708	-1.113	0.277
Time*Time	0.00002	0.00001	1.94	0.065
Solid Loading*Solid Loading	0.00218	0.000937	2.325	0.029
Enzyme Loading*Enzyme Loading	0.00048	0.000185	2.618	0.015
S =0.063623	**PRESS** = 0.161458			
R-Sq = 77.63%	**R-Sq(pred)** = 61.20%		**R-Sq(adj)** = 71.79%	

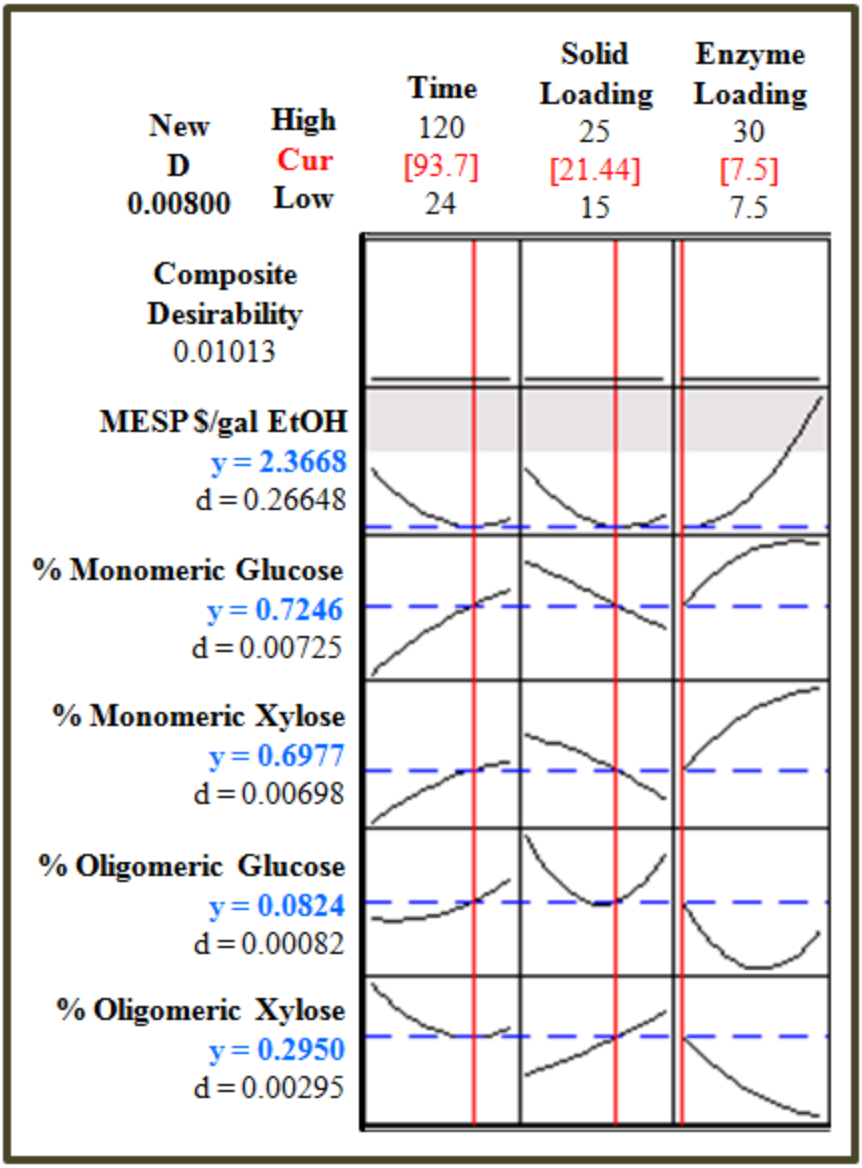

Figure 8-8 Optimization plots for defining enzymatic hydrolysis conditions that minimize MESP ($/gallon ethanol). % sugar conversions are also presented in the left side on the plots in blue numbering. These values were calculated for base case EA pretreated corn stover.

REFERENCES

REFERENCES

1. Sousa, L.D., et al., *'Cradle-to-grave' assessment of existing lignocellulose pretreatment technologies.* Current Opinion in Biotechnology, 2009. **20**(3): p. 339-347.

2. Roberts, K.M., et al., *The effects of water interactions in cellulose suspensions on mass transfer and saccharification efficiency at high solids loadings.* Cellulose, 2011. **18**(3): p. 759-773.

3. Kristensen, J.B., C. Felby, and H. Jorgensen, *Yield-determining factors in high-solids enzymatic hydrolysis of lignocellulose.* Biotechnology for Biofuels, 2009. **2**.

4. Jin, M., et al., *A novel integrated biological process for cellulosic ethanol production featuring high ethanol productivity, enzyme recycling and yeast cells reuse.* Energy & Environmental Science, 2012. **5**(5): p. 7168-7175.

5. Monti, A., N. Di Virgilio, and G. Venturi, *Mineral composition and ash content of six major energy crops.* Biomass and Bioenergy, 2008. **32**(3): p. 216-223.

6. Pettersen Roger, C., *The Chemical Composition of Wood*, in *The Chemistry of Solid Wood*. 1984, American Chemical Society. p. 57-126.

7. Sun, Y. and J. Cheng, *Hydrolysis of lignocellulosic materials for ethanol production: a review.* Bioresource Technology, 2002. **83**(1): p. 1-11.

8. G. W. Huber, B.E.D., *Grassoline at the Pump.* Scientific American Magazine, 2009. **301**(1): p. 8.

9. Wyman, C.E., et al., *Coordinated development of leading biomass pretreatment technologies.* Bioresource Technology, 2005. **96**(18): p. 1959-1966.

10. Cosgrove, D.J., *Growth of the plant cell wall.* Nat Rev Mol Cell Biol, 2005. **6**(11): p. 850-861.

11. Fengel D, W.W., *Wood - Chemistry, Ultrastructure, Reactions*. 1989, Berlin, Germany: Walter de Gruyter. 613.

12. Wada, M., T. Okano, and J. Sugiyama, *Allomorphs of native crystalline cellulose I evaluated by two equatoriald-spacings.* Journal of Wood Science, 2001. **47**(2): p. 124-128.

13. Goro Honjo, M.W., *Examination of cellulose fiber by the low-temperature specimen method of electron diffraction and electron microscopy* Nature 1958. **181**: p. 326.

14. Jeffries, T., *Biodegradation of lignin and hemicelluloses,* in *Biochemistry of microbial degradation*, C. Ratledge, Editor. 1994, Springer Netherlands. p. 233-277.

15. Chundawat, S.P.S., *Ultrastructural and Physicochemical Modifications Within Ammonia Treated Lignocellulosic Cell Walls and Their Influence on Enzymatic Digestibility*. 2009: UMI.

16. Laine, C., *Structures of Hemicelluloses and Pectins in wood and Pulp*, in *KCL communications* 2005, Helsinki University of Technology.

17. Sederoff, R.R., et al., *Unexpected variation in lignin.* Current Opinion in Plant Biology, 1999. **2**(2): p. 145-152.

18. Besle, J.-M., A. Cornu, and J.-P. Jouany, *Roles of structural phenylpropanoids in forage cell wall digestion.* Journal of the Science of Food and Agriculture, 1994. **64**(2): p. 171-190.

19. Himmel, M., et al., *Biomass recalcitrance: Engineering plants and enzymes for biofuels production.* Science, 2007. **315**: p. 804 - 807.

20. Aden, A., et al., *National renewable energy laboratory.* Golden, Colorado, 2002.

21. Wooley, R., et al., *Process Design and Costing of Bioethanol Technology: A Tool for Determining the Status and Direction of Research and Development.* Biotechnology Progress, 1999. **15**(5): p. 794-803.

22. Gao, D., et al., *Mixture optimization of six core glycosyl hydrolases for maximizing saccharification of ammonia fiber expansion (AFEX) pretreated corn stover.* Bioresource Technology, 2010. **101**(8): p. 2770-2781.

23. Chundawat, S.P., *Ultrastructural and physicochemical modifications within ammonia treated lignocellulosic cell walls and their influence on enzymatic digestibility*, in *Chemical Engineering and Materials Science*. 2009, Michigan State University: East Lansing.

24. Wu, Z. and Y.Y. Lee, *Inhibition of the enzymatic hydrolysis of cellulose by ethanol.* Biotechnology Letters, 1997. **19**(10): p. 977-979.

25. Zyl, W.H.v., R.d. Haan, and D.C.l. Grange, *Developing Organisms for Consolidated Bioprocessing of Biomass to Ethanol*, in *Biofuel Production-Recent Developments and Prospects*, D.M.A.D.S. Bernardes, Editor. 2011, InTech.

26. Zakzeski, J., et al., *The Catalytic Valorization of Lignin for the Production of Renewable Chemicals.* Chemical Reviews, 2010. **110**(6): p. 3552-3599.

27. Lora, J.H. and W.G. Glasser, *Recent industrial applications of lignin: A sustainable alternative to nonrenewable materials.* Journal of Polymers and the Environment, 2002. **10**(1-2): p. 39-48.

28. Kadla, J.F., et al., *Lignin-based carbon fibers for composite fiber applications.* Carbon, 2002. **40**(15): p. 2913-2920.

29. Nishikawa, N., R. Sutcliffe, and J. Saddler, *The influence of lignin degradation products on xylose fermentation by Klebsiella pneumoniae.* Applied Microbiology and Biotechnology, 1988. **27**(5-6): p. 549-552.

30. Pan, X., *Role of functional groups in lignin inhibition of enzymatic hydrolysis of cellulose to glucose.* J Biobased Mater Bioenergy, 2008. **2**: p. 25 - 32.

31. Weiss, N., et al., *Enzymatic lignocellulose hydrolysis: Improved cellulase productivity by insoluble solids recycling.* Biotechnology for Biofuels C7 - 5, 2013. **6**(1): p. 1-14.

32. Lee, D., A.H.C. Yu, and J.N. Saddler, *Evaluation of cellulase recycling strategies for the hydrolysis of lignocellulosic substrates.* Biotechnology and Bioengineering, 1995. **45**(4): p. 328-336.

33. Cantu, D., et al., *Strangers in the matrix: plant cell walls and pathogen susceptibility.* Trends in plant science, 2008. **13**(11): p. 610-617.

34. Ishizawa, C.I., et al., *Porosity and Its Effect on the Digestibility of Dilute Sulfuric Acid Pretreated Corn Stover.* Journal of Agricultural and Food Chemistry, 2007. **55**(7): p. 2575-2581.

35. Zadrazil, F. and A.K. Puniya, *Studies on the effect of particle size on solid-state fermentation of sugarcane bagasse into animal feed using white-rot fungi.* Bioresource Technology, 1995. **54**(1): p. 85-87.

36. Fan, L.T., Y.H. Lee, and D.R. Beardmore, *The influence of major structural features of cellulose on rate of enzymatic hydrolysis.* Biotechnology and Bioengineering, 1981. **23**(2): p. 419-424.

37. Chang, V. and M. Holtzapple, *Fundamental factors affecting biomass enzymatic reactivity.* Applied Biochemistry and Biotechnology, 2000. **84-86**(1): p. 5-37.

38. Laureano-Perez, L., et al., *Understanding Factors that Limit Enzymatic Hydrolysis of Biomass.* , in *Twenty-Sixth Symposium on Biotechnology for Fuels and Chemicals*. 2005, Humana Press. p. 1081-1099.

39. Sidiras, D.K. and E.G. Koukios, *Acid saccharification of ball-milled straw.* Biomass, 1989. **19**(4): p. 289-306.

40. Tassinari, T., et al., *Energy requirements and process design considerations in compression-milling pretreatment of cellulosic wastes for enzymatic hydrolysis.* Biotechnology and Bioengineering, 1980. **22**(8): p. 1689-1705.

41. Alvo, P. and K. Belkacemi, *Enzymatic saccharification of milled timothy (Phleum pratense L.) and alfalfa (Medicago sativa L.).* Bioresource Technology, 1997. **61**(3): p. 185-198.

42. Heinze, T. and A. Koschella, *Solvents applied in the field of cellulose chemistry: a mini review.* Polímeros, 2005. **15**: p. 84-90.

43. Pan, X., et al., *Bioconversion of hybrid poplar to ethanol and co-products using an organosolv fractionation process: Optimization of process yields.* Biotechnology and Bioengineering, 2006. **94**(5): p. 851-861.

44. Arato, C., E.K. Pye, and G. Gjennestad, *The Lignol Approach to Biorefining of Woody Biomass to Produce Ethanol and Chemicals*, in *Twenty-Sixth Symposium on Biotechnology for Fuels and Chemicals*, B. Davison, et al., Editors. 2005, Humana Press. p. 871-882.

45. Zhang, Y.-H.P., et al., *Fractionating recalcitrant lignocellulose at modest reaction conditions.* Biotechnology and Bioengineering, 2007. **97**(2): p. 214-223.

46. Moxley, G., Z. Zhu, and Y.H.P. Zhang, *Efficient Sugar Release by the Cellulose Solvent-Based Lignocellulose Fractionation Technology and Enzymatic Cellulose Hydrolysis.* Journal of Agricultural and Food Chemistry, 2008. **56**(17): p. 7885-7890.

47. Swatloski, R.P., et al., *Dissolution of Cellose with Ionic Liquids.* Journal of the American Chemical Society, 2002. **124**(18): p. 4974-4975.

48. Turner, M.B., et al., *Ionic liquid salt-induced inactivation and unfolding of cellulase from Trichoderma reesei.* Green Chemistry, 2003. **5**(4): p. 443-447.

49. Joglekar, H.G., I. Rahman, and B.D. Kulkarni, *The Path Ahead for Ionic Liquids.* Chemical Engineering & Technology, 2007. **30**(7): p. 819-828.

50. Lee, S.H., et al., *Ionic liquid-mediated selective extraction of lignin from wood leading to enhanced enzymatic cellulose hydrolysis.* Biotechnology and Bioengineering, 2009. **102**(5): p. 1368-1376.

51. Weil, J., et al., *Pretreatment of corn fiber by pressure cooking in water.* Applied Biochemistry and Biotechnology, 1998. **73**(1): p. 1-17.

52. Weil, J.R., et al., *Removal of Fermentation Inhibitors Formed during Pretreatment of Biomass by Polymeric Adsorbents.* Industrial & Engineering Chemistry Research, 2002. **41**(24): p. 6132-6138.

53. Klinke, H.B., A.B. Thomsen, and B.K. Ahring, *Inhibition of ethanol-producing yeast and bacteria by degradation products produced during pre-treatment of biomass.* Applied Microbiology and Biotechnology, 2004. **66**(1): p. 10-26.

54. Lloyd, T.A. and C.E. Wyman, *Combined sugar yields for dilute sulfuric acid pretreatment of corn stover followed by enzymatic hydrolysis of the remaining solids.* Bioresource Technology, 2005. **96**(18): p. 1967-1977.

55. Kim, J., Y.Y. Lee, and R. Torget, *Cellulose hydrolysis under extremely low sulfuric acid and high-temperature conditions.* Applied Biochemistry and Biotechnology, 2001. **91-93**(1-9): p. 331-340.

56. Buhner, J. and F.A. Agblevor, *Effect of detoxification of dilute-acid corn fiber hydrolysate on xylitol production.* Applied Biochemistry and Biotechnology, 2004. **119**(1): p. 13-30.

57. Chen, H., et al., *New process of maize stalk amination treatment by steam explosion.* Biomass and Bioenergy, 2005. **28**(4): p. 411-417.

58. Playne, M.J., *Increased digestibility of bagasses by pretreatment with alkalis and steam explosion.* Biotechnology and Bioengineering, 1984. **26**(5): p. 426-433.

59. Ewanick, S.M., R. Bura, and J.N. Saddler, *Acid-catalyzed steam pretreatment of lodgepole pine and subsequent enzymatic hydrolysis and fermentation to ethanol.* Biotechnology and Bioengineering, 2007. **98**(4): p. 737-746.

60. Brownell, H.H., E.K.C. Yu, and J.N. Saddler, *Steam-explosion pretreatment of wood: Effect of chip size, acid, moisture content and pressure drop.* Biotechnology and Bioengineering, 1986. **28**(6): p. 792-801.

61. Wyman, C., *Handbook on bioethanol: production and utilization*. 1996: Taylor & francis.

62. Mosier, N., et al., *Features of promising technologies for pretreatment of lignocellulosic biomass.* Bioresource Technology, 2005. **96**(6): p. 673-686.

63. Mosier, N., et al., *Optimization of pH controlled liquid hot water pretreatment of corn stover.* Bioresource Technology, 2005. **96**(18): p. 1986-1993.

64. Mosier, N.S., C.M. Ladisch, and M.R. Ladisch, *Characterization of acid catalytic domains for cellulose hydrolysis and glucose degradation.* Biotechnology and Bioengineering, 2002. **79**(6): p. 610-618.

65. Peter van Walsum, G. and H. Shi, *Carbonic acid enhancement of hydrolysis in aqueous pretreatment of corn stover*. Bioresource Technology, 2004. **93**(3): p. 217-226.

66. Luo, C., D.L. Brink, and H.W. Blanch, *Identification of potential fermentation inhibitors in conversion of hybrid poplar hydrolyzate to ethanol.* Biomass and Bioenergy, 2002. **22**(2): p. 125-138.

67. Öhgren, K., M. Galbe, and G. Zacchi, *Optimization of Steam Pretreatment of SO2-Impregnated Corn Stover for Fuel Ethanol Production*, in *Twenty-Sixth Symposium on Biotechnology for Fuels and Chemicals*, B. Davison, et al., Editors. 2005, Humana Press. p. 1055-1067.

68. Wyman, C.E., et al., *Comparative sugar recovery data from laboratory scale application of leading pretreatment technologies to corn stover.* Bioresource Technology, 2005. **96**(18): p. 2026-2032.

69. Wyman C, K.R., Dale B, Elander R, Holtzapple M, Ladisch M, Lee Y, Moniruzzaman M, Saddler J, *Comparative data for enzymatic digestion of corn stover and poplar wood after pretreatment by leading technologies.*, in *AIChE Annual Meeting*. 2006: San Francisco, California.

70. Öhgren, K., et al., *Effect of hemicellulose and lignin removal on enzymatic hydrolysis of steam pretreated corn stover*. Bioresource Technology, 2007. **98**(13): p. 2503-2510.

71. Kim, T.H. and Y.Y. Lee, *Pretreatment and fractionation of corn stover by ammonia recycle percolation process.* Bioresource Technology, 2005. **96**(18): p. 2007-2013.

72. Laureano-Perez, L., *Spectroscopic and chemical characterization of biomass*. 2005, Michigan State University: East Lansing.

73. Kim, S. and M.T. Holtzapple, *Lime pretreatment and enzymatic hydrolysis of corn stover.* Bioresource Technology, 2005. **96**(18): p. 1994-2006.

74. Kim, S. and M.T. Holtzapple, *Delignification kinetics of corn stover in lime pretreatment.* Bioresource Technology, 2006. **97**(5): p. 778-785.

75. Chang, V. and M. Holtzapple, *Fundamental factors affecting biomass enzymatic reactivity.* Applied Biochemistry and Biotechnology, 2000. **84-86**(1-9): p. 5-37.

76. Laureano-Perez, L., et al., *Understanding factors that limit enzymatic hydrolysis of biomass.* Applied Biochemistry and Biotechnology, 2005. **124**(1-3): p. 1081-1099.

77. Sendich, E., et al., *Recent process improvements for the ammonia fiber expansion (AFEX) process and resulting reductions in minimum ethanol selling price.* Bioresource Technology, 2008. **99**(17): p. 8429-8435.

78. Lau, M.W. and B.E. Dale, *Cellulosic ethanol production from AFEX-treated corn stover using Saccharomyces cerevisiae 424A(LNH-ST).* Proceedings of the National Academy of Sciences, 2009. **106**(5): p. 1368-1373.

79. Lau, M.W., B.E. Dale, and V. Balan, *Ethanolic fermentation of hydrolysates from ammonia fiber expansion (AFEX) treated corn stover and distillers grain without detoxification and external nutrient supplementation.* Biotechnology and Bioengineering, 2008. **99**(3): p. 529-539.

80. Lewin, M. and L.G. Roldan, *The effect of liquid anhydrous ammonia in the structure and morphology of cotton cellulose.* Journal of Polymer Science Part C: Polymer Symposia, 1971. **36**(1): p. 213-229.

81. Weimer, P.J., et al., *Effect of supercritical ammonia on the physical and chemical structure of ground wood*. 1986. Medium: X; Size: Pages: 5-18.

82. Kim, S. and Y. Lee, *Fractionation of herbaceous biomass by ammonia-hydrogen peroxide percolation treatment.* Applied Biochemistry and Biotechnology, 1996. **57-58**(1): p. 147-156.

83. García-Cubero, M.T., et al., *Effect of ozonolysis pretreatment on enzymatic digestibility of wheat and rye straw*. Bioresource Technology, 2009. **100**(4): p. 1608-1613.

84. Martin, C. and A.B. Thomsen, *Wet oxidation pretreatment of lignocellulosic residues of sugarcane, rice, cassava and peanuts for ethanol production.* J. Chem. Technol. Biotechnol., 2007. **82**: p. 174-181.

85. Gould, J.M., *Alkaline peroxide delignification of agricultural residues to enhance enzymatic saccharification.* Biotechnology and Bioengineering, 1984. **26**(1): p. 46-52.

86. Lee, J.-W., et al., *Evaluation of waste mushroom logs as a potential biomass resource for the production of bioethanol.* Bioresource Technology, 2008. **99**(8): p. 2736-2741.

87. Christian, V., et al., *Degradation of xenobiotic compounds by lignin-degrading white-rot fungi: enzymology and mechanisms involved.* Indian journal of experimental biology, 2005. **43**(4): p. 301.

88. Balan, V., et al., *Mushroom spent straw: a potential substrate for an ethanol-based biorefinery.* Journal of Industrial Microbiology & Biotechnology, 2008. **35**(5): p. 293-301.

89. Searchinger, T., et al., *Use of U.S. Croplands for Biofuels Increases Greenhouse Gases Through Emissions from Land-Use Change.* Science, 2008. **319**(5867): p. 1238-1240.

90. Yang, B. and C.E. Wyman, *Pretreatment: the key to unlocking low-cost cellulosic ethanol.* Biofuels, Bioproducts and Biorefining, 2008. **2**(1): p. 26-40.

91. E, C.J., J.S. V, and D.B. E, *Technical and Financial Feasibility Analysis of Distributed Bioprocessing Using Regional Biomass Pre-Processing Centers.* Journal of Agricultural & Food Industrial Organization, 2007. **5**(2): p. 1-29.

92. Weimer, P.J., et al., *FIBEX-treated rice straw as a feed ingredient for lactating dairy cows.* Animal Feed Science and Technology, 2003. **103**(1–4): p. 41-50.

93. Fengel, D. and G. Wengener, *Wood. Chemistry, Ultrastructure, reactions.* Walter de Gruyter, Berlin, Germany, 1989: p. 613.

94. Sjöström, E., Tappi 60, 1977. **9**: p. 151-154.

95. Chundawat, S.P.S., et al., *Multifaceted characterization of cell wall decomposition products formed during ammonia fiber expansion (AFEX) and dilute acid based pretreatments.* Bioresource Technology, 2010. **101**(21): p. 8429-8438.

96. Buanafina, M.M.D., *Feruloylation in Grasses: Current and Future Perspectives.* Molecular Plant, 2009. **2**(5): p. 861-872.

97. Vismeh, R., et al., *Profiling of diferulates (plant cell wall cross-linkers) using ultrahigh-performance liquid chromatography-tandem mass spectrometry.* Analyst, 2013. **138**(21): p. 6683-6692.

98. French, H.E. and G.G. Wrightsman, *Action of Ammonia on Esters.* Journal of the American Chemical Society 1938. **60**: p. 50-51.

99. Gordon, M., J.G. Miller, and A.R. Day, *Effect of Structure on Reactivity.1 II. Influence of Solvents on Ammonolysis of Esters.* Journal of the American Chemical Society, 1949. **71**(4): p. 1245-1250.

100. Williamson, P.M., R.C. Anderson, and G.W. Watt, *Electrolyte Catalysis in the Ammonolysis of 9-Phenyl-9-chlorofluorene by Liquid Ammonia1*. Journal of the American Chemical Society, 1944. **66**(3): p. 376-379.

101. Fellinger, L.L. and L.F. Audrieth, *Acid Catalysis in Liquid Ammonia. II. Ammonolysis of Ethyl Benzoate.* Journal of the American Chemical Society, 1938. **60**(3): p. 579-581.

102. Shibamoto, T., et al., *A study of pyrazine formation.* Journal of Agricultural and Food Chemistry, 1979. **27**(5): p. 1027-1031.

103. Wada, M., et al., *Cellulose IIII Crystal Structure and Hydrogen Bonding by Synchrotron X-ray and Neutron Fiber Diffraction.* Macromolecules, 2004. **37**(23): p. 8548-8555.

104. Wada, M., Y. Nishiyama, and P. Langan, *X-ray Structure of Ammonia-Cellulose I: New Insights into the Conversion of Cellulose I to Cellulose IIII.* Macromolecules, 2006. **39**(8): p. 2947-2952.

105. Chundawat, S.P.S., et al., *Restructuring the Crystalline Cellulose Hydrogen Bond Network Enhances Its Depolymerization Rate.* Journal of the American Chemical Society, 2011. **133**(29): p. 11163-11174.

106. Cheng, G., et al., *Transition of Cellulose Crystalline Structure and Surface Morphology of Biomass as a Function of Ionic Liquid Pretreatment and Its Relation to Enzymatic Hydrolysis.* Biomacromolecules, 2011. **12**(4): p. 933-941.

107. Zhang, Y.H.P., et al., *A transition from cellulose swelling to cellulose dissolution by o-phosphoric acid: Evidence from enzymatic hydrolysis and supramolecular structure.* Biomacromolecules, 2006. **7**(2): p. 644-648.

108. Humpula, J.F., et al., *Probing the nature of AFEX-pretreated corn stover derived decomposition products that inhibit cellulase activity.* Bioresource Technology, 2013. **152**(0): p. 38-45.

109. Jin, M., et al., *Quantitatively understanding reduced xylose fermentation performance in AFEX^{TM} treated corn stover hydrolysate using Saccharomyces cerevisiae 424A (LNH-ST) and Escherichia coli KO11.* Bioresource Technology, 2012(available online).

110. Shao, X., et al., *Conversion for Avicel and AFEX pretreated corn stover by Clostridium thermocellum and simultaneous saccharification and fermentation: Insights into microbial conversion of pretreated cellulosic biomass.* Bioresource Technology, 2011. **102**(17): p. 8040-8045.

111. Mooney, C.A., et al., *The effect of initial pore volume and lignin content on the enzymatic hydrolysis of softwoods.* Bioresource Technology, 1998. **64**(2): p. 113-119.

112. Palonen, H., et al., *Adsorption of Trichoderma reesei CBH I and EG II and their catalytic domains on steam pretreated softwood and isolated lignin.* Journal of Biotechnology, 2004. **107**(1): p. 65-72.

113. Ximenes, E., et al., *Deactivation of cellulases by phenols.* Enzyme and Microbial Technology, 2011. **48**(1): p. 54-60.

114. Hall, M., et al., *Cellulose crystallinity – a key predictor of the enzymatic hydrolysis rate.* FEBS Journal, 2010. **277**(6): p. 1571-1582.

115. Nishiyama, Y., et al., *Crystal Structure and Hydrogen Bonding System in Cellulose IÎ± from Synchrotron X-ray and Neutron Fiber Diffraction.* Journal of the American Chemical Society, 2003. **125**(47): p. 14300-14306.

116. Finkenstadt, V.L. and R.P. Millane, *Crystal Structure of Valonia Cellulose Iβ.* Macromolecules, 1998. **31**(22): p. 7776-7783.

117. Igarashi, K., M. Wada, and M. Samejima, *Activation of crystalline cellulose to cellulose IIII results in efficient hydrolysis by cellobiohydrolase.* FEBS Journal, 2007. **274**(7): p. 1785-1792.

118. Gao, D., et al., *Increased enzyme binding to substrate is not necessary for more efficient cellulose hydrolysis.* Proceedings of the National Academy of Sciences, 2013.

119. Schleicher, H., C. Daniels, and B. Philipp, *Changes of cellulose accessibility to reactions in alkaline medium by activation with ammonia.* Journal of Polymer Science: Polymer Symposia, 1974. **47**(1): p. 251-260.

120. Barry, A.J., F.C. Peterson, and A.J. King, *x-Ray Studies of Reactions of Cellulose in Non-Aqueous Systems. I. Interaction of Cellulose and Liquid Ammonia1.* Journal of the American Chemical Society, 1936. **58**(2): p. 333-337.

121. Davis, W.E., et al., *X-Ray Studies of Reactions of Cellulose in Non-Aqueous Systems. II. Interaction of Cellulose and Primary Amines1.* Journal of the American Chemical Society, 1943. **65**(7): p. 1294-1299.

122. Clark, G.L. and E.A. Parker, *An X-ray Diffraction Study of the Action of Liquid Ammonia on Cellulose and Its Derivatives.* The Journal of Physical Chemistry, 1937. **41**(6): p. 777-786.

123. Mittal, A., et al., *Effects of alkaline or liquid-ammonia treatment on crystalline cellulose: changes in crystalline structure and effects on enzymatic digestibility.* Biotechnology for Biofuels, 2011. **4**(1): p. 41.

124. Zhang, J., et al., *Dissolution of Microcrystalline Cellulose in Phosphoric Acid-Molecular Changes and Kinetics.* Molecules, 2009. **14**(12): p. 5027-5041.

125. Ruland, W., *X-ray determination of crystallinity and diffuse disorder scattering.* Acta Cryst, 1961. **14**: p. 1180 - 1185.

126. Park, S., et al., *Cellulose crystallinity index: measurement techniques and their impact on interpreting cellulase performance.* Biotechnology for Biofuels, 2010. **3**(1): p. 10.

127. Hult, L., T. Iversen, and J. Sugiyama, *Characterization of the supramolecular structure of cellulose in wood pulp fibres.* Cellulose, 2003. **10**: p. 103 - 110.

128. Garvey, C., I. Parker, and G. Simon, *On the interpretation of X-ray diffraction powder patterns in terms of the nanostructure of cellulose I fibres.* Macromol Chem Phys, 2005. **206**: p. 1568 - 1575.

129. He, J., S. Cui, and S.-Y. Wang, *Preparation and crystalline analysis of high-grade bamboo dissolving pulp for cellulose acetate.* J Appl Polym Sci, 2008. **107**: p. 1029 - 1038.

130. Schuerch, C., *Plasticizing wood with liquid ammonia.* J Ind Eng Chem, 1963. **55**: p. 39.

131. Thygesen, A., et al., *On the determination of crystallinity and cellulose content in plant fibres.* Cellulose, 2005. **12**(6): p. 563-576.

132. Barry, A., F. Peterson, and A. King, *X-ray studies of reactions of cellulose in non-aqueous systems. I. Interaction of cellulose and liquid ammonia.* J Am Chem Soc, 1936. **58**: p. 333 - 337.

133. Clark, G. and E. Parker, *An X-ray diffraction study of the action of liquid ammonia on cellulose and its derivatives.* J Phys Chem, 1937. **41**: p. 777 - 786.

134. Sinitsyn, A., A. Gusakov, and E. Vlasenko, *Effect of structural and physico-chemical features of cellulosic substrates on the efficiency of enzymatic hydrolysis.* Appl Biochem Biotechnol, 1991. **30**: p. 43 - 59.

135. Gharpuray, M.M., Y.-H. Lee, and L.T. Fan, *Structural modification of lignocellulosics by pretreatments to enhance enzymatic hydrolysis.* Biotechnology and Bioengineering, 1983. **25**(1): p. 157-172.

136. Murnen, H.K., et al., *Optimization of Ammonia Fiber Expansion (AFEX) Pretreatment and Enzymatic Hydrolysis of Miscanthus x giganteus to Fermentable Sugars.* Biotechnology Progress, 2007. **23**(4): p. 846-850.

137. Garlock, R.J., V. Balan, and B.E. Dale, *Optimization of AFEX^{TM} pretreatment conditions and enzyme mixtures to maximize sugar release from upland and lowland switchgrass.* Bioresource Technology, 2012. **104**(0): p. 757-768.

138. Mielenz, J.R., et al., *Lignocellulosic Biomass Pretreatment Using AFEX*, in *Biofuels*. 2009, Humana Press. p. 61-77.

139. Wada, M., et al., *Improved structural data of cellulose IIII prepared in supercritical ammonia.* Macromolecules, 2001. **34**: p. 1237 - 1243.

140. Bellesia, G., et al., *Probing the early events associated with liquid ammonia pretreatment of native crystalline cellulose.* J Phys Chem B, 2011. **115**(32): p. 9782-8.

141. Saafan, A., S. Kandil, and A. Habib, *Liquid-ammonia and caustic mercerization of cotton fibers using X-ray, infrared, and sorption measurements.* Text Res J, 1984. **54**: p. 863 - 867.

142. Wadehra, I.L., R.S.J. Manley, and D.A.I. Goring, *Permanently amorphous cellulose.* Journal of Applied Polymer Science, 1965. **9**(7): p. 2634-2636.

143. Bel'chev, F.V., N.I. Shuikin, and S.S. Novikov, *The catalytic amination of alcohols.* Bulletin of the Academy of Sciences of the USSR, Division of chemical science, 1961. **10**(4): p. 599-602.

144. Klinkenberg, J.L. and J.F. Hartwig, *Catalytic Organometallic Reactions of Ammonia.* Angewandte Chemie International Edition, 2010. **50**(1): p. 86-95.

145. Chundawat, S.P.S., et al., *Multi-scale visualization and characterization of lignocellulosic plant cell wall deconstruction during thermochemical pretreatment.* Energy & Environmental Science, 2011. **4**(3): p. 973-984.

146. Iyer, P., et al., *Ammonia recycled percolation process for pretreatment of herbaceous biomass.* Applied Biochemistry and Biotechnology, 1996. **57-58**(1): p. 121-132.

147. Morrison, W.H., et al., *Investigation of the ester- and ether-linked phenolic constituents of cell wall types of normal and brown midrib pearl millet using chemical isolation, microspectrophotometry and 13C NMR spectroscopy.* Journal of the Science of Food and Agriculture, 1993. **63**(3): p. 329-337.

148. McMillan, J., et al., *Corn Stover Fractions and Bioenergy*, in *Twenty-Seventh Symposium on Biotechnology for Fuels and Chemicals*. 2006, Humana Press. p. 104-116.

149. Argillier, O., et al., *Genotypic variation in phenolic components of cell-walls in relation to the digestibility of maize stalks.* Agronomie, 1996. **16**(2): p. 123-130.

150. Bergvinson, D.J., J.T. Arnason, and L.N. Pietrzak, *Localization and quantification of cell wall phenolics in European corn borer resistant and susceptible maize inbreds.* Canadian Journal of Botany, 1994. **72**(9): p. 1243-1249.

151. Lu, F. and J. Ralph, *Detection and Determination of p-Coumaroylated Units in Lignins.* Journal of Agricultural and Food Chemistry, 1999. **47**(5): p. 1988-1992.

152. Ralph, J., J.H. Grabber, and R.D. Hatfield, *Lignin-ferulate cross-links in grasses: active incorporation of ferulate polysaccharide esters into ryegrass lignins.* Carbohydrate Research, 1995. **275**(1): p. 167-178.

153. Grabber, J.H., J. Ralph, and R.D. Hatfield, *Cross-Linking of Maize Walls by Ferulate Dimerization and Incorporation into Lignin.* Journal of Agricultural and Food Chemistry, 2000. **48**(12): p. 6106-6113.

154. Riboulet, C., et al., *Genetic variation in maize cell wall for lignin content, lignin structure, p-hydroxycinnamic acid content, and digestibility in set of 19 lines at silage harvest maturity* Maydica, 2008. **53**(1): p. 11-19.

155. Huang, G., C. Zhang, and Z. Chen, *Pulping of Wheat Straw with Caustic Potash-Ammonia Aqueous Solutions and Its Kinetics.* Chinese Journal of Chemical Engineering, 2006. **14**(6): p. 729-733.

156. Bludworth, J. and F. Carl Knopf, *Reactive extraction of lignin from wood using supercritical ammonia-water mixtures.* The Journal of Supercritical Fluids, 1993. **6**(4): p. 249-254.

157. Liu, Z., et al., *Aqueous-ammonia delignification of miscanthus followed by enzymatic hydrolysis to sugars.* Bioresource Technology, 2012. **135**(0): p. 23-29.

158. Zhang, Y.-j., et al., *Effects of supercritical ammonia on bamboo pulping.* Forestry Studies in China, 2011. **13**(1): p. 80-84.

159. Obst, J.R., *Kinetics of Alkaline Cleavage of β-Aryl Ether Bonds in Lignin Models: Significance to Delignification.* Holzforschung, 1983. **37**(1): p. 23-28.

160. Huang, G., J.X. Shi, and T.A.G. Langrish, *NH_4OH-KOH pulping mechanisms and kinetics of rice straw.* Bioresource Technology, 2007. **98**(6): p. 1218-1223.

161. del Rio, J.C., et al., *Structural Characterization of Wheat Straw Lignin as Revealed by Analytical Pyrolysis, 2D-NMR, and Reductive Cleavage Methods.* Journal of Agricultural and Food Chemistry, 2012. **60**(23): p. 5922-5935.

162. Stewart, D., *Lignin as a base material for materials applications: Chemistry, application and economics.* Industrial Crops and Products, 2008. **27**(2): p. 202-207.

163. Agarwal, U.P., R.R. Reiner, and S.A. Ralph, *Estimation of Cellulose Crystallinity of Lignocelluloses Using Near-IR FT-Raman Spectroscopy and Comparison of the Raman and Segal-WAXS Methods.* Journal of Agricultural and Food Chemistry, 2013. **61**(1): p. 103-113.

164. Agarwal, U., R. Reiner, and S. Ralph, *Cellulose I crystallinity determination using FT-Raman spectroscopy: univariate and multivariate methods.* Cellulose, 2010. **17**(4): p. 721-733.

165. Yu, Z., et al., *The effect of delignification of forest biomass on enzymatic hydrolysis.* Bioresource Technology, 2011. **102**(19): p. 9083-9089.

166. Dien, B.S., M.A. Cotta, and T.W. Jeffries, *Bacteria engineered for fuel ethanol production: current status.* Applied Microbiology and Biotechnology, 2003. **63**(3): p. 258-266.

167. Jin, M., et al., *Quantitatively understanding reduced xylose fermentation performance in AFEXTM treated corn stover hydrolysate using Saccharomyces cerevisiae 424A (LNH-ST) and Escherichia coli KO11.* Bioresource Technology, 2012. **111**(0): p. 294-300.

168. Hodge, D., et al., *Model-Based Fed-Batch for High-Solids Enzymatic Cellulose Hydrolysis.* Appl Biochem Biotechnol, 2009. **152**: p. 88 - 107.

169. Hodge, D., et al., *Soluble and insoluble solids contributions to high-solids enzymatic hydrolysis of lignocellulose.* Bioresour Technol, 2008. **99**: p. 8940 - 8948.

170. Kristensen, J., C. Felby, and H. Jorgensen, *Yield-determining factors in high-solids enzymatic hydrolysis of lignocellulose.* Biotechnology for Biofuels, 2009. **2**(1): p. 11.

171. Lau, M.W., et al., *An integrated paradigm for cellulosic biorefineries: Utilization of lignocellulosic biomass as self-sufficient feedstocks for fuel, food precursors and Saccharolytic enzyme production.* Energy & Environmental Science, 2012.

172. Caminal, G., J. López-Santín, and C. Solà, *Kinetic modeling of the enzymatic hydrolysis of pretreated cellulose.* Biotechnology and Bioengineering, 1985. **27**(9): p. 1282-1290.

173. Okazaki, M. and M. Moo-Young, *Kinetics of enzymatic hydrolysis of cellulose: Analytical description of a mechanistic model.* Biotechnology and Bioengineering, 1978. **20**(5): p. 637-663.

174. Xiao, Z., et al., *Effects of sugar inhibition on cellulases and beta-glucosidase during enzymatic hydrolysis of softwood substrates.* Appl Biochem Biotechnol, 2004. **113-16**: p. 1115 - 1126.

175. Studer, M.H., et al., *Lignin content in natural Populus variants affects sugar release.* Proceedings of the National Academy of Sciences, 2011. **108**(15): p. 6300-6305.

176. Gellerstedt, G., J. Pranda, and E.L. Lindfors, *Structural and Molecular Properties of Residual Birch Kraft Lignins.* Journal of Wood Chemistry and Technology, 1994. **14**(4): p. 467-482.

177. Shimada, K., S. Hosoya, and T. Ikeda, *Condensation Reactions of Softwood and Hardwood Lignin Model Compounds Under Organic Acid Cooking Conditions.* Journal of Wood Chemistry and Technology, 1997. **17**(1-2): p. 57-72.

178. Guerra, A., et al., *Toward a Better Understanding of the Lignin Isolation Process from Wood.* Journal of Agricultural and Food Chemistry, 2006. **54**(16): p. 5939-5947.

179. Holtman, K.M., et al., *Quantitative 13C NMR Characterization of Milled Wood Lignins Isolated by Different Milling Techniques.* Journal of Wood Chemistry and Technology, 2006. **26**(1): p. 21-34.

180. Granata, A. and D.S. Argyropoulos, *2-Chloro-4,4,5,5-tetramethyl-1,3,2-dioxaphospholane, a Reagent for the Accurate Determination of the Uncondensed and Condensed Phenolic Moieties in Lignins.* Journal of Agricultural and Food Chemistry, 1995. **43**(6): p. 1538-1544.

181. Allison L, R.A., Hsieh J, *Metal profiling of southeastern U.S. softwood and hardwood furnish.* Tappi J, 2000. **83**(8): p. 97-1.

182. Balan, V., et al., *Overview to ammonia pretreatments for lignocellulosic biorefineries*. Dynamic Biochemistry, Process Biotechnology and Molecular Biology. Vol. 6. 2012: Global Science Books.

183. Withers, S., et al., *Identification of Grass-specific Enzyme That Acylates Monolignols with p-Coumarate.* Journal of Biological Chemistry, 2012. **287**(11): p. 8347-8355.

184. Fornale, S., et al., *Altered Lignin Biosynthesis Improves Cellulosic Bioethanol Production in Transgenic Maize Plants Down-Regulated for Cinnamyl Alcohol Dehydrogenase.* Molecular Plant, 2011. **5**(4): p. 817-830.

185. Chabbert, B., et al., *Biological variability in lignification of maize: Expression of the brown midrib bm3 mutation in three maize cultivars.* Journal of the Science of Food and Agriculture, 1994. **64**(3): p. 349-355.

186. Hu, Z., M. Foston, and A.J. Ragauskas, *Comparative studies on hydrothermal pretreatment and enzymatic saccharification of leaves and internodes of alamo switchgrass.* Bioresour Technol, 2011. **102**(14): p. 7224-8.

187. Hallac, B.B., et al., *Biomass Characterization of Buddleja davidii: A Potential Feedstock for Biofuel Production.* Journal of Agricultural and Food Chemistry, 2009. **57**(4): p. 1275-1281.

188. Crestini, C. and D.S. Argyropoulos, *Structural Analysis of Wheat Straw Lignin by Quantitative 31P and 2D NMR Spectroscopy. The Occurrence of Ester Bonds and α-O-4 Substructures.* Journal of Agricultural and Food Chemistry, 1997. **45**(4): p. 1212-1219.

189. Samuel, R., et al., *Structural Characterization and Comparison of Switchgrass Ball-milled Lignin Before and After Dilute Acid Pretreatment.* Applied Biochemistry and Biotechnology, 2010. **162**(1): p. 62-74.

190. Akim Leonid, G., et al., *Quantitative 31P NMR Spectroscopy of Lignins from Transgenic Poplars*, in *Holzforschung*. 2001. p. 386.

191. Sun, X.-F., et al., *Extraction and characterization of lignins from maize stem and sugarcane bagasse.* Journal of Applied Polymer Science, 2011. **120**(6): p. 3587-3595.

192. Jiang, G., D.J. Nowakowski, and A.V. Bridgwater, *Effect of the Temperature on the Composition of Lignin Pyrolysis Products.* Energy & Fuels, 2010. **24**(8): p. 4470-4475.

193. Black, L.T., G.F. Spencer, and O.L. Brekke, *Reactions of lipids in corn with ammonia.* Journal of the American Oil Chemists' Society, 1978. **55**(6): p. 526-529.

194. Parashar, V., S.K. Pandey, and A.C. Pandey, *Low-temperature synthesis of quantum size gadolinium monosulfide (GdS) nanoparticles and their pathogen capture efficiency.* Chemical Communications, 2010. **46**(18): p. 3143-3145.

195. Hurtta, M., I. Pitkanen, and J. Knuutinen, *Melting behaviour of d-sucrose, d-glucose and d-fructose.* Carbohydrate Research, 2004. **339**(13): p. 2267-2273.

196. Räisänen, U., et al., *Formation of the main degradation compounds from arabinose, xylose, mannose and arabinitol during pyrolysis.* Journal of Thermal Analysis and Calorimetry, 2003. **72**(2): p. 481-488.

197. Cho, J., et al., *Kinetics and reaction chemistry for slow pyrolysis of enzymatic hydrolysis lignin and organosolv extracted lignin derived from maplewood.* Green Chemistry, 2011. **14**(2): p. 428-439.

198. Ho, N.Y., et al., *Successful Design and Development of Genetically Engineered Saccharomyces Yeasts for Effective Cofermentation of Glucose and Xylose from Cellulosic Biomass to Fuel Ethanol*, in *Recent Progress in Bioconversion of Lignocellulosics*. 1999, Springer Berlin Heidelberg. p. 163-192.

199. Jin, M., et al., *Continuous SSCF of AFEX™ pretreated corn stover for enhanced ethanol productivity using commercial enzymes and Saccharomyces cerevisiae 424A (LNH-ST).* Biotechnology and Bioengineering, 2013. **110**(5): p. 1302-1311.

200. Howell, J.A. and M. Mangat, *Enzyme deactivation during cellulose hydrolysis.* Biotechnology and Bioengineering, 1978. **20**(6): p. 847-863.

201. Kumar, R. and C.E. Wyman, *Does change in accessibility with conversion depend on both the substrate and pretreatment technology?* Bioresource Technology, 2009. **100**(18): p. 4193-4202.

202. Zhou, W., Y. Xu, and H.-B. Schüttler, *Cellulose hydrolysis in evolving substrate morphologies III: Time-scale analysis.* Biotechnology and Bioengineering, 2010. **107**(2): p. 224-234.

203. Zhang, S., D.E. Wolfgang, and D.B. Wilson, *Substrate heterogeneity causes the nonlinear kinetics of insoluble cellulose hydrolysis.* Biotechnology and Bioengineering, 1999. **66**(1): p. 35-41.

204. Dawes, E., D. Ribbons, and L. PJ, *The route of ethanol formation in Zymomonas mobilis.* Biochem J. , 1966. **98**(3): p. 795-803.

205. Long, T.M., et al., *Cofermentation of Glucose, Xylose, and Cellobiose by the Beetle-Associated Yeast Spathaspora passalidarum.* Applied and Environmental Microbiology, 2012. **78**(16): p. 5492-5500.

206. Humbird, D., et al., *Process Design and Economics for Biochemical Conversion of Lignocellulosic Biomass to Ethanol: Dilute-Acid Pretreatment and Enzymatic Hydrolysis of Corn Stover*. 2011, NREL.

207. Voitkevich, O.V., et al., *Thermodynamic Properties of Plant Biomass Components. Heat Capacity, Combustion Energy, and Gasification Equilibria of Lignin.* Journal of Chemical & Engineering Data, 2012. **57**(7): p. 1903-1909.

208. Blokhin, A.V., et al., *Thermodynamic Properties of Plant Biomass Components. Heat Capacity, Combustion Energy, and Gasification Equilibria of Cellulose.* Journal of Chemical & Engineering Data, 2011. **56**(9): p. 3523-3531.

209. Adjei, T., *Characterization of a novel biodegradable material to reduce emission of ammonia*, in *Biological Systems Engineering*. 2007, Virginia Polytechnic Institute and State Univeristy: Blacksburg, Virginia.

210. Perry, R.H. and D. Green, *Perry's Chemical Engineers' Handbook*. 6th ed. 1984, New York: McGraw-Hill.

211. Peters, M.S. and K.D. Timmerhaus, *Plant Design and Economics for Chemical Engineers*. 1991, New York: McGraw-Hill.

212. Page, J.S., *Conceptual Cost Estimating Manual*. 1996, Houston: Gulf Publishing.

213. Matches. *http://matche.com*. 2013 [cited 2013.

214. *http://www.duncanseddon.com/docs/pdf/c9-the-price-of-ammonia.pdf*. 2013 [cited 2013.

215. *http://www.alibaba.com/showroom/lignin.html*. 2013 [cited 2013.

216. Eranki, P.L., B.D. Bals, and B.E. Dale, *Advanced Regional Biomass Processing Depots: a key to the logistical challenges of the cellulosic biofuel industry.* Biofuels, Bioproducts and Biorefining, 2011. **5**(6): p. 621-630.